

Respiratory viruses in childhood: surveillance, analysis, and modelling of their epidemiological dynamics. The case of Catalonia.

Aida Perramon Malavez

Thesis advisors: Prof. Ph.D. Clara Prats Soler, Ph.D. MD. Antoni Soriano Arandes



PhD programme in Applied and Computational Physics
Research group on Computational Biology and Complex Systems
Department of Physics
Castelldefels, May 2025

Respiratory viruses in childhood: surveillance, analysis, and modelling of their epidemiological dynamics. The case of Catalonia.

Doctoral thesis by:

Aida Perramon Malavez

Thesis advisors:

Prof. PhD. Clara Prats Soler

PhD. MD. Antoni Soriano Arandes

Front and back cover illustration:

Qiaoling Ye (叶俏伶)

Universitat Politècnica de Catalunya (UPC)

Department of Physics

Castelldefels, May 2025

A l'Avi Jordi,
I a la nena que somiava en física quàntica.



Abstract

This PhD thesis focused on the characterisation and understanding of the dynamics of SARS-CoV-2, influenza, and respiratory syncytial virus (RSV) in children in Catalonia over the last decade. Through a combination of empirical epidemiological analyses and dynamic modelling approaches, the study explored how the COVID-19 pandemic disrupted the seasonality and interaction patterns of respiratory viruses, altering their epidemiological behaviour and public health impact.

We described epidemiological changes before, during and after the pandemic, highlighting the distinct post-pandemic behaviour of SARS-CoV-2 in children, that after the emergence of the Omicron variant and together with vaccination, has ceased to produce severe outcomes and predictable epidemic waves like influenza and RSV. Influenza and RSV, in turn, showed a progressive return to their pre-pandemic epidemic patterns, but they are not in a stationary state yet.

The thesis introduced new epidemiological indicators, such as the epidemic potential growth (EPG), risk diagrams and risk panels, which were successfully applied for real-time epidemic surveillance. Additionally, empirical Gompertz models were employed to retrospectively analyse pre-pandemic epidemic dynamics of influenza and RSV, providing a quantitative framework for comparing the two viruses' epidemic curves and identifying consistent patterns in their magnitude and timing and to verify post pandemic changes. These models served as well for predicting pre- and post-pandemic (when possible) epidemic peaks almost a month in advance with a maximum of a one-week error margin and magnitude falling within the 95% CI of the models, while human supervision and intervention enhanced their performance.

To better understand the factors modulating influenza transmission, a SEIR compartmental model was developed, using a two-step transmissivity function that was ultimately related to meteorological factors. This model revealed a significant association between temperature and influenza transmissivity,

following a two-week delayed effect, offering valuable insights into the environmental drivers of seasonal influenza epidemics.

We also evaluated the real-world effectiveness of preventive strategies against RSV, particularly the monoclonal antibody nirsevimab, which demonstrated high effectiveness in reducing hospital admissions and paediatric intensive care unit (PICU) admissions by more than 80%.

Furthermore, this work questioned long-standing assumptions regarding the role of children as primary drivers of respiratory virus epidemics. While confirming their value as a sentinel population for early epidemic detection given their frequent contact rates and active surveillance, the results suggest that children may not necessarily initiate epidemics, especially for viruses like influenza. This finding invites a reconsideration of public health strategies and control measures traditionally directed at the paediatric population.

In conclusion, this thesis contributed to a deeper understanding of paediatric respiratory virus epidemiology in Catalonia, validated new modelling tools and surveillance indicators, and laid the groundwork for improving epidemic forecasting and prevention strategies in the post-pandemic context: placing children in the spotlight but safeguarding them from assuming responsibilities that belong to all of us.

Keywords: Mathematical modelling, infectious diseases, RSV, influenza, SARS-CoV-2, nirsevimab, SEIR, Gompertz, paediatrics, epidemiology.

Resum

Aquesta tesi doctoral s'ha centrat en la caracterització i estudi de la dinàmica del SARS-CoV-2, el virus de la influència (grip) i el virus respiratori sincitial (VRS) en nens i nenes de Catalunya durant l'última dècada. Per mitjà d'una combinació d'anàlisis empíriques epidemiològiques i de modelització dinàmica, hem explorat com la pandèmia de la COVID-19 ha alterat l'estacionalitat i els patrons d'interacció dels virus respiratoris, modificant el seu comportament epidemiològic i impacte en la salut pública.

Hem descrit els canvis epidemiològics abans, durant i després de la pandèmia, destacant el comportament distintiu del SARS-CoV-2 en nens i nenes després de l'aparició de la variant Òmicron i l'inici de la vacunació, deixant de generar malaltia greu i onades epidèmiques previsibles com la grip i el VRS. Aquests, d'altra banda, han mostrat un retorn progressiu als seus patrons epidèmics pre-pandèmia, tot i que encara no es troben en un estat estacionari.

També hem introduït nous indicadors epidemiològics, com el potencial de creixement epidèmic (EPG per les sigles en anglès), i els diagrames i panells de risc, que s'han aplicat amb èxit per a la vigilància epidèmica en temps real. A més, hem emprat models empírics basats en la corba de Gompertz per analitzar retrospectivament la dinàmica epidèmica pre-pandèmia de la grip i el VRS, proporcionant un marc quantitatiu per comparar les corbes epidèmiques dels dos virus i identificar patrons consistents en la seva magnitud i cronologia, permetent-nos verificar canvis post-pandèmics. Aquests models també han servit per predir els seus pics epidèmics pre- i post-pandèmia (quan fou possible) amb gairebé un mes d'antelació, amb un marge màxim d'error d'una setmana i una magnitud que cau dins de l'interval de confiança del 95% dels models, tot i que la supervisió i intervenció humana milloren el seu rendiment.

Per comprendre millor els factors que modulen la transmissió de la grip, hem desenvolupat un model SEIR de compartiments, utilitzant una funció de transmissibilitat en dos passos que s'ha aconseguit relacionar amb factors meteorològics. Aquest model ha revelat una associació significativa entre la

temperatura i la transmissivitat de la grip, amb un retard de dues setmanes, el que ofereix indicis sobre l'impacte que poden tenir variables mediambientals en les epidèmies estacionals de grip.

També s'ha avaluat l'efectivitat pràctica de les estratègies preventives contra el VRS, particularment l'anticòs monoclonal nirsevimab, que ha demostrat una alta efectivitat en la reducció d'hospitalitzacions i d'ingressos a la unitat de cures intensives pediàtriques (UCIP), de més del 80%.

A més, aquest treball ha qüestionat suposicions històriques sobre el paper dels nens i les nenes com a principals impulsors de les epidèmies de virus respiratori. Tot i que s'ha confirmat el seu valor com a població sentinella per a la ràpida detecció de les infeccions que circulen donada la seva elevada taxa de contacte i vigilància activa, els resultats suggereixen que no necessàriament inicien les epidèmies, especialment per a virus com la grip. Aquest descobriment convida a reconsiderar les estratègies de salut pública i mesures de control tradicionalment dirigides a la població pediàtrica.

En conclusió, aquesta tesi ha contribuït a una comprensió més profunda de l'epidemiologia dels virus respiratoris pediàtrics a Catalunya, ha validat noves eines de modelització i indicadors de vigilància i ha establert les bases per millorar la predicció d'epidèmies i les estratègies de prevenció en el context post-pandèmia: posant els nens i nenes al centre, però protegint-los d'assumir responsabilitats que ens corresponen a tots i totes.

Paraules clau: Modelització matemàtica, malalties infeccioses, VRS, influenza, SARS-CoV-2, nirsevimab, SEIR, Gompertz, pediatria, epidemiologia.

Resumen

Esta tesis doctoral se ha centrado en la caracterización y estudio de la dinámica del SARS-CoV-2, el virus de la influenza (gripe) y el virus respiratorio sincitial (VRS) en niños y niñas de Cataluña durante la última década. A través de una combinación de análisis empíricos epidemiológicos y de modelización dinámica, hemos explorado cómo la pandemia de la COVID-19 ha alterado la estacionalidad y los patrones de interacción de los virus respiratorios, modificando su comportamiento epidemiológico e impacto en la salud pública.

Hemos descrito los cambios epidemiológicos antes, durante y después de la pandemia, destacando el comportamiento distintivo del SARS-CoV-2 en niños y niñas tras la aparición de la variante Ómicron y la introducción de la vacunación, tal que ha dejado de producir enfermedad grave y epidemias previsibles como hacen la gripe y el VRS. La gripe y el VRS, a su vez, han mostrado un retorno progresivo a sus patrones epidémicos prepandemia, aunque aún no parecen estar en un estado estacionario.

También hemos introducido nuevos indicadores epidemiológicos, como el potencial de crecimiento epidémico (EPG, por las siglas en inglés) y los diagramas y paneles de riesgo, que se han aplicado con éxito para la vigilancia epidémica en tiempo real. Además, hemos empleado modelos empíricos basados en la ecuación de Gompertz para analizar retrospectivamente la dinámica epidémica prepandemia de la gripe y el VRS, proporcionando un marco cuantitativo para comparar las curvas epidémicas de los dos virus e identificar patrones consistentes en su magnitud y cronología y verificar cambios postpandemia. Estos modelos también han servido para predecir sus picos epidémicos, pre- y postpandemia (cuando fuere posible) con casi un mes de antelación, con un margen máximo de error de una semana y una magnitud que cae dentro del intervalo de confianza del 95% de los modelos, pero mejorando su rendimiento gracias a la intervención y supervisión humana continua.

Para comprender mejor los factores que modulan la transmisión de la gripe, hemos desarrollado un modelo SEIR compartimental, utilizando una función de transmisividad en dos pasos que se ha conseguido relacionar con factores meteorológicos. Este modelo ha revelado una asociación significativa entre la temperatura y la transmisividad de la gripe, con un retraso de dos semanas, lo que evidencia el potencial efecto de las variables medioambientales en las epidemias estacionales de gripe.

También se ha evaluado la efectividad práctica de las estrategias preventivas contra el VRS, particularmente el anticuerpo monoclonal nirsevimab, que ha demostrado una alta efectividad en la reducción de hospitalizaciones y de ingresos en la unidad de cuidados intensivos pediátricos (UCIP), de más del 80%.

Además, este trabajo ha cuestionado suposiciones históricas sobre el papel de los niños y niñas como principales impulsores de las epidemias de virus respiratorios. Aunque se ha confirmado su valor como población centinela para la detección temprana de las infecciones circulantes, dada su elevada tasa de contacto y vigilancia activa, los resultados sugieren que no necesariamente inician las epidemias, especialmente para virus como la gripe. Este hallazgo invita a reconsiderar las estrategias de salud pública y medidas de control tradicionalmente dirigidas a la población pediátrica.

En conclusión, esta tesis ha contribuido a una comprensión más profunda de la epidemiología de los virus respiratorios pediátricos en Cataluña, ha validado nuevas herramientas de modelización e indicadores de vigilancia y ha sentado las bases para mejorar la predicción de epidemias y las estrategias de prevención en el contexto postpandemia: poniendo a los niños y niñas en el centro, pero protegiéndolos de asumir responsabilidades que nos corresponden a todos y todas.

Palabras clave: Modelización matemática, enfermedades infecciosas, VRS, influenza, SARS-CoV-2, nirsevimab, SEIR, Gompertz, pediatría, epidemiología.

Acknowledgements

Veureu que aquesta tesi està escrita en format llibre, però amb parts de llibre llibre, dels d'aventures i fantasia, de poemes i paraules estranyes que et porten a un món on tot és possible. I és que la lectura ha format part de la meva vida des de ben petita, i va ser justament per un llibre que vaig decidir estudiar física. Així que entre això i que en aquesta tesi la infància hi té un gran pes, no hi podia faltar aquest toc màgic en el document que m'acreditarà per poder dir: "papa, mama, soc doctora en física". I és que és als meus pares a qui he d'agrair poder estar escrivint aquestes paraules. No pel fet de donar-me la vida, que també, si no per haver potenciat la meva passió pel coneixement des de ben petita i per haver-me criat amb un amor infinit. Quan la mama tornava de la seva jornada de feina després d'estar 12h fora de casa i es posava amb mi a jugar i fer els deures, quan el papa m'ensenyava matemàtiques i divisions de molts números; quan amb la mama fèiem quaderns d'estiu i llegíem llibres, i quan el papa s'inventava cada dia una història diferent per entretenir-me de camí a l'escola i deixar volar la meva imaginació. En tots aquests moments, que per mi van ser fonamentals, vosaltres vau haver de fer un gran esforç. Gràcies, mama, papa, per no parar de respondre els meus dubtes mai, i per creure'm capaç de tot. Per donar-me ales, per permetre'm seguir el meu camí. Gràcies, papa, mama, per tot el que heu fet fins ara i pel que sé que seguireu fent. Aquesta tesi i la persona que soc avui no serien possibles sense vosaltres.

També vull donar el meu més sincer agraiïment a la Clara Prats i el Toni Soriano, els meus supervisors de tesi. Quin camí més llarg hem fet. Toni, gràcies per portar la pediatria i les infecciose a la meva vida, i per ensenyarme a parlar la "llengua dels metges". He pogut aprendre d'un gran professional i persona, que m'ha obligat a sortir de la meva zona de confort i m'ha portat a oportunitats de col-laboració nacionals i internacionals que no m'hauria pogut mai imaginar. Gràcies per ser el meu company de congressos i per permetre'm aprendre de la teva perseverança, rigor, resolució i empenta. Gràcies per ampliar els meus horitzons i acompañar-me i guiar-me en aquest camí. Clara, a tu et vaig conèixer per primer cop el 2016 a una classe de Biofísica i d'Enginyeria Física. Qui s'imaginava que quasi deu anys després no tindria

suficients paraules per agrair-te haver forjat el meu camí com a investigadora i com a persona. Gràcies per donar-me exemple, a mi i moltes més, de com ser una dona intel·ligent, capaç, líder, resolutiva i ferma, alhora que empàtica, amable, dedicada i generosa. Gràcies per ser més que una supervisora de tesi, qualitat que compartiu amb el Toni, ja que m'heu acompanyat en els moments d'estrès, de bloqueig, de síndrome de l'impostor... I gràcies per la teva qualitat humana, molt a l'estil del BIOCOM-SC. I és que no hi ha grup de recerca més acollidor. El BIOCOM-SC ha estat per mi una gran família adoptiva, amb el Dani fent de pare de tant en tant, essent la veu de la saviesa i de la innovació, ajudant-me a créixer i reptant-me a donar el millor de mi mateixa. Gràcies Dani per acompanyar-me també des de farà quasi 10 anys, per fer que la ciència sigui sempre divertida, i per treure'm una mica de pes de les espatlles sempre que ho he necessitat. Gràcies al Sergio també per mantenir-me connectada a la física de les epidèmies, ajudant-me a raonar les meves idees més estranyes i aportant-me les seves solucions, moltes de les quals queden pendents i espero poder implementar plegats en un futur. Gràcies per ajudar-me sempre. Gràcies també a l'Enric, per les idees, pels ànims, per lluitar pels i les doctorandes al departament de física, per la passió i entrega que posa en la seva feina i que són contagioses. Gràcies al Blas, a l'Adrià, al David, al Jordi, al Laure i a tots els sèniors del BIOCOM-SC amb qui he compartit camí. Pel vostre suport, les vostres aportacions a les BIOCOMverses, per l'acollida i amabilitat que mostreu sempre amb els i les vostres alumnes i companyes. Gràcies en especial al Víctor, per ser el *postdoc* més competent, amable, divertit i implicat que podria haver desitjat. Els teus consells han fet millor aquesta tesi i n'he pogut aprendre moltíssim. També vull donar les gràcies al Quim Valls, que tot i que vam coincidir poquet dins del grup, em va donar els millors consells i avui dia encara penso en ell cada cop que escolto música clàssica. I al Martí. Gràcies, per totes les oportunitats que m'has donat, per totes les portes que m'has obert, per haver cregut en mi.

He estat molt afortunada a la meva etapa universitària, perquè contínuament m'han envoltat i guiat persones amb grans valors i passió per la seva feina. Gràcies al David Pino i a la Cristina Montañola per donar-me suport durant aquests anys i per involucrar-me en la vostra recerca podent aprendre de

vosaltres, grans professionals i millors persones. A l'Ermen i l'Edu, i tot l'equip del SISAP de l'ICS, per integrar-me com a una més, per ensenyar-me, per obrir-me portes, per la companyonia. A la Carmen Cabezas per la gran tasca que ha fet i el legat que deixa, gràcies. Gràcies a tot el COPEDICAT, aquesta tesi no s'hauria pogut dur a terme sense el vostre amor i vocació. En especial, gràcies al Pepe, l'Anna, l'Almudena, el Ramón, i a tots aquells i aquelles que m'heu acollit com a una més, m'heu guiat en el món complicat dels metges i m'heu fet sentir sempre una professional capaç. Gràcies per totes les oportunitats que m'heu donat. També, gràcies a l'Anna Creus i la Maria Piñana pels dinars, l'amistat, i per ser referents.

Aquest camí hagués estat molt més solitari també sense l'equip de futbol de l'EPSEB i el meu capi preferit, David, gràcies per compartir la teva originalitat amb la resta, per ser una persona tan divertida i única. Gràcies per estendre'm la mà. A l'Allison, per ensenyar-me a divertir-me treballant i mostrar-me què és ser excel·lent amb humilitat. Moltes gràcies, tant de bo assemblar-me a tu algun dia. També gràcies al Carles, per ser el meu company de congressos, de sortides i de queixes del doctorat; i per fer els dies a Castelldefels menys solitaris. I als meus primers alumnes de TFG, el Mario i la Qiao, que s'han convertit en companys a qui admiro moltíssim i que m'ensenyen molt més del que jo vaig poder fer-ho. Gràcies per fer que tot valguia la pena. Per l'amistat, per la ciència compartida i el camí que ens queda per davant. I per l'amistat també, sense cap ordre concret, al Simon, la Naiara, el Pau, el Miquel, l'Oscaritu, el Roger, la Inma, l'Anna, el Xema i l'Eric. Naiara, gràcies per obligar-me a descansar, pel suport emocional i per ser una referent. Eric, gràcies per ser el meu confident i passar hores a l'altra banda del telèfon des de l'altra punta d'Europa. Simon, gràcies per accompanyar-me sempre independentment dels quilòmetres que ens separin. Anna, gràcies per entrar a formar part de la meva vida. Una amiga com tu té un valor incalculable. Roger, gràcies per fer-me riure en els pitjors moments. Dones tant la tabarra que a una se li oblien els seus problemes. Xema, gràcies pels riures, pels balls, pels jocs, per compartir aquesta alegria tant teva amb la resta i fer el nostre món una mica millor. Oscaritu, gràcies pels moments compartits i per les converses que duren hores. Pau, Miquel, gràcies per les estones al bar de la FIB, per escoltar-me

hores queixant-me de la tesi, per donar-me espais on relaxar-me i ser jo mateixa, per fer camí amb mi. Pau, gràcies pels dinars, els debats, els riures, la muntanya i, en general, la companyia. Miquel, gràcies pels àudios interminables, per l'art, per compartir passions, per escoltar sempre. També, enhorabona, doctors. Ho hem aconseguit! Inma, vam fer el grau i el màster juntes i, tot i anar per camins diferents pel doctorat, aquí segum. Gràcies per tot el que has fet per mi sempre. Per evitar-me atacs de pànic, per compartir inquietuds, per deixar-me aprendre de tu. T'admiro tant que les paraules es queden curtes. Sergi, Gerard, no m'oblidó de vosaltres. Moltes gràcies per acompañar-me a dia d'avui, per deixar-me aprendre de vosaltres.

Tirant cap a casa, Jordi, gràcies per ensenyar-me com de curativa pot ser una bona riallada, pels sopars i les caminades, per fer-me respirar una mica d'aire fresc. Txell, gràcies per ser la meva brúixola moral, per acompañar-me des de l'època de les ulleres i els bràquets, per abraçar-me sempre que ho he necessitat, per treure'm un somriure en la pitjor de les situacions. Gràcies per créixer amb mi, i seguir fent-ho. Per les trucades, per les idees esbojarrades idèntiques que tenim per casualitat en el mateix moment des de llocs que estan a quilòmetres de distància. Gràcies per ensenyar-me què vol dir ser una bona amiga. Alexito, tu sí que m'has aguantat tota la vida, i el que et queda. Gràcies per ser el germà que no he tingut, per renyar-me quan calia, per centrar-me quan em feia falta, per no deixar-me mai sola. Gràcies per caminar sempre al meu costat, i deixar-me aprendre de tu. Sense vosaltres no seria aquí avui.

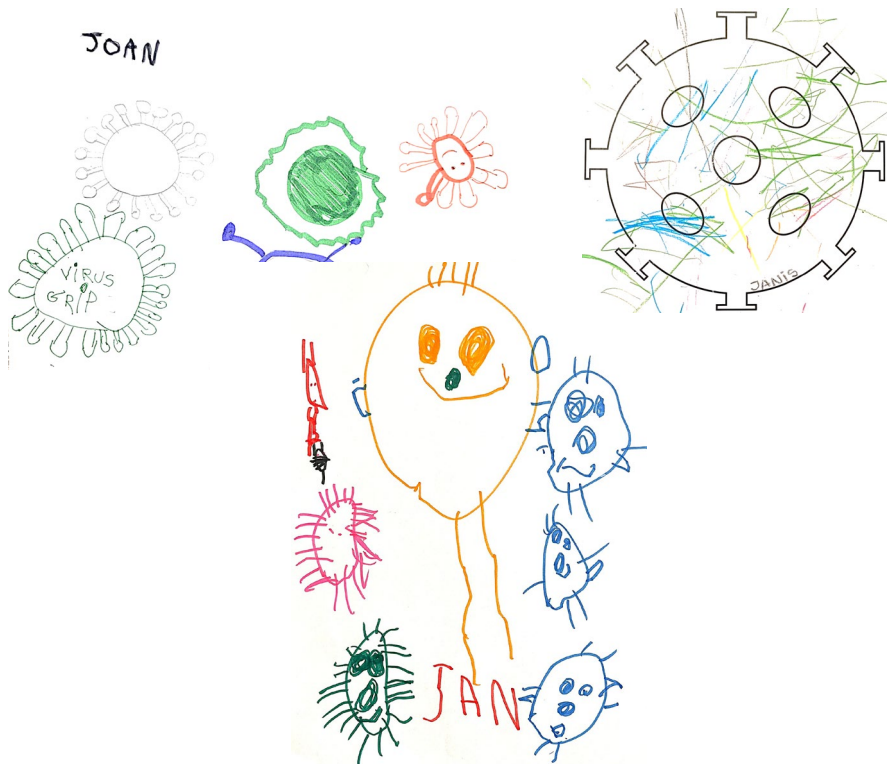
I sobretot gràcies a l'Adrià, i també a la teva família (i a la Nara) que amb tant d'amor m'ha acollit. Has passat els millors i els pitjors moments d'aquest camí amb mi, acompañant-me, comprant-me xocolata quan em veies molt desesperada, compartint rentadores i armari – cosa que no és tan fàcil com sembla –, plorant al meu costat i rient i jugant com si tornéssim a ser petits i despreocupats. Estar amb tu no només em fa feliç, em fa millor. Moltes gràcies per formar una llar amb mi, per les ales que em dones, per com de fàcil fas que sembli tot. Gràcies per impulsar-me, per ser un exemple. T'estimo.

I gràcies de nou a la meva família. A totes les tatas, tetes, tiets, tietes. Als més peques, a qui espero que ajudi la meva recerca. A l'avi Jordi que ja no hi és i a

la iaia Rosa, el iaio Quillo i la iaia Carmen que tant de bo fossin eterns. A la tita Raquel, que sempre ha estat al meu costat. Al tito Juan i la tita Angels, que han estat sempre per mi com uns segons pares.

Podria fer una llista interminable de les persones amb les que he tingut la sort de compartir espais i vivències i a les que admiro profundament tant a nivell personal com professional, però ho deixaré aquí. Us tinc molt presents tot i no poder mencionar-vos a tots i totes. Tanmateix, tinc clar que aquest camí no l'he fet sola i no l'hauria pogut fer sense cap de vosaltres. Però sobretot, i de nou expressant el meu més sincer agraiament que no serà mai suficient, no seria aquí sense l'amor i suport dels meus pares, Pere i Ana. Us estimo moltíssim.

Gràcies a totxs. També a tu, que estàs dedicant el teu temps en llegir aquestes pàgines.



Scientific work

About the author



Aida Perramon Malavez graduated in Engineering Physics at the Polytechnical University of Catalonia (2016-2020). She holds a master's degree in Computational Biomedical Engineering (Pompeu Fabra University, 2020-2021). In September 2021, she joined as a predoctoral fellow the Computational Biology and Complex Systems (BIOCOM-SC) group led by Prof. PhD. Clara Prats at Universitat Politècnica de Catalunya in Castelldefels, Spain. Her PhD studies were funded by la Fundació la Marató de TV3 and were co-supervised by Prof. PhD. Clara Prats and MD. PhD. Antoni Soriano-Arandes. During her doctoral studies, she obtained a master's degree in Bioinformatics and Biostatistics (Universitat de Barcelona and Universitat Oberta de Catalunya, 2023-2025) and pursued a three-months scholarship on Planetary Health Informatics at the Nuffield Department of Orthopaedics, Rheumatology and Musculoskeletal Sciences (NDORMS) at the University of Oxford under the supervision of PhD. Sara Khalid. As part of her PhD training, in 2024 she did a research stay at the Catalan Healthcare Institute (Institut Català de la Salut, in Catalan) under the supervision of MD. Ermengol Coma. A summary of the scientific work conducted by the author during her Thesis is provided below.

Peer-reviewed publications in indexed journals

- I. Perramon-Malavez, A.; Buonsenso, D.; Morello, R.; Coma, E.; Foster, S.; Leonard, P.; Marlow, R.; Martínez-Marcos, M.; Mendioroz, J.; Vila, J.; Creus-Costa, A.; Prats, C.; Roland, D.; Williams, T.C.; Soriano-Arandes, A. Real-world impact of nirsevimab immunisation against respiratory disease on emergency department attendances and admissions among infants: a multinational retrospective analysis. *The Lancet Regional Health – Europe*. 2025. <Accepted in means of publication>
- II. Soriano-Arandes, A.; Andrés, C.; Perramon-Malavez, A.; Creus-Costa, A.; Gatell, A.; Martín-Martín, R.; Solà-Segura, E.; Rierra-Bosch, M.T.; Fernández, E.; Biosca, M.; et al. Implementing Symptom-Based Predictive Models for Early Diagnosis of Pediatric Respiratory Viral Infections. *Viruses*. 2025. Volume: 17. <<https://doi.org/10.3390/v17040546>>

- III. Perramon-Malavez, A.; Hermosilla, E.; Coma, E.; Fina, F.; Refié, A.; Martinez, M.; Mendioroz, J.; Prats, C.; Soriano-Arandes, Antoni; Cabezas, C. Effectiveness of nirsevimab immunoprophylaxis against respiratory syncytial virus-related outcomes in hospital care settings: a seasonal cohort study of infants in Catalonia (Spain). *Pediatric infectious disease journal*. 2025. <<https://doi.org/10.1097/INF.0000000000004672>>
- IV. Soriano Arandes, Antoni; Creus, A.; Perramon-Malavez, A.; Andrés, C.; Vila, J.; Gatell, A.; Piñana, M.; Serrano, P.; González, A.; Capdevila, R.; Prats, C.; Soler-Palacín, P.; Antón, A. Early experience on universal prophylaxis in infants against respiratory syncytial virus: facts and expectations. *Seminars in respiratory and critical care medicine*. 2025. <<https://doi.org/10.1055/a-2531-0968>>
- V. Andrés, C.; Perramon-Malavez, A.; Creus-Costa, A.; Gatell, A.; Martín-Martín, R.; Solà-Segura, E.; Ribera-Bosch, M.; Biosca, M.; Soler, I.; Chiné, M.; Sanz, L.; Quezada, G.; Pérez, S.; Salvadó, O.; Sau, I.; Prats, C.; Antón, A.; Soriano-Arandes, A. Respiratory viral coinfections in pediatric patients in the primary care setting: a multicenter prospective study within the COPEDICAT network. *Journal of infectious diseases*. 2024. Volume: 230. Number: 6. pp.: 1337 ~ 1341. <<https://doi.org/10.1093/infdis/jiae279>>
- VI. López-Sánchez, I.; Perramon-Malavez, A.; Soriano-Arandes, A.; Prats, C.; Duarte-Salles, T.; Raventós, B.; Roel, E. Socioeconomic inequalities in COVID-19 infection and vaccine uptake among children and adolescents in Catalonia, Spain: a population-based cohort study. *Frontiers in Pediatrics*. 2024. Volume: 12. <<https://doi.org/10.3389/fped.2024.1466884>>
- VII. Pistillo, A.; Warkentin, S.; Abellan, A.; de Bont, J.; Ranger, T.; Pérez, L.; Cirach, M.; Perramon-Malavez, A.; Khalid, S.; Nieuwenhuijsen, M.; Vrijheid, M.; Duarte-Salles, T. Residential relocation and changes in patterns of environmental exposures by health determinants among children and adolescents in Catalonia, Spain. *Environmental research*. 2024. Volume: 263, part 2. Number: article 120152. <<https://doi.org/10.1016/j.envres.2024.120152>>
- VIII. Perramon-Malavez, A.; Lopez de Rioja, V.; Coma, E.; Hermosilla, E.; Fina, F.; Martínez-Marcos, M.; Mendioroz, J.; Cabezas, C.; Montañola-Sales, C.; Prats, C.; Soriano-Arandes, A. Introduction of nirsevimab in Catalonia, Spain: description of the incidence of bronchiolitis and respiratory syncytial virus in the 2023/2024 season. *European journal of pediatrics*. 2024. Volume: 183. pp.: 5181 ~ 5189. <<https://doi.org/10.1007/s00431-024-05779-x>>
- IX. Lopez de Rioja, V.; Perramon-Malavez, A.; Alonso, S.; Andrés, C.; Antón, A.; Bordoy, A.; Càmara, J.; Cardona, P.J.; Català, M.; Lopez, D.; Martí, S.; Martró, E.; Saludes, V.; Prats, C.; Alvarez-Lacalle, E. Mathematical modeling

- of SARS-CoV-2 variant substitutions in European countries: transmission dynamics and epidemiological insights. *Frontiers in public health*. 2024. Volume: 12. <<https://doi.org/10.3389/fpubh.2024.1339267>>
- X. Villanueva, M.; Conesa, D.; Català, M.; Perramon-Malavez, A.; Lopez de Rioja, V.; Lopez, D.; Alonso, S.; Cardona, P.J.; Prats, C.; Alvarez-Lacalle, E.; López, M.; Molinuevo, D.; Montañola, C. Country-report pattern corrections of new cases allow accurate 2-week predictions of COVID-19 evolution with the Gompertz model. *Scientific reports*. 2024. Volume: 14. Number: article 10775. <<https://doi.org/10.1038/s41598-024-61233-w>>
- XI. Lopez de Rioja, V.; Basile, L.; Perramon-Malavez, A.; Martinez-Solanas, È.; Lopez, D.; Medina-Maestro, S.; Coma, E.; Fina, F.; Prats, C.; Mendioroz, J.; Alvarez-Lacalle, E. Severity of Omicron subvariants and vaccine impact in Catalonia, Spain. *Vaccines*. 2024. Volume: 12. Number: 5, article 466. <<https://doi.org/10.3390/vaccines12050466>>
- XII. Perramon-Malavez, A.; Bravo, M.; Lopez de Rioja, V.; Català, M.; Alonso, S.; Alvarez-Lacalle, E.; Lopez, D.; Soriano Arandes, A.; Prats, C. A semi-empirical risk panel to monitor epidemics: multi-faceted tool to assist healthcare and public health professionals. *Frontiers in public health*. 2024. Volume: 11. Number: 1307425. <<https://doi.org/10.3389/fpubh.2023.1307425>>
- XIII. Coma, E.; Martinez, M.; Hermosilla, E.; Mendioroz, J.; Reñé, A.; Fina, F.; Perramon-Malavez, A.; Prats, C.; Cereza, M.; Ciruela, P.; Pineda, V.; Antón, A.; Ricós Furió, G.; Soriano Arandes, Antoni; Cabezas, C. Effectiveness of nirsevimab immunoprophylaxis against respiratory syncytial virus-related outcomes in hospital and primary care settings: a retrospective cohort study in infants in Catalonia (Spain). *Archives of disease in childhood*. 2024. Number: 109. pp.: 736 ~ 741. <<https://doi.org/10.1136/archdischild-2024-327153>>
- XIV. Perramon-Malavez, A.; Lopez de Rioja, V.; Montañola-Sales, C.; Vila, J.; Antón, A.; Piñana, M.; Soler-Palacín, P.; Prats, C.; Soriano-Arandes, A.; Creus, A.; Andrés, C.; Lera, E.; Wörner, N.; Balcells, J. Unraveling the effects of the COVID-19 pandemic on the hospital burden of respiratory syncytial virus. *Pediatric pulmonology*. 2023. Volume: 58. Number: 10. pp.: 2979 ~ 2982. <<https://doi.org/10.1002/ppul.26616>>
- XV. Coma, E.; Pino, D.; Moras, N.; Mora, N.; Fina, F.; Perramon-Malavez, A.; Prats, C.; Medina, M.; Planella, A.; Mompart, A.; Mendioroz, J.; Cabezas, C. Mortality in Catalonia during the summer of 2022 and its relation with high temperatures and COVID-19 cases. *Frontiers in public health*. 2023. Volume: 11. <<https://doi.org/10.3389/fpubh.2023.1157363>>

- XVI. Pino, R.; Antoñanzas, J.; Paredes-Carmona, F.; Perramon-Malavez, A.; Rivière, J.; Martínez, A.; Gatell, A.; Soler-Palacín, P.; Fina, F.; Prats, C.; Soriano-Arandes, A. Multisystem inflammatory syndrome in children and SARS-CoV-2 variants: a two-year ambispective multicentric cohort study in Catalonia, Spain. *European journal of pediatrics*. 2023. Volume: 182. Number: 4. pp.: 1897 ~ 1909. <<https://doi.org/10.1007/s00431-023-04862-z>>
- XVII. Soriano Arandes, A.; Brett, A.; Buonsenso, D.; Emilsson, L.; de la Fuente, I.; Gkentzi, D.; Helve, O.; Kepp, K.; Mossberg, M.; Muka, T.; Munro, A.; Papan, C.; Perramon-Malavez, A.; Schaltz, F.; Smeesters, P.; Zimmermann, P. Policies on children and schools during the SARS-CoV-2 pandemic in Western Europe. *Frontiers in public health*. 2023. Volume: 11. Number: Article 1175444. pp.: 1 ~ 20. <<https://doi.org/10.3389/fpubh.2023.1175444>>
- XVIII. Buonsenso, D.; Perramon-Malavez, A.; Català, M.; Torres, J.; Camacho, G.; Rojas, M.; Ulloa, R.; Camacho, K.; Pérez, C.; Cotugno, N.; Yamazaki, M.; Estripeaut, D.; Buddingh, E.; von Asmuth, E.; van Rossum, A.; Rivière, J.; Pino, R.; Prats, C. Multisystem inflammatory syndrome in children in western countries: decreasing incidence as the pandemic progresses? An observational multicenter international cross-sectional study. *Pediatric infectious disease journal*. 2022. Volume: 41. Number: 12. pp.: 1 ~ 7. <<https://doi.org/10.1097/INF.0000000000003713>>
- XIX. Antoñanzas, J.; Perramon-Malavez, A.; López, C.; Boneta, M.; Aguilera, C.; Capdevila, R.; Gatell, A.; Serrano, P.; Poblet, M.; Canadell, D.; Vilà, M.; Catásus, G.; Valldepérez, C.; Català, M.; Soler-Palacín, P.; Prats, C.; Soriano-Arandes, A. Symptom-based predictive model of COVID-19 disease in children. *Viruses*. 2021. Volume: 14. Number: 1. pp.: 63. <<https://doi.org/10.3390/v14010063>>
- XX. Perramon-Malavez, A.; Soriano-Arandes, A.; Pino, D.; Andres, C.; Català, M.; Gatell, A.; Poblet, M.; Prats, C. Schools as a Framework for COVID-19 Epidemiological Surveillance of Children in Catalonia, Spain: A Population Based Study. *Frontiers in Pediatrics*. 2021. Volume: 9. Number: 745744.
- XXI. Soriano-Arandes, A.; Perramon-Malavez, A.; Gatell, A.; Serrano, P.; Prats, C.; Soler, P. Reply to Darcis, et al. *Clinical infectious diseases*. 2021. pp.: ciab572.

Peer-reviewed publications in non-indexed journals

- XXII. Perramon-Malavez, A.; Lopez de Rioja, V.; Lopez, D.; Prats, C. Transition from the old to the new viral normality: Where are we? *Enfermedades Emergentes*. 2023. Volume: 22. Number: 2. pp.: 71 ~ 75. <http://hdl.handle.net/2117/390935>

- XXIII. Perramon-Malavez, A.; Alvarez-Lacalle, E.; Català, M.; Lopez de Rioja, V.; Alonso, S.; Prats, C.; Lopez, D. Analysis of the epidemiological dynamic of monkeypox from 15th May to 31st August 2022. *Enfermedades emergentes*. 2022. Volume: 21. Number: 3. pp.: 160 ~ 167. <http://hdl.handle.net/2117/384328>

Other scientific and technical documents

- XXIV. Català, M.; Cardona, P.J.; Prats, C.; Alonso, S.; Alvarez-Lacalle, E.; Conesa, D.; Perramon-Malavez, A.; Echebarria, B.; Lopez, D. Analysis and prediction of COVID-19 for EU-EFTA-UK and other countries. 11/10/2021. pp.: 80.
- XXV. Català, M.; Cardona, P.J.; Prats, C.; Alonso, S.; Alvarez-Lacalle, E.; Conesa, D.; Perramon-Malavez, A.; Echebarria, B.; Lopez, D. Analysis and prediction of COVID-19 for EU-EFTA-UK and other countries. 08/10/2021. pp.: 86.
- XXVI. Català, M.; Cardona, P.J.; Prats, C.; Alonso, S.; Alvarez-Lacalle, E.; Conesa, D.; Perramon-Malavez, A.; Echebarria, B.; Lopez, D. Analysis and prediction of COVID-19 for EU-EFTA-UK and other countries. 06/10/2021. pp.: 117.
- XXVII. Català, M.; Cardona, P.J.; Prats, C.; Alonso, S.; Alvarez-Lacalle, E.; Conesa, D.; Perramon-Malavez, A.; Echebarria, B.; Lopez, D. Analysis and prediction of COVID-19 for EU-EFTA-UK and other countries. 04/10/2021. pp.: 94.
- XXVIII. Català, M.; Cardona, P.J.; Prats, C.; Alonso, S.; Alvarez-Lacalle, E.; Conesa, D.; Perramon-Malavez, A.; Echebarria, B.; Lopez, D. Analysis and prediction of COVID-19 for EU-EFTA-UK and other countries. 01/10/2021. pp.: 90.

Contributions to national and international conferences

- I. Perramon-Malavez, A.; Hermosilla, E.; Coma, E.; Martinez, M.; Mendioroz, J.; Soriano Arandes, Antoni; Prats, C.; Cabezas, C. Efectividad de la inmunoprofilaxis con nirsevimab frente a la infección relacionada con el virus respiratorio sincitial en el ámbito hospitalario: estudio de la cohorte estacional en lactantes de Cataluña (España). *XII Congreso de la Asociación Española de Vacunología*. 26/10/2024.
- II. Perramon-Malavez, A.; Prats, C.; Alonso, S.; Alvarez-Lacalle, E.; Lopez, D. Análisis dinámico de la mortalidad infantil, un indicador de la salud global en la infancia. *XIII - Congreso SEMTSI Salud Global en la Infancia*. 02/10/2024.
- III. Perramon-Malavez, A.. Association of temperature and absolute humidity with influenza illness in Catalonia, Spain. Weather and Well-Being Symposium. *European Meteorological Society*. 06/09/2024.
- IV. Perramon-Malavez, A.; Lopez de Rioja, V.; Coma, E.; Fina, F.; Martínez, M.; Mendioroz, J.; Cabezas, C.; Prats, C.; Soriano Arandes, A. The effect of the first nirsevimab immunisation campaign in the respiratory syncytial virus

community incidence in Catalonia, Spain. *42nd Annual Meeting of the European Society of Paediatric Infectious Diseases*. 22/05/2024.

- V. Perramon-Malavez, A.; Warkentin, S.; Pistillo, A.; Abellan, A.; de Bont, J.; Vrijheid, M.; Duarte Salles, T.; Khalid, S. Changes in environmental and socioeconomic determinants of child health: a descriptive analysis of spatio-temporal movement patterns of 237,316 children. *2024 Planetary Health Summit & 6th Annual Meeting*. 17/04/2024.
- VI. Bravo, M.; Perramon-Malavez, A.; Lopez de Rioja, V.; Alonso, S.; Alvarez-Lacalle, E.; Lopez, D.; Prats, C. Development of mathematical SEIR models to study the epidemiology of influenza in Catalonia. *XVII International Congress of the Spanish Biophysical Society*. 28/06/2023.
- VII. Perramon-Malavez, A.; Lopez de Rioja, V.; Alvarez-Lacalle, E.; Alonso, S.; Lopez, D.; Piñana, M.; Andrés, C.; Vila, J.; Coma, E.; Antón, A.; Soriano Arandes, Antoni; Prats, C. Epidemiological characterization and modelling for short-term prediction of bronchiolitis in Catalonia, Spain. *RSVW'23 – A Global Conference On Novel RSV Preventive and Therapeutic Interventions*. 22/02/2023.
- VIII. Perramon-Malavez, A.; Lopez de Rioja, V.; Català, M.; Alonso, S.; Alvarez-Lacalle, E.; Prats, C.; Lopez, D. Epidemiological characteristics and modelling for short-term prediction of the Respiratory Syncytial Virus (RSV) and influenza spreading in Catalonia (Spain). *XXXVII Trobades Científiques de la Mediterrània Josep Miquel Vidal*. 19/10/2022.
- IX. Perramon-Malavez, A.; Lopez de Rioja, V.; Català, M.; Alonso, S.; Alvarez-Lacalle, E.; Prats, C.; Lopez, D. Analysis of the epidemiological dynamics of monkeypox from May 15 to August 31, 2022. *XXXVII Trobades Científiques de la Mediterrània Josep Miquel Vidal*. 19/10/2022.
- X. Soriano Arandes, Antoni; Perramon-Malavez, A.; Català, M.; Villanueva, M.; Piñana, M.; Vila, J.; Andrés, C.; Lopez, D.; Antón, A.; Prats, C. Característiques i models epidemiològics per a la predicción a curt termini de l'infecció per virus respiratori sincítial (VRS) a Catalunya. *XXVI Reunió Annual de la Societat Catalana de Pediatria*. 11/06/2022.
- XI. Perramon-Malavez, A.; Català, M.; Villanueva, M.; Piñana, M.; Vila, J.; Andrés, C.; Lopez, D.; Soriano Arandes, Antoni; Antón, A.; Prats, C. Epidemiological characteristics and modelling for short-term prediction of the respiratory syncytial virus (RSV) spreading in Catalonia (Spain). *European Society for Paediatric Infectious Diseases Meeting*. 11/05/2022.

Supervision or tutoring of bachelor theses

- I. **Supervisor/s:** Lopez, D.; Perramon-Malavez, A. Work author: Mokhtari Khaled, Chaimae. Analisi del treball en salut comunitària realitzat a la Unitat de Salut Internacional Drassanes-Vall d'Hebron. Bachelor's thesis. 13/02/2025. Mark: Very Good.
- II. **Supervisor, Vocal:** Perramon-Malavez, A. Work author: Valette Hohn, Berta. Avaluació dels efectes de la introducció del Nirsevimab en la dinàmica de les bronquiolitis i el VRS a Catalunya. Bachelor's thesis. 22/07/2024. Mark: A with honours.
- III. **Supervisor/s:** Lopez de Rioja, V.; Perramon-Malavez, A. Work author: Ruiz De la cuesta castaño, Elena. Prediction and Modelling of Influenza with Machine Learning. Bachelor's thesis. 08/07/2024. Mark: Excellent.
- IV. **Supervisor/s:** Lopez, D.; Perramon-Malavez, A. Work author: Samuelson Gonzalez, Lidia. Anàlisi de la dinàmica epidemiològica de la grip als països europeus. Bachelor's thesis. 05/02/2024. Mark: Pass. Universitat Politècnica de Catalunya.
- V. **Supervisor:** Perramon-Malavez, A. Work author: Alvarez Bernal, Arnau. Utilització del model de Gompertz per avaluar la dinàmica epidemiològica del Monkeypox. Bachelor's thesis. 23/10/2023. Mark: Very Good.
- VI. **Supervisor/s:** Lopez, D.; Perramon-Malavez, A. Work author: Ye, Qiaoling. Anàlisi dels efectes epidemiològics de la interacció entre virus respiratoris. Bachelor's thesis. 19/07/2022. Mark: A with honours.
- VII. **Supervisor/s:** Lopez, D.; Perramon-Malavez, A. Work author: Bravo Masferrer, Mario. Desenvolupament de models matemàtics tipus SEIR per estudiar les epidèmies de grip a Catalunya. Bachelor's thesis. 20/01/2022. Mark: A with honours.

Grants and awards

- Prats, C.; Alonso, S.; Alvarez-Lacalle, E.; Arias, S.; Benitez, R.; Echebarria, B.; Ginovart, M.; Lopez, D.; Oriola, D.; Tauste Campo, A.; Gonzalez, R.; Ramirez de La Piscina, L.; Oliveira AD; Vila, M.; Abecia, S.; Conesa, D.; Perramon-Malavez, A.; Lopez de Rioja, V. *Placa Josep Trueta al mèrit sanitari 2022*. 2022. First prize. Govern de la Generalitat de Catalunya.

Academic training during the PhD programme

- Master's in Bioinformatics and Biostatistics. Universitat Oberta de Catalunya and Universitat de Barcelona. Barcelona, Spain. 2023-2025,

- Introducció al software estadístic R. Castelldefels Campus. Castelldefels, Spain. 2023.
- Oxford Real World Evidence Summer School. NDORMS, University of Oxford. Oxford, United Kingdom. 2022.
- XV MESIO UPC-UB Summer School. Universitat Politècnica de Catalunya and University of Barcelona. Barcelona, Spain. 2022.

Journal peer-review activities

- Scientific Reports (x1)
- European Journal of Pediatrics (x1)
- BMC Public Health (x2)

Education and outreach activities

- Interview. RTVE - Radio y Televisión Española. 5 anys del primer cas de Covid-19: estem preparats per a una nova pandèmia? 25/02/2025 - 25/02/2025.
- Tècniques d'optimització, millora de models. Postgrau en Agrifood Data Science. Universitat Politècnica de Catalunya. 2024.
- Prats, C.; Perramon-Malavez, A. Pòdcast UPC: Algorritmes. Description: "Les matemàtiques, aliades inesperades en la lluita contra les malalties" Accessible a: https://www.ivoox.com/en/les-matematiques-aliades-inesperades-lluitacontra-audios-mp3_rf_103148943_1.html. 15/02/2023 - 15/02/2023.
- Física + Matemàtiques = Salut2. ConscienciArte. Red ConscienciArte. Platja d'Aro, Espanya. 2023.
- No és una bola de vidre: és ciència. El paper de la física en la biologia i la medicina. Societat Catalana de Física. 2022.

Preface

*"Ample are time and space—ample the fields
of Nature."*

Walt Whitman

Dear reader, in 2020 the world suffered a watershed event: the COVID-19 pandemic. Responsible for it was the SARS-CoV-2, a novel virus that arose with uncertainty and unpreparedness, and, with it, death and prejudice followed. Nonetheless, after the initial dismay, this public health hazard highlighted for us, as a society, the significant benefits of global and interdisciplinary collaboration. It also underscored the critical importance of epidemiological surveillance and the necessity of proactively anticipating changes in the environmental status quo. This thesis is born in this regard and focuses on the population that suffers the most the consequences of adults' decisions: children.

In 2020, our infants were unfoundedly singled out as key contributors to the accelerated transmission of SARS-CoV-2, leading to various governmental measures that impacted their functional and emotional development. In response, and to safeguard the interests of children in Catalonia—the geographic focus of this thesis—the COPEDICAT research group was established. This group has played an instrumental role in the advancement of this thesis. COPEDICAT spearheaded the surveillance of respiratory viruses among Catalan children, particularly SARS-CoV-2, influenza viruses and the respiratory syncytial virus. This initiative was conducted within the framework of a competitive project funded by the Fundació la Marató de TV3. The objective of this thesis is to understand the dynamics of the most prevalent respiratory viral infections in childhood in Catalonia, being able to predict their epidemics, assess how SARS-CoV-2 and other factors such as preventive strategies might affect the previous dynamics of the respiratory syncytial virus and influenza; to determine the COVID-19 effects on children, their role on epidemics and to study what new viral normality is established.

Table of Contents

Abstract	i
Acknowledgements	vii
Scientific work.....	xii
Preface	xx
Introduction.....	1
1.1. Lower respiratory tract infections	2
1.1.1. Worldwide.....	3
1.1.2. In Catalonia	5
1.2. Dynamics of viral transmission	8
1.2.1. Airborne transmission of respiratory viruses	8
1.2.2. The immune system response	18
1.3. The Catalan healthcare system.....	23
1.3.1 Catalan databases	27
1.4. Epidemiological models.....	30
1.4.1. Empirical models.....	30
1.4.2. Mechanistic models.....	34
1.5. Aim, approach, and outline of this thesis.....	38
Indicators and surveillance	41
2.1. The <i>tripledemy</i>	43
2.2. Epidemiological indicators	47
2.2.1. Semi-empirical risk panel to monitor epidemics.....	48
SARS-CoV-2	69
3.1. Characteristics of SARS-CoV-2	71
3.2. COVID-19 disease	72
3.3. Epidemiology of SARS-CoV-2 in Catalonia.....	74
3.3.1. The role of children in COVID-19 epidemics.....	75
3.4. Multisystem inflammatory syndrome in children.....	81
3.4.1. In Catalonia and Western countries	82
Influenza	87
4.1. Characteristics of influenza viruses	89

4.2. Influenza disease	92
4.3. Epidemiology of influenza	93
4.3.1. Children as the drivers for influenza epidemics	95
4.4. Modelling the influenza epidemic	104
4.4.1. Empirical modelling of influenza epidemics	104
4.4.2. Mechanistic modelling of influenza epidemics	119
Respiratory Syncytial Virus.....	141
5.1. Characteristics of the respiratory syncytial virus	143
5.2. Bronchiolitis disease.....	145
5.3. Epidemiology of the respiratory syncytial virus	147
5.4. Modelling the respiratory syncytial virus epidemic	149
5.4.1. Empirical modelling of the respiratory syncytial virus epidemics	149
5.5. Immunisation with nirsevimab	173
5.5.1. Dynamic changes after the introduction of nirsevimab	175
5.5.2. Nirsevimab effectiveness in Catalonia	182
Conclusions.....	195
6.1. Summary of results and discussion.....	196
6.2. Conclusions.....	204
6.3. Future work	207
Note on language support.....	211
References	212

Chapter 1

Introduction

"I am a child, I am a child, although my needs may be different from yours, it does not make me any different from you."

Cleric Tembwe

*O*n this chapter, the reader will begin their adventure into knowledge, the most thrilling of affairs. This may be a perilous adventure, but with science on your side, you are certain to navigate it triumphantly. Your first encounter will be the enigmatic world of viruses that assail the lower respiratory tract, uncovering their impact on children. As the saying goes: think globally and act locally. Thus, we shall converge our adventure by focusing on Catalonia, the cradle of this thesis. We will embark on an exploration of the labyrinthine workings of the Catalan healthcare system, plumbing the depths of the precious public data it offers, alongside other complementary data sources that await discovery. Subsequently, we shall introduce the realm of epidemiological models. Though they may resemble crystal balls, these models are grounded in science and logic, guiding us through the intricate domain of mathematics as it intertwines with life sciences, an art often known as physics. To conclude this chapter, the grand objective of this thesis will be unveiled, alongside a compelling outline of the ensuing stages of our adventure.

1.1. Lower respiratory tract infections

Our planet Earth functions as a vast ecosystem, with humans constituting just one of its many animal inhabitants, alongside plants and microbial beings among others. When we step away from screens and social media, we engage synergistically with our environment and come into contact with other organisms contributing to the planet's development and maintenance. These interactions can be neutral, beneficial, or detrimental to our survival. In fact, the context of these interactions can alter their impact on our well-being. For instance, brief exposure to sunlight is valuable for our bodies, supporting proper metabolic and hormonal function. However, prolonged exposure can lead to severe sunburn and an increased risk of skin cancer [1].

In our interactions with the world, we also encounter viruses. These microorganisms can infect us and cause diseases, but they can also play a role in our survival, as evidenced by therapies for autoimmune diseases [2]. Ultimately, these interactions are inevitable and contribute to our evolution as a species.

Respiratory viruses are among the most common types of viruses we encounter. This prevalence is due to their ability to cause mild symptoms that often go unnoticed, the scarce antiviral therapies and the challenges in containing airborne transmission [3], which will be discussed later. These viruses primarily target the respiratory system. Depending on the area affected, infections are categorized as either upper respiratory tract infections (URTI) or lower respiratory tract infections

(LRTI) (**Figure 1.1**). The LRTI are typically more severe, as they may cause inflammation of the bronchi and result in breathing difficulties. The most common and known LRTI in children are bronchiolitis and pneumonia [4]. In contrast, URTI usually cause epiglottitis and

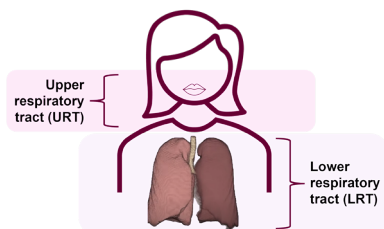


Figure 1.1. Diagram of the respiratory system, indicating the upper and lower respiratory tracts.

pharyngitis which are generally not as relentless [5]. These types of infections are particularly severe in children under five years old, whose immature anatomy and naïve immune systems struggle to combat viral pathogens [6], [7].

1.1.1. Worldwide

To provide some insight into how certain diseases strike worldwide, it was developed a practical yet devastating tool: the VizHub of the Institute for Health Metrics and Evaluation (IHME) at the University of Washington [8]. This tool graphically illustrates the impact of various diseases, including non-communicable diseases (depicted in blue), communicable, maternal, neonatal, and nutritional diseases (in red), and injuries (in green). The burden is measured in terms of years lived with disability (YLDs), disability-adjusted life years (DALYs), and deaths (**Figure 1.2**). Besides, the size of each element is proportional to the percentage of outcome they represent among the total.

It is particularly striking to observe that the highest percentage of under-five deaths attributable to communicable diseases is due to LRTIs, accounting for nearly 11% of annual under-five deaths in 2021. Fortunately, this percentage has been decreasing year by year.

Of the more than 500,000 annual deaths in children <5 years, more than 50% happen in regions of the Global South.

However, a more disheartening perspective emerges when examining the rate of under-five deaths per 100,000 population by country (U5MR). Central Africa and Southeast Asia have the highest rates of U5MR due to LRTIs (**Figure 1.2**). Consequently, of the more than half a million annual deaths attributed to LRTIs globally [6], a significant proportion occurs in these regions. These results are shattering and ethically challenging, as they suggest that LRTI deaths can be prevented in the Global North, hence they should also be preventable in these regions of the Global South.

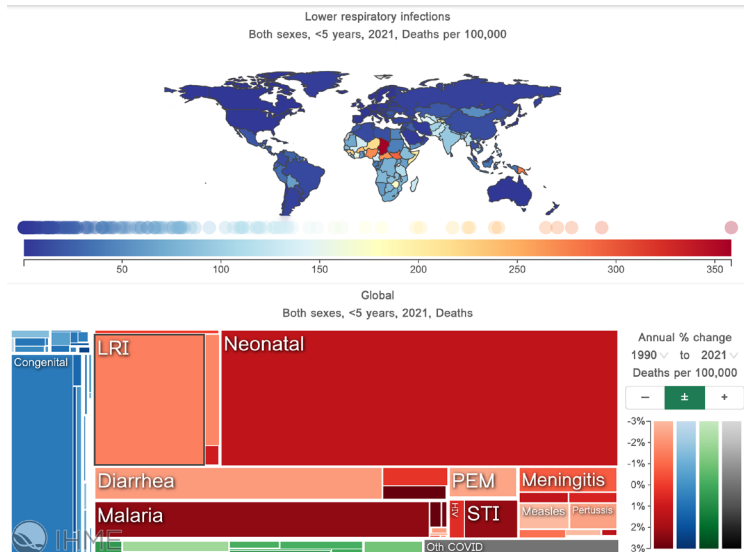


Figure 1.2. Map of lower respiratory tract infections deaths per 100,000 inhabitants; the colors represent magnitude from least (blue) to maximum (red) (**top**). Main causes of death for under-five years old children worldwide including non-communicable diseases (depicted in blue), communicable, maternal, neonatal, and nutritional diseases (in red), and injuries (in green). The size of each element is proportional to the percentage of outcome they represent from the total (**bottom**). Retrieved from Vizhub – GBD Compare [8].

Understanding these disparities is essential for critically assessing this work or any of a similar calibre. It is important to contextualize that this thesis focuses on Catalonia, a region of Spain that is part of the European Union. Given this context, we recognize that while we have a significant healthcare burden due to LRTIs and a non-negligible U5MR – ideally, this rate would be zero – we also have access to containment and prevention measures that mitigate the severity of LRTI impact on our children.

Conducting epidemiological studies that highlight the necessity, advantages, and drawbacks of these measures is crucial. Such research can inform and facilitate the gradual global adaptation of effective strategies to reduce LRTI impact and improve child health outcomes universally.

By examining the impact of these viral infections and the effectiveness of both non-pharmacological and pharmacological containment measures within Catalonia, this thesis aims to provide valuable insights that can contribute to broader efforts to address LRTIs and enhance public health on a global scale.

1.1.2. In Catalonia



Figure 1.3. Map of the Iberian Peninsula with Catalonia highlighted.

Catalonia is an autonomous community located in the north-east of Spain (**Figure 1.3**). According to the Statistical Institute of Catalonia (IDESCAT in Catalan), on 1st January 2024, the total population of Catalonia was 8,016,606 people, 15% of them being under fifteen years old [9], [10], considered children

for the Catalan healthcare system. Besides, in 2023, there were 54,182 births, following the decreasing tendency in natality that started in 2008 [11].

Limited information exists on LRTIs at a local level, and the scarce data available has been diluted amidst the plethora of articles published during the coronavirus disease 2019 (COVID-19) pandemic. Fortunately, in 2022, Vila, J. *et al.* [4] conducted a comprehensive analysis of the burden of non-SARS-CoV2 viral LRTIs in hospitalized children in Barcelona, Spain. In addition, these data can be complemented with the study of Macías Reyes, M.J. *et al.* [12] that assessed the prevalence of respiratory infections in central Catalonia.

The Vila, J. *et al.* [4] work analysed data from October 2012 to December 2020 at the Vall d'Hebron University Hospital in Barcelona (Catalonia), the largest hospital complex in the Catalan Health System, which is also a tertiary paediatric hospital dealing with around 9,200 paediatric hospitalizations per year. As they state, the hospital has 16 Paediatric Intensive Care Unit (PICU) beds that can be increased to 20 during seasonal periods and 55 in a general paediatric ward. Besides, the Vall d'Hebron University Hospital is a reference

hospital in the northern part of Barcelona's metropolitan area for the 30,508 children under 15 years old living in its surroundings.

Their study presents that 8% of the children that end up in the PICU in the Vall d'Hebron University Hospital were diagnosed with an LRTI, and yearly there are hundreds of hospitalizations due to these diseases, which cost up to €2,000,000 a year to the Catalan healthcare system, being this just a single hospital in Barcelona alone.

There are hundreds of hospitalizations yearly due to LRTI, which cost up to €2,000,000 a year for a single hospital in the Catalan healthcare system.

For central Catalonia, these numbers repeat themselves. The work of Macías Reyes, M.J. *et al.* [12] was conducted during the 2018-2020 period in the primary care centres of the Catalan Institute of Health of central Catalonia. The reference population was 523,328 inhabitants, of which 80,884 were under 15 years. In this age group, there were 110,478 visits due to respiratory infections, all of which were included in the study. Yearly, there were approximately 40,000 consultations for respiratory infections in the paediatric population. In children under one year of age, bronchiolitis predominated with approximately 25% of prevalence. This suggests that 1 out of 4 infants from 0 to 11 months of age have bronchiolitis in central Catalonia. Besides, the equivalent to half the whole population of children under 15 years old have a consultation for respiratory infections yearly.

Yearly, 1 out of 4 infants 0-11 months old have bronchiolitis (in central Catalonia).

Therefore, indeed, although in Catalonia we do not suffer the misfortune of having 11% of annual deaths due to LRTI, we do experience significant rates of illness and hospitalization. These lead to substantial economic burdens on the Catalan health system, as well as physical and emotional impacts on both patients and healthcare professionals. In fact, the long-term consequences of suffering from an LRTI during early childhood are well-documented, with

research indicating a doubled risk of both premature death from respiratory diseases in adulthood and the likelihood of developing chronic conditions such as asthma. Additionally, such early-life infections significantly increase the probability of developing recurrent episodes of wheezing, later in life [13], [14], [15].

1.2. Dynamics of viral transmission

But the question now should be, how do these numbers get that high? How is it possible for such a significant percentage of the population to contract a viral LRTI annually? Well, we find the answer in the dynamics of the airborne transmission.

1.2.1. Airborne transmission of respiratory viruses

Respiratory viruses can be transmitted via respiratory secretions. Traditional knowledge exposed that these viruses are transmitted through direct physical contact between an infected individual and an individual susceptible to infection, indirectly via contact with contaminated surfaces or objects (fomites), or directly through the air (**Figure 1.4**). However, how this transmission through the air happens has been a subject of debate. The airborne transmission used only to encompass large respiratory droplets, but the vast spread of severe acute respiratory syndrome coronavirus 2 (SARS-CoV-2) could not be explained without considering virus-laden fine respiratory aerosols that can travel long distances and that remained in the air for enough time to infect several people [16].

- **Aerosols:** particles of $<100\mu\text{m}$ exhaled by an individual, which can be infected or not. Can travel distances longer than a meter and can be suspended in air for hours. Can be inhaled.
- **Droplets:** particles of $>100\mu\text{m}$ exhaled by an individual, which can be infected or not. Can travel distances shorter than a meter, since almost immediately they fall to the ground. Can be inhaled at short range.
- **Fomites:** surfaces contaminated with viruses, where virus-laden droplets and aerosols are deposited.

The COVID-19 pandemic has significantly advanced our understanding of viral transference, providing substantial evidence for the role of aerosols in airborne transmission. Today, we can confidently include them as key factors in viral transportation, alongside droplets and fomites, thanks to the extensive research and findings of the past four years [3], [16], [17].

Chapter 1 – Introduction: Dynamics of viral transmission

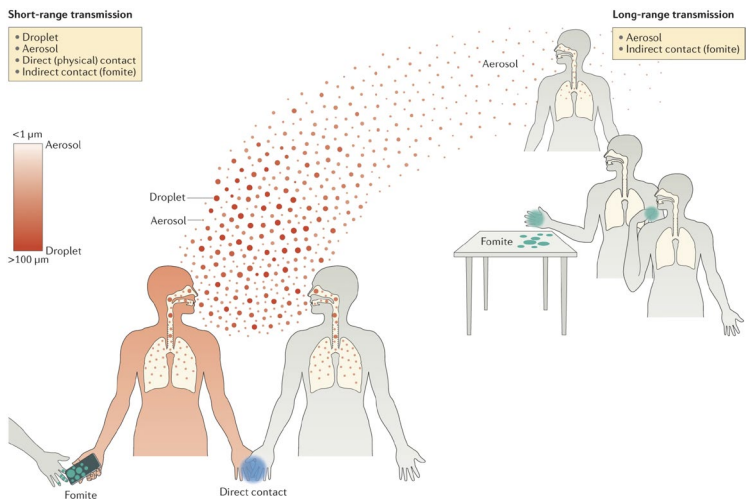


Figure 1.4. Scheme of the major modes of transmission of respiratory viruses during short-range and long-range transmission. Retrieved from Leung, N. [3].

Individuals can exhale particles of varying sizes depending on the type of respiratory activity they are engaged in. During actions such as sneezing or coughing, large droplets are expelled, which can settle on the mucous membranes of the eyes, nose, or mouth of nearby individuals, potentially leading to transmission. Additionally, even during speaking or exhalation, smaller aerosols are released. These aerosols, due to their reduced size, are capable of penetrating deeper into the respiratory system of close contacts, increasing the potential for infection. The number and viral load of aerosols produced through speaking and other expiratory activities are much higher than those of droplets and they are small enough to remain airborne, can accumulate in poorly ventilated spaces, and are likely to be inhaled over both short and long distances. Complementary, fomite transmission can occur when these droplets and aerosols settle on surfaces, allowing viruses to be transmitted to susceptible people. This can happen when contaminated surfaces are touched, and the virus is subsequently transferred to the mucous membranes, entering later to the circulatory system [16].

Once viruses reach the potential host's respiratory tract, the individual can be infected. Nevertheless, it is important to note that infection does not necessarily lead to disease. Infection occurs when the viruses enter to the circulatory system and begin to replicate. Disease, which is only developed by a certain proportion of infected people, occurs when the cells are damaged as a result of infection, and signs and symptoms of an illness appear. The immune system can prevent disease by effectively fighting off the infection [18], [19].

Infection does not necessarily lead to disease.

But, why do viruses disrupt our cells? A virus is, essentially, a simple structure composed of nucleic acid – either DNA or RNA – encased in a protein shell, and sometimes enveloped by fatty substances known as lipids. In the extracellular state, a virus is inert, lacking the necessary components for reproduction. Upon entering a host cell, the virus becomes active, using the cell's metabolic machinery to replicate itself. The viral replication cycle begins with the binding of an infectious virion to a host cell surface receptor, facilitating attachment and entry. Once internalized, the virion disassembles into its genome and associated proteins. Using a mix of viral and host proteins, the virus transcribes, translates its genes, and replicates its genome. Newly synthesized genomes are then packaged into virus particles, which mature, traffic to the cell surface, and are ultimately released as infectious virions [20]. This release process can result in the virus either bursting out of the host cell breaking it or budding off from the cell membrane, which means that the virus exits the cell by forming a small bud from the cell membrane, which then separates from the cell to release the virus so that they can continue infecting cells and reproducing. This mechanism is highly efficient for viral replication and transmission, ensuring that the virus can spread without being easily contained. Importantly, the disease we experience is not just due to the destruction of cells but also largely from the immune system's inflammatory response. The body detects the viral presence and initiates a defence, often resulting in systematic symptoms such as fever and fatigue. These symptoms, triggered by the immune system, are responsible for much of the discomfort we feel during an infection.

Respiratory viruses, in particular, often induce mild symptoms, which enable infected individuals to remain mobile and socially active, facilitating the viruses' transmission to new hosts and ensuring its continued replication [21]. This mild symptomatology is advantageous for the viruses' spread, as it promotes ongoing contact between individuals. In that way, respiratory viruses stimulate the production of excess nasal secretions by activating the host's immune response, which increases mucus production to trap and expel the virus. Additionally, these viruses can irritate the mucosal lining, triggering reflexes such as sneezing or coughing. These reflexes generate airflows that scatter fluid – composed of both virally infected and non-infected cells – into small airborne droplets and aerosols. The forcibly expelled droplets and aerosols are then released into the surrounding air, where they can be inhaled by other potential hosts, facilitating further transmission of the virus. But similarly to how infection does not necessarily lead to disease, the transmission of a virus from one person to another is not guaranteed. The likelihood of infection depends on various factors, including the viral load in the different-sized exhaled particles, susceptibility to infection of close contacts, the dose-response relationship for each virus, i.e., the probability of infection given exposure to a certain number of virions through a particular exposure route, and the stability and transmission efficiency of the virus in the surrounding environment. These factors are collectively influenced by the virus and host characteristics, but also environmental conditions such as humidity, temperature, airflow, ultraviolet (UV) radiation and ventilation [3], [16], [18], [19].

Viral determinants of transmission

The transmission and survival of viruses are determined by key structural and functional components of their internal and external structures and genomic content. One of the primary factors is the presence of a viral envelope and capsid. The capsid, a protein shell encasing the viral genome, plays a crucial role in maintaining viral stability under various environmental conditions. Its structure not only ensures protection for the nucleic acid but also contributes to the virus' capacity to withstand harsh external conditions until it reaches a suitable host. Moreover, modifications in the surface proteins of the envelope are of great significance. These proteins determine the viruses' binding

specificity and affinity to host cell receptors, directly influencing the site of infection and the viruses' capacity to infect specific cell types. Additionally, surface proteins can facilitate the formation of viral aggregates, which might enhance viral infectivity by shielding the virus from host immune defences and aiding in transmission [3], [16], [21].

As for the internal structure's role in viral transmission, one might particularly focus on the viral genome and associated proteins. Densely packaged viral genomes confer added stability to the virus, making it more resilient in environments where it might otherwise degrade. Internal viral proteins, especially polymerases, play an essential role in viral replication. These polymerases are enzymes responsible for replicating the viral genome, and they are often host-adapted, meaning they evolve to operate efficiently within the specific cellular environment of the host organism. This host adaptation is a significant advantage for the virus, as it allows for rapid and efficient replication once inside a host cell, thus supporting the production of new virions. Host-specific adaptations of polymerases are observed in many RNA viruses, including influenza and coronaviruses, where errors introduced by RNA polymerase during replication contribute to the genetic diversity and mutation rates of the virus.

Surface proteins determine the viruses' binding specificity, while internal proteins affect their mutation rate and host adaptability.

This allows the virus to evade the host immune system and adapt to new hosts, further enhancing its transmission potential. In this regard, the viral genome itself is a key factor in viral adaptation and evolution. Genetic mutations within the viral genome can lead to significant changes in viral behaviour, including increased adaptability to new hosts. These mutations may enhance viral fitness, allowing the virus to evade the immune system or adapt to different environmental conditions, thereby facilitating more effective transmission and long-term survival. Thus, the viral genome, along with its structural and functional components, represents a dynamic system that ensures the virus' evolutionary success in a wide range of hosts and conditions [3], [22], [23], [24].

Environmental determinants of transmission

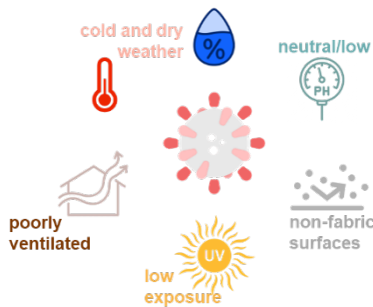


Figure 1.5. Environmental determinants that contribute to viral transmission.

Environmental factors play a critical role in modulating the transmission dynamics of respiratory viruses by influencing both viral survival and host response. For instance, temperature, humidity, airflow, and UV radiation can significantly impact how long respiratory viruses remain infectious after

being expelled into the environment [3] (Figure 1.5). A poorly ventilated space can withhold aerosols in the air for almost three times longer than in well-ventilated environments, and in spaces with no ventilation, aerosol suspension can extend up to ten times longer [25]. After some time in the air, the virus-laden particles fall to the ground or different surfaces, where fomite transmission can occur. Evidence suggests that some fabrics (contaminated plastic, stainless steel, copper, and/or cardboard material surfaces) may facilitate transmission better than others for some viruses [26], [27], [28] such as SARS-CoV-2, for which it has been reported that the virus remains infectious for more than 72h in polyester but up to 48h or 66h less in cotton and polycotton respectively. For the respiratory syncytial virus (RSV), it has been described to remain activated on the skin for up to 25 minutes, on rubber gloves for more than 1h and in clothing gowns for 30-45 minutes. On non-fabric surfaces, the virus can persist for several hours. Other viruses often exhibit even longer survival times, although some of them are not affected by surface type, like influenza. This evinces the key role that UV radiation and pH have on viral inactivation. Studies have shown that high levels of UV radiation effectively inactivate viruses, while most viruses thrive in acidic pH environments and are inactivated in basic or alkaline conditions [29], [30], because an alkaline pH can disrupt viral protein structures or interfere with the virus' ability to attach to host cells, rendering it inactive. However, it has to be considered that all these factors are influenced

by temperature and humidity. Lower temperatures tend to prolong the survival of many viruses, whereas higher temperatures generally reduce their viability. The relationship between humidity and viral persistence is complex and variable. Some studies [31], [32], [33] suggest an inverse correlation between relative humidity and virus survival, while others report a U-shaped relationship [34], [35], where both very low and very high humidity levels can support viral persistence. Additionally, seasonal patterns of viral transmission differ across climates. In temperate regions, influenza transmission generally peaks during cold, dry winter months, whereas in tropical regions, it is more prevalent in humid, rainy seasons. These variations likely result from a combination of factors, underscoring the intricate interactions between viruses and environmental conditions.

Temperature and humidity also contribute to viral infection by altering the oral mucosal protection of the potential host [36], [37]. A consistently moist environment with high humidity can encourage the growth of harmful bacteria and fungi, the perfect environment for viral replication too. On another hand, cold and dry climates can lead to dehydration of the oral mucosa, reducing saliva production and causing dryness. Saliva is crucial for maintaining oral health because it contains antimicrobial enzymes, acid neutralising substances, and proteins that help protect and repair the mucosal surface. When saliva production decreases, these protective functions are weakened, making the mucosa more vulnerable to infection and irritation. Additionally, rapid changes in temperature can cause microdamage to the mucosal tissues, creating openings where pathogens can enter. Most importantly, environmental conditions can also influence human behaviour, particularly in Catalonia, where we increase indoor crowding during colder months or rainy days, which facilitates closer contact between individuals and enhances viral transmission.

Host determinants of transmission

By now, we have learned the environmental and virus' characteristics that draw viral transmission of respiratory viruses. However, to develop a comprehensive understanding of viral transmission, it is essential to consider host-specific determinants, as these factors play critical roles in shaping the dynamics of both the infectors (individuals transmitting the virus) and the infectees (those susceptible to infection). Host-related factors can modulate key aspects of the transmission process, including the efficiency of viral replication, the magnitude and duration of viral shedding, the anatomical sites of viral entry and exit, and the immune response [3]. Consequently, these determinants have a profound influence on the likelihood of transmission and the pathways through which respiratory viruses are disseminated (**Figure 1.6**).

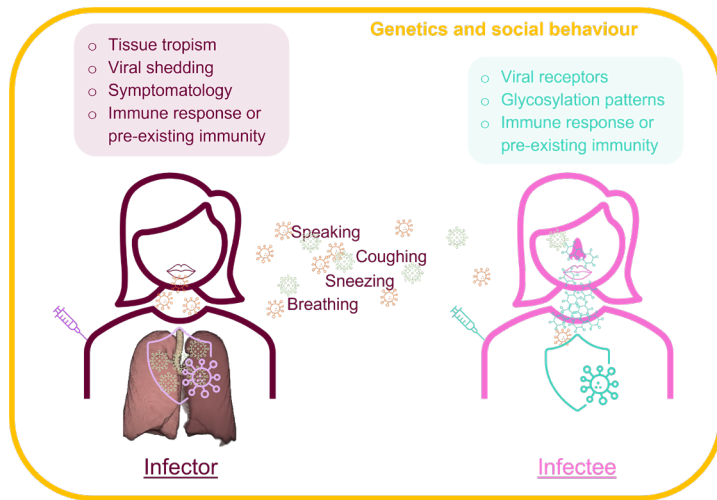


Figure 1.6. Scheme of the main host determinants of transmission.

Viral shedding, defined as the release of virus-laden particles from the host, is fundamental to contagiousness. High levels of viral excretion from the nasal or throat mucosa in the URT are particularly effective in driving transmission via respiratory droplets and aerosols, which are the primary vehicles for spread. Notably, asymptomatic individuals can shed virus at levels comparable to symptomatic ones, contributing to silent transmission [38]. This complicates

epidemic control efforts and increases the likelihood of widespread outbreaks. The variability in shedding and aerosol production between individuals is thought to drive superspreading events, where a single individual disproportionately infects many others. Besides, the immune status of the infector – shaped by prior infections, vaccination history, or partial immunity – can influence the level and duration of viral shedding. Individuals with partial immunity often shed virus at lower levels, reducing their transmissibility. Thus, we can highlight the dual role of vaccination: not only it prevents disease but also limits the spread of viruses within populations.

A key factor in viral transmission is tissue tropism, influencing both the ability of the infector to shed the virus and the susceptibility of the infectee to become infected. This term describes a virus' preference for specific tissues or cell types for replication. For respiratory viruses, the replication site within the respiratory tract significantly shapes viral shedding pathways and transmissibility. Viruses with broader tissue tropism, which allows replication at multiple sites, can facilitate expulsion from both the upper and lower respiratory tracts, thereby increasing their potential for widespread transmission. This ability to productively infect various tissues stems from a complex interplay between the virus and the host [20].

Tissue tropism influences both the ability of the infector to shed the virus (multiple site replication) and the susceptibility of the infectee to become infected (viral receptors).

The importance of tissue tropism extends to the infectee, particularly in the expression of viral receptors. The presence and density of these receptors are critical for a virus' ability to establish infection. Respiratory viruses typically gain entry through mucosal surfaces in the respiratory tract by binding to specific receptors. For example, SARS-CoV-2 uses the angiotensin-converting enzyme 2 (ACE2) receptor [39], while rhinovirus targets the intercellular adhesion molecule 1 (ICAM1). The distribution of these receptors along the respiratory tract influences not only the site of initial infection but also the severity of disease outcomes. For instance, although aerosols predominantly deposit in the lower

respiratory tract due to their small size, SARS-CoV-2 usually initiates infection in the nasal cavity, where ACE2 expression is highest [3]. Additionally, host cell N-glycosylation patterns, including glycan structures, can modulate viral entry. N-glycosylation refers to the attachment of glycans – complex carbohydrate molecules with a protective function – to the asparagine (N) residues of proteins, and this process is vital for proper protein folding, stability, and cellular localization. Glycan structures formed through N-glycosylation may either facilitate or inhibit viral binding, depending on their composition and distribution along the respiratory tract. For many viruses, including respiratory pathogens, these glycans serve as co-receptors or enhance the accessibility of primary receptors, affecting which cells within the respiratory tract are most susceptible. Such receptor specificity ultimately determines both the infection's location within the host and the dominant transmission routes (e.g., airborne, droplet, or fomite) in different scenarios [40].

Furthermore, host genetics can play a role in modulating the severity of infection, but its influence on transmissivity is less clear. Some evidence suggests that genetic factors could affect the expression of viral receptors or the immune response to infection, thereby influencing how easily an individual can transmit the virus. However, more research is needed to fully understand the genetic determinants of viral transmissibility. Nevertheless, what is clear is that social behaviours and contact patterns significantly affect transmission dynamics. Heterogeneous social contacts, such as age-related mixing patterns, can determine the likelihood of transmission between different groups. The structure of social networks is also important. While dense, overlapping networks in workplaces or households promote rapid transmission, sparser networks or bubble-like contact groups serve as a protective measure by limiting the number of interactions and reducing the likelihood of infection transmission. This characteristic of social networks was particularly important in containing the spread of SARS-CoV-2 during the pandemic [3].

In addition to network structure, several behavioural factors also influence transmission risk. Practices such as handshaking, saluting with kisses as we do in Catalonia, mask-wearing, and mobility patterns significantly impact how a

virus spreads through a population. However, it is important to note that we are unlikely to limit our social interactions to inhibit viral spread in the long term. Instead, the host's immune response is the heavy driver of protection against epidemics. An infection may either be productive – leading to the generation of progeny viruses and subsequent spread – or abortive, where replication is blocked, and the infection does not progress. The latter is different from pre-existing immunity and can happen due to various factors, such as strong intracellular immune responses or the virus lacking essential factors for replication in that particular cell type. All in all, the outcome of infection is largely determined by the host's immune system, which mounts a defence against the virus.

1.2.2. The immune system response

The human immune system can be compared to a sophisticated medieval castle, complete with layered defences, responsive guards, and an evolving strategy for repelling invaders. Understanding its operation requires a view not only of its biological components but also its dynamic, system-level behaviour. From a physics perspective, the immune system is a remarkable example of signal detection, amplification, and feedback control, ensuring effective protection against pathogens while minimising collateral damage to the host.

The first line of defence in our body is the innate immune system (IIS). Much like a castle's outer walls, the IIS is the body's first barrier against invading pathogens such as viruses. This layer of defence is rapid, generalised, and always on alert. It is also non-specific; it is not precise in response to certain pathogens. It operates using pattern-recognition receptors (PRRs), which could correspond to motion detectors embedded in the castle's walls, that sense common features of invaders. For respiratory viruses, the most important are toll-like receptors (TLRs), which detect conserved molecular patterns on pathogens, like viral RNA or proteins. In mammals, TLRs are a family of 15 unique receptors expressed by different cell types. TLR3, TLR7 and TLR9 are particularly important in respiratory viral infections (RVIs) as they recognize products of viral replication. On the other hand, TLR4, for example, is key for the identification of RSV, as it identifies its fusion protein F [41], [42].

Dendritic cells (DCs) are also a vital component of this front-line defence. DCs are strategically positioned throughout the respiratory tract, residing beneath and within the conducting airway epithelium and in the alveolar walls. This placement enables them to sample antigens across both the upper and lower respiratory tract. These diverse cells not only detect invaders but also orchestrate the broader immune response [43], [44].

Once an invader is detected (by TLRs, DCs, etc.) the system triggers an alarm signal, releasing molecules such as cytokines, chemokines, and interferons. These signalling molecules alert nearby cells and recruit immune cells like neutrophils and natural killer (NK) cells to the site of infection. Neutrophils, the castle's infantry, engage in a fast but indiscriminate attack, while NK cells are the elite shock troops targeting infected cells. This stage operates like a feedback-driven emergency response, amplifying the defence where the threat is detected [41]. The IIS prioritises speed over precision, ensuring that most threats are neutralised early at minimal energy cost.

The innate immune system provides the fast action, while the adaptive immune system improves the specificity of the response.

The second line of defence in this castle of our immune response is the adaptive immune system (AIS). If the pathogen breaches the outer defences, the AIS is mobilised. This system functions like the castle's strategists and elite guards, offering a slower but highly specialised response. For that, the AIS relies on antigen presentation, where cells display fragments of the pathogen to T and B cells, triggering a highly specific immune response. The highlight of the AIS is that it also has a memory function, recording the details of past infections, enabling faster and more efficient responses to familiar pathogens. Vaccines, for example, leverage this memory, preparing the immune system in advance without requiring actual infection [42], [44].

- **Cytokines:** the castle's messengers, rapidly delivering orders to mobilise the immune system's defences. These secreted proteins have vital roles in growth, differentiation, and activation, regulating the intensity and type of immune response. They ensure that the castle's defenders (immune cells) are properly directed to the site of invasion and coordinate their efforts.
- **Chemokines:** the castle's signal flares, guiding reinforcements to where they are needed most. These proteins direct immune cells to specific tissues or locations, orchestrating a targeted response. When an external pathogen enters the body, chemokines create a beacon, ensuring our defences converge on the site of intrusion incisively.
- **Interferons:** the castle's alarm bells, raised at the first sign of an attack. Interferons are also proteins, secreted to alert neighbouring cells of the presence of a viral invader, instructing them to fortify their defences. By inducing an antiviral state, interferons ensure that the cells become harder to penetrate, slowing the advance of the viral infection and giving the immune system time to mount a coordinated counterattack.
- **T cells:** the castle's knights, patrolling the land and neutralising any invaders. These immune cells have specialised roles:
 - Helper or CD4+ T cells serve as commanders, coordinating the defence secreting cytokines and activating macrophages.
 - Cytotoxic or CD8+ T cells are the elite warriors, directly attacking infected cells – that they recognize thanks to their T cell receptors – to halt the spread of the virus. Some become memory T cells, ensuring they can rapidly respond if the same pathogen returns.
- **B cells:** the castle's alchemists, crafting antibodies that act like enchanted arrows, precisely locking onto the invader pathogen, neutralising their ability to spread, or marking them for destruction by cytotoxic T cells and others.

Based on Commins, S. et al. [45]

From a physics perspective, the immune system is a dynamic network where the innate and adaptive systems operate in parallel and feedback-driven loops, ensuring an optimised defence response. The IIS is broad-spectrum and energy-efficient, like an early warning system detecting generic patterns, while AIS is high-precision, but its response requires more time and resources [45].

Additionally, the immune system's ability to regulate its response, i.e., escalating during infection and de-escalating once the threat is resolved, demonstrates a homeostatic feedback loop. This is vital since dysregulated immune responses can lead to collateral damage in host tissues, primarily through inflammation and cellular injury. In the context of LRTI, the recruitment of inflammatory cells in response to signals from infected epithelium exacerbates oedema, vascular congestion, and tissue swelling. These pathological changes further narrow the already compromised airways, particularly in smaller bronchi and bronchioles, causing e.g., bronchiolitis in children. The accumulation of oedematous fluid and mucus in these airways severely obstructs airflow to distal alveoli, hindering effective gas exchange. Moreover, increased intravascular pressure promotes the leakage of fluid into the airspaces, enhancing the obstruction. As these factors converge, the restricted airways may become occluded by clots and plugs, culminating in clinical symptoms such as wheezing and dyspnoea. In severe cases, this progressive respiratory compromise requires oxygen therapy to maintain adequate oxygenation [43], [44].

Recent research has elucidated the connection between such inflammation and disruptions within the gut-lung axis, a bidirectional relationship of the interplay between gut microbiota and pulmonary immunity. The RVIs, such as those causing LRTI, can induce significant gut dysbiosis characterized by a reduction in beneficial microbes and an increase in pathogenic species (**Figure 1.7**), being this the reason behind RVIs also causing digestive symptoms. This dysbiosis amplifies systemic inflammation by diminishing protective microbial metabolites, such as short-chain fatty acids (SCFAs), which are vital for mitigating inflammatory responses.

Reduced SCFA levels impair type I interferon signalling, which we saw it is a critical mechanism for antiviral defence, and exacerbate inflammatory complications observed in conditions like bronchiolitis [46], [47], [48], [49]. Conversely, the bidirectional nature of the gut-lung axis implies that exploring therapeutic interventions targeting this axis – such as probiotics, prebiotics, or microbiota-focused treatments – offers a promising pathway to modulate inflammation, restore microbial homeostasis, and potentially improve recovery in RVIs. These interventions represent an emerging area of focus that could redefine strategies for managing both gut and lung health in the context of systemic inflammation [46], [47], [48].

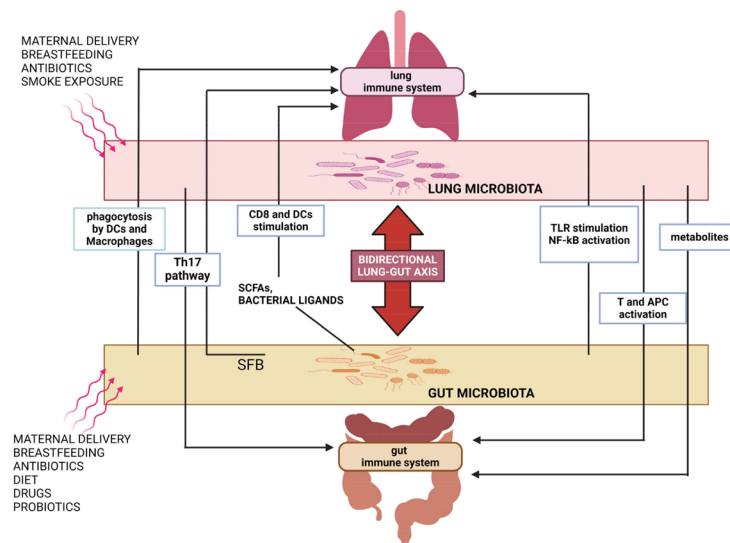


Figure 1.7. Schematic representation of the main interactions underlying the gut-lung axis. Gut microbiota and microbial metabolite stimulate and promote the differentiation of Helper T cells. Moreover, the gut microbes enter the intestinal mucosa and may be phagocytosed by antigen presenting cells (APCs), DCs, and macrophages. Travelling to the lung, APCs stimulate T cells and lung immune responses. On the other hand, the lung microbiota exhibits similar effects influencing the immune system and homeostasis of the gut. Retrieved from Marella, V. et al. [49].

1.3. The Catalan healthcare system

In Catalonia (and all Spain), healthcare is universal and free, ensuring that any resident seeking healthcare is entitled to receive it without financial burden.

The healthcare services available in Catalonia are organized into several care lines to address different aspects of health and wellbeing [50], [51]:

- ❖ Primary and community care: the basic care, providing general medical, paediatric, and nursing care, as well as health promotion and disease prevention programs. Primary care practices (*centres d'atenció primària*, CAPs; PCPs in English) are the first point of contact for most health concerns and manage most non-specialized healthcare needs. In rural areas, these centres are called local consults (*consultoris locals*, CL).
- ❖ Specialized and hospital acute care: for conditions requiring specialized medical expertise or inpatient care, there are hospitals and specialized outpatient clinics. This includes access to advanced diagnostics, surgical services, and multidisciplinary care teams of different medical specialties.
- ❖ Sociosanitary care: this sector integrates healthcare and social services to provide support for individuals with chronic illnesses, disabilities, or dependency. It includes home-based care, palliative care, and long-term institutional care for vulnerable populations.
- ❖ Mental health and addictions care: specialized mental health services, addiction treatment programs, and community-based support for individuals with psychological or psychiatric needs.
- ❖ Continuous and urgent care: this covers emergency services that ensure 24/7 access to medical attention for urgent health concerns, including emergency departments (ED) in hospitals and ambulance services, but also some PCPs that include urgent care.
- ❖ Pharmaceutical care: network of pharmacies to dispense medications, with partial or full reimbursement for prescriptions covered under the public healthcare system.

- ❖ Telephone and online assistance: digital health platforms and hotlines that provide immediate guidance for minor health concerns, appointment scheduling, and health information.
- ❖ Complementary services: including diagnostic imaging, laboratory services, and programs of rehabilitation from injuries.
- ❖ Other services: very specialized care units, such as maternal and child health services, geriatric care, and preventive health initiatives.

Hence, the first step for the parents of a sick child would be to contact the corresponding PCP to seek basic paediatric attention. If the child's symptoms evolve to more severe presentations, such as wheezing and respiratory distress, the paediatrician would refer the child to hospital care. In cases where the health condition escalates urgently, the parents may go directly to the ED of a hospital, where the child would likely be admitted for further care.

Healthcare in Catalonia is territorially organised into sanitary regions (*Regions Sanitàries*). Several reforms were made regarding these regions and subsequent centres in Catalonia. The most recent, in 2023, implied the establishment of ten sanitary regions (**Figure 1.8**), comprising Alt Pirineu i Aran, Lleida, Camp de Tarragona, Terres de l'Ebre, Catalunya Central, Girona, Barcelona City, Northern Metropolitan Barcelona, Southern Metropolitan Barcelona and Penedès [52].

Catalonia is organised in districts called *comarca*, a similar territorial division to the *counties* of England. Each sanitary region comprises several districts or *comarques*, which in turn are made of multiple municipalities. In each of these sanitary regions, there are basic health areas (*Àrea Básica de Salut*, ABS) through which primary health care services are organised. The ABS are territorial units formed by neighbourhoods or districts in urban areas, or by one or more municipalities in rural areas. Each PCP is under control of one of those ABS, that act as the foundational unit for primary care services. There is at least one PCP per municipality. The Department of Health of the Catalan government has enabled a tool to search which PCP is closest to your address [53].

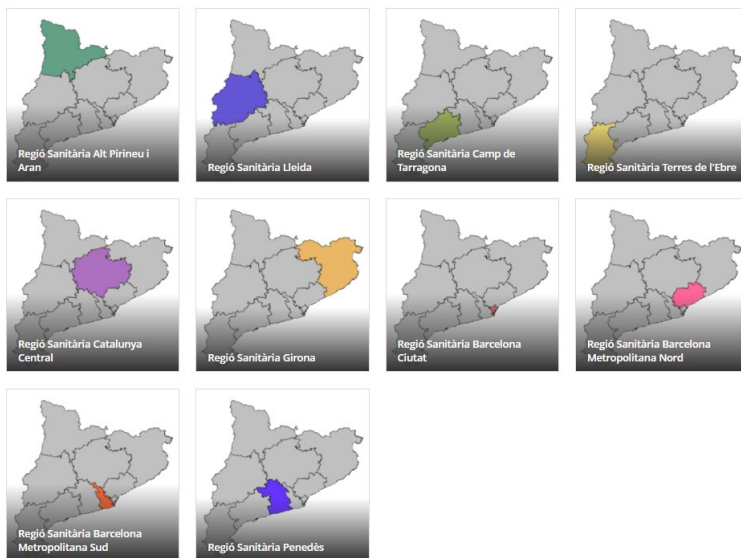


Figure 1.8. Catalan sanitary regions. Retrieved from [52].

Regarding hospital care, emergency services are available at any hospital, ensuring immediate attention regardless of location. However, for scheduled specialized or outpatient visits, patients are generally referred to the hospital closest to their municipality to streamline access and optimize resource allocation.

Once the territorial organization of healthcare is clear, the following question arises: who is responsible for providing these healthcare services? In Catalonia, healthcare services are delivered by the Catalan Health Service (*Servei Català de la Salut*, CatSalut). The CatSalut has evolved through historical reforms, notably influenced by the Spanish Constitution of 1978 and the Statute of Autonomy of Catalonia in 1979, which decentralized healthcare responsibilities to the Catalan government. In the 1990s, the passage of the Catalan Healthcare Organization Act (*Llei d'Ordenació Sanitària de Catalunya*, LOSC) further formalized this system. Although complex, CatSalut is just an administrative organization, enforcing the mandates of the health department and in charge of emphasizing universal coverage, integrated healthcare services, and the

equitable distribution of resources across territories [51], [54]. CatSalut manages several healthcare networks that provide services to different parts of Catalonia, whether they are private or public, or private with public services (e.g., certain vaccines).

A central pillar of this system is the Catalan Healthcare Institute (*Institut Català de la Salut*, ICS), the largest public healthcare provider in Catalonia. The ICS manages more than 289 primary care teams (*equips d'atenció primària*, EAP) – which are the professionals working in a PCP – and three large high-tech tertiary hospitals (Vall d'Hebron, Bellvitge and Germans Trias), four regional referral hospitals (Arnaud de Vilanova in Lleida, Joan XXIII in Tarragona, Josep Trueta in Girona and Verge de la Cinta in Tortosa) and one regional hospital (Viladecans). It operates alongside other public and private providers within the principal healthcare network of Catalonia that CatSalut administers, called the integral sanitary system of public usage of Catalonia (*sistema sanitari integral d'utilització pública de Catalunya*, SISCAT). In fact, the private healthcare sector is an integral component of Catalonia's mixed healthcare model, operating in coordination with public services. Private providers participate in the SISCAT, sometimes delivering services funded by the public system through agreements and contracts with CatSalut. This arrangement enables private entities, including hospitals, diagnostic centres, and specialized clinics, to complement public healthcare services and address patient demand efficiently [51], [54], [55].

However, the private healthcare sector also operates independently, providing services to individuals with private health insurance or those choosing to pay out-of-pocket. As a result, certain patient data, including vaccination records and disease incidence, may not be fully accessible to public health services.

In 2008, CatSalut allocated a budget of €1,250 per person annually, which decreased to €1,150 by 2013. This amount saw a modest recovery, reaching €1,186 in 2019. Following the COVID-19 pandemic and the revised budget for 2023, the per capita allocation increased significantly to €1,502.10, reflecting the heightened demand for healthcare resources and services [54], [56], [57], [58].

1.3.1 Catalan databases

Open data initiatives are a cornerstone of Catalonia's government commitment to transparency and public information access, as outlined in the Open Government Plan 2017-2018. These data are available to the public through the Generalitat's – the name of the government in Catalonia – Open Data Portal [59], [60], that serves as a centralized platform aggregating all publicly available datasets from its various governmental bodies. These datasets are provided in reusable formats, such as CSV and XML, designed for integration into external programs and applications. Some of the public datasets available and that are of interest for this thesis are those of primary care daily syndromic diagnoses of respiratory diseases, as well as rapid antigen test (RAT) results for certain respiratory viruses, gathered by the information system for surveillance of infections in Catalonia (SIVIC) [61]. SIVIC extracts the data from the primary care clinical history (PCCH), and all public healthcare centres in Catalonia use the same PCCH. Another important database for this thesis is the data on meteorological variables all across Catalonia provided by the network of automatic meteorological stations (*xarxa d'estacions meteorològiques automàtiques*, XEMA) [62], that gives information on meteorological station and different variables such as temperature or relative humidity. Other interesting data that are available under demand are these included in the minimum basic data set (*conjunt minim bàsic de dades*, CMBD) [63], which comprise diverse causes hospitalizations data and associated severity, for instance. In addition, sociodemographic data from the Catalan population is available thanks to the IDESCAT [64].

Nevertheless, these data are not always available daily and frequently suffer from delays that can significantly impact analyses performed with them. For instance, SIVIC is updated weekly on Wednesdays – although daily data can be provided upon request – but diagnoses reported during the last three days are typically incomplete. In fact, electronic medical records and diagnostic reports are only considered consolidated 30 days after the date of entry [65]. Additionally, the data often exhibit a weekly reporting pattern, with case counts on Mondays typically doubling those reported over the weekend, and similar

patterns observed around holidays [66], [67]. Consequently, data obtained from these kinds of repositories must undergo pre-processing prior to analysis.

Several other public organizations provide public data on healthcare, economic development, socioeconomic factors, etc. But there are also some smaller entities providing data under demand. An example of particular interest for this thesis is the COPEDICAT research group.

COPEDICAT research group

The research group COPEDICAT (Coronavirus Pediatría Catalunya) was established during the COVID-19 pandemic under the management of PhD. MD. Antoni Soriano Arandes, to investigate the impact of the disease on children and their role in the transmission of the virus. This initiative brought together a wide range of healthcare institutions and research groups to ensure a coordinated and comprehensive approach to studying paediatric COVID-19 cases. Beyond its clinical focus, COPEDICAT emphasizes the integration of research and healthcare, working as a multidisciplinary team in close collaboration with the computational biology and complex systems (BIOCOM-SC) research group at the Universitat Politècnica de Catalunya (UPC) and the Agency for Health Quality and Assessment of Catalonia (AQuAS).

The COPEDICAT network comprises numerous healthcare centres across Catalonia, including hospitals, primary care units, and specialized paediatric teams. Among its hospital members are the Hospital Universitari Vall d'Hebron in Barcelona – together with its microbiology and immunology teams – as well as Hospital Universitari Dexeus, Hospital General de Granollers, Hospital Universitari d'Igualada, Hospital Universitari Arnau de Vilanova de Lleida, Althaia Xarxa Assistencial Universitària de Manresa, Espitau dera Val d'Aran, Hospital Universitari del Mar, Hospital de Mataró (part of the Consorci Sanitari del Maresme), Fundació Hospital Sant Joan de Déu de Martorell, Hospital Universitari Sant Joan de Reus, Hospital Joan XXIII Tarragona, Hospital Josep Trueta Girona, Hospital General Universitari de Vic, Hospital Pius de Valls, Hospital Mútua de Terrassa, and the Consorci Corporació Sanitària Parc Taulí de Sabadell.

In addition, the network includes specialized paediatric territorial teams, such as Equip Territorial de Pediatría de l'Alt Penedès, Equip Territorial de Pediatría del Garraf, Equip Territorial Pediatría Sabadell Nord, and Equip de Pediatría dels Pirineus, Alt Urgell i Pallars. Primary care units also play a crucial role in COPEDICAT's operations, including ABS Almacelles, ABS Les Borges Blanques, ABS Pla d'Urgell, ABS Seròs, CAP Les Hortes, CAP Rural Sud-Granadella, CAP Bordeta-Magraners, CAP Cappont, CAP Mont-roig del Camp, CAP Llibertat, CAP Marià Fortuny, CAP Remei, CAP Onze de Setembre, CAP Sant Quirze, EAP Vic Nord, EAP Vic Sud, EAP Baix Berguedà, EAP Manlleu, EAP Ripollet, EAP Poble Nou, EAP Polinyà, EAPT Horta-Carmel-Sant Rafael, and EAPT Drassanes.

COPEDICAT provided vital patient-level data, encompassing not only clinical and diagnostic variables but also sociodemographic factors that were particularly relevant for understanding the dynamics and infection characteristics of specific diseases. The data collected by COPEDICAT was meticulously designed to enable well-defined studies on COVID-19 and other respiratory illnesses. These comprehensive datasets included unique insights into population characteristics, such as the number of cohabitants and household size, which would have otherwise been difficult, if not impossible, to analyse.

1.4. Epidemiological models

Given the significant burden of LRTIs in Catalonia and globally, and the availability of comprehensive and accurate data on respiratory diseases alongside other relevant variables, coupled with teams of professionals dedicated to analysing such data, the next step is to explore the mathematical tools employed to study these epidemiological datasets. These tools, known as mathematical models, provide a framework for applying a physics-based perspective to the study of diseases.

Mathematical models allow us to represent a simplified version of a part of reality in a simulated environment, enabling the investigation of disease mechanisms and the prediction of their evolution. In other words, mathematical models are tools that physicists use to address specific questions about reality in a controlled environment after formulating a set of hypotheses and choosing relevant variables. We rely on a set of equations that can be adjusted to fit real data or whose parameter values can be derived from empirical knowledge. Once these equations are calibrated, we can simulate a specific situation or scenario, such as the evolution of a disease, and modify them as needed to reflect changes in the system being studied.

These models can operate at different scales, depending on the nature and scope of the available data. At a microscopic level, models can simulate how a disease interacts with the human body, elucidating its physiological effects. At a macroscopic level, they can model the dynamics of disease spread and impact within populations. This versatility makes mathematical modelling an invaluable approach for understanding and addressing complex epidemiological challenges. And precisely depending on the nature of these challenges, we classify mathematical models as empirical or mechanistic.

1.4.1. Empirical models

Empirical models are primarily statistical tools designed to analyse and describe patterns in surveillance data without explicitly incorporating the underlying biological, social, or behavioural mechanisms. They are useful to deal with large volumes of data to detect patterns, predict outcomes (for example, new

diagnoses), and evaluate temporal changes in disease incidence or prevalence [68]. While these approaches are powerful for short-term forecasting, they often lack the ability to generalize to novel scenarios, such as the emergence of new variants of a virus or the implementation of new public health interventions. For instance, an empirical model might detect and be able to reproduce a seasonal pattern in number of diagnoses but would not explain whether this pattern arises from changes in human behaviour, meteorological factors, or pathogen biology. This lack of mechanistic insight constrains the model's ability to provide actionable guidance for public health decision-making, while still being a very powerful forecasting tool.

Despite these limitations, empirical models play a crucial role in epidemiological research and public health. Their simplicity and computational efficiency make them invaluable for real-time monitoring and surveillance, particularly in rapidly evolving situations like infectious disease outbreaks, as demonstrated during the COVID-19 pandemic, where numerous research was focused on predicting new cases using this kind of models [67], [69], [70]. Furthermore, they can complement mechanistic models by providing robust statistical frameworks for parameter estimation or hypothesis testing.

The choice to use empirical models should depend on the research question and the context of the analysis. When the goal is to quickly assess trends or make short-term predictions, empirical models offer an accessible and effective solution. However, for a deeper understanding of the drivers of disease dynamics or the evaluation of intervention strategies, they are often most effective when combined with mechanistic models that explicitly incorporate the processes governing disease transmission and progression.

**Empirical models are quick and effective for short-term forecasting
but fail to provide a deeper understanding of the system.**

Empirical models in infectious disease research can be broadly divided into two categories: traditional models and artificial intelligence (AI)-based models. Among the traditional approaches, the Gompertz and logistic models hold a

prominent place due to their ability to capture the growth dynamics of epidemics.

The logistic model [71], [72], [73], [74], [75] is a sigmoidal growth curve that describes how a population evolves over time, assuming that the rate of growth is proportional to both the existing population size and the remaining capacity for growth. It is widely used for its interpretability and effectiveness in modelling idealized epidemic curves. However, its assumption of symmetry can be limiting in cases where real-world data exhibit prolonged or uneven saturation phases. When this happens, the Gompertz model, another sigmoidal function, would be the gold standard.

The Gompertz model [68], [74], [76], [77], [78], [79] also describes how a population evolves over time, but starting with exponential growth before gradually slowing as it approaches a plateau or stationary state:

$$N(t) = K \cdot e^{-\ln\left(\frac{K}{N_0}\right) \cdot e^{-a \cdot t}} \quad \text{Eq. 1.1. } \checkmark$$

Where $N(t)$ in Eq. 1.1 represents in epidemiology the cumulative new infections of a disease, K the maximum number of people infected over the course of the epidemic, N_0 the initial infections and a a parameter related to the decrease of growth rate of infections.

The specific growth rate μ of infections is derived from the first derivative of $N(t)$, it can be expressed as the relative change in infections:

$$\frac{dN(t)}{dt} = K \cdot a \cdot \ln\left(\frac{K}{N_0}\right) \cdot e^{-\ln\left(\frac{K}{N_0}\right) \cdot e^{-a \cdot t}} \cdot e^{-a \cdot t} \quad \text{Eq. 1.2. } \checkmark$$

$$\mu(t) = \frac{1}{N(t)} \frac{dN(t)}{dt} = a \cdot \ln\left(\frac{K}{N_0}\right) \cdot e^{-a \cdot t} \quad \text{Eq. 1.3. } \checkmark$$

Hence when $t \rightarrow 0$, we have the maximum growth rate:

$$\mu_{max} = \mu(t \rightarrow 0) = a \cdot \ln\left(\frac{K}{N_0}\right) \quad \text{Eq. 1.4. } \checkmark$$

Which allows us to describe the growth rate evolving in time as:

$$\mu(t) = \mu_{max} \cdot e^{-a \cdot t} \quad \text{Eq. 1.5. } \checkmark$$

Therefore, α governs the rate at which the exponential growth of infections slows down as the epidemic progresses towards its carrying capacity (K , **Figure 1.9**). The fact that the specific growth rate decreases exponentially over time is what makes the Gompertz model applicable to many different situations. In other words, it is an empirical model, but it is not merely a fit; it identifies the presence of a phenomenon whose rate of change decreases exponentially with time. This model is particularly well-suited to modelling the cumulative number of infections or deaths during an epidemic because usually the growth rate diminishes due to factors such as increasing immunity, changes in behaviour due to infection or media alert, or the impact of interventions. The asymmetry of this function distinguishes it from the logistic model and makes it a better choice to reproduce real world scenarios.

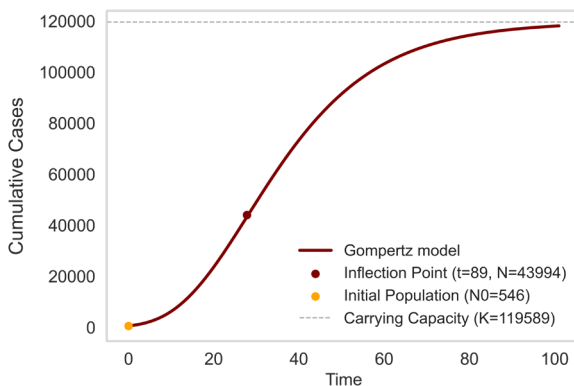


Figure 1.9. Representation of the Gompertz model.

Traditional models like these are particularly valuable because they can be applied with relatively limited data and are computationally efficient, making them practical for use in settings where resources are constrained or uncertainty is the norm, like during the pandemic. Furthermore, their parameters often have clear epidemiological interpretations, such as the maximum growth rate or the carrying capacity, which facilitate their explanation to public health managers. In contrast, AI-based models are gaining popularity due to their ability to handle large, complex datasets and capture temporal dependencies and hidden patterns in the data. This has a counterpart, that is the need for

large sets of data which are not common in epidemiological settings, at least in Catalonia, where the surveillance data begins from 2014 onwards. Besides, the COVID-19 pandemic disturbed viral synergies and stationarity rendering pre-pandemic data unreliable for understanding post-pandemic dynamics. A deep learning (DL) neural network broadly used for forecasting are long-short term memory networks (LSTMs), as they are a type of recurrent neural network (RNN) that retains information over long sequences, enabling them to predict disease dynamics accurately in scenarios with intricate temporal patterns, such as varying transmission rates or non-linear intervention effects, in which traditional models might be less reliable [80], [81], [82], [83], [84]. But their *black box* nature often limits interpretability, making it difficult for researchers and policymakers to understand the underlying mechanisms driving predictions. For public health managers, acting on recommendations derived from such opaque systems can be daunting, as decision-making requires trust in methodologies that may not be easily explainable. Despite these limitations, AI models, including LSTMs, are increasingly being combined with traditional approaches to enhance their predictive power while maintaining interpretability [85], [86]. Still, empirical models, whether traditional or AI-based, often fall short in providing a deeper understanding of the underlying epidemiological processes driving disease dynamics. Their focus on statistical relationships, rather than biological mechanisms, limits the interpretability of their results in a real-world public health context.

1.4.2. Mechanistic models

Mechanistic models play a key complementary role. They can explicitly incorporate known epidemiological mechanisms, such as transmission rates, recovery rates, and population structures, as well as additional covariates like behavioural components, preventive measures, or meteorological factors, offering a more structured framework for understanding and interpreting disease dynamics.

Mechanistic models offer deeper system understanding by incorporating underlying processes but are often more complex.



Figure 1.10. Scheme of how an agent-based model (ABM) categorises population.

Two common approaches to mechanistic modelling are compartmental models, such as SIR (Susceptible-Infectious-Recovered) and agent-based models (ABMs) [87]. While compartmental models study populations

macroscopically, dividing them into compartments of different characteristics, ABMs are more microscopically oriented, labelling each individual of a population instead (**Figure 1.10**). This is what is called a bottom-up approach, so that the actions and interactions of individual agents are simulated to study the whole population evolution. This allows for the model to capture unique attributes and behaviours and to be highly granular and stochastic, hence detecting heterogeneities in populations and easily adding confounders, introducing variations in contact patterns, compliance with interventions, or movement dynamics. ABMs are particularly advantageous for exploring scenarios with complex dynamics, such as localized outbreaks, the impact of targeted interventions, or the effects of network structures on transmission [88], [89], [90], [91]. However, a major limitation of ABMs is their reliance on a deep understanding of transmission dynamics and risk factors, as well as the need for extensive individual-level data, which may not always be available. Additionally, they come with high computational costs. In contrast, while SIR-like models are still mechanistic, they do not have such stringent requirements.

Thus, for a broader overview of epidemic trends, we can rely on compartmental models. In epidemiology, these models are based on dividing the population into homogeneous compartments, representing distinct disease states. For instance, the SIR model categorises the population in three groups: susceptible, infected, and recovered (SIR). If we take into account that infected individuals are susceptible individuals that become exposed to the pathogen and then might become infected, then we add another compartment with exposed

people, hence having a SEIR model (**Figure 1.11**). This particular model is the one that will be employed in this thesis. The flow of individuals between the determined

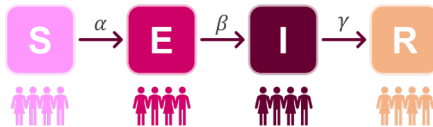


Figure 1.11. Scheme of how a Susceptible-Exposed-Infected-Recovered (SEIR) model categorises population.

states is described using a system of ordinary differential equations (ODEs), which govern the transitions between compartments based on parameters such as transmission and recovery rates. Similar to the Gompertz model, these equations are adjusted to fit observed infection data, yet the mathematical framework is more complex. The ODEs that describe the SEIR model are expressed in **Eq. 1.6** to **Eq. 1.10**:

$$S_0 = f \cdot N \quad \text{Eq. 1.6. } \checkmark$$

$$\frac{ds}{dt} = -\alpha SI \quad \text{Eq. 1.7. } \checkmark$$

$$\frac{dE}{dt} = \alpha SI - \beta E \quad \text{Eq. 1.8. } \checkmark$$

$$\frac{di}{dt} = \beta E - \gamma I \quad \text{Eq. 1.9. } \checkmark$$

$$\frac{dR}{dt} = \gamma I \quad \text{Eq. 1.10. } \checkmark$$

Where f is the fraction of people susceptible to be infected, N the total number of inhabitants of the population, α is the transmissivity rate, β is the inverse of the incubation period of the virus and γ the inverse of the recovery ratio from the infection.

The SEIR model provides a structured framework for studying infectious disease dynamics and enables the derivation of fundamental epidemiological metrics, essential for understanding disease transmission and guiding public health interventions, such as the basic reproduction number, the effective reproduction number, or the critical vaccination coverage [92], [93], [94], [95], [96].

- **Basic reproduction number (R_0):** estimates how many people one infected individual can transmit the disease to in a fully susceptible population → $R_0 = \frac{\alpha}{\gamma}$
- **Effective reproduction number (R_{eff}):** adjusts R_0 considering that some individuals in the population may already be immune or that control measures are in place → $R_{eff}(t) = R_0 \cdot f \cdot \frac{S(t)}{N}$, where f is a contact reduction factor and N the considered population.
- **Critical vaccination coverage (V_c):** defines the proportion of the population that needs to be immunized to stop disease spread →

$$V_c = 1 - \frac{1}{R_0}$$

1.5. Aim, approach, and outline of this thesis

The aim of this PhD thesis, under the sponsoring of **Fundació La Marató de TV3**, is to characterize and understand the dynamics of the most prevalent RVI in childhood in Catalonia along the last decade, exploring specific factors and interventions for SARS-CoV-2, RSV and influenza. Specific objectives are:

- O1** To define epidemiological indicators and thresholds for the surveillance and early detection of respiratory diseases in Catalonia, with special focus on the paediatric population.
- O2** To describe and analyse changes in the epidemiological patterns of respiratory viral infections in children before, during, and after the COVID-19 pandemic, through prospective monitoring and dynamic modelling.
- O3** To analyse pre-pandemic data on RSV and influenza epidemics in children in Catalonia using empirical epidemiological models (based on the Gompertz equation) to describe their epidemic dynamics.
- O4** To develop compartmental epidemiological models for influenza, incorporating meteorological factors as potential modulators of transmissivity.
- O5** To assess the predictive performance of the models at short- and mid-term and their potential application in public health monitoring and response systems.
- O6** To analyse the epidemiological characteristics and impact of multisystem inflammatory syndrome in children associated with SARS-CoV-2 in Catalonia.
- O7** To evaluate the role of the paediatric population as a sentinel group for detecting and anticipating respiratory virus epidemics in the general population, particularly during the COVID-19 pandemic.
- O8** To assess the role of children in the transmission dynamics of seasonal influenza epidemics in Catalonia.
- O9** To analyse the epidemiological impact of new immunisation strategies for RSV in children in Catalonia, through statistical analysis and dynamic modelling approaches.

Outline

This thesis is about the mathematical modelling and analysis of dynamics of different respiratory viral infections in children. To be able to cover such an ample topic, we have structured the thesis into 6 chapters. **Chapter 1** has been the introduction, where we have presented the concepts, methods and data behind this thesis, and that concludes with this section. In **Chapter 2**, we cover surveillance and general dynamics (specific objectives 1 and 2) of the viral infections of study, to provide a general basis from which to proceed. This chapter is based on peer-reviewed publications XII and XXII (see **Scientific Work**). We then focus on each virus of study for **Chapter 3**, **Chapter 4** and **Chapter 5**, which correspond to SARS-CoV-2, influenza and RSV, respectively.

Starting with SARS-CoV-2 specific questions (specific objectives 6 and 7), in **Chapter 3** of this thesis we include peer-reviewed publications XVI to XX (see **Scientific Work**). Afterwards, we delve into the influenza specific questions (specific objective 8), explored in the **Chapter 4** of this thesis. And, finally, we conclude the viral chapters with RSV specific questions (specific objective 9) in the **Chapter 5** of this thesis, in which we cover peer-reviewed publications III, VIII and XIII (see **Scientific Work**).

As part of the RSV specific objective 9, with regards to the impact of nirsevimab, a short research stay was carried out at the Catalan Healthcare Institute's primary healthcare services information system (SISAP, in Catalan), under the supervision of MD. Ermengol Coma, to work with electronic health records from both primary and hospital care covering the entire Catalan public healthcare system.

In addition to this, **Chapter 4** and **Chapter 5** comprehend predictive modelling for RSV and influenza analyses (specific objectives 3, 4 and 5), based on our peer-reviewed methodology in publication X and reports XXIV to XXVIII (see **Scientific Work**) and currently under peer-review.

Last but not least, **Chapter 6** serves as a closure for this thesis, with a final discussion and specific conclusions from these years of research.

Chapter 1 – Introduction: Aim, approach, and outline of this thesis

Table 1.1 shows the outline of this thesis, gathering the objectives that are addressed in each chapter together with the corresponding publications.

Table 1.1. Summary of the outline of this thesis with each chapter linked to its corresponding specific objectives and publications.

Chapter	Specific objectives	Publications
<i>Chapter 1. Introduction</i>		
<i>Chapter 2. Surveillance</i>	O1, O2	XII, XXII
<i>Chapter 3. SARS-CoV-2</i>	O6, O7	XVI to XX
<i>Chapter 4. Influenza</i>	O3, O4, O5, O8	X
<i>Chapter 5. RSV</i>	O3, O4, O5, O9	III, VIII, X, XIII
<i>Chapter 6. Conclusions</i>		

Chapter 2

Indicators and surveillance

*"Tot canta o brunz en el món
sa cançó misteriosa;
tot és un concert immens
per qui no té ànima sorda."*

Caterina Albert

*L*s the reader must know, the shadow of the great plague of SARS-CoV-2 is slowly fading, and thus a new chapter begins. With it, the reader must cast their gaze upon the other familiar yet elusive maladies that once plagued the children of our lands. These afflictions, which had retreated in the wake of the terrible scourge, now return—yet they are not as they once were, for they have been transformed, wearing new and unfamiliar faces. In the coming pages of our tale, the reader shall embark upon a journey to uncover how we keep vigilant watch over these astute viruses and the ailments they birth, and how we might craft new and powerful indicators to gauge the state of epidemics—shielding our realm from the unseen forces that threaten its peace.

In this chapter we will discuss the current viral landscape and introduce epidemiological indicators and surveillance tools based on the following published and peer-reviewed articles:

Scientific work article XII: Perramon-Malavez, A., *et al.* Frontiers in public health. 2024.

Scientific work article XXII: Perramon-Malavez, A., *et al.* Enfermedades Emergentes. 2023.

2.1. The *tripledemy*

In March 2020, Catalonia – in fact, all Spain – stopped. The Spanish government declared the state of alarm, enforcing a strict lockdown that initially confined the population to their homes for two weeks, later extended to two months [97], [98]. This was the first of many non-pharmaceutical interventions (NPIs) implemented to control the spread of SARS-CoV-2. Following the lockdown, additional measures such as curfews, mobility restrictions, school closures, social distancing, and mandatory mask use were enforced. While these interventions were highly effective in reducing COVID-19 transmission, they also had unintended consequences on the circulation of other respiratory viruses [99], [100].

Respiratory infections such as influenza and bronchiolitis, which typically exhibit well-defined seasonal patterns, were significantly disrupted by the widespread implementation of NPIs. The drastic reduction in social interactions, enhanced hygiene practices, and school closures led to an almost complete suppression of these diseases during the 2020-2021 season (Figure 2.1). However, as NPIs were gradually lifted and social mixing resumed, the viruses behind these infections re-emerged, fuelled by a population with waning immunity due to prolonged periods of low exposure [101]. This progressive resurgence led to a new epidemiological phenomenon, the continuous, and still in a transitory state, co-circulation of SARS-CoV-2, influenza, and RSV – the main cause of bronchiolitis [102], [103] –, which we refer to as the *tripledemy*. These dynamics can be seen represented in Figure 2.1 for the paediatric population (<15 years), using the data extracted from SIVIC and population data from IDESCAT to compute disease incidence (cases per 100,000 population).

Incidence of disease is defined as reported cases per 100,000 population.

The period represented in the figure states for the COVID-19 pandemic period described in Spain, from March 2020 to July 2023 [104], with a few months margin for further insight on the influenza-bronchiolitis synergy.

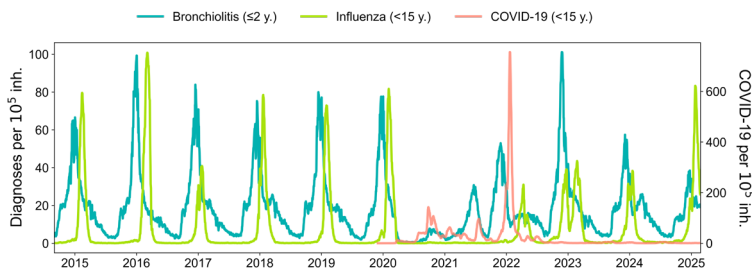


Figure 2.1. Evolution of COVID-19 (coral), influenza (green) and bronchiolitis (teal) incidence dynamics from September 2015 to February 2025.

Before the COVID-19 pandemic, influenza and RSV followed predictable seasonal patterns, with a well-established seasonal synergy between bronchiolitis and influenza. However, the introduction of SARS-CoV-2 disrupted this equilibrium, fundamentally altering the dynamics of respiratory virus transmission. This disruption shifted the system from a stationary state into a transitory phase, where the previous seasonal synergy could no longer occur under the same conditions. As a result, the three viruses began to co-circulate in an unpredictable manner, leading to overlapping and sometimes prolonged epidemic waves.

This shift has created persistent healthcare challenges, as the once-stable seasonal cycles have given way to a more complex and volatile viral landscape. It is expected that the system will eventually reach a new state of stationarity, but the timing and characteristics of this equilibrium remain uncertain. As of February 2025, incidences in children of SARS-CoV-2 after the Omicron subvariant arose have been neglectable, while influenza and bronchiolitis have been slowly returning to pre-pandemic dynamics, although the latter has been recently affected by the introduction of an immunoprophylaxis antibody against RSV called nirsevimab in October 2023 in Catalonia [105], [106], which will be discussed further on this thesis. The current state of this *tripledemy* and the historical synergy of bronchiolitis and influenza can be observed in [Figure 2.2](#), an ampliation of the data on [Figure 2.1](#).

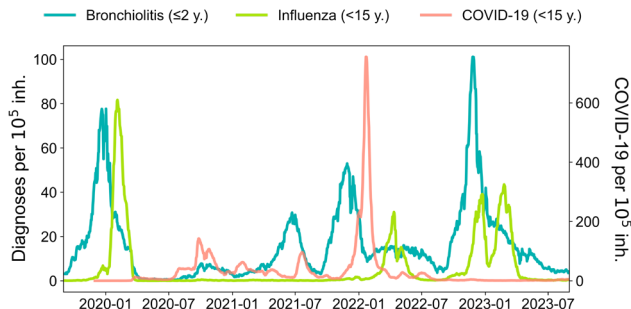


Figure 2.2. Evolution of COVID-19 (coral), influenza (green) and bronchiolitis (teal) incidence dynamics from September 2019 to August 2023, containing the COVID-19 pandemic period March 2020 to July 2023.

Since August 2022, COVID-19 infections in children have been sporadic. However, some circulation of SARS-CoV-2 likely continues, potentially going underdiagnosed. As discussed in the previous chapter, COVID-19 symptoms have become less specific and can easily be mistaken for influenza or other RVIs unless confirmed by diagnostic testing. As introduced in [Section 1.3.1](#), in primary care settings, paediatricians often use RATs to diagnose children with RVI symptoms. These tests screen for adenovirus, SARS-CoV-2, RSV A and B, and influenza A and B. However, testing practices vary. Although a testing protocol was established in 2020 [107], its current implementation depends largely on individual paediatricians' criteria. Consequently, children with mild symptoms may not be tested or even brought to primary care by parents, introducing a potential bias when analysing clinical diagnosis data.

For this reason, [Figure 2.3](#) is provided. It illustrates the testing and positive cases per 100,000 inhabitants for SARS-CoV-2, influenza viruses A and B, RSV A and B, and adenovirus from the introduction of RAT in Catalonia through to February 2025. Notably, the magnitude of the data in this figure differs significantly from that in [Figure 2.2](#), despite both representing the same population, the children in Catalonia. This discrepancy arises because only a small percentage of symptomatic cases are actually tested, highlighting the limitations in surveillance data. Additionally, clinical diagnosis data are more stochastic and exhibit greater variability because multiple viruses or pathogens

can cause similar symptoms. This overlap contributes, for instance, to the plateaus observed for bronchiolitis in [Figure 2.1](#) and [Figure 2.2](#). These plateaus occur because not all bronchiolitis cases are caused by RSV; instead, the overall epidemic represents a combination of smaller overlapping waves from various pathogens. Moreover, some bronchiolitis cases may result from less seasonal pathogens, leading to sporadic occurrences that further influence the overall trend. This complex interplay of multiple viral agents contributes to the distinct epidemic patterns seen in the data, not only for bronchiolitis but for any other disease reports.

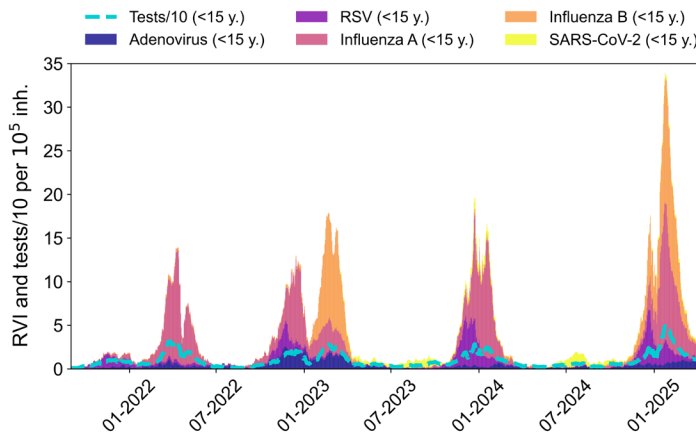


Figure 2.3. Evolution of rapid antigen tests scaled by 10 (dashed blue), adenovirus (navy), RSV (purple), influenza A (pink), influenza B (orange) and SARS-CoV-2 (yellow) incidence dynamics from January 2021 to February 2025.

This evolving epidemiological scenario and the difference between data sources highlight the critical need for adaptive surveillance systems and modelling tools, predictive or not. By better understanding and anticipating viral interactions and epidemic patterns, these tools can help optimise vaccination strategies and support public healthcare management in the coming seasons.

2.2. Epidemiological indicators

One of the epidemiological tools that we have for surveillance are indicators. But what do we mean by *indicators*? In epidemiology, indicators are measurable variables that provide valuable information about the state and dynamics of a disease within a population, even about its evolution. They are essential for monitoring, assessing, and predicting health trends, enabling public health officials and researchers to make informed decisions.

Organizations like the Centre for Disease Prevention and Control (CDC) of the United States (US) and the European Centre for Disease Prevention and Control (ECDC) monitor incidence alongside other indicators, such as cumulative hospitalization incidence, deaths, and paediatric deaths, to track diseases like influenza [108], [109], [110].

- **Incidence:** occurrence of new cases within a specific population and timeframe, often expressed as $Incidence = 100,000 * \frac{new\ cases}{population}$.
- **Prevalence:** occurrence of total number of existing cases within a specific population and timeframe.
- **Mortality rate:** quantifying the rate of deaths over a certain period, thus related to severity of illness.
- **Hospitalization and intensive care admission:** monitoring severe cases that require hospital care and healthcare system burden.
- **Testing rates:** quantifying the number of tests per inhabitant and timeframe, including positivity rates for specific viruses ($Positivity = 100 * \frac{positives}{tests}$), that track viral circulation and disease transmission.
- **Reproductive number:** defining the average number of secondary infections generated by an infected individual, it provides insight into disease transmissibility and the potential for epidemic growth.
- **Growth rate:** relative change in cumulative infections from one week to the next, provides complementary information to the reproductive number regarding epidemic growth.

The ECDC also monitors laboratory data to detect circulating virus variants and uses sentinel groups to estimate epidemic incidence levels across different countries [111], [112]. By analysing these indicators, public health agencies can identify potential outbreaks and monitor the progression of a disease over time, as was demonstrated crucial during the COVID-19 pandemic.

Epidemic indicators are therefore vital for guiding public health surveillance and response strategies. Some of them are computed empirically, while others are estimated from model parameters, such as the reproduction number, but hence they require further mathematical expertise.

2.2.1. Semi-empirical risk panel to monitor epidemics

To assist in the allocation of health resources and to offer direct knowledge of the current and short-term expected disease burden we defined a set of semi-empirical indicators to assess the risk level of seasonal respiratory epidemics in Catalonia but translatable to the whole world, based on both incidence and their dynamics, and considering epidemic thresholds. This risk evaluation system has been published [66] and builds upon a previously developed method for monitoring COVID-19 [113]. By limiting the use of complex models, we strived to provide a practical and effective tool for public health surveillance and decision-making, especially straightforward for those professionals without expertise in mathematical epidemiological modelling.

Methods

We used publicly available data from SIVIC [61] on daily clinical diagnoses of influenza for the whole Catalan population and bronchiolitis in children less than 2 years old, from September 1st, 2011 to March 31st, 2023. Previous studies showed that SIVIC data are a good proxy of the epidemiological dynamics of respiratory diseases like influenza, because their results have been representative of laboratory confirmed diagnoses and sentinel systems but entail a shorter delay [114]. We used data from children ≤2 years for assessing bronchiolitis because this disease mainly affects this age group. Otherwise, influenza is not only focused on a determined age group and can have an impact among the general population. To use the data, first we needed to pre-

process it. Every time we used SIVIC data of influenza or bronchiolitis for analysis throughout this thesis, we followed the same pre-processing strategy, as described in Perramon-Malavez, A *et al.* [66] and summarized below. We divided the data pre-processing into three different stages: two of *nowcasting* and one of smoothing. The first *nowcasting* approach is to account for the delayed notification or report in medical databases, while the second one is to consider the differences in data reporting (i.e., influenza cases) depending on whether the day of the week is a working day or a holiday. Finally, to the pre-processed data we performed a smoothing 7-day moving average.

Nowcasting delayed reporting or notifications

There is a well-described problem when working with medical diagnostic databases, the data are constantly being updated and the true number of infections for a certain day cannot be verified after some time. The global agreement is to use these data after one month since being reported once it has been consolidated [115]. In this regard, we had been downloading the SIVIC database each week since the beginning of 2021. We performed a week-to-week comparison of the daily reports in the different databases and ascertained that while records were generally coherent after 30 days from their entry, the most recent registers were still being updated. With a retrospective analysis, we intended to define the percentage of data completion for the last 30 entries in the database and use them to weight the data into a more accurate approximation of the real number of cases.

Since the reporting methods in Catalan healthcare have changed substantially during the last years, we focused our process only in the datasets downloaded in mid-October, November, and December 2022, because we considered them as consolidated (more than three months before the end of the study period), and their reporting pattern was closer to the ongoing one than that of 2021. We decided to take records after 30 days from entry as ground truths and iteratively compute the percentage of completion of each day from October to December 2022, ending up with thirty 30-last days iterations. Thereafter, we averaged the results to obtain the mean percentage of completion per each of the days, which we named *reporting weights*:

$$\omega_j = \frac{c_i}{c_{i+30}}, \text{for } i = 1, \dots, 30 \text{ days, for } j = \text{day 1, \dots, day 30} \quad \text{Eq. 2.1.} \quad \checkmark$$

$$\text{reporting weights} = \overline{\omega_r} = \frac{\sum_{j=1}^{30} \omega_j}{N_{\text{repetitions}}}, \text{for } j = \text{day 1, \dots, day 30} \quad \text{Eq. 2.2.} \quad \checkmark$$

In Eq. 2.1, ω_j states for the normalized percentage of completion, C_i is the number of cases reported in a day and C_{i+30} the number of cases reported for the same day but 30 days later. The *reporting weights* in Eq. 2.2 ($\overline{\omega_r}$) are constructed as the average ω_j for all iterations performed. In our case, $N_{\text{repetitions}} = 30$ since we started computing ω_j from 20/10/2022 to 20/11/2022 and ended at the iteration from 20/11/2022 to 20/12/2022.

Finally, we estimated the daily cases for the last month since the day the data is downloaded from SIVIC as:

$$C_i^{(i)} = \frac{c_i}{\overline{\omega_r}}, \text{for } i = 1, \dots, 30 \quad \text{Eq. 2.3.} \quad \checkmark$$

In Eq. 2.3, $C_i^{(i)}$ states for the estimated diagnoses in the 30 days previous to the last update of the database. Former works share this approximation [67], [113], [115].

To end the pre-processing and smooth the data of bronchiolitis infections, we apply to $C_i^{(i)}$ a cumulative 7-day moving average filter, while the influenza series undergo the weekly pattern correction detailed in the next subsection.

Nowcasting weekly patterns

SIVIC data followed a weekly pattern, as reported in the article [66]. However, bronchiolitis cases usually follow a highly stochastic nature thus their pattern of report is not stable nor avoidable. Hence, this approach can only be applied when an evident pattern is present like in the influenza diagnoses.

We labelled every day in the study period as Monday (1), Tuesday (2), Wednesday (2), Thursday (2), Friday (2), Saturday (3), Sunday (3) or Holiday (3) as stated by the working calendar in Catalonia for each year. Therefore, we created three groups of days, the regular working days from Tuesday to Friday, the weekends and festivities when the healthcare centres only attend

emergencies, and Mondays when all non-urgent cases occurring in weekends are finally attended. In addition, days after a festivity are labelled as Mondays (1) to capture the same effect as described.

Afterwards, we took daily windows of 7-days from the start to the end of the study period and computed the weights per type of day as the difference between the raw number of diagnoses reported in SIVIC and the daily filtered number of diagnoses with a 7-day moving average (MM7), that is:

$$\delta_j = \frac{C(j)}{CMM7(j)}, \text{for } j = 1,2,3 \quad \text{Eq. 2.4. } \checkmark$$

In Eq. 2.4, δ_j are the weights computed for Mondays, regular workdays and weekends and festivities in a certain 7-days window. C states for the raw daily reports in SIVIC and CMM7 for the 7-day moving mean of C. The (j) indicates that to compute a certain weight, we only consider the cases of its kind. We saved all the iterative computations per type of day and graphically observed a time-varying pattern in which stochasticity was reduced when epidemic peaks were reached. Therefore, we took the weights per kind of day as the median among the intervals in which the values were more stable, which were detected with a signal processing algorithm detecting local maxima. We decided to take the median value instead of the average to account for instability.

However, we wanted to account for the stochasticity present in the data. Hence, instead of using a constant weight value we used a random Gaussian distribution in which the aforementioned computed weights are the mean of the distribution, but its standard deviation is inversely proportional to the recorded number of diagnoses. Consequently, the more daily cases, i.e., the closer to the epidemic peak, the more the final weight resembles the average. Besides, we only apply this modification when CMM7 are over 100 influenza infections, a threshold fixed empirically, since the fluctuations when there are few infections are very high and applying the weights to that data may detriment them.

Finally, we applied the weekly reporting pattern to the daily estimated diagnoses $C_i^{(i)}$ that we already computed in order to obtain more balanced data:

$$D = \frac{c_i^{(i)}}{\delta_j}, \text{ for } i = \text{days in the study period and } j = 1, 2, 3 \quad \text{Eq. 2.5.} \checkmark$$

In Eq. 2.5, D represents the final weighted diagnoses. We based this approach on the work of Català, M. et al. [67], [113] and Villanueva, I. et al. [79]. Further information can be found in [66]. To end the pre-processing and smooth the data of influenza infections, we apply to D a cumulative 7-day moving average filter.

Epidemic levels

To define epidemic levels, we employed a novel approach based on the Moving Epidemic Method (MEM) which is used in European institutions such as the ECDC [116], [117]. But first, we needed to compute the weekly incidence for each disease and set an epidemic threshold from which to compute these stages.

From the pre-processed dataset, we measured the weekly incidence of bronchiolitis and influenza computing the number of daily diagnoses per 10^5 population (≤ 2 years and all Catalonia respectively) and resampling them to weekly frequency. To determine the start of the epidemic, we used the first derivative of daily diagnoses. The first derivative represents the rate of change of the number of reported cases with respect to time. By looking at a certain value of the derivative, we can identify the day when the number of reported cases started to increase rapidly. We set this value to a three-fold increase in the number of reported cases over a single day. We then looked for the number of cases reported that day from 2011 to 2019 and averaged them. The exclusion of pandemic years is deliberate to avoid skewing the result. Once we found the epidemic threshold, we selected the epidemic as the first and last days when we are over this boundary.

With the epidemic delimited, we computed an average epidemic among the pre-pandemic ones and calculated the 25th, 50th, 75th and 95th percentiles of cases. The number of cases up to the threshold represent the basal level of the epidemic, from the threshold to the 25th percentile correspond to a very low level of the epidemic, from the 25th to the 50th percentile indicates a low level, from

50th to 75th signifies a medium level, from 75th to 95th represents a high level and above the 95th constitutes very high epidemic levels. Since with this method we obtained epidemic thresholds for weekly incidence, we divided the values obtained by 7 to also have the daily incidence levels.

Epidemic indicators

In our semi-empirical risk panel, we used three different epidemic indicators: the daily incidence of disease, the weekly growth rate, and the effective potential growth (EPG) [113]. All of them are computed from the pre-processed datasets. All analyses were done using Python and R.

Daily incidence

To calculate the daily incidence of bronchiolitis and influenza, we took the daily number of diagnoses weighted and filtered with a cumulative 7-day moving average and computed cases per 100,000 population. The population was considered constant intra-yearly but variable inter-annually.

Weekly growth rate

To assess the weekly growth rate, we first needed to define weekly incidence as previously explained, resampling daily incidence to weekly frequency. With this, we defined weekly growth rate as the percentage of more (or less) cases that a week reports compared to the previous week:

$$\mu_j = \frac{\varphi_j}{\varphi_{j-1}}, \text{for } j = \text{all weeks in the study period} \quad \text{Eq. 2.6.} \checkmark$$

In Eq. 2.6, μ_j stands for the weekly growth rate, obtained from φ_j that represents the weekly incidence of disease in a certain week. The higher the weekly growth rate, the faster the disease is spreading.

Effective reproduction number

The effective reproduction number (R) is an estimation of the average number of infections produced by a single infected individual over their infectious period. It is computed taking into account the generation time, which is defined as the average interval between the infection of an individual and the infection of its

secondary cases. It usually corresponds to the incubation period. For influenza, the generation time is between $\gamma = 2$ and $\gamma = 6$ days [118]. For bronchiolitis, the generation time is in the order of $\gamma = 5$ days [119]. This index is usually computed through the equations of mathematical mechanistic models such as the SIR model, as anticipated in previous sections. However, it has undergone several redefinitions to enable alternative (rough) estimations without detailed knowledge of specific disease characteristics or the need to solve complex equations [94], [95], [120]. When the effective reproduction number has temporal resolution, it can be used to predict disease dynamics and evolution. An $R>1$ means the number of new infections is increasing while $R<1$ indicates that the new infections have decreased over the generation time.

For our particular study case, we defined a semi-empirical reproduction number (ρ_γ), as the ratio of new cases with respect to cases γ days ago, with γ the most contagious period of the disease that also corresponds to the time between cases, and filtered with a 3-day moving mean:

$$\rho_\gamma^i = \frac{D_{i-1} + D_i + D_{i+1}}{D_{i-\gamma-1} + D_{i-\gamma} + D_{i-\gamma+1}}, \text{ for } i = 1, \dots, N \text{ days} \quad \text{Eq. 2.7.} \checkmark$$

In Eq. 2.7 the semi-empirical reproduction number is presented, with N the number of days of the study period, D the filtered and pre-processed diagnoses either of bronchiolitis (Eq. 2.3) or of influenza (Eq. 2.5), and $\gamma = 5$ both for bronchiolitis and influenza. We decided to use $\gamma = 5$ for influenza after analysing the robustness of the results obtained for $\gamma = 2$ to $\gamma = 6$ days, which is the interval that literature proposes as time between infections. Since the resulting ρ_γ , especially for bronchiolitis, were strongly fluctuating, we decided to apply a 7-day moving mean filter to smooth the effects of the stochasticity of certain diagnostic reports.

From all possible estimations of the reproduction number, we decided to use the semi-empirical ρ_γ , from now on ρ_5 , (Eq. 2.7) due to its simplicity.

Effective Potential Growth

The EPG hereby is based on the one defined for COVID-19 [113]. EPG is an epidemic index that combines the incidence level and the incidence trend into

a single parameter, and it has shown to be a useful risk indicator for the monitoring of COVID-19. In this work, we defined it as the product of the daily 7-day cumulated incidence of infections (A_7) by the semi-empirical reproduction number (ρ_γ). Since the time $t = 7$ for A_7 , and the generation interval are different, the reproduction number has to be corrected as Gostic, K.M. *et al.* [121] described:

$$\rho_{\gamma_c} = (\rho_\gamma)^{\frac{t}{\gamma}} \quad \text{Eq. 2.8. } \checkmark$$

$$EPG = A_7 \cdot \rho_{\gamma_c} \quad \text{Eq. 2.9. } \checkmark$$

We defined in Eq. 2.8 the corrected semi-empirical reproduction number, with $t = 7$ and $\gamma = 5$ in our particular case. In Eq. 2.9 we presented the EPG index as the product of A_7 and the ρ_{γ_c} , from now on ρ'_5 , afore introduced. The semi-empirical reproduction number is an estimation of how many new infections generates one infected individual. EPG amplifies or narrows the weekly incidence according to whether there has been an increase ($\rho'_5 > 1 \Rightarrow EPG > A_7$) or decrease ($\rho'_5 < 1 \Rightarrow EPG < A_7$) in cases over the last γ days. In this way, the rate of growth is considered when looking at the weekly incidence of infections and we can anticipate a threshold crossing of the epidemic. Hence, the EPG can be interpreted as a forecaster of trend changes, the anticipation of which needs to be determined. However, EPG is not a predictor of incidences, but of the dynamic changes in the evolution of an epidemic, anticipating the level of risk to which we are going to be exposed. The EPG has an advantage over using ρ_5 or A_7 alone in that it is more easily interpretable for healthcare or public health professionals. It presents, in incidence terms, the effects of the reproduction number on the evolution of the epidemic. In addition, it can be combined with risk levels to provide a short-term snapshot.

Measure of anticipation

The objective of creating a monitoring and risk panel for RVIs is not only to assess the current epidemiological situation but to be able to forecast how the course of events will unfold. Subsequently, we performed a Pearson correlation analysis for EPG to determine its suitability and anticipation to the surpassing

of epidemic levels. For that, we analysed how influenza and bronchiolitis incidences correlate and what lag they have with their EPG sequences globally, for their whole series, but also for each of their seasons separately. We also looked at how many days EPG advances the different epidemic levels, computing the difference in days when a certain threshold is reached. A representation of the process is provided in the published work [66].

Results and discussion

Epidemic levels and threshold

After performing the extensive pre-processing, we obtained smooth visualizations of daily number of diagnoses of bronchiolitis and influenza throughout the study period. With them, we were able to compute daily and weekly incidence of disease, allowing us to define epidemic stages. The resulting computations of daily and weekly epidemic incidence threshold and levels for influenza and bronchiolitis are collected in [Table 2.1](#). Furthermore, weekly thresholds are represented in [Figure 2.4](#) and [Figure 2.5](#), for influenza and bronchiolitis respectively, together with their weekly incidences.

These results suggest that when we have a weekly incidence of 9/27 or a daily incidence of 1/4 for influenza/bronchiolitis, we can consider the epidemic wave to have started and we will remain at very low numbers of infections until we cross the low epidemic thresholds, after which we should already observe effects at the level of occupancy in health care facilities.

We can notice from [Figure 2.4](#) and [Figure 2.5](#) the disappearance of influenza when the COVID-19 pandemic spread in March 2020, until mid-2022 when a small epidemic occurred. Meanwhile, diagnoses of bronchiolitis were reported in winter 2020 and two consecutive relatively small epidemics in 2021, both during summer and winter, surpassing the epidemic thresholds defined but not reaching very high levels. Nonetheless, as [Figure 2.5](#) shows, the latter epidemic of bronchiolitis has been the historically greatest appearing 1 month earlier. As concerning influenza, in [Figure 2.4](#) we can ascertain that we are still moving towards a new “normal” seasonality. The latter epidemic wave of influenza was advanced also 1 month from previous seasons, and actually

consisted of two different outbreaks, the first one mainly corresponding to influenza A and the subsequent to mainly influenza B viruses [122].

Table 2.1. Epidemic threshold and levels of daily and weekly incidence for influenza and bronchiolitis diseases. Retrieved from Perramon-Malavez, A. et al. [66].

Level	Daily		Weekly	
	Influenza (diagnoses / 10^5)	Bronchiolitis (diagnoses / 10^5)	Influenza (diagnoses / 10^5)	Bronchiolitis (diagnoses / 10^5)
Threshold	1	4	9	27
Low	3	13	21	89
Medium	8	20	53	141
High	20	36	138	250
Very High	31	65	214	453

On another note, these visualizations allow us to contrast the nature of both diseases. Bronchiolitis is of a highly stochastic nature, partially because it affects a smaller population (only children) and because the disease can be caused by several viral agents creating plateaus before and after the epidemic peak, which is mostly caused by RSV. On the other hand, influenza presents a smoother signal, mainly because the number of daily diagnoses is higher [116].

Comparing [Figure 2.4](#) and [Figure 2.5](#), the distance between the low and medium epidemic thresholds is narrower for bronchiolitis than for influenza, as an effect of that previously described *plateau* present in the bronchiolitis infections data. This indicates that for bronchiolitis, the epidemic thresholds defined might only be useful from the medium threshold, when the clear epidemic wave started before the pandemic. Besides, we still have to be cautious with the levels calculated since there are still many unknowns about how future epidemics of influenza and bronchiolitis will unfold in Catalonia after COVID-19.

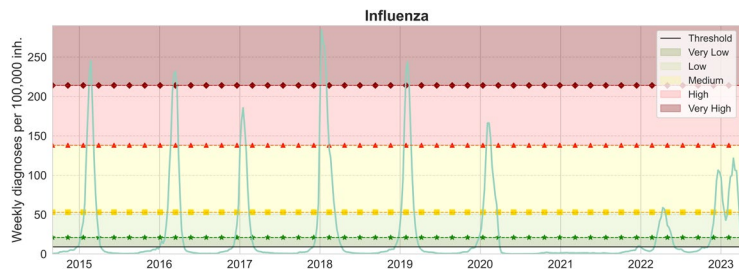


Figure 2.4. Weekly influenza cases per 100,000 inhabitants in Catalonia. From bottom to top, the epidemic threshold (black), the low (green, stars), medium (yellow, squares), high (red, triangles) and very high (maroon, diamonds) epidemic levels are also displayed. Retrieved from Perramon-Malavez, A. et al. [66].

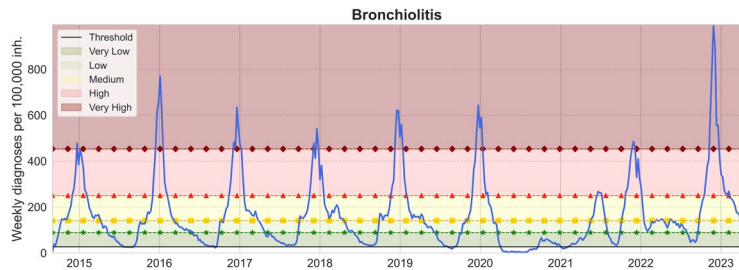


Figure 2.5. Weekly bronchiolitis cases per 100,000 inhabitants <2 years in Catalonia. From bottom to top, the epidemic threshold (black), the low (green, stars), medium (yellow, squares), high (red, triangles) and very high (maroon, diamonds) epidemic levels are also displayed. Retrieved from Perramon-Malavez, A. et al. [66].

Effective Potential Growth

With a correlation coefficient higher than 0.98, we found that the EPG anticipates weekly influenza incidence by 6 to 7 days and bronchiolitis by 4 to 5 days. It is noteworthy that the EPG effectively predicted the incidence of bronchiolitis and influenza almost a week in advance, maintaining strong correlation coefficients even during and after the pandemic. During the first epidemic following the SARS-CoV-2 outbreak, it experienced only a slight decrease in predictive ability, losing 1-2 days of anticipation. However, the 2020-2021 epidemic period should be excluded from the analysis due to the

negligible incidence of influenza and the low occurrence of bronchiolitis cases. We also looked at how many days EPG anticipates the different epidemic levels, and the results are collected in **Table 2.2**. Notice that not all columns in the table are filled. That is because not all epidemic seasons reach all the different thresholds, some of them only achieve medium levels of incidence. In addition, the robustness of EPG in influenza anticipation is palpable when compared to the results for bronchiolitis, a consequence of the nature of the data used, with much fewer daily diagnoses than influenza. Hence the bronchiolitis reports present and therefore can cause artifacts leading to less robust results, presented as >10 days. For the same reason, for bronchiolitis, only EPG anticipating high and very high risks should be considered, since lower incidences still present reporting variability that adds noise to the metric.

Table 2.2. Number of days in which EPG advances the reaching of the different epidemic thresholds with respect to A_7 . For (top) bronchiolitis and (bottom) influenza diseases. Retrieved from Perramon-Malavez, A. et al. [66].

Bronchiolitis				
Season	Threshold			
	Low	Medium	High	Very High
2014-2015	>10	9	6	6
2015-2016	7	>10	7	10
2016-2017	7	>10	7	9
2017-2018	5	9	6	8
2018-2019	6	9	>10	6
2019-2020	>10	>10	7	>10
2020-2021	9	-	-	-
2021-2022	0	5	>10	>12
2022-2023	0	6	>10	4

Influenza				
Season	Threshold			
	Low	Medium	High	Very High
2014-2015	8	3	8	8
2015-2016	>10	>10	10	7
2016-2017	7	6	7	-
2017-2018	5	5	6	8
2018-2019	>10	8	6	9
2019-2020	>10	6	7	-
2020-2021	-	-	-	-
2021-2022	9	5	-	-
2022-2023	0	>10	-	-

Medium risk is also faithfully anticipated, but one should be cautious as to read the results because artifacts appear in some seasons as a result of the plateaus occupying these incidence ranges, plateaus caused by the many viruses that can produce bronchiolitis before the RSV predominates.

For further insight into the results, we present the historical diagnoses, incidences, p_5 and EPG measurements in [Figure 2.6](#) and [Figure 2.7](#) for influenza and bronchiolitis, respectively. Once again, the stochastic nature of epidemic medical records is ascertained, in particular when looking at the estimated reproduction numbers p_5 . In addition, we see how before an epidemic peak there is a raise of p_5 up to 3, which means that a large number of contagions are taking place. The similarity between the incidence of diagnoses and the EPG for both diseases can be corroborated, as well as the slight advancement of EPG, and how it reaches incidences higher than the equivalent weekly diagnoses, due to prompt growths in infections. This way, it indicates the risk of growth of an epidemic.

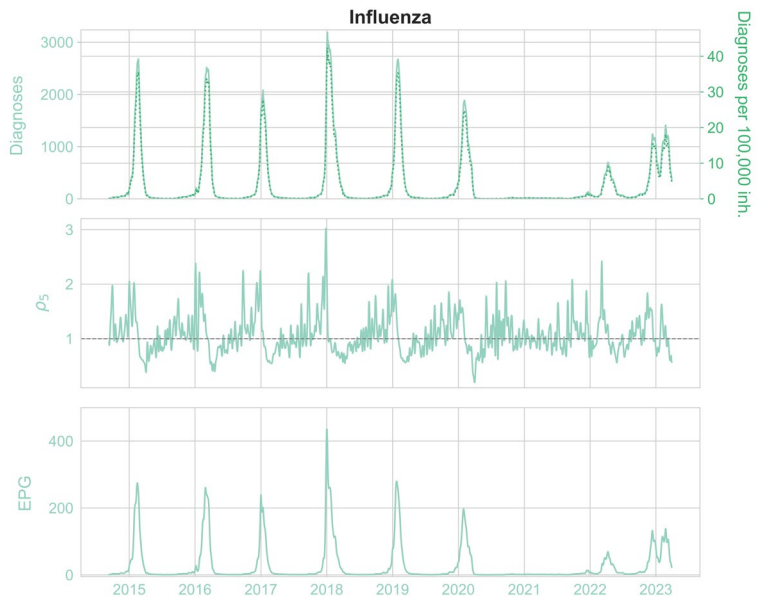


Figure 2.6. From top to bottom, the daily diagnoses (left) and daily diagnoses per 100,000 population (right, pointed), ρ_5 rate and EPG (weekly) infections per 100,000 population, for influenza. Retrieved from Perramon-Malavez, A. et al. [66].

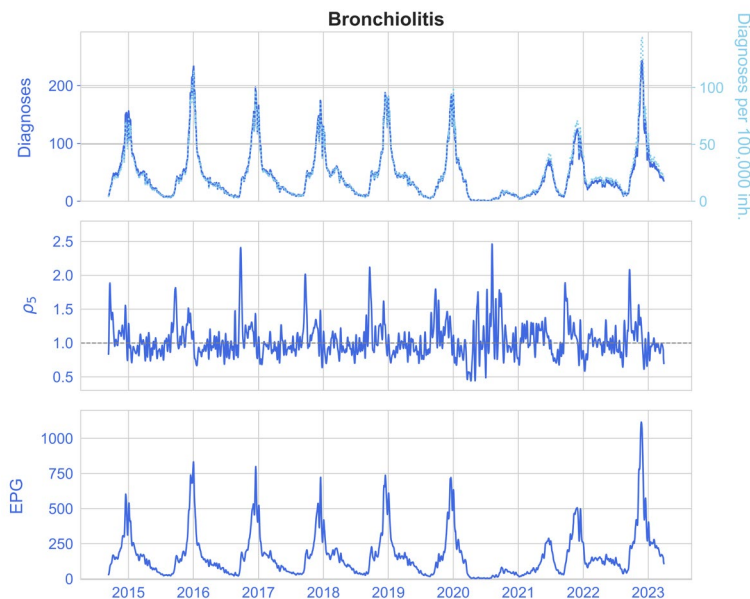


Figure 2.7. From top to bottom, the daily diagnoses (left) and daily diagnoses per 100,000 population (right, pointed), ρ_5 rate and EPG (weekly) infections per 100,000 population, for bronchiolitis. Retrieved from Perramon-Malavez, A. et al. [66].

Risk diagrams

To assist the visualization of EPG to better interpret it, we plotted the so-called risk diagrams [113] in which we have ρ_5 in front of A_7 and a shaded background in a colour scale representing the different epidemiological levels defined: dark green for very low or basal level, light green for low, yellow for medium, red for high and maroon for very high weekly incidence levels. To enhance readability and assist all readers, we have incorporated distinct symbols in our presentation. We differentiate between very low and low levels by “**”, low and medium levels by a square, medium and high levels by triangles and high and very high levels by diamonds. The growth/decrease threshold ($\rho_5=1$) is shown as a dotted line. Each dot in the plot depicts an EPG value for the corresponding A_7 and ρ_5 in a certain day, and the dashed line joins two consecutive days. The more separated the points, the greater the increase or decrease in incidence

(horizontal direction) or growth rate (vertical direction). The day the epidemic threshold is crossed initially is drawn as a blue dot and the final day of the epidemic, when we cross that value again, is in red. The x-axes are limited to only show A_7 incidences above the weekly epidemic threshold. An example of risk diagram can be found in [Figure 2.8](#) but the complete set of risk diagrams for all epidemic seasons during the period of study can be found in the material of the published article [66].

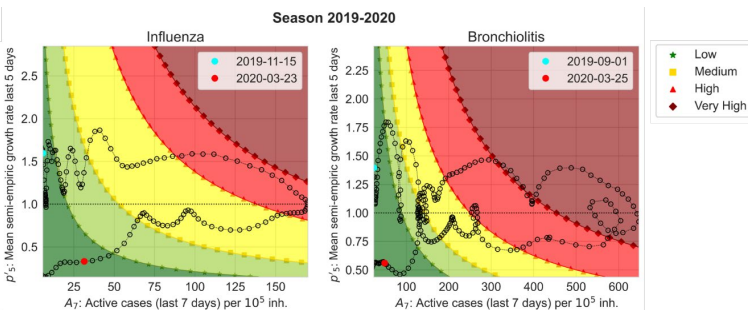


Figure 2.8. Risk diagrams for season 2019-2020 for influenza (left) and bronchiolitis (right). They show p_5 with respect to A_7 starting from the cyan point and finishing at the red point. The background colours correspond to EPG values classified by the epidemic levels. Very low (dark green) and low (light green) levels are separated by “*”, low and medium (yellow) levels by a square, medium and high (red) level by triangles and high and very high (maroon) levels by diamonds. Retrieved from Perramon-Malavez, A. et al. [66].

The risk diagrams allow us to anticipate the evolution of an epidemic in a very straightforward way. If we have an influenza incidence of 50 cases per 10^5 inhabitants but we are above the dotted line that separates growth from decrease, we expect that the number of active cases will continue to increase, following the pattern of the last 5 years. On the other hand, if the same incidence is located below the dotted line, it will not. Then, the colour scale helps us to define where we are in the epidemic, whether we are at low (dark and light green), medium (yellow) or high (bright and dark red) incidence values.

Surveillance table

To enhance and simplify surveillance of respiratory diseases in Catalonia, and facilitate the visualization of the epidemiological indicators, we have developed

an automatized control panel, as depicted in [Figure 2.9](#), that displays the weekly incidence rates for the previous and current weeks, the growth rates for the previous and current weeks, and the EPG. These data are updated daily, and the weekly incidence rates and growth rates are calculated by grouping the reported diagnoses over the last 7 days. In [Figure 2.9](#) we represented the panel on 5th December 2022, when the epidemic of bronchiolitis started vanishing and the influenza wave started to increase.

The last three columns present a colour scale such that *Current week growth rate (%)* is green if it is lower than the previous week one, orange if it is the same and red if it is higher; *Semi-empirical reproduction number ρ_5* is green when below 1, orange if equal to 1, and red if greater than 1; and *EPG (diagnoses per 100,000 population)* is white if the epidemic threshold is not surpassed, dark green if we are in very low level, green for low level, yellow for medium level, orange for high level and maroon for very high level. In [Figure 2.9](#), we observe that we are in a period where the bronchiolitis epidemic is over and we are slowly decreasing incidence, although maintained in high incidences, while at the height of the flu epidemic, with a high number of infections and moving towards greater incidences.

Risk Panel for Seasonal Epidemics						
	Previous week incidence (diagnoses per 100,000 population)	Current week incidence (diagnoses per 100,000 population)	Previous week growth rate (%)	Current week growth rate (%)	Semi-empirical reproduction number ρ_5	EPG (diagnoses per 100,000 population)
Bronchiolitis	899.00	899.00	23.00	-9.00	0.80	683.00
Influenza	61.00	61.00	41.00	56.00	1.35	92.00

Figure 2.9. Capture of the Risk Panel for seasonal epidemics in Catalonia, as of 5th of December 2022. Retrieved from Perramon-Malavez, A. et al. [66]. A better resolution image can be seen in the publisher's website.

Certainly, our proposed scheme has some limitations, and the EPG indicator is more robust for influenza than for bronchiolitis, in particular until the medium level threshold. That is due to the stochastic nature of bronchiolitis data, as stated before, and because of the plateau present in its epidemic waves. Nonetheless, in most cases we are able to anticipate the change in epidemic threshold by approximately a week in advance. Another limitation is the simplicity of the calculation of the effective reproduction number, which might not be accurately describing the epidemic dynamics. However, is within the error that we accept in exchange for simplicity of interpretation, and we observe

that it performs adequately. We could also use it in an anticipatory way, but this is not the objective of this work, since its output is more complex to interpret than that of the incidence, which is why we rely on the EPG.

In addition, currently, hospitalizations are not publicly available, which restricts us to using only primary healthcare data. With hospital admissions, further information could be introduced in our risk panel, such as the severity of the infections by a certain disease, including the ratio of people admitted to the hospital versus clinical diagnoses in primary healthcare, or the percentage of PICUs occupied. From these data, other risk indicators could be designed, such as a PICU-increase associated risk indicator. Besides, data on mortality could also be a good indicator of the sternness of the disease, but these data are not provided in a daily manner in our region. Additionally, pre-processing medical records is a hard task and there is not a standardized way to do so, yet. The bronchiolitis diagnoses' stochasticity limits both our pre-processing and predictions abilities with the disease.

To summarise

We redefined the Effective Potential Growth (EPG) indicator, which anticipates epidemic incidence changes by nearly a week for influenza and bronchiolitis. This, alongside a semi-empirical reproduction number and growth rates, forms the core of our epidemic surveillance panel. The method provides a simple yet effective tool for short-term forecasting, offering early warnings for healthcare systems without requiring advanced mathematical expertise. While more robust for influenza than bronchiolitis due to data variability, the approach remains a valuable asset for public health. As of 2025, we continue to use this method and have integrated it into a publicly accessible surveillance website [123], while during the epidemic period we provide constant updates to paediatricians and public health authorities using the risk panel data.

As of 2025, we have adapted the MEM to compute epidemic thresholds for influenza in paediatric age groups (0-11 months, 1-2 years, 3-4 years, and 5-14 years) and only the age group 0-11 months has been incorporated for

bronchiolitis, since additional age stratifications have been deemed unnecessary. The results are depicted in **Table 2.3**. Noteworthy, a key limitation of this method is that MEM is designed to be recalculated yearly using data from the previous five years. Given that our dataset starts in 2014, the earliest year we can compute epidemic thresholds is 2019. Besides, the COVID-19 pandemic disrupted the regular seasonality of influenza and RSV, while SARS-CoV-2 was still establishing itself within the *tripledemic* landscape, leading to highly irregular post-2019 data. As a result, for influenza and bronchiolitis, we continue using pre-pandemic epidemic thresholds, despite evidence that current epidemics have slightly different dynamics than before, especially for bronchiolitis following the introduction of nirsevimab.

Table 2.3. Epidemic threshold and levels of weekly incidence for (top) influenza and (bottom) bronchiolitis diseases.

Level	Influenza					
	0-11 months	1-2 years	3-4 years	5-14 years	<15 years	All population
Threshold	6	10	13	9	9	9
Low	12	21	35	21	22	21
Medium	43	64	123	81	82	53
High	141	282	359	242	259	138
Very High	223	469	689	471	488	214

Level	Bronchiolitis	
	0-11 months	<2 years
Threshold	83	27
Low	266	89
Medium	412	141
High	767	250
Very High	1417	453

In a few years, when these epidemics finally become stationary, we will be able to redefine these epidemic levels to better reflect the post pandemic reality. Despite these challenges, the epidemic risk panel, along with the risk diagrams, remains a reliable surveillance tool for accurately describing and predicting the

state and evolution of epidemics. The current risk panel follows the structure shown in **Figure 2.10**, which represents data as of January 17th, 2025, and it is publicly available and updated weekly in <https://epidemiologia.upc.edu/> [123]. One might notice that, currently, we introduced COVID-19 to our surveillance panel. We had not incorporated this disease in our analysis since during the pandemic several indicators were already developed for COVID-19, serving as a basis for the present study. However, for monitoring purposes, we included the disease in our panel and mimicked the methodology developed for influenza and bronchiolitis for COVID-19. Nevertheless, we did not compute any thresholds for its epidemics, due to its high instability and currently uncertain epidemic state, especially in children, where SARS-CoV-2 is very rarely found nowadays, as we will see in the next chapter.

Risk Panel for Seasonal Epidemics						
	Incidence of previous week (diagnoses per 100,000 inh.)	Incidence of current week (diagnoses per 100,000 inh.)	Previous rate of growth (%)	Current rate of growth (%)	Semi-empirical reproduction number (ρ)	EPG (diagnoses per 100,000 inh.)
COVID-19 (all)	11.00	15.00	32.00	36.00	1.28	19.00
COVID-19 (0 y.)	33.00	34.00	76.00	1.00	0.90	0.00
COVID-19 (1-2 y.)	3.00	6.00	24.00	104.00	1.45	7.00
COVID-19 (3-4 y.)	3.00	3.00	625.00	0.00	0.90	0.00
COVID-19 (5-14 y.)	3.00	3.00	103.00	11.00	0.98	0.00
COVID-19 (>15 y.)	4.00	5.00	95.00	14.00	0.97	5.00
Bronchiolitis (0 y.)	606.00	473.00	4.00	-22.00	0.88	436.00
Bronchiolitis (>2 y.)	183.00	149.00	-14.00	-29.00	0.95	146.00
Influenza (all)	241.00	281.00	52.00	17.00	0.98	280.00
Influenza (0 y.)	327.00	466.00	70.00	42.00	1.47	668.00
Influenza (1-2 y.)	268.00	451.00	55.00	68.00	1.69	725.00
Influenza (3-4 y.)	193.00	391.00	5.00	103.00	2.20	778.00
Influenza (5-14 y.)	128.00	237.00	-7.00	96.00	2.02	437.00
Influenza (<15 y.)	159.00	288.00	7.00	81.00	1.93	514.00

Figure 2.10. Capture of the Risk Panel for seasonal epidemics in Catalonia, as of 17th of January 2025. Retrieved from [123]. A better resolution image can be seen in the source website.

Chapter 3

SARS-CoV-2

"What's true of all the evils in the world is true of plague as well. It helps men to rise above themselves."

Albert Camus

The title of this new chapter may evoke the reader a sense of unease. Nevertheless, to grasp the future, we must first comprehend the past. Thus, embarking courageously on this new journey will present the reader with a novel perspective on the pandemic precipitated by the virus after which this chapter is named. Together, we will delve into the dystopic reality with which SARS-CoV-2 confined us, exploring its origins, the emergence of variants, and surfing among the complex waves of its epidemiology and dynamics in Catalonia. We will also uncover its impact on children, including its prevalence and side effects, for every magical potion carries unforeseen consequences, and the illness known as COVID-19 was no exception. It gave rise to the dreaded multisystem inflammatory syndrome in children (MIS-C), a condition that wrought severe consequences, even claiming the lives of some. However, I implore the reader not to be alarmed, for this journey ultimately culminates in hope.

In this chapter we will introduce SARS-CoV-2 and COVID-19 and discuss how it has remained in the viral landscape, which role had children and schools during the pandemic regarding transmission and how did the multisystem inflammatory syndrome in children cases evolved throughout the years, based on the following published and peer-reviewed articles:

Scientific work article XVI: Pino, R., *et al.* European journal of pediatrics. 2023.

Scientific work article XVII: Soriano Arandes, A., *et al.* Frontiers in public health. 2023.

Scientific work article XVIII: Buonsenso, D., *et al.* Pediatric infectious disease journal. 2022.

Scientific work article XIX: Antoñanzas, J. and Perramon-Malavez, A., *et al.* Viruses. 2021.

Scientific work article XX: Perramon-Malavez, A., *et al.* Frontiers in Pediatrics. 2021.

3.1. Characteristics of SARS-CoV-2

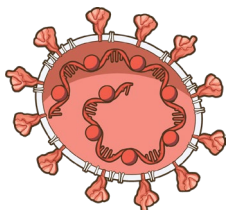


Figure 3.1. Scheme of SARS-CoV-2. Retrieved from Bioart [124].

The SARS-CoV-2 requires no introduction to those who lived through the events of late 2019. The virus, responsible for the COVID-19 pandemic, is a single-stranded RNA enveloped virus of the *Coronaviridae* family, which name comes from the unique feature on their surfaces resembling a solar corona (**Figure 3.1**) [124]. These characteristic spikes are S proteins on the virion surface that play a crucial role in the virus's

ability to infect and spread. Once SARS-CoV-2 reaches a host cell, the S protein strongly binds to ACE2 receptors on the cell membrane, allowing the virus to enter and release its genetic material, hijacking the host's organelles to produce the proteins necessary for replication. The newly formed virions are released to infect other cells, continuing the cycle of infection [125]. Mutations in the S protein have led to the emergence of variants with enhanced transmissibility such as the Alpha, Delta, and Omicron variants. These mutations altered the virus's interaction with antibodies, reducing the effectiveness of prior immunity and generating different transmission dynamics and epidemiological patterns [126], [127].

Beyond its ability to mutate and spread, SARS-CoV-2 can trigger a complex and sometimes dysregulated immune response. While most infections from the original pre-Alpha strain remained mild or moderate, severe cases have often been linked to a magnified inflammatory reaction called cytokine storm. In this scenario, the castle's messengers or pro-inflammatory cytokines, overwhelmed and disoriented, deliver conflicting signals, leading to widespread chaos instead of an organized defence. This results in extensive tissue damage, endothelial dysfunction, and, in the worst cases, multiorgan failure. Moreover, SARS-CoV-2 can also inhibit interferon signalling, thus our castle's bells fail to sound the alarm in time, granting the virus a critical advantage, increasing viral replication and prolonging infection, further contributing to severe disease outcomes [128].

3.2. COVID-19 disease

Describing the clinical presentation of COVID-19 is challenging, as its symptomatology has evolved alongside the emergence of new SARS-CoV-2 variants. Initially, the disease caused by the pre-Alpha strain was characterized by moderate severity, with an incubation period of up to 14 days. The most frequently reported symptoms included fever, fatigue, cough, shortness of breath, and loss of smell or taste (anosmia and ageusia), the latter being particularly distinctive features [129], [130]. Nowadays, with the Omicron variant being prevalent, the COVID-19 symptoms are those of a URTI such as the common cold or the flu, with fever, cough and nasal congestion [131]. However, it is important to note that not all individuals infected with SARS-CoV-2 developed symptomatic COVID-19. Asymptomatic carriers constitute a significant proportion of viral shedders, contributing to the silent transmission of the virus within populations [38].

Moreover, symptom presentation also varied with age before the emergence of the Omicron variant. Literature describes that in individuals aged 16 to 39 years, loss of smell, chest pain, abdominal pain, shortness of breath, and eye soreness were among the most relevant symptoms. For individuals aged 40 to 59 years, significantly different than for the older age groups, persistent cough was more relevant in detecting COVID-19, while chills or shivers were less relevant when compared with individuals aged 80 years or older. As participant age increased beyond 60 years, anosmia became less relevant, and in individuals over 80 years, it was no longer a primary diagnostic feature. Instead, symptoms such as diarrhoea, sore throat, chest pain, unusual muscle pain, eye soreness, and chills or shivers gained prominence. Notably, these older age groups also exhibited the highest mortality rates [91], [129], [132].

However, what about children, the focus of this thesis? In terms of symptomatology, we observed that in younger children, the absence of high-grade fever was a strong predictor of COVID-19, whereas in older children, loss of taste or smell was the most determinant symptom [133]. Nonetheless, as SARS-CoV-2 evolved, so did the clinical manifestation of COVID-19. The Alpha variant (B.1.1.7), which emerged in late 2020, was associated with a higher risk

of hospitalization and mortality compared to the original strain. Patients infected with Alpha reported more frequent cough and fatigue, and anosmia remained a key distinguishing feature. The Delta variant (B.1.617.2), which became dominant in mid-2021, exhibited increased transmissibility and a distinct symptom profile. Reports indicated that anosmia and ageusia became less common for the general population, while headaches, sore throats, and rhinorrhoea became more prevalent. Delta also had a higher propensity to cause severe illness, particularly in unvaccinated individuals [134], [135], [136] and children, who, unlike adults, saw their symptoms magnified [137].

By late 2021, the Omicron variant (B.1.1.529) rapidly replaced Delta as the dominant strain due to its increased immune evasion and transmissibility. Omicron infections presented with significantly different symptoms, resembling an URTI like the flu or a strong cold, as anticipated, and anosmia and ageusia were reported much less frequently. Omicron tended to cause milder disease, particularly in children and vaccinated individuals, with a lower risk of hospitalization compared to Delta [134], [135], [138], [139].

Overall, COVID-19 has consistently presented with nonspecific and often ambiguous clinical manifestations in children, closely resembling other common respiratory viral infections. However, during the period spanning the Alpha to Delta variants, the increased overall severity of COVID-19 was also reflected in a rise in cases of multisystem inflammatory syndrome in children (MIS-C), a severe hyperinflammatory condition associated with SARS-CoV-2 infection. MIS-C, which will be discussed in detail later in this thesis, emerged as the primary cause of SARS-CoV-2-related mortality in children due to its potential for severe cardiovascular and systemic complications [140], [141].

3.3. Epidemiology of SARS-CoV-2 in Catalonia

Fortunately, at the time of writing, SARS-CoV-2 circulation remains at low levels in both adult and paediatric populations. The irregular wave-like pattern of disease incidence observed from 2020 to mid-2022 has largely subsided ([Figure 3.2](#)). In Catalonia, four major SARS-CoV-2 strains have predominated over time, as previously mentioned.

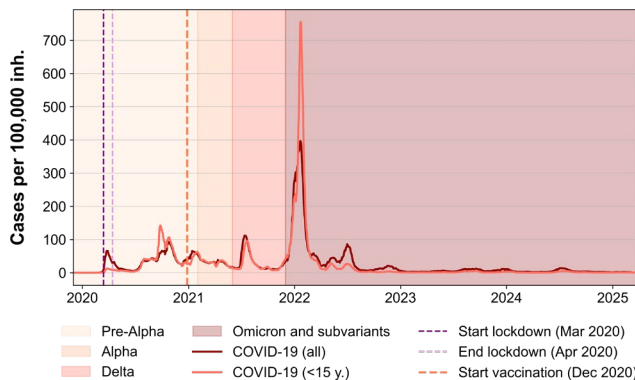


Figure 3.2. Evolution of SARS-CoV-2 cases per 100,000 inhabitants in Catalonia from December 2019 to February 2025. For the whole (dark red) and paediatric population (coral). The different variants periods are depicted as coloured background, from the lightest shade for pre-alpha strain to the darkest for omicron and subvariants, which are the ones circulating as of 2025. The lockdown period (dashed purple), and the beginning of the vaccination campaign in Catalonia (dashed orange) are also depicted.

The pre-Alpha strain, originating in Wuhan and circulating from December 2019 to February 2021; the Alpha variant, which was dominant from February to June 2021; the Delta variant, which prevailed from June to December 2021; and the Omicron strain, which has remained dominant since December 2021. While multiple Omicron subvariants have since emerged, they have not diverged significantly enough to warrant distinct classification. Despite the reduced impact of SARS-CoV-2, periodic vaccination remains an essential public health measure to mitigate the risk of severe disease and maintain population immunity [142].

Throughout the SARS-CoV-2 integration into our viral ecosystem multiple variants of the virus coexisted, although one typically predominated in different periods of time. In Catalonia, these were Alpha, Delta, and Omicron, but the dominant variant often varied between countries due to geographic factors, population density, and the timing of variant introductions. While the Alpha and Delta variants were associated with more severe disease, Omicron demonstrated the highest transmissibility. However, its rapid spread was mitigated by acquired immunity through natural infection and vaccination, which started on 27th December 2020 in Catalonia, as well as periodic booster immunisation efforts that continue to this day [127]. As illustrated in [Figure 3.2](#), the incidence of COVID-19 in children during the Omicron wave was substantially higher than in adults. However, throughout the pandemic, overall incidence rates in children were comparable to or even lower than those observed in adults. Despite initial concerns that children were major drivers of SARS-CoV-2 transmission, evidence did not fully support this claim, yet numerous public health measures, including school closures, were directed towards children [143], [144].

3.3.1. The role of children in COVID-19 epidemics

We conducted a collaborative international study demonstrating that school closures were not associated with a reduction in COVID-19 cases ([Figure 3.3](#)) [144]. This study highlighted the considerable uncertainty and debate surrounding mitigation policies for children during the pandemic. Although some children with comorbidities were at increased risk of severe COVID-19, or complications such as MIS-C, most paediatric cases were mild. Therefore, being unjustifiable that so many measures were implemented targeting them. Moreover, substantial evidence indicates that mass mitigation measures had significant adverse effects on children, not only on their physical health but also on their mental development [145]. This raised a fundamental question: to what extent should children bear the burden of mitigation measures for a disease that disproportionately affects older populations? We analysed differences in epidemiology, policies, mitigation strategies, and outcomes between children and adults in several countries in Western Europe. The highly heterogeneous policies applied to children across European countries did not lead to significant

differences in outcomes. Besides, in most countries school closures did not lead to a reduction in cases or prevented the epidemic waves, as seen in Ireland or Cyprus in **Figure 3.3.**

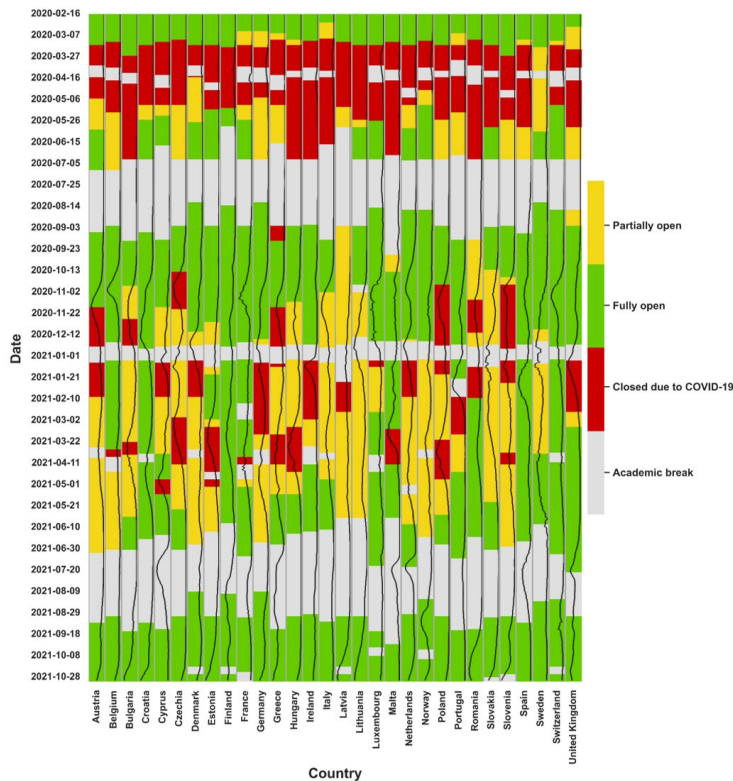


Figure 3.3. Closure of primary schools in European countries during the pandemic. The black line is showing the COVID-19 incidence per 10⁵ population for each country. Retrieved from Soriano-Arandes, A. et al. [144]. A better resolution figure can be found in the publisher's website.

Notably, when we did the study the relative role of school-aged children in transmitting SARS-CoV-2 to other age groups remained uncertain, with existing evidence suggested that school transmission generally followed, rather than drove, community transmission. However, more recent literature has clarified that children were not the primary drivers of the pandemic in its early stages,

despite policies being heavily focused on them. Their role in transmission became more significant later on, particularly with the emergence of the Omicron variant [146], but vaccination was then implemented.

**School transmission generally followed, rather than drove,
community transmission.**

In Catalonia, we conducted an extensive study analysing the incidence of SARS-CoV-2 in individuals under 18 years old during the 2020-2021 school year [147], with the aim of further justifying that NPIs should not be just directed at them and defending their relative role in general transmission dynamics.

Methods

We obtained public data on the total tested and confirmed SARS-CoV-2 cases in Catalonia, provided by AQuAS (see [Section 1.3.1](#)) that had downloaded the original data from the Catalan Epidemiological Surveillance Network's clinical microbiological laboratories [148]. No additional data were available.

A confirmed COVID-19 case was defined as any individual testing SARS-CoV-2 positive by molecular assays or RAT in symptomatic patients, according to the company information. RAT had only been available since 23rd October 2020 (7th week of the school-course) in primary care settings. All the close contacts of the confirmed cases were tested, mainly with polymerase chain reaction (PCR). Nevertheless, in the schools, all the classroom contacts were tested by PCR and not by RAT.

Results

Our findings revealed that, despite a significantly higher diagnostic effort in children – with up to 1,154 more tests per 100,000 population compared to adults – the relative incidence of paediatric cases remained slightly lower than that of the general population. Notably, incidence rates increased with age within the paediatric group ([Figure 3.4](#)).

Moreover, we observed a lower positivity rate among children (5.7%) compared to adults (7.2%), with the lowest rates (4.9%) recorded during periods of school attendance, outside of holiday breaks. This outcome was closely linked to the

implementation of mass screening initiatives and systematic whole-group contact tracing whenever a case was detected within a classroom.

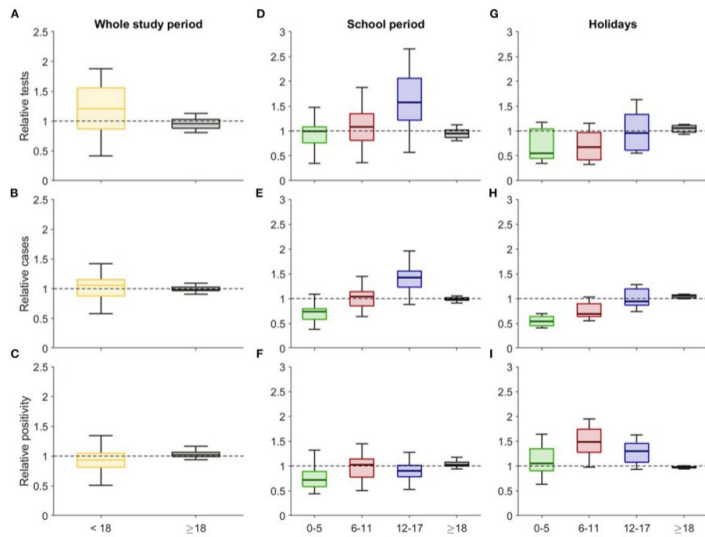


Figure 3.4. Box plots of the relative daily values of (A) number of tests, (B) incidence, and (C) positivity during the whole study period. Box plots for the relative daily (D,G) number of tests, (E,H) incidence, and (F,I) positivity during the school period and holidays. For each age group, the variables are presented relative to the general population (i.e., value in the age group divided by the value in the general population). Retrieved from Perramon-Malavez, A. et al. [147].

These targeted measures not only helped contain potential outbreaks but also reinforced the role of schools as vital epidemiological surveillance hubs. Regarding the influence of Spain's COVID-19 vaccine rollout, adult vaccination started on the 27th of December 2021, and the coverage (full vaccination) went from 0.84% at the end of January 2021 to 17.53% at the end of the study period (see Perramon-Malavez, A. et al. [147]). Considering the age <69 years, which is the age-group of active employees, only 5.45% were fully vaccinated by the end of May 2021, while 23.52% had received at least the first dose of a vaccine. Moreover, essential workers, such as teachers and staff working in educational centres, were also vaccinated with a scheduled interval of 12 weeks between the first and the second dose. In particular, in Catalonia, the second dose of the

vaccine began to be administered to essential workers on 27th May 2021 [149]. Therefore, considering the rollout procedure, the incidence among children during the last part of the analysed period was probably not affected by the vaccination of teachers and other school workers.

To summarise

While schools played an important role in monitoring SARS-CoV-2 transmission, children were not the main drivers of the pandemic in Catalonia. Although schools remained open with NPIs in place, the incidence of COVID-19 among children was comparable to that of adults and slightly higher among adolescents. However, test positivity rates in children consistently remained lower, largely due to increased diagnostic efforts, particularly the systematic testing of entire classrooms following a positive case, as well as several mass screening campaigns conducted in educational settings. Given the typically mild course of SARS-CoV-2 infection in children, often with a high proportion of asymptomatic cases, our findings highlighted the importance of systematic screening in schools when a case was detected. Furthermore, supporting evidence from other Western European regions showed that school closures were not associated with a significant reduction in SARS-CoV-2 incidence, despite being a central focus of public health policies.

However, our study has some limitations. Firstly, we do not know the percentage of asymptomatic children in the study period. Nevertheless, we found a correlation between diagnostic effort and positivity because of the testing protocols in the schools: the greater the diagnostic effort, the lower the positivity. Secondly, we do not know the exact percentage of students and teachers who strictly followed the NPIs at each educational centre. Thirdly, we cannot disaggregate the effect of NPI measures implemented in the community which could affect the dynamics of adults and children in a different manner and that were not constant throughout the course. Nevertheless, the epidemiological differences between children and adults in scholar vs. holiday periods reported in this study are expected to be mainly caused by whether the

schools were open or not in these two periods, and it is further supported by the evidence of [Figure 3.3](#) and Soriano-Arandes, A. *et al.* [144]. Fourthly, the percentage of younger children (under 5) tested by RAT was higher than in older age-groups. This is likely because they were mostly tested out of the school contact tracing studies, and therefore incidence in this age-group could be underestimated. Finally, childhood SARS-CoV-2 incidence during the school year has not been demonstrated to be a determining factor in the levels of community transmission, but mitigation measures, mainly NPIs applied at the educational centres, could have been crucial to obtaining such a favourable outcome.

3.4. Multisystem inflammatory syndrome in children

While children were not the main drivers of the COVID-19 pandemic early on, they became a focal point due to a severe complication that some experienced: MIS-C. This rare but serious condition caused widespread inflammation in multiple organs and, in severe cases, led to PICU admission and even death. The MIS-C is similar to Kawasaki disease and early on the pandemic both were confused, but MIS-C distinctively presents as a severe, hyperinflammatory condition temporally associated with SARS-CoV-2 infection, and some population have an increased risks for developing it, for instance children with male sex, age 5-11 years, foreign-born parents, asthma, obesity, and life-limiting conditions [150]. At the beginning of the pandemic, the syndrome was understudied, and our research in Catalonia provided valuable insights into the incidence, clinical manifestations, and trends of MIS-C throughout different phases of the pandemic.

In a comprehensive two-year ambispective multicentric cohort study conducted across Catalonia from April 2020 to April 2022 by Pino, R. *et al.* [141], we found that common clinical manifestations of MIS-C included gastrointestinal symptoms (88.2%) and high-grade fever exceeding 39°C (81.6%) while cardiac involvement was significant, with nearly 40% of patients exhibiting abnormal echocardiographic findings. Besides, we observed that the monthly incidence of MIS-C was of one case per 3,700 SARS-CoV-2 infections (0.03%) before the Omicron variant period, where the rate ratio of MIS-C significantly decreased. In fact, taking Omicron as the reference period, we found an 8.9 (95%CI: 5.7-13.8), 2.1 (95%CI: 0.8-5.5) and 6.6 (95%CI: 4.1-10.4) RR of MIS-C for pre-Alpha, Alpha and Delta strains, respectively. This change in the MIS-C proportion suggested that immunisation was acquired through vaccination or that the variant presented a decreased severity. The evolution of MIS-C cases and SARS-CoV-2 throughout the study period, per age ranges, is depicted in **Figure 3.5**.

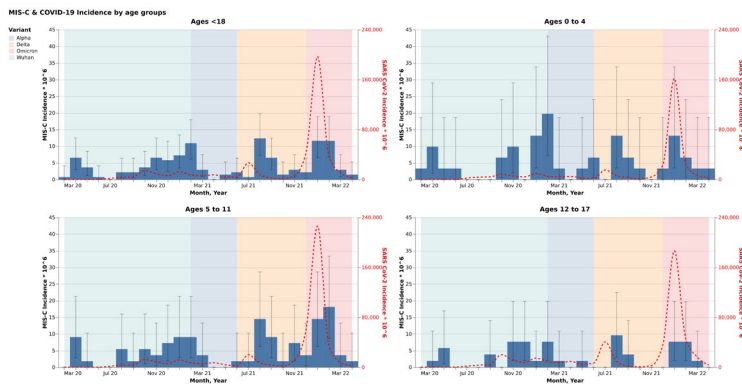


Figure 3.5. Blue boxes show the MIS-C incidences ($\times 10^6$) by age-groups (< 18 years old, 0-4 years old, 5-11 years old, and 12-17 years old) for each variant period. The discontinuous red line describes the SARS-CoV-2 incidence ($\times 10^6$) through the periods. Retrieved from Pino, R. et al. [141]. A better resolution figure can be seen in the publisher's website.

3.4.1. In Catalonia and Western countries

But MIS-C cases were not exclusive of Catalonia, but a global concern. On a broader international context, we performed an observational multicentre cross-sectional study examining MIS-C cases in Western countries to assess trends in incidence as the pandemic progressed [151]. The findings were coherent with the Catalonia study, since they suggested a decreasing incidence of MIS-C over time, attributed to factors such as increased population immunity, either through natural infection or vaccination, and the emergence of new SARS-CoV-2 variants with different pathogenic profiles.

Methods

MIS-C cases were reported by the participant researchers. In the study, we included data from Chile, The Netherlands, Costa Rica and Catalonia (Spain), where the researchers compiled all the MIS-C cases for the whole region or country. We also covered Lazio (Italy), Mexico DF, Panamá and Bogotá (Colombia), where we included the MIS-C cases diagnosed at a paediatric referral hospital. In most of the sites, it was possible to split the cases per age ranges. With respect to COVID-19 diagnosis we included the available data of the total number of cases and tests in each country, the number of cases and

tests for paediatric ages in each region and the number of paediatric hospitalizations. Additionally, we retrieved data about SARS-CoV-2 variants, vaccination introduction date and vaccine coverage for adolescents and children from all the participating sites. We assessed the ratio between MIS-C cases and COVID-19 paediatric cases diagnosed 4 weeks earlier (average time for the temporal association observed in this disease) for 5 participating sites – Catalonia (Spain), Chile, Bogotá (Colombia), Costa Rica and The Netherlands –. For 3 other sites where COVID-19 paediatric cases were not available, we assessed the same ratio of MIS-C cases but using the total COVID-19 cases among the general population – Panamá, Ciudad de México and Lazio (Italy) –. A probit linear regression model with binomial distribution was performed for each site obtaining the *p*-value for the fit to define the statistical significance of the observed trend. For those sites where paediatric COVID-19 cases were not available, the probit linear regression model was applied to the monthly ratio between MIS-C cases and the total COVID-19 cases reported in the region 4 weeks before – Mexico DF, Panamá and Lazio (Italy) –. The *p*-value for the fit was also assessed to define the statistical significance of the observed trend. We finally used the probit linear regression model to predict the MIS-C cases (**Figure 3.6**). The analysis was implemented in MATLAB using the *glmfit* function for the probit linear regression analysis with binomial distribution for the response variable.

Results

As previously stated, and consistently with our other studies, we observed a global significant decreasing trend with the time-series binomial analysis for the ratio between MIS-C cases and COVID-19 diagnosed cases in the previous month (*p*-value < 0.001).

When analysing each of the participating sites, Chile and The Netherlands kept a significant decrease trend (*p*-value < 0.001), but this trend was not statistically significant for Catalonia (Spain), Bogotá (Colombia), Costa Rica, Lazio (Italy), Mexico DF or Panamá, although all regions presented a negative slope in the evolution of MIS-C cases, showing a decrease in incidence despite not being statistically significant. The varying results across the countries or sites could

be associated with the sample size, because the higher the number of MIS-C cases are, the better the binomial regression analysis fits with the decreased trend, as shown when we include all the sites at once.

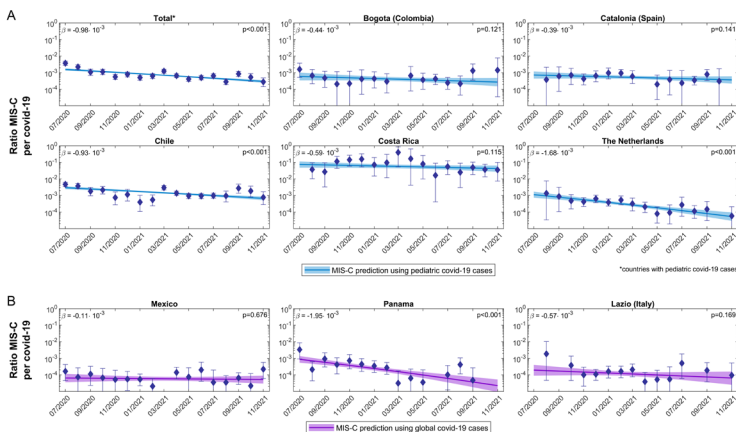


Figure 3.6. Monthly evolution of the ratios between monthly MIS-C cases and the COVID-19 paediatric (or total) cases the month before. **A:** Timeline for the monthly ratio between MIS-C cases and COVID-19 paediatric cases for Bogota (Colombia), Catalonia (Spain), Chile, Costa Rica and The Netherlands. **B:** Timeline for the monthly ratio between MIS-C cases and total COVID-19 cases for México DF, Panama and Lazio (Italy). For the Netherlands and Catalonia (Spain), it should be noted that testing strategies for children changed through the course of the pandemic, resulting in an underestimation in the beginning and increasing positive findings through screening asymptomatic schoolchildren in the last months. The slopes and the p-values for the significance of the observed trends are indicated in each case. Note that the y-axis uses a logarithmic scale so that the same axis can be used for all countries. Retrieved from Buonsenso, D. et al. [151]. A better resolution image can be found in the publisher's website.

Additionally, the decrease through time in the MIS-C to cases ratio in The Netherlands or Catalonia could also be partly due to changing testing strategies during the course of the pandemic, with school children rarely being tested for SARS-CoV-2 in the beginning and routinely screened bi-weekly in the later months and mainly during the school-periods [147]. Furthermore, different coverage of fully COVID-19 vaccination in adolescents and children in the participating sites could explain the differences in trend between countries, since the impact of the vaccines on viral transmission in the community depends

on the vaccination coverage, dosage and schedules, as well as type of vaccines administered in the adolescents but also in the adults. The vaccination in the households reduces SARS-CoV-2 transmission in familiar contacts [152] and may also contribute to reducing MIS-C cases.

To summarise

We observed a global significant decrease in trend for the ratio between MIS-C cases and paediatric COVID-19 diagnosed cases in the previous month. If we consider that the majority of countries have introduced mRNA and/or inactivated vaccines against COVID-19 in children 12-17 years of age since mid-2021, our findings suggest that vaccination could have an impact not only in preventing severe paediatric COVID-19 but also MIS-C. Besides, after the Omicron wave in winter 2021, no new MIS-C cases have been reported in Catalonia up to the time of writing in April 2025.

Our findings have been ascertained by other studies from around the world [153], [154]. Collectively, these studies highlight the dynamic nature of MIS-C incidence throughout the pandemic. Fortunately, the infrequent occurrence of this complication, coupled with the current low incidence of COVID-19 in children, has made MIS-C an increasingly uncommon phenomenon in today's clinical landscape.

Chapter 4

Influenza

*"Sol, sóc etern. M'és present el paisatge
De fa mil anys, l'estrany no m'és estrany"*

JV Foix

Dear reader, let us cast aside the tattered scrolls of old knowledge, for the tale of influenza is not one of mere winter ailments and fleeting fevers. Nay, it is a saga of unseen forces, an adversary whose form shifts like a trickster spirit, eluding the grasp of those who dare to pursue it. And yet, as the alchemists of old transmuted lead to gold, so too have scholars and healers sought to decipher its secrets—not with potions and leeches, but with the wisdom of numbers, the spells of models. In Catalonia, we have traced its path, deciphering past epidemics to foresee those yet to come. We wield the tools of prophecy, models forged in the crucible of knowledge, to chart contagion's course. No longer do we speak of mere chance but of transmissivity shaped by the world itself—by heat and cold, by the very rhythm of the climate. So walk with me through this realm of science and foresight, where we shall unveil the true nature of this elusive foe, and in which way children are intricately involved.

In this chapter we will define the role of children in influenza transmission, study its relationship with meteorology using mechanistic models and, based on the following published and peer-reviewed article, we will empirically model the influenza epidemics for monitoring and short- to mid- term prediction:

Scientific work article X: Villanueva, M., *et al.* Scientific reports. 2024.

4.1. Characteristics of influenza viruses

It is well understood that influenza viruses undergo frequent mutations, necessitating the development of a new vaccine every year based on the most recent circulating strains. It is also widely known that these viruses cause influenza, commonly referred to as the flu, and that influenza A and B are responsible for seasonal epidemics. However, are these two strains truly alike? Do additional strains exist? And what drives the rapid mutation of these viruses? In this section, we will examine these questions in detail.

The influenza viruses are enveloped viruses that belong to the *Orthomyxoviridae* family. Their name derives from the Greek word *myxo*, meaning mucus, as these viruses have an affinity for mucoproteins on cell surfaces. These proteins are a type of glycoprotein (G protein, see [Section 1.2](#)) and the major component of mucus [155]. Because of that, they are found on the surfaces of epithelial cells, particularly in the respiratory and gastrointestinal tracts. These proteins play a crucial role in protecting and lubricating mucosal surfaces, trapping pathogens, and facilitating immune responses. Influenza viruses specifically bind to mucoproteins via their hemagglutinin (HA) protein ([Figure 4.1](#)) [156], [157], [158]. This interaction allows the virus to attach to and enter host cells, initiating infection. Different influenza strains have varying affinities for specific types of linkages, influencing their host range and transmission patterns.

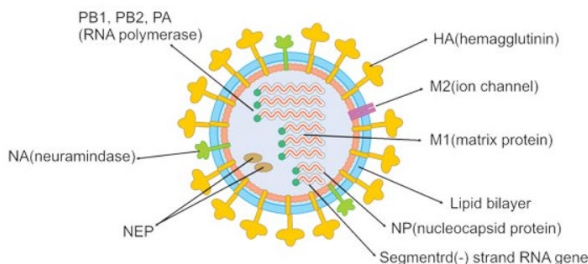


Figure 4.1. Influenza viruses' general structure. Retrieved from [155].

In this regard, there are four types of influenza viruses: A, B, C, and D. While types A-C can infect humans, type D viruses have been recognized to infect

vertebrate animals like swine, cattle, and sheep but not humans. Among these strains, influenza A and B are of significant concern due to their role in seasonal epidemics. Influenza A viruses are further divided into subtypes based on combinations of HA and neuraminidase (NA) proteins on their surface [156], [157], [158]. Currently circulating in humans are subtype A(H1N1) and A(H3N2) influenza viruses, although one may find A(H1N1) also written as A(H1N1)pdm09, as it caused the influenza pandemic in 2009 and replaced the previous A(H1N1) virus which had circulated prior to that year. In Catalonia, A(H3N2) was the predominant subtype before 2017; however, since then, A(H1N1)pdm09 has emerged as the most often leading cause of seasonal influenza A associated epidemics [159], [160]. Notably, only influenza A viruses have been associated with pandemics, and are usually the ones producing the most severe symptoms. In contrast, influenza B viruses are categorized into two main lineages: B/Yamagata and B/Victoria. Recent studies suggest that the B/Yamagata lineage may have become extinct [161], [162], which has implications for vaccine formulation and public health strategies. In regions like Catalonia, the annual influenza vaccination program includes coverage for both influenza A subtypes and the B/Victoria lineage, reflecting the current epidemiological landscape described by the World Health Organisation (WHO) [163]. Researchers are exploring new strategies for next-generation influenza A virus vaccines to better prepare for future pandemics. The goal is to create broader immunity that protects against multiple strains, not just the ones predicted for each flu season.

Antigenic drift is a process of small and continuous mutations within a viral subtype, while antigenic shift is a major mutation that defines a new subtype.

The current problem when developing influenza vaccines is the rapid mutation of influenza viruses, primarily driven by antigenic drift and antigenic shift. Antigenic drift involves small, continuous genetic changes that accumulate over time, leading to new virus strains that may evade the immune system. For instance, influenza B viruses undergo both intra- and inter-lineage reassortment [164], an infrequent but crucial process that necessitates continuous

surveillance to optimize vaccine composition. Antigenic shift, on the other hand, is a sudden and significant change that could lead to the emergence of a novel influenza A subtype with pandemic potential [158]. Traditional flu shots mainly target the globular head of the HA protein, that changes frequently due to the antigenic drift, which is why the flu vaccine needs to be updated every year. In contrast, next-generation vaccines are aimed to more conserved regions of the virus, such as the HA stem or NA, to provide broader and longer-lasting protection as they trigger stronger, cross-protective immune responses. These innovations could reduce infections, severe illness, and even transmission, though they also raise questions about how they interact with existing immunity and influence virus evolution [165].

4.2. Influenza disease

Influenza is an acute respiratory illness that, despite being generally self-limiting, can impose a significant health and economic burden. Seasonal influenza is responsible for a significant burden of LRTIs in children under 5 years, with an estimated 120,000 deaths annually [166], although most of those deaths happen in the Global South, as stated in [Section 1.1.1](#). It is characterized by symptoms such as fever, headache, fatigue, runny nose, and chills, typically appearing around two days after infection (incubation period: $\tau = 2$) [118]. While most individuals recover within a week without medical intervention, symptoms can persist for over two weeks, and severe cases may lead to complications such as pneumonia, sepsis, or exacerbation of pre-existing conditions, particularly in high-risk groups such as older adults, young children – where influenza viruses can also cause bronchiolitis [167] –, pregnant women, and individuals with chronic diseases [157], [168]. Furthermore, influenza is highly contagious; infected individuals can transmit the virus from the day before symptom onset, with adults remaining infectious for 3 to 5 days and children for up to 10 days [169], [170], and recovering approximately after a week.

Beyond its clinical impact, influenza places a substantial burden on healthcare systems. In Catalonia, influenza-related hospitalizations incur mean costs exceeding €10,000 per case, based on data from 16 sentinel hospitals [171]. However, only a small proportion of cases require hospitalization, with most being managed in primary care settings, leading to significant strain and saturation in these facilities. Not only this, but the disease also contributes to absenteeism and productivity losses during seasonal epidemics since it can be a debilitating disease.

Given its high transmissibility and potential for severe outcomes – it is worth recalling how COVID-19 was frequently compared to influenza – this virus remains a major public health concern, underscoring the need for effective surveillance, vaccination programs, and preparedness strategies.

4.3. Epidemiology of influenza

Influenza epidemiology is driven by a complex interplay of factors, in which viral strain, meteorological variables and host demographics, particularly age, play a key role. Age influences not only susceptibility to different influenza strains but also disease severity and immune response. Children, for example, are thought to be the key drivers of influenza transmission due to their high contact rates and often naïve immune systems [172], [173]. This will be further explored and challenged later in this section. Older adults and individuals with chronic conditions, on the other hand, experience higher morbidity and mortality due to weaker immune responses [159], [172].

On another note, in the post-pandemic context, the relationship between viral strain and influenza dynamics has become increasingly evident. While generally influenza A is predominant and influenza B appears in alternate seasons, notably, dual epidemic waves – typically characterized by an initial peak driven by influenza A followed by a second peak dominated by influenza B or vice versa – have been observed, as exemplified by the 2022-2023 season (see [Figure 4.2](#)). Interestingly, the subsequent 2024-2025 epidemic also exhibited a bimodal pattern; however, in this case, influenza A followed influenza B and the temporal separation between the peaks does not appear to be clearly linked to specific viral subtypes. This can be seen in [Figure 4.2](#), where the RAT daily data for children <15 years were extracted from SIVIC ([Section 1.3.1](#)) has been represented after applying a 7-day average moving filter, with incidence computed using age-segregated population data (which can be obtained from SIVIC or IDESCAT). The data has been zoomed for September 2022 onwards and represented only for influenza, but a more complete version of the RAT results landscape can be observed in [Figure 2.3](#). This raises the possibility that other factors may be influencing the observed dynamics, such as shifts in the timing and intensity of RSV epidemics, e.g., due to nirsevimab introduction, which are thought to be closely interrelated with influenza circulation [174], [175]. In addition, meteorological variations may also contribute to the altered epidemic structure. Notably, reporting biases linked to

holiday periods, particularly around Christmas when influenza often peaks, must also be taken into account.

Despite these complexities, meteorological conditions remain a fundamental driver of influenza transmission. In temperate climates, such as those in the northern hemisphere, influenza follows a highly predictable seasonal cycle, peaking during the winter months when colder temperatures, lower absolute humidity, and increased indoor crowding facilitate viral transmission (see [Section 1.2.1](#)) [31]. In Catalonia, the influenza season typically extends from November to April, though variations in timing and intensity occur annually, probably due to changes in viral evolution, vaccination coverage, and/or environmental conditions [176], [177].

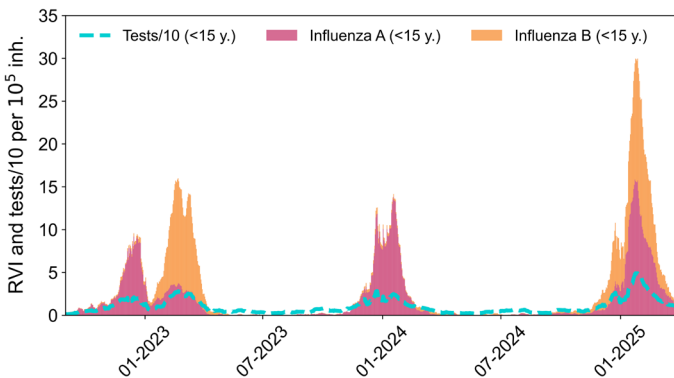


Figure 4.2. Evolution of incidence of diagnostic effort and viral detection of influenza A and B with RAT in Catalonia for children <15 years old, from September 2021 to March 2025. Test incidence is provided in tests per 10^6 instead of 10^5 to maintain scale with viral incidence.

Still, these seasonal patterns are largely influenced by environmental factors, as they affect both virus stability and host susceptibility (see [Section 1.2.1](#)). As stated, in temperate regions, influenza typically peaks during the colder months, when absolute humidity (AH) is low. However, in tropical climates, influenza transmission behaves differently, with outbreaks occurring in a less predictable, non-seasonal trend. In these regions, influenza activity is often correlated with periods of high humidity and rainfall rather than temperature drops. For example, in Panama, influenza does not follow a fixed seasonal cycle but is

instead aligned with the rainy season, a pattern also observed in other equatorial regions [178], [179]. This seems to be contradictory, as both high and low AH correlate with influenza cases: low AH can dry out the mucosal surfaces of the respiratory tract, impairing the first line of immune defence and making it easier for viruses like influenza to enter and infect host cells; but high AH creates an environment that can support viral stability and replication, particularly in tropical regions ([Section 1.2.1](#)). Thus, both extremes of AH (low in temperate winters and high during tropical rainy seasons) may facilitate different aspects of influenza transmission. All things considered, this behaviour reinforces the hypothesis that meteorological conditions play a central role in shaping influenza transmission dynamics; maybe not only due to the effects they have on viruses and hosts, but because these associations may reflect behavioural changes during such weather conditions. Cold or rainy days often result in increased indoor crowding, reduced ventilation, and closer interpersonal contact, all of which facilitate viral spread and may act as indirect drivers of seasonal influenza epidemics.

Meteorological conditions play a key role in shaping influenza dynamics: not only due to their effects on viruses and hosts, but because of the behavioural changes they entail to the society.

The global diversity in influenza seasonality highlights the importance of region-specific surveillance and tailored public health strategies. While temperate regions benefit from well-established vaccination schedules aligned with seasonal epidemics, tropical and subtropical areas require more flexible approaches to vaccination timing and outbreak preparedness. Furthermore, climate change and immunisation strategies – both for influenza and for other viruses such as RSV – may alter the future landscape of influenza epidemiology, potentially shifting transmission patterns in both temperate and tropical settings.

4.3.1. Children as the drivers for influenza epidemics

As previously mentioned, children are often considered superspreaders of influenza, playing a central role in the propagation of seasonal epidemics. To

critically assess this widely held assumption, we analysed influenza diagnosis data from PCPs in Catalonia, obtained from the SIVIC surveillance system.

Methods

Data gathering and pre-processing

We retrieved daily influenza case data spanning ten influenza seasons, from 2014-2015 to 2024-2025 (since season 2020-2021 did not occur due to the COVID-19 pandemic). The data were pre-processed following the procedures detailed in [Section 2.2](#). Age groups considered were 0-11 months old, 1-2 years, 3-4 years, 5-14 years, 15-44 years, 45-59 years, 60-69 years, 70-79 years and 80+ years old, in accordance with SIVIC data visualisations.

Statistical analyses

Three complementary analyses were conducted in Python. First, we computed a lagged Pearson correlation with a 60-day window (30 in advance and 30 in delay), between the different age groups and the general population epidemic for each season after z-normalising the curves. The goal was to determine which age groups experienced the epidemic peak first. Secondly, we calculated the daily proportion of incidence by age group relative to the total incidence of cases on that day. This was examined within a temporal window of four weeks before and after the crossing of the epidemic threshold, as defined in [Section 2.2](#), and in the same time span but for the epidemic peak of the general population infections. We use incidence instead of cases to normalise by population to avoid bias from larger age cohorts contributing more simply because they are more numerous. Consequently, values can exceed 100% for the age groups experiencing the highest disease burden and potentially the greatest role in epidemic propagation. Thus, to ensure comparability across seasons, the percentages were normalized so that the sum of all age-group contributions equalled 100% per season. This normalization facilitates a clear visualization of the age-specific distribution of influenza cases over time. Additionally, we calculated the seasonal burden of disease by age group, using the proportion of incidence relative to the total seasonal incidence. Finally, we assessed which age group reached 5% of its total seasonal cases first. For

these analyses, the 2024-2025 season – still ongoing at the time of writing – was considered complete as of March 2025. All other seasons were analysed from the first to the last day above the daily epidemic threshold established for the general population, which is of 1 case per 100,000 inh. ([Section 2.2](#)).

Results and discussion

First of all, we displayed the daily diagnoses of influenza for the different age groups from September 1st, 2014 to March 31st, 2025 in [Figure 4.3](#). Notice that season 2020-2021 did not happen, as explained, because of the COVID-19 pandemic. Besides, season 2021-2022 was not during the regular months of influenza epidemic, but it was delayed to spring 2022, followed by a 2022-2023 season showing its characteristic dual peak because of the epidemics created by influenza strains A and B.

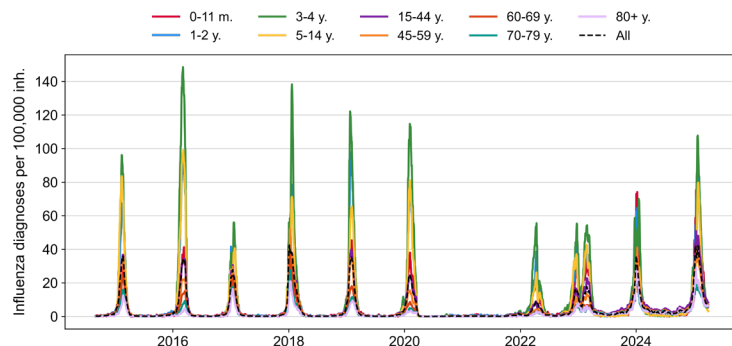


Figure 4.3. Historical evolution of influenza daily infections per 100,000 inhabitants in Catalonia, per age range, from September 2014 to March 2025.

Undoubtedly, the greatest burden of disease is carried by 3-4 years old, reaching incidences greater than 100 cases per 100,000 inhabitants, and usually followed in incidence by 5-14 years old children. However, they do not seem to be the first to reach the epidemic peak. By computing the lagged correlation between age groups for each season, we were able to determine which age groups experienced the epidemic peak first. These results are presented in [Figure 4.4](#), where the heatmaps display the Pearson correlation coefficients for each age group compared to the general trend.

Chapter 4 – Influenza: Epidemiology of influenza

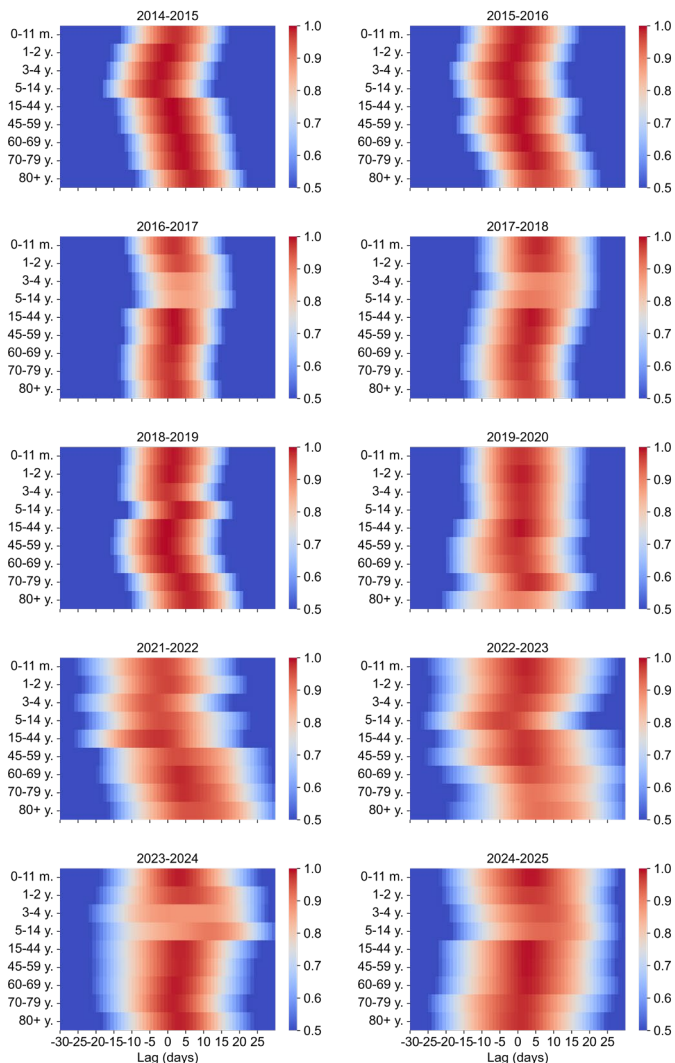


Figure 4.4. Seasonal heatmap of the lagged correlation in a 60-day window (30 in advance and 30 in delay) between the epidemic of each age group and the general epidemic for the total population. Blue is the lowest correlation (0.5) and dark red the highest (1.0). Negative lags correspond to advancement and positive lags to delay.

The darkest shade of red represents the highest correlation. Interestingly, there are no clear patterns on which age group reaches the epidemic peak first; however, the 3-4 years old group is usually the most advanced. Nonetheless, adults (15-59 years) have shown earlier epidemics in several seasons, such as 2017-2018, 2018-2019, and 2019-2020. Even when young children (1-4 years) are the first to reach the epidemic peak, a similar trend is observed in adults, particularly within the 45-59 years-old group, as evidenced in the 2015-2016, 2016-2017, 2021-2022, and 2022-2023 seasons. This suggests that infections in children and their parents may be closely linked, although further analysis is required.

However, our analysis has limitations. Firstly, it is based on clinical diagnoses that are not laboratory-confirmed across all age groups. While children are typically tested using RAT in primary care from 2021 onwards [107], making their diagnoses more reliable, this is not consistently the case for adults. As a result, some adult cases recorded as influenza may actually be due to other respiratory pathogens. Consequently, the conclusions drawn apply only to clinical diagnoses of influenza. Furthermore, the data are grouped into broad age ranges, meaning that a more detailed analysis could be conducted using more disaggregated data, or even patient-level data, rather than population-level data, which would allow for a precise identification of familial relationships or household transmittal patterns. These limitations carry through to the subsequent analyses presented in this section.

To analyse deeper the age group carrying the influenza epidemic each season, we computed the normalized percentage of incidence during the whole epidemic ([Figure 4.5](#)) to see which has the greatest burden of disease, and during the four weeks before and after crossing the epidemic threshold ([Figure 4.6](#)) and the epidemic peak ([Figure 4.7](#)) to ascertain which epidemic starts first and which age group dominates during the epitome of the season. Once again, the age groups consistently showing the greatest burden of disease are children aged 1 to 14 years (paediatric patients, though notably not the youngest). This could be because infants are primarily affected by RSV, which could help

explain the increasing prominence of these 0-11 months old infants in influenza incidence following the COVID-19 pandemic.

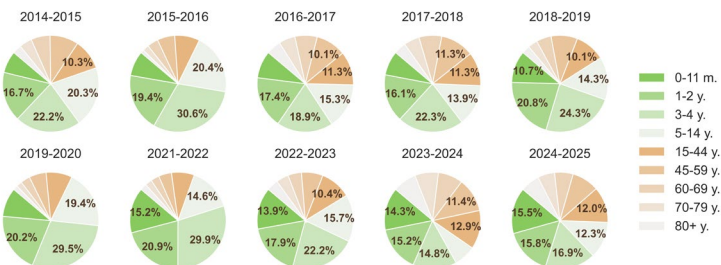


Figure 4.5. Normalized percentage of incidence of influenza disease carried seasonally by each age group. Numbers are shown for ratios greater than 10%.

This shift may be partially attributed to an immunity debt as a result of a naïve immune system during the pandemic years [180], as well as to the introduction of nirsevimab in 2023, that offers immunisation against RSV in infants [105], [181], [182]. But what has nirsevimab to do with influenza epidemics? Well, prior to the availability of nirsevimab, coinfections between RSV and influenza were uncommon, likely due to RSV outcompeting influenza in cases of viral interference [174], [183]. In fact, RSV epidemic is usually a precursor of the influenza epidemic [184]. A plausible hypothesis is that, following the rollout of nirsevimab, coinfections could have become more frequent, raising the possibility that influenza may now have a competitive advantage in these dual infections. Nevertheless, the analysis of epidemiological data remains to be done and there is no published literature supporting this at the moment.

On another note, even though children have the greatest burden of influenza, they do not seem to be the initiators of influenza epidemics in Catalonia. As **Figure 4.6** shows, during the 4 weeks before and after the day when the epidemic threshold is surpassed, adults (population > 14 years) are the population groups with the greatest burden of disease, except for season 2022-2023. Besides, the last two seasons 2023-2024 and 2024-2025, it is clear that people ≥80 years have gotten an increasing importance in the beginning of the epidemic, while the paediatric age groups do not even reach the 30% of relative incidence in the first weeks analysed.

Chapter 4 – Influenza: Epidemiology of influenza

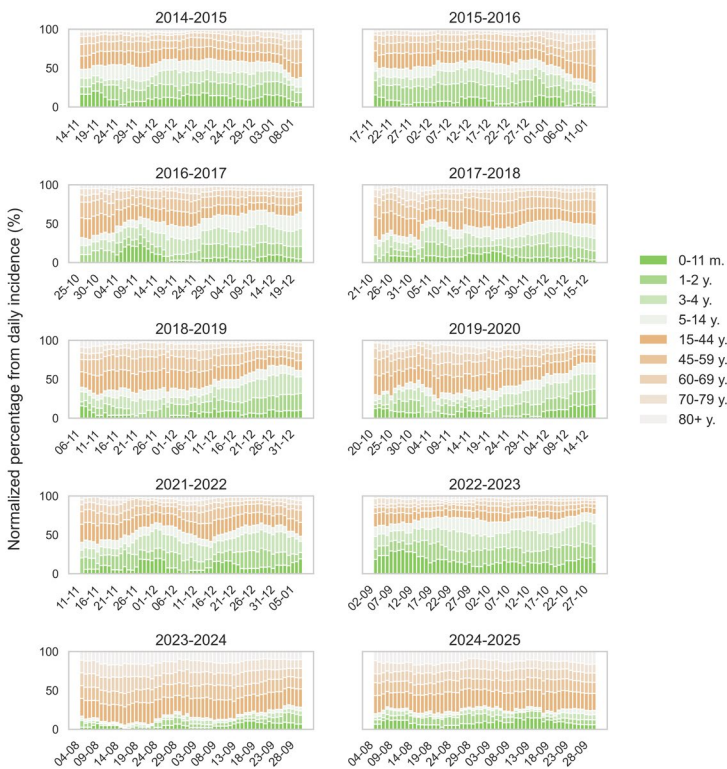


Figure 4.6. Representation of the normalized percentage of daily incidence per age group in an exploration of the 4 weeks prior and post epidemic threshold surpassing per season.

However, around the epidemic peak, this pattern gets inverted ([Figure 4.7](#)). Children dominate more than 50% of the epidemic weight surrounding the epidemic peak, even reaching 80% in all seasons but 2016-2017, 2017-2018, 2023-2024 and 2024-2025. Interestingly, vaccination rates for influenza have decreased these last two seasons [185], while data before 2020 is unavailable. This is verified when checking the first age group to reach the 5% of its total cases each season, reported in [Table 4.1](#), where it is clear than from the 10 seasons studied, the 70% of the times adult age groups are the first to reach

5% of the total epidemic cases, showing that they are more advanced in their epidemic season.

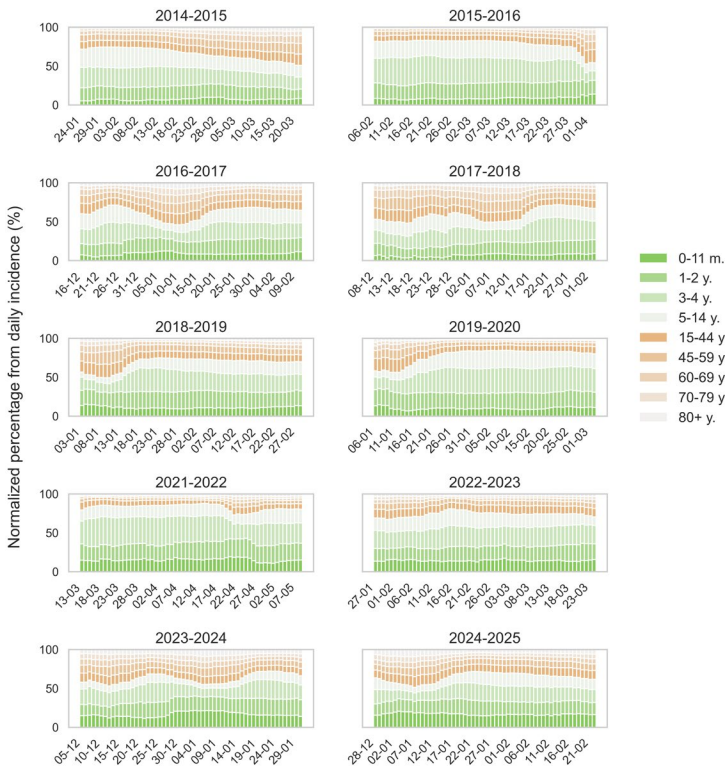
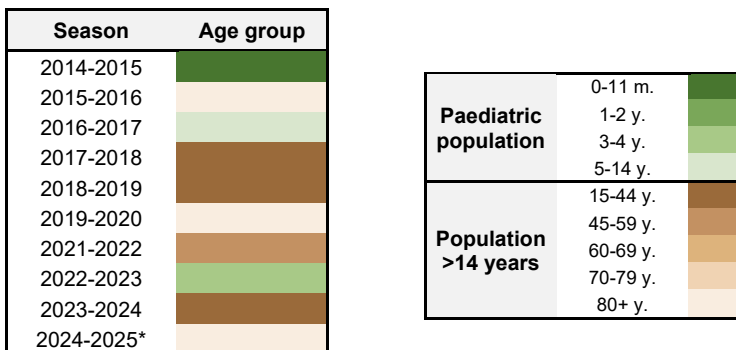


Figure 4.7. Representation of the normalized percentage of daily incidence per age group in an exploration of the 4 weeks prior and post epidemic peak per season.

Notwithstanding this, it is to note that the same incidence threshold has been considered for post pandemic epidemics than for pre-pandemic ones. Since after the COVID-19 pandemic there has been a higher level of basal clinical diagnoses of influenza, for seasons after 2022-2023 the epidemic threshold is surpassed in September, while for the previous seasons the mean month of epidemic start was November. This has a relevant implication, since schools are not open yet in early September hence the transmission of influenza among

infants is less probable. Although, this could be considered another argument for that children are not the initiators of the influenza epidemic – despite being very much affected by it – but the first detections of influenza occur in the older age groups.

Table 4.1. Table representing the first age group to reach the 5% of its total cases per season. Each age group is represented by a colour, green scale for children and brown scale for adults. Season 2024-2025 has an “*” as it is incompletely at the moment of writing this thesis.



To summarise

After analysing data on influenza disease incidence in primary care, we reached the conclusion that although children suffer the greatest burden of the influenza seasonal epidemics, they are not their main initiators.

4.4. Modelling the influenza epidemic

Given the significant health and economic burden posed by seasonal influenza epidemics globally, considerable attention has been devoted to developing models capable of predicting not only the onset of epidemics [186] but also their overall trajectory and peak intensity [187], [188], [189]. A variety of modelling approaches have been employed for this purpose [190]. Among the most widely used are mechanistic models (see [Section 1.4.2](#)), such as SIR and SEIR frameworks [191], [192], [193], but empirical models (see [Section 1.4.1](#)) like the logistic equation, regression or Bayesian models, are not the most common approach [190], [194]. In recent years, AI-based models have gained popularity [195], [196], although they often require extensive historical datasets that are not always available or accessible. While these existing models have been proven effective, many tend to be overly complex, with a level of sophistication that does not always strike an ideal balance between complexity and performance, and that can even present overfitting issues. Besides, a great proportion of the current literature focuses on anticipating hospitalizations, whereas primary care remains largely unexamined. Moreover, in Catalonia, predictive modelling tools had not been implemented within the public health system. In this section, we present the two modelling strategies developed and provided to the Catalan Public Health Secretariat to support epidemic preparedness and anticipate influenza epidemic peaks in the post-COVID-19 context.

4.4.1. Empirical modelling of influenza epidemics

Unlike hospitalization-based forecasting models, which rely on delayed and highly selective datasets, empirical models ([Section 1.4.1](#)) can be effectively applied to primary care data, offering timely predictions that reflect real-time disease circulation in the general population. To assist public healthcare managers in Catalonia for decision-making and inform healthcare providers of the epidemiological situation and perspectives, we aimed to streamline the modelling process for real-time prediction, focusing on a simpler, more balanced approach that maintains accuracy without unnecessary intricacy and that is suitable for influenza epidemics in primary care settings: the Gompertz

model ([Section 1.4.1](#)). While this model has been widely used in epidemic modelling, hereby we present the first application of the Gompertz model to primary care data for influenza in Catalonia. This simplification has proven effective in previous studies [67], [79], and it is under review for publication at the moment of writing.

Methods

Data gathering

We used publicly available data on daily clinical diagnoses of influenza across the entire Catalan population, covering the period from September 1st, 2018, to August 31st, 2024. Additionally, we collected annual data on the reference population corresponding to these diagnoses. All data were sourced from the SIVIC system [61] ([Section 1.3.1](#)).

The influenza dataset includes all age groups, reflecting the virus's broad impact on the general population. Although this thesis is focused on the paediatric population, developing separate models for each age group would not necessarily enhance accuracy, as larger datasets improve model performance, and influenza affects all the population indiscriminately. Notably, children consistently exhibit the highest incidence rates. Therefore, a model based on the entire population serves as an effective tool for epidemic surveillance and prediction, including for paediatric populations, which are intrinsically linked to broader community transmission dynamics.

Data pre-processing

The data pre-processing for influenza was described in [Section 2.2](#). A season was defined as September one year to August the next, but for modelling purposes, we used as starting and end points the first and last dates, respectively, where the medium epidemic threshold ([Section 2.2.1](#)) was reached, which corresponds to daily 7 cases per 100,000 inh. for influenza.

Modelling epidemics

We adjusted seasons 2018-2019, 2019-2020 and 2023-2024 to the Gompertz model, as defined in [Section 1.4.1](#). We use this model because it is an empirical

model, but it is not merely a fit; it identifies the presence of a phenomenon whose rate of change decreases exponentially with time. This is the reason why we find the Gompertz model advantageous in front of the logistic model, for instance, which inflection point occurs at 50% of the final case count. The Gompertz model allows for an earlier inflection point, making it more realistic for respiratory diseases where the growth rate slows down before reaching half of the total cases, as it is the case for the influenza disease. For real-time prediction, this difference is crucial, as the Gompertz model better anticipates changes in transmission rates early in the epidemic, improving peak estimation.

Similarly as reported in Català, M. et al. [67], we computed the estimated empirical reproductive number at the beginning and throughout the epidemics, following:

$$\rho(t - \tau) = \frac{\frac{dN(t)}{dt}}{\frac{dN(t - \tau)}{dt}} = \frac{\frac{K \cdot a \cdot \ln\left(\frac{K}{N_0}\right) \cdot e^{-\ln\left(\frac{K}{N_0}\right) \cdot e^{-a \cdot t}} \cdot e^{-a \cdot t}}{K \cdot a \cdot \ln\left(\frac{K}{N_0}\right) \cdot e^{-\ln\left(\frac{K}{N_0}\right) \cdot e^{-a \cdot (t - \tau)}} \cdot e^{-a \cdot (t - \tau)}}}{\frac{e^{-\ln\left(\frac{K}{N_0}\right) \cdot e^{-a \cdot (t - \tau)}} \cdot e^{-a \cdot (t - \tau)}}{e^{-\ln\left(\frac{K}{N_0}\right) \cdot e^{-a \cdot (t - \tau)}} \cdot e^{-a \cdot (t - \tau)}}} \quad \text{Eq. 4.1. } \checkmark$$

Namely, ρ the empirical reproductive number estimation defined as the number of newly infected divided by the number of newly infected τ days ago, where τ is the incubation period, hence $\tau = 2$ for influenza [118].

The reproductive number, which represents the average new infections by each case, typically decreases along the epidemic progression, from an initial $\rho_0 = \rho(t \rightarrow 0)$ to a number below one once the epidemic peak is reached, representing a decrease in the ratio of new diagnoses.

We transformed the new daily infections data into daily cumulative diagnoses and used the `curve_fit` function in the `optimize` package of Python v.3.12.7, adding empirically chosen bounds to our adjustments. To determine the predictive ability of the model, we iteratively added data for adjustment until the day of the epidemic peak was reached. To evaluate the model's fit, we used the R^2 metric for adjustments and assessed its accuracy in predicting the week of the peak (`wop`) and daily peak magnitude. Additionally, we computed the mean

absolute percentage error (MAPE) to measure predictive accuracy. Given the stochasticity in daily reported diagnoses, we focused on weekly peak magnitude (wM) as a predictive metric together with the wop , as it provides more actionable information for public health professionals. However, we included daily peak magnitude in our evaluation of the global adjustments to offer a higher-resolution assessment of the model's performance.

The model adjustments were performed on a daily basis, while predictions were expressed on a weekly scale to align with the weekly framework of publicly available data. For the prediction phase, we established parameter boundaries based on the minimum and maximum values derived from prior adjustments for the same disease. This approach assumes consistency in epidemic dynamics across seasons for a given disease. However, an exception was made for the 2023-2024 season, because there are disruptions on the regularity of the epidemic caused by the COVID-19 pandemic. Under normal circumstances, parameter boundaries are adjusted iteratively to reflect new data, making seasonal adjustments a standard part of the methodology. For this study, we assessed the accuracy of predictions at 32, 30, 28, 21, 14, 7 and 0 days prior to the peak. Broader time delays could not be evaluated due to the limited duration of the growth phase leading up to the peak. Some of the time delays could not be assessed for certain seasons for the same reason.

Results and discussion

Full-season Gompertz fittings

The Gompertz model was adjusted for all non-pandemic seasons of study. Results for seasons 2018-2019, 2019-2020 and 2023-2024 can be seen in [Figure 4.8](#), [Figure 4.9](#) and [Figure 4.10](#), respectively. The parameters values for all epidemics are reported in [Table 4.2](#).

Interestingly, the 2019-2020 influenza season saw significantly fewer cases than 2018-2019, whereas the 2023-2024 season exhibited a similar epidemic magnitude. This trend may be linked to the emergence of SARS-CoV-2, which could have altered the influenza epidemic dynamics. Additionally, NPIs

implemented to control the COVID-19 pandemic may have also influenced the spread of other respiratory viruses.

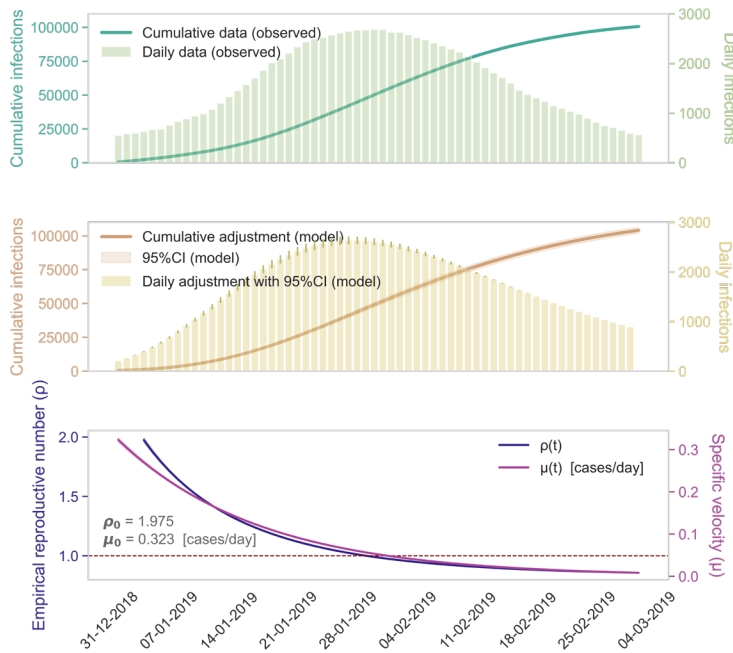


Figure 4.8. Gompertz model adjustments for influenza season 2018-2019. Top panel: influenza diagnoses counts, considering daily and cumulative counts. Middle panel: fitted model outcome in terms of cumulative and daily counts. Bottom panel: model-derived specific growth rate and empiric reproductive number, with their initial values; the dotted line represents the $\rho = 1$ threshold, that stands for the inflection point of decrease in caseload.

Another notable impact of the pandemic is the altered epidemic growth and decline rates. Influenza now exhibits slower initial growth rates (μ_0) and prolonged decline phases, leading to broader epidemics despite their overall magnitude remaining similar to or exceeding pre-pandemic levels. This slower progression may explain why clinicians perceived post-pandemic epidemics as more severe, even when case numbers were comparable to past seasons.

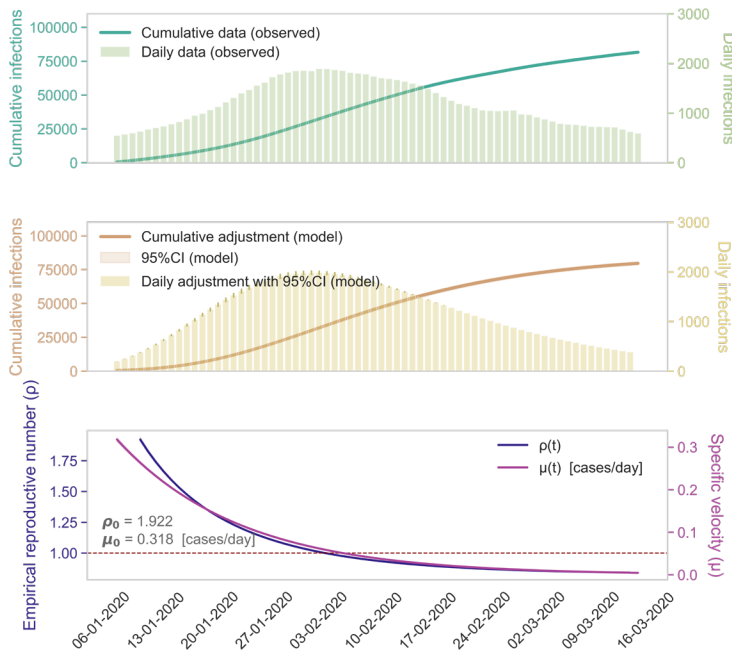


Figure 4.9. Gompertz model adjustments for influenza season 2019-2020. Top panel: influenza diagnoses counts, considering daily and cumulative counts. Middle panel: fitted model outcome in terms of cumulative and daily counts. Bottom panel: model-derived specific growth rate and empiric reproductive number, with their initial values; the dotted line represents the $\rho = 1$ threshold, that stands for the inflection point of decrease in caseload.

Influenza cases decline fast, resulting in a more symmetrical epidemic that spans a shorter time frame. Besides, estimates of the empirical reproduction number indicate that each influenza case results in only two secondary infections. To compare this result with a better known one, the empirical reproduction number estimates for COVID-19 at the beginning of the pandemic in Spain were 2 to 4 depending on the autonomous community [197].

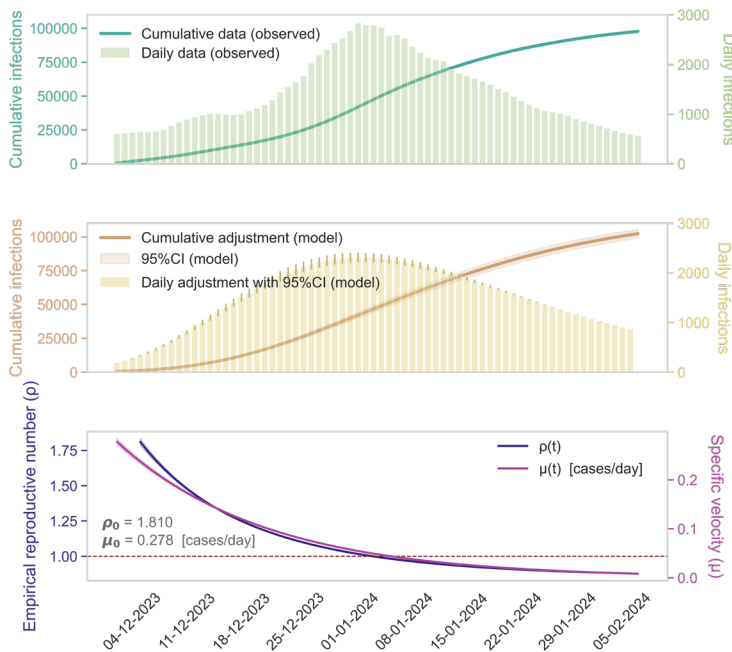


Figure 4.10. Influenza diagnoses Gompertz model adjustments for season 2023-2024. Top panel: influenza diagnoses counts, considering daily and cumulative counts. Middle panel: fitted model outcome in terms of cumulative and daily counts. Bottom panel: model-derived specific growth rate and empiric reproductive number, with their initial values; the dotted line represents the $\rho = 1$ threshold, that stands for the inflection point of decrease in caseload.

Table 4.2. Parameter values for the Gompertz model adjustment of influenza. The last two columns show the values of empirical reproductive number and specific growth rate at the onset of the fitted epidemic curve.

Season	K (cumulative cases)	a (day ⁻¹)	ρ_0	μ_0 (cases·day ⁻¹)
2018-2019	119,588 (117,772-121,403)	0.060 (0.059-0.061)	1.975	0.323
2019-2020	85,880 (84,965-86,794)	0.063 (0.062-0.064)	1.922	0.318
2023-2024	119,824 (117,112-122,535)	0.052 (0.051-0.053)	1.810	0.278

These conclusions have been extracted from the adjustment's parameters, that are as rigorous as to observe $R^2 > 0.99$ in all cases. The model also accurately adjustes to the wop for all epidemic. Also, the peak magnitude is slightly underestimated. Specifically, the model underestimates the peak magnitude by

19% in season 2023-2024. Although the results vary by season, they demonstrate consistency in capturing the correct week of the peak, with errors in magnitude typically less than 5% across all other seasons, as detailed in **Table 4.3**. The magnitude underestimation is computed based on the day the peak in reported cases is reached, which is highly stochastic due to irregularities in case reporting. However, visually, the model captures the peak quite well in general terms.

Table 4.3. Adjusted and observed week and magnitude (in daily cases) of the peak per season and disease, depending on the data used for forecasting defined as days before the epidemic peak. R^2 of the adjustments.

Season	Adjusted wop	Observed wop	Weeks of delay	Adjusted magnitude	Observed magnitude	Difference in magnitude (%)	R^2
2018-2019	2019-W6	2019-W6	0	2638.36	2685.13	-1.7	0.998
2019-2020	2020-W6	2020-W6	0	1986.79	1892.93	5.0	0.998
2023-2024	2024-W2	2024-W2	0	2310.68	2837.66	-18.6	0.997

The discrepancies obtained could be influenced by differences in diagnostic behavior at the epidemic peak, as well as healthcare system capacity constraints. In some cases, peak days coincide with high healthcare demand, potentially leading to underreporting due to saturation or reporting delays. Moreover, notably, the pre-pandemic seasons are adjusted with greater accuracy, which suggests that after the pandemic the Gompertz model may not be able to fully capture disease dynamics, or that the adjustment should be started in a different threshold since we are dealing with a different scenario. Aligned with this, an unusual trend is observed in the influenza data during the 2023-2024 season, where the flu case numbers do not follow the typical pattern, as influenza cases normally decline to zero by the spring, but season 2023-2024 has a clear onset compared to previous epidemics.

Predictive performance of Gompertz model

In **Table 4.4**, we summarize the predictive accuracy of the model, reporting the predicted week of peak at each iteration as well as its magnitude and comparing these values to the observed data. We show the accuracy obtained in the simulation of real-time successive predictions, from one month before the peak

onwards. We also provide the MAPE of each adjustment. A plot of the model prediction per each iteration and the parameters values evolution are also reported in [Figure 4.11](#) to [Figure 4.16](#).

Table 4.4. Predicted and observed week and maximum magnitude (in terms of weekly diagnoses, wM) of the peak per season and disease, depending on the data used for forecasting defined as days before the epidemic peak. MAPE of the adjustments.

Season	Days before peak	Predicted wop	Observed wop	Weeks of delay	Predicted wM	Observed wM	Difference in magnitude (%)	MAPE (%)
2018-2019	28	2019-W5	2019-W6	-1	19,090	18,532	3.01	9.10
	21	2019-W5		-1	19,090		3.01	9.10
	14	2019-W5		-1	19,090		3.01	9.10
	7	2019-W5		-1	18,011		-2.81	6.78
2019-2020	21	2020-W6	2020-W6	0	18,858	12,773	47.64	31.00
	14	2020-W6		0	18,858		47.64	31.00
	7	2020-W6		0	16,115		26.16	17.76
2023-2024	28	2024-W1	2024-W2	-1	16,662	18,863	-11.67	12.21
	21	2024-W1		-1	16,662		-11.67	12.21
	14	2024-W1		-1	16,662		-11.67	12.21
	7	2024-W1		-1	14,825		-21.41	11.95

For most seasons, our model successfully predicts the epidemic peak week, with an error margin of only one week, even with a one-month anticipation, always predicting the peak earlier than the actual occurrence. This early prediction provides public health authorities with a crucial window to act and allocate resources effectively to mitigate the epidemic's impact. Furthermore, the error in the predicted magnitude of the peak is mostly below 15% when predictions are made 28 days in advance and below 10% 21 days in advance.

An exception to this trend is seen in the 2019-2020 season, which was affected by the arrival of the COVID-19 pandemic, disrupting the usual influenza patterns. In addition, in the 2023-2024 season we see how the magnitude is progressively less well captured. This could be due to a diverging trend on the number of basal influenza cases but also on its growth that could be related to the pandemic's lasting effects. A reason behind the higher number of basal influenza reports might be that people are now more likely to visit PCPs than before 2020, leading to more cases being recorded.

Chapter 4 – Influenza: Modelling the influenza epidemic

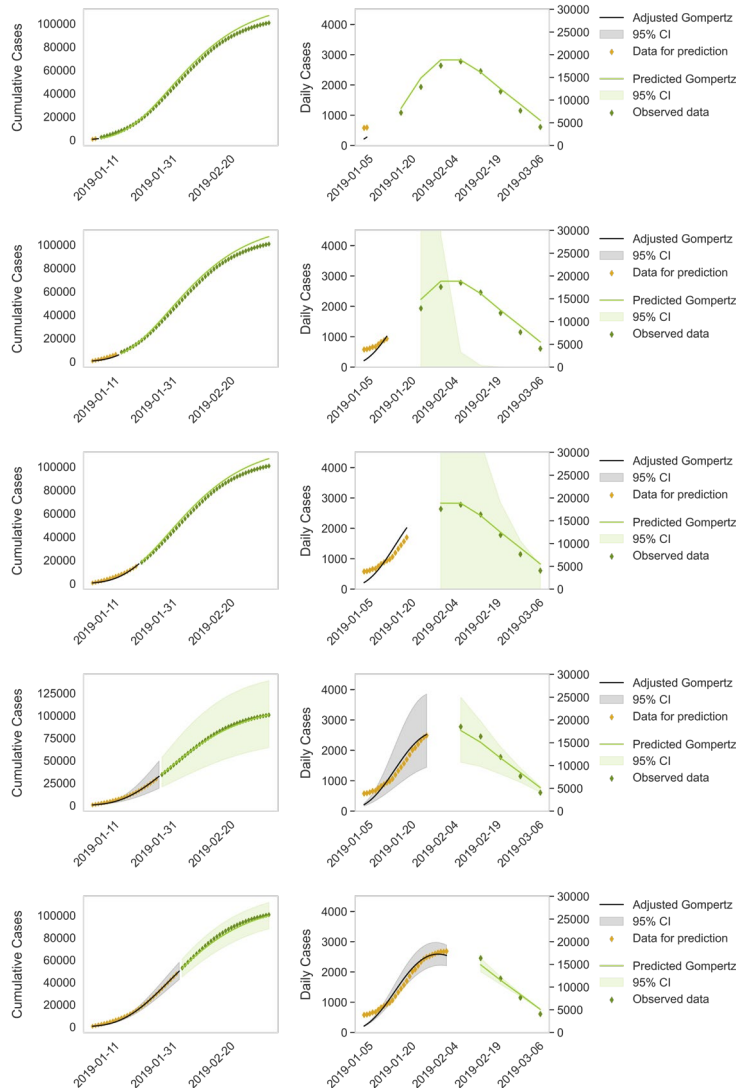


Figure 4.11. Iterative adjustment and predictions for 2018-2019 season of influenza. From top to bottom, iteration with data for prediction of 28, 21, 14, 7 and 0 days until the peak.

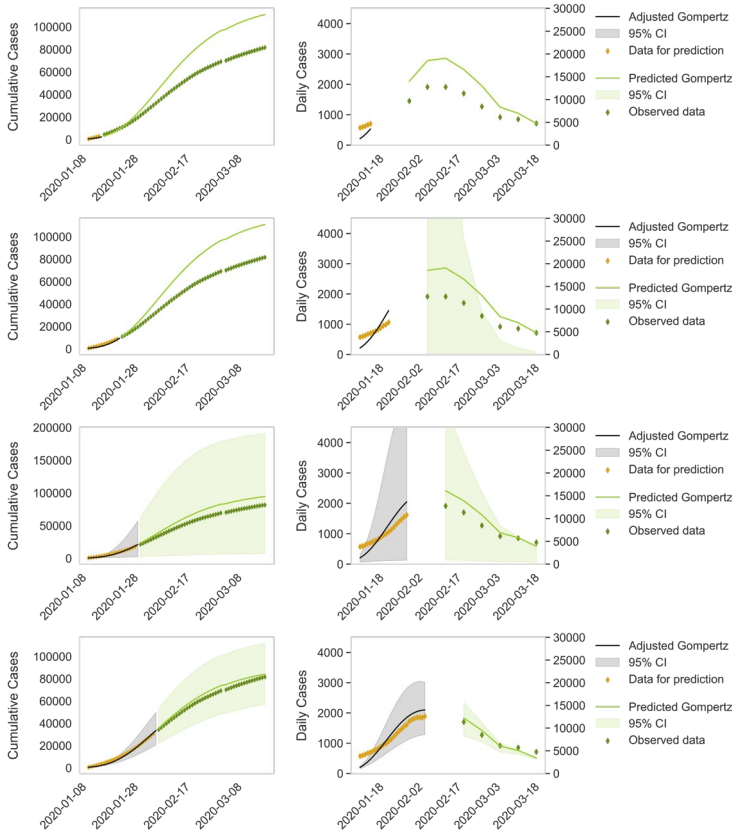


Figure 4.12. Iterative adjustment and predictions for 2019-2020 season of influenza. From top to bottom, iteration with data for prediction of 21, 14, 7 and 0 days until the peak.

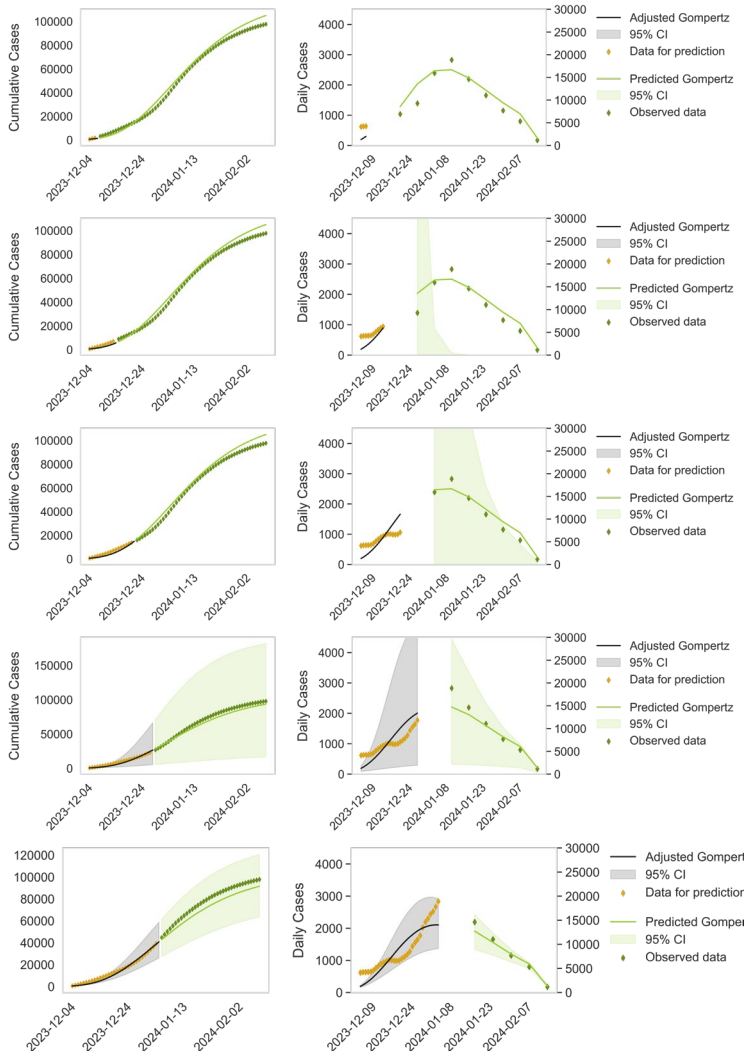


Figure 4.13. Iterative adjustment and predictions for 2023-2024 season of influenza. From top to bottom, iteration with data for prediction of 28, 21, 14, 7 and 0 days until the peak.

Also, as explained in [Section 4.3](#), changes in the RSV season during 2023–2024 – possibly due to the introduction of nirsevimab – may have played a role in changing how the influenza spread that year. Notably, the true magnitude of the peak lies within the confidence intervals of the prediction for all seasons ([Figure 4.11](#) to [Figure 4.13](#)).

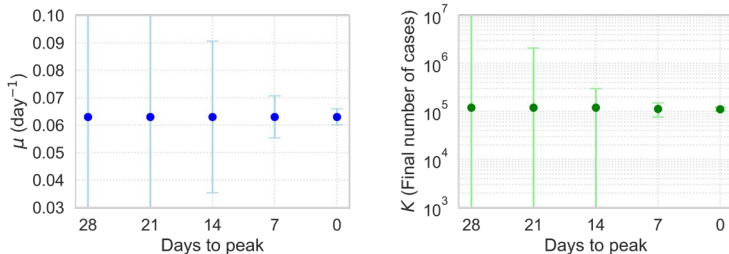


Figure 4.14. Parameter values evolution for the iterative adjustment and predictions for 2018-2019 season of influenza. Parameter K values are shown in a logarithmic axis.

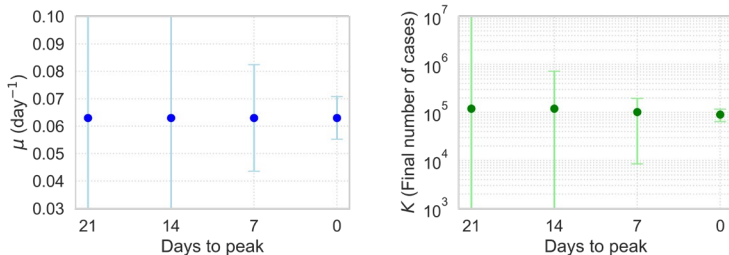


Figure 4.15. Parameter values evolution for the iterative adjustment and predictions for 2019-2020 season of influenza. Parameter K values are shown in a logarithmic axis.

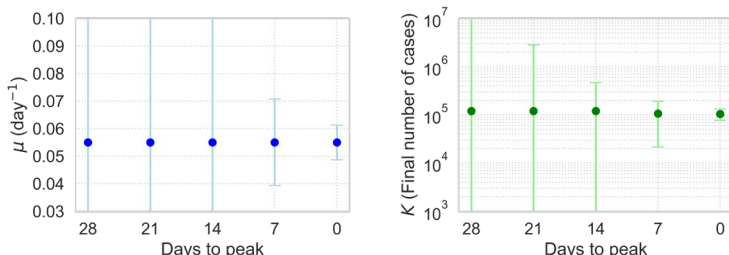


Figure 4.16. Parameter values evolution for the iterative adjustment and predictions for 2023-2024 season of influenza. Parameter K values are shown in a logarithmic axis.

It is important to highlight that the presence of outliers, likely resulting from irregularities in case reporting, can create discrepancies in identifying the true epidemic peak. These outliers often result from delays in data aggregation, sudden spikes due to reporting corrections, or local outbreaks that are not representative of the broader epidemic trend. When the peak is defined by the single highest reported daily case count, it may differ from the model's prediction, which more accurately reflects the epidemic's wave-like progression. However, the model's prediction remains accurate, as the outlier occurred during the week with the highest total reported cases, which is the basis for evaluating predictions. A similar effect is observed for the peak magnitude, since while reported data may fluctuate due to stochastic irregularities, the model provides a more accurate estimation of the epidemic's true impact. In fact, in all seasons the observed cases consistently fall within the confidence intervals of the model's predictions.

In addition, it is worth noting that the MAPE metric reaches up to 30% for all epidemic seasons when predicting 28 days before the peak. This result is based on fixed parameter boundaries across all iterations, whereas in real-life scenarios, these boundaries are typically adjusted manually to better fit new data. Consequently, while the maximum prediction error in this study is 30%, it would likely be significantly lower with human supervision, as it has demonstrated to be in a real-world scenario.

All things considered, the Gompertz model is a good approach to study influenza daily diagnoses data in primary care in Catalonia. These findings are critically important for providing public health managers with timely information, enabling them to take proactive measures to mitigate epidemics and reduce associated health risks and costs. Despite this, the study has some limitations. On one hand, we are using pre and post pandemic data, and as one can see in the value of the adjusted parameters, influenza post pandemic season was larger and slower than the pre-pandemic ones. The introduction of nirsevimab represents a significant change in RSV epidemiology but perhaps in influenza dynamics too, potentially altering transmission patterns, seasonal intensity and timing of the epidemic peak. This transformation poses new challenges for real-

time prediction, as past epidemic trends may not be directly applicable to future seasons. Another limitation of this study is that healthcare databases such as SIVIC often suffer from underreporting biases, which tend to be compensated over time. It is also important to note that influenza thresholds are computed in pre-pandemic data ([Section 2.2.1](#)). These thresholds should be yearly updated, but we assume them constant due to the restricted period in which to compute them. The starting point for modelling defined, as well as the parameter bounds for forecasting, will probably change from pre to post pandemic data once the epidemics stabilize, which has not happened yet. Post-pandemic seasons for influenza have a clear onset of cases compared to previous epidemics. That is, cases after the epidemic do not reach zero but a basal level. This anomaly may indicate that other respiratory viruses are being classified as influenza in the surveillance data or that after the pandemic there is a greater circulation of the virus. While we acknowledge this limitation as dealing with primary care diagnoses data, it is unlikely to affect the prediction of peak timing, as during the rise of the epidemic, the influenza virus remains the primary driver. Additionally, the increasing promotion of influenza vaccination in Catalonia, especially among children which suffer the greatest burden of disease ([Section 4.3.1](#)), could significantly impact epidemic dynamics over time, making it crucial to factor in these shifts as part of future models. The methodology developed in this study can be applied for other diseases such as RSV-bronchiolitis (see [Section 5.4](#)) and it has significant global applicability, as it can be adapted to different regions with varying healthcare structures and surveillance systems. In low-resource settings, where real-time primary care data may be incomplete, integrating syndromic surveillance systems or sentinel networks could enhance predictions. In countries with robust electronic health records (EHRs), linking primary care and hospitalization data could improve forecasting accuracy. By tailoring the model to local data sources, thresholds, and epidemiological patterns, the approach could support public health decision-making worldwide, fostering a proactive response to seasonal epidemics.

To summarise

The Gompertz growth equation can be applied to empirically model influenza epidemics, both before and after the COVID-19 pandemic. The epidemic peak can be predicted several weeks in advance, with only a week in advancement error margin. The magnitude of the epidemic is anticipated with less precision but covered within the 95% CI of the model. Human supervision is key to improve the model's performance, adjusting parameter boundaries following empirical data.

4.4.2. Mechanistic modelling of influenza epidemics

We have seen that empirical epidemiological models can be employed to model and forecast influenza, not only in Catalonia ([Section 4.4.1](#)) but in other countries, where mechanistic models have also been found useful [187], [188], [189], [190]. Despite significant advances, many uncertainties remain regarding the transmissibility of the influenza virus and its underlying drivers. One widely accepted hypothesis is that meteorological factors may influence influenza dynamics. Current state-of-the-art research links temperature (T), absolute humidity (AH) and relative humidity (RH) to the onset and transmissivity of influenza outbreaks in temperate and even some equatorial regions [16], [198], [199], [200], [201], [202], potentially explaining the seasonal epidemics that occur between November and March in these climates [177], [203], [204]. However, a study performed in Australia [205] presents conflicting evidence, challenging this association, which has not yet been quantified.

We explored the possibility of modelling influenza epidemics in Barcelona, the capital of Catalonia with 1.7 million inhabitants, using temperature and/or absolute humidity as primary drivers of disease transmissibility to better understand their relationship with influenza dynamics. While both AH and RH are influenced by temperature, AH provides a more direct measure of atmospheric moisture content, which has been shown to play a crucial role in viral stability and transmission (see [Section 1.2.1](#)). In contrast, RH is a relative measure that varies greatly with temperature fluctuations, making it a less informative variable.

Methods

Data gathering

We gathered data on daily influenza diagnoses in Catalonia's PCPs from September 1st, 2014 to May 31st, 2024 (both included), publicly available in SIVIC ([Section 1.3.1](#)) [61]. We have excluded the 2024-2025 season from this study, as the influenza epidemic had not yet concluded at the time of writing. These data are segregated by sanitary region, and we extracted the subset of diagnoses in Barcelona city. The use of regional data allows for high-resolution modelling within a well-characterized urban environment. Since SIVIC is updated every week, we considered the weekly basis as the time scale for the output of the model on its real-world application, like in the previous modelling studies presented. In addition, we obtained T and RH (codes 32 and 33 respectively) hourly daily data for the same study period from the public database XEMA (see [Section 1.3.1](#)) [62]. Meteorological data were obtained from three representative stations in Barcelona: the Barcelona Zoo (green area), el Raval (urban downtown), and Zona Universitària (low-density residential area) ([Figure 4.17](#)).

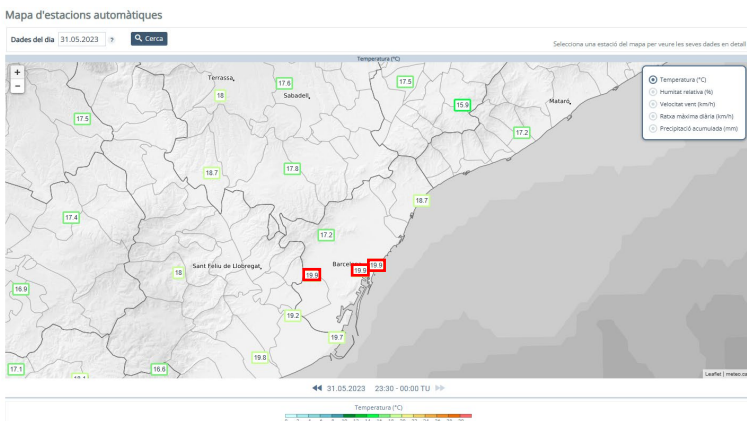


Figure 4.17. Map of the meteorological stations, highlighted in red the ones we used in our work, showing the temperature the day May 31st, 2023 at 23:30h. Retrieved from [206].

These stations were selected for their coverage of distinct urban zones within Barcelona city, while maintaining similar longitude, latitude, and altitude, ensuring comparable meteorological conditions [206].

Data pre-processing

Epidemiological data

We pre-processed the raw epidemiological data provided by SIVIC as explained in [Section 2.2.1](#). Usually, this kind of data has reporting biases that depend on whether the day when the patient was visited by the doctor was a workday or festive. Besides, the last 30 days of data are usually incomplete as delayed reporting of cases are common. We accounted for those biases in our pre-processing strategies, performing a pattern analysis and weighting the data. Once we obtained the weighted diagnoses, we applied a final last-7-day average filter to the data for smoothing purposes. While these steps mitigate short-term fluctuations and reporting inconsistencies, residual biases may still impact model predictions.

An epidemic season was defined as spanning from 1st September of one year to 31st August of the following year. The seasons 2020-2021, 2021-2022, and 2022-2023 were excluded from this study due to their distinct characteristics compared to pre-pandemic seasons, because of the short and mid-term impacts of the new SARS-CoV-2 circulation, together with the NPI that were in-place for several months. Specifically, the 2020-2021 season did not experience an influenza epidemic, the 2021-2022 season marked the first post-pandemic epidemic and was characterized by an out-of-season low number of infections, since there were still some NPI measures applied, and the 2022-2023 season exhibited a dual epidemic peak due to consecutive outbreaks of influenza A and influenza B, probably due to a higher number of people susceptible to infection as a result of the previous two scarce epidemics. In contrast, the 2023-2024 season was included in the analysis due to its alignment with pre-pandemic epidemic patterns ([Figure 4.18](#)).

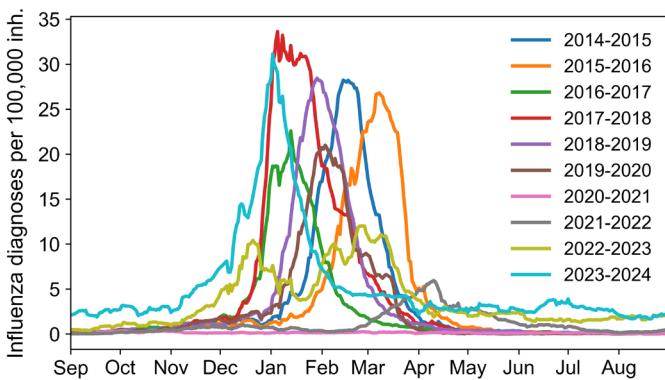


Figure 4.18. Influenza epidemics in Catalonia from 2014-2015 to 2023-2024, layered one on top of the other.

Meteorological data

To convert the hourly data from XEMA into daily estimates, we computed the daily mean temperature and RH for each observatory. The daily city-wide average for Barcelona is then derived as the arithmetic mean of the three observatory-specific daily values. For smoothing purposes, we applied a 7-day moving average filter to the data, afterwards. Finally, we computed absolute humidity from the previous variables combining Eq. 4.2 with the Clausius-Clapeyron equation in Eq. 4.3 [207] which results in the following Eq. 4.4:

$$AH = \frac{eM_{H_2O}}{R \cdot T} \quad \text{Eq. 4.2. } \checkmark$$

$$\epsilon = \epsilon_0 e^{\left[\frac{L}{R_v} - \left(\frac{1}{T_0} - \frac{1}{T} \right) \right]} \frac{RH}{100} \quad \text{Eq. 4.3. } \checkmark$$

$$AH = \epsilon_0 e^{\left[\frac{L}{R_v} - \left(\frac{1}{T_0} - \frac{1}{T} \right) \right]} \frac{RH}{100} \frac{M_{H_2O}}{R \cdot T} \quad \text{Eq. 4.4. } \checkmark$$

Where e is the water vapor pressure, $\epsilon_0 = 0.611 \text{ kPa}$, $M_{H_2O} = 18.02 \frac{\text{g}}{\text{mol}}$, $R = 8.31 \frac{\text{J}}{\text{mol} \cdot \text{K}}$, $L = 2.5 \cdot 10^6 \frac{\text{J}}{\text{kg}}$, $R_v = 461 \frac{\text{J}}{\text{kg} \cdot \text{K}}$, $T_0 = 273 \text{ K}$, T is the temperature in Kelvin and RH is the relative humidity in percentage.

Mathematical models

SEIR without meteorology

To characterize the dynamics of influenza epidemics, we employed a modified SEIR model (see [Section 1.4.2](#)) incorporating a step function to account for temporal variations in the transmissibility coefficient. A detailed analysis of daily influenza diagnoses revealed two distinct inflection points in the epidemic curve across all seasons studied. Based on this observation, we implemented a two-step transmissibility function, as illustrated in [Figure 4.19](#), which depicts the model structure.

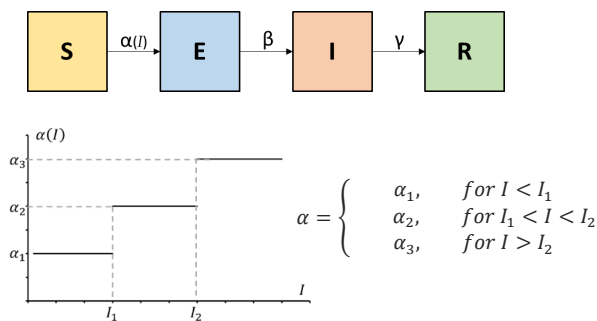


Figure 4.19. Scheme of the SEIR model with a 2-step transmissivity function.

This approach offers a balance between simplicity and epidemiological relevance, enabling the capture of key shifts in transmission dynamics while maintaining interpretability and computational efficiency. Compared with more complex frameworks incorporating continuously varying transmissibility or additional compartments [208], [209], the two-step function provides a pragmatic yet effective means of modelling epidemic progression. By explicitly representing phase transitions in disease spread, it facilitates real-time estimation and forecasting. While it is not yet widely adopted, it aligns with existing literature, such as the model proposed by Liu, X. and Stechlinski, P. [210].

We determined I_1 and I_2 empirically, initially choosing 26 and 67 daily cases as thresholds for seasons 2014-2015 to 2019-2020, corresponding to the medium and high levels of disease ([Section 2.2.1](#)) considering that Barcelona accounts

for approximately the 20% of the population in Catalonia [211]; and we chose 50 and 100 for season 2023-2024 empirically, because it has an increased number of baseline influenza cases. The model definition is that of a regular SEIR ([Eq. 1.6](#) to [Eq. 1.10](#)), but in its implementation, a condition on the choice of the α value is added depending on the number of daily cases. Besides, we defined separately I_n , the daily new number of infected people, since this is the variable that we adjusted our data to, as SIVIC does not provide active cases data ([Eq. 4.5](#)):

$$\frac{dI_n}{dt} = \beta E$$

[Eq. 4.5.](#) ✓

Since influenza infectious and recuperation periods are of 4 days in average and of more or less a week, respectively ([Section 4.2](#)), we set $\beta = \frac{1}{4} \text{days}^{-1}$ and $\gamma = \frac{1}{7} \text{days}^{-1}$. Once the model is defined, we implemented it in Python v.3.9.20 and adjusted it to each season of the epidemiological data through the minimization of the error between our SIVIC data and I_n using the *curve_fit* function. We empirically adjusted the parameters boundaries, setting as a condition that $\alpha_1 < \alpha_2 < \alpha_3$ for coherence. The parameters being optimized are the three transmissivity values α_1 , α_2 and α_3 , the fraction of initial susceptible population f and the I_1 and I_2 thresholds that define the change in α . Since no change was observed in the I_1 and I_2 thresholds values, the model was adjusted again only for f , α_1 , α_2 and α_3 .

We assessed the accuracy of the model computing the R^2 of the adjustment, as well as root mean square error (RMSE) and the difference in the expected weekly magnitude and week of the peak of each epidemic and the modelled ones. To account for real-life needs, we aimed to estimate the week of the peak instead of its day, as it is a more valuable information for public health managers. Finally, to evaluate the sensitivity of our SEIR model's outputs to its parameters, we implemented a global sensitivity analysis combining latin hypercube sampling (LHS) with the partial rank correlation coefficient (PRCC) method, using as a basis the code provided by Massey, S.C. [212].

The LHS is a stratified sampling technique used to generate a diverse set of parameter combinations efficiently across multidimensional space [213], [214]. For each parameter in the SEIR model – in our case, the susceptible fraction f and the transmissibility coefficients α_1 , α_2 and α_3 – we defined normal distributions based on season-specific means and variances derived from previous estimations. Each parameter distribution was divided into equally probable intervals, from which a random sample was drawn. This ensured a thorough exploration of the parameter space without requiring an exhaustive number of simulations. We generated 100 such samples, resulting in 100 simulations of the SEIR model per epidemic season.

Using each set of sampled parameters, we simulated epidemic curves for the four compartments of the SEIR model and our fifth compartment In . After obtaining the simulation outputs, we applied the PRCC method to assess the sensitivity of each model output to its input parameters over time. PRCC measures the monotonic relationship between the model input and output while controlling for the effects of other inputs [215]. For each time step in the epidemic simulation, we computed the Spearman correlation between the residuals of ranked inputs and outputs after removing the linear effects of other variables. This allowed us to estimate which parameters most influenced each compartment at different points in time.

The PRCC results included the correlation values, their associated p -values, and an indicator of statistical 95% significance. The outputs were visualized over time to provide insight into when and how strongly each parameter affected disease dynamics during the epidemic period.

SEIR with meteorology

Building upon previous research on the relationship between T , AH , and influenza transmission, we introduced refinements to the SEIR model described earlier. Specifically, we explored the potential time-lagged effects of meteorological variables by evaluating three possible delays: 0, 7, and 14 days. Correlation analyses computing an exponential fit of the relationship between the epidemiological data and meteorological variables at the thresholds defined

for the model – 26 and 67 daily cases or 50 and 100 for 2023-2024 – were made. R^2 metric was used to assess goodness of the fit. We included a first threshold set to 1, representing the start of the epidemic. The transmissibility parameter α_2 was redefined as a function of the variables and delays that indicated a strong correlation. In other words, to construct these new α_2 functions, each threshold was linked to its corresponding temperature or absolute humidity value observed τ days earlier for each influenza season, with $\tau = 14, 7$ or 0 days prior to the day of surpassing the epidemic levels if these values showed a correlation in the previous exploratory analysis. To describe the relationship between α_2 and the meteorological variable, we fitted an exponential function. This approach enabled the derivation of a specific transmissibility function for each meteorological variable and lag in relation to α_2 (for instance, $\alpha_2(T) = A \cdot e^{B \cdot T(t-\tau)}$ for temperature).

Separate models were then constructed using each of the individual transmissibility functions. Once these models were fully defined, they were calibrated to fit the epidemiological data using the same parameter adjustment procedure previously described: the other transmissivity coefficients α_1 and α_3 , as well as the f value, were readjusted for each season with the same empirically set boundaries as before. Again, we assessed the accuracy of the model computing the R^2 of the adjustment, as well as RMSE and the difference in the expected magnitude and date of the peak of each epidemic and the modelled ones. The PRCC analysis was not repeated for these results to avoid redundancy.

Results and discussion

Figure 4.20 illustrates an apparent inverse relationship between influenza epidemics and both temperature and absolute humidity, with influenza cases peaking when T and AH reach their lowest values. This peak appears to occur with a slight temporal delay relative to the meteorological conditions, thereby supporting the rationale behind our modelling approach.

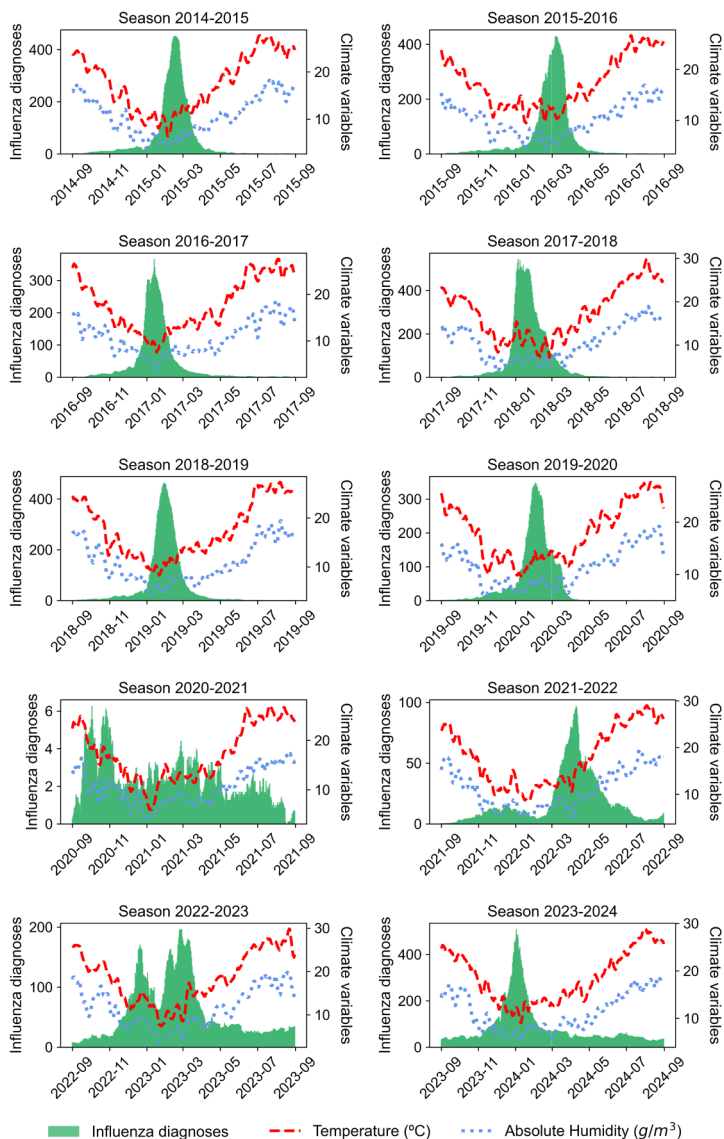


Figure 4.20. Influenza daily diagnoses (green), mean temperature (dashed red) and mean absolute humidity (dotted blue) from 2014-2015 to 2023-2024.

SEIR without meteorology

The SEIR model for influenza diagnoses in Barcelona accurately reproduces all epidemic peaks from season 2014-2015 to 2023-2024, except for the latter ([Figure 4.21](#)). The model effectively captures the magnitude and timing of the epidemic peak across all but the last season, achieving an adjustment of $R^2 \geq 0.8$, but an R^2 of 0.37 for the 2023-2024 epidemic, that approaches the epidemic peak week but not its magnitude. The RMSE is in most seasons under 30 cases, being the greatest (RMSE = 83 cases) for season 2023-2024, the only post COVID-19 pandemic epidemic that was analysed and that also posed a challenge for being adjusted with our empirical approach ([Section 4.4.1](#)).

The parameter values obtained for each season and its metrics can be seen in [Table 4.5](#) and [Figure 4.22](#). The values of the transmissivity parameters have been plotted in the latter figure instead of given in the table for a better visualization of their values and for simplicity.

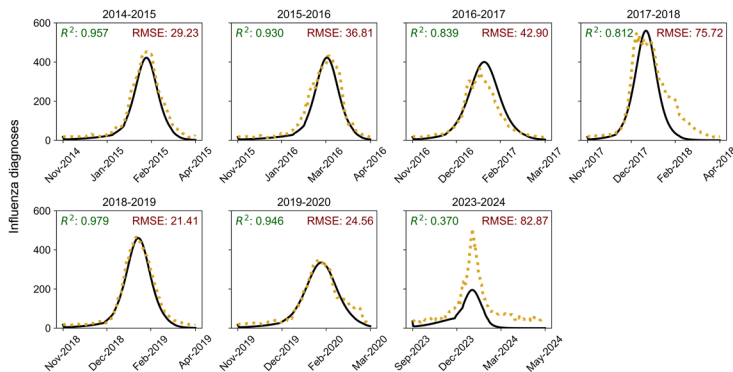


Figure 4.21. SEIR model adjustment to every epidemic season of study, with metrics R^2 and RMSE. For the model with a 2-step transmissivity function.

When looking at the values obtained for the fraction of people susceptible to influenza infection, we can see that this is of approximately the 1% of the population in all seasons. While we restricted this value from the 0.1% to the 10% when adjusting the model, we observe that in Barcelona, consistently, the population that seasonally gets infected with influenza viruses remains stable at the 1%, which stands for around 20,000 people.

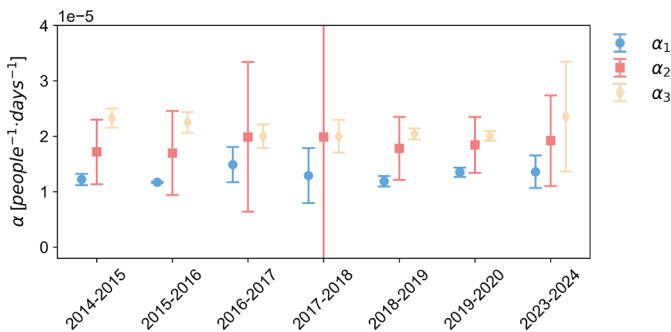


Figure 4.22. Values for the three different transmissivities considered in our SEIR model for influenza diagnoses in Barcelona.

Table 4.5. Estimated parameters and performance metrics of the SEIR model for influenza diagnoses in Barcelona using a step function for transmissivity.

Seasons	f	R ²	RMSE [cases]	Weeks of delay	wM (%)
2014-2015	0.011 (0.010-0.011)	0.96	29.23	0	-10.37
2015-2016	0.010 (0.010 - 0.011)	0.93	36.81	-1	-5.76
2016-2017	0.011 (0.010-0.012)	0.84	42.90	1	18.79
2017-2018	0.012 (0.011 - 0.014)	0.81	75.72	1	5.25
2018-2019	0.011 (0.011 - 0.012)	0.98	21.41	0	-0.21
2019-2020	0.010 (0.010 - 0.011)	0.95	24.56	0	-0.29
2023-2024	0.008 (0.005 - 0.012)	0.37	82.87	-1	-72.8

Overall, our model is well adjusted to the influenza epidemics with one week of delay or advancement at most, comparable to the performance of the empirical model defined in the previous section. Besides, except for season 2023-2024, the model captures the magnitude of the peak with less than a 20% error, even reaching values of less than 5% and usually underestimating the epidemic peak.

The sensitivity of the model to the different parameters' values was studied with our PRCC analysis, and its results can be observed in [Figure 4.23](#) to [Figure 4.29](#) for seasons 2014-2015 to 2023-2024. When the compartments are depicted, GT stands for the ground truth of each, i.e., the result of the base model.

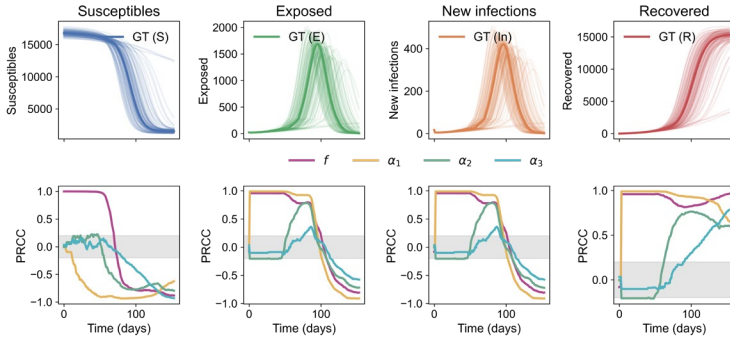


Figure 4.23. Simulations of the SEIR model for influenza diagnoses in Barcelona with the parameters estimated using LHS and PRCC in time for the parameters f (purple), α_1 (yellow), α_2 (dark green) and α_3 (light blue) for each compartment (S – blue, E – green, I_n – orange and R – red). For 2014-2015.

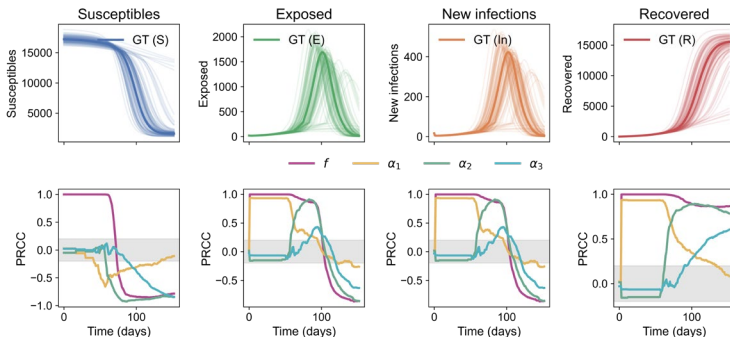


Figure 4.24. Simulations of the SEIR model for influenza diagnoses in Barcelona with the parameters estimated using LHS and PRCC in time for the parameters f (purple), α_1 (yellow), α_2 (dark green) and α_3 (light blue) for each compartment (S – blue, E – green, I_n – orange and R – red). For 2015-2016.

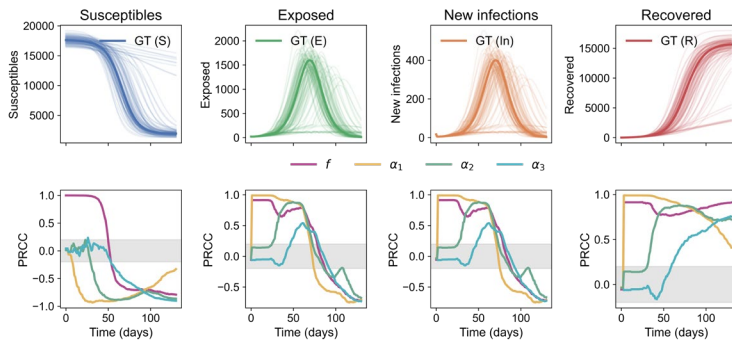


Figure 4.25. Simulations of the SEIR model for influenza diagnoses in Barcelona with the parameters estimated using LHS and PRCC in time for the parameters f (purple), α_1 (yellow), α_2 (dark green) and α_3 (light blue) for each compartment (S – blue, E – green, I_n – orange and R – red). For 2016-2017.

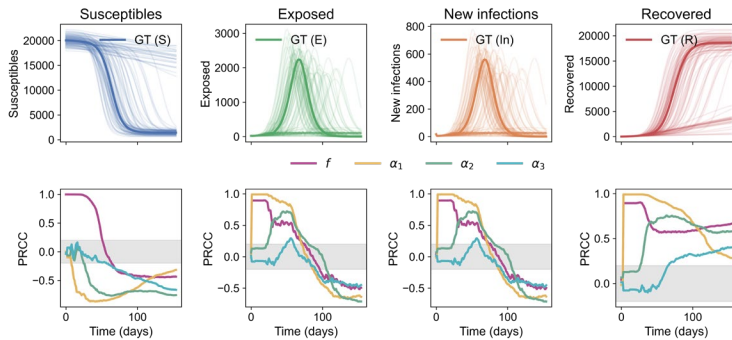


Figure 4.26. Simulations of the SEIR model for influenza diagnoses in Barcelona with the parameters estimated using LHS and PRCC in time for the parameters f (purple), α_1 (yellow), α_2 (dark green) and α_3 (light blue) for each compartment (S – blue, E – green, I_n – orange and R – red). For 2017-2018.

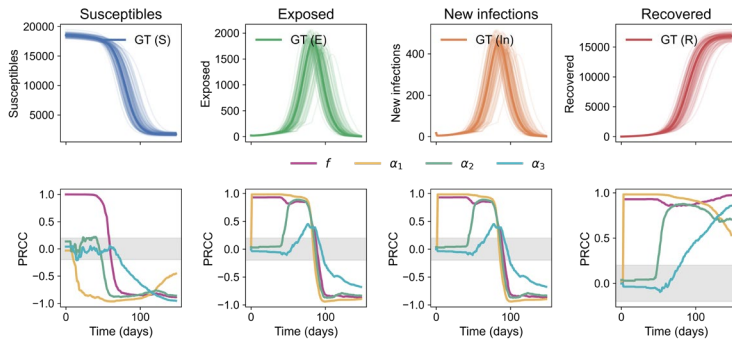


Figure 4.27. Simulations of the SEIR model for influenza diagnoses in Barcelona with the parameters estimated using LHS and PRCC in time for the parameters f (purple), α_1 (yellow), α_2 (dark green) and α_3 (light blue) for each compartment (S – blue, E – green, I_n – orange and R – red). For 2018-2019.

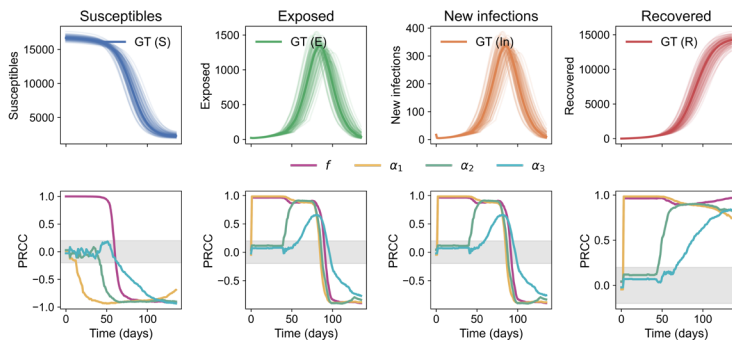


Figure 4.28. Simulations of the SEIR model for influenza diagnoses in Barcelona with the parameters estimated using LHS and PRCC in time for the parameters f (purple), α_1 (yellow), α_2 (dark green) and α_3 (light blue) for each compartment (S – blue, E – green, I_n – orange and R – red). For 2019-2020.

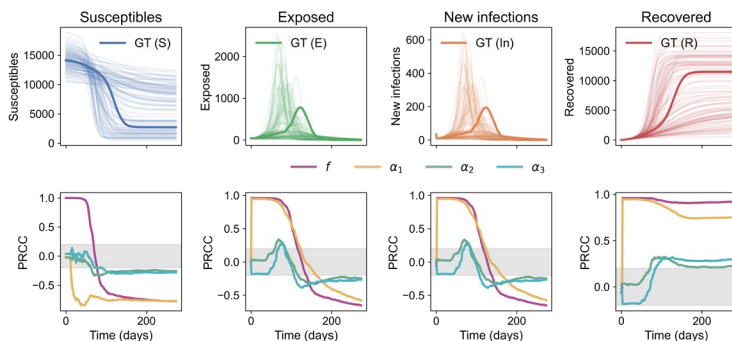


Figure 4.29. Simulations of the SEIR model for influenza diagnoses in Barcelona with the parameters estimated using LHS and PRCC in time for the parameters f (purple), α_1 (yellow), α_2 (dark green) and α_3 (light blue) for each compartment (S – blue, E – green, I_n – orange and R – red). For 2023-2024.

When examining the new infections compartment, it becomes evident that each transmissivity parameter only begins to show substantial influence (with a correlation exceeding 0.2) after surpassing the predefined infection threshold used for model adjustment. This behaviour is coherent with the model structure, as transmissivity is expressed as a two-step function. Interestingly, the proportion of susceptible individuals f is highly influential at the start and toward the end of the epidemic, but its importance diminishes around the epidemic peak. In contrast, the transmissivity parameters reach their highest influence during the peak period, reflecting the critical role of transmission rates in driving epidemic intensity once a substantial number of individuals are exposed. Another notable observation is that the PRCCs of all parameters tend to shift towards strong negative values towards the end of the epidemic. This pattern highlights the cumulative effect of these parameters as the susceptible population depletes and recovery progresses, exerting a limiting effect on further transmission. Lastly, it is worth emphasizing that seasons with better model fits exhibit greater consistency and smoother trends in SEIR model results, but some seasons display more stochastic and erratic parameter sensitivities. This is revealing of the model's sensitivity to parameter values and potentially reflecting variability in epidemic dynamics or limitations in data quality for those seasons.

SEIR with meteorology

At this point, where the base SEIR model is verified and consolidated, we studied the lagged correlation between influenza diagnoses and the meteorological variables, adjusting an exponential fit and observing its R^2 (**Figure 4.30**).

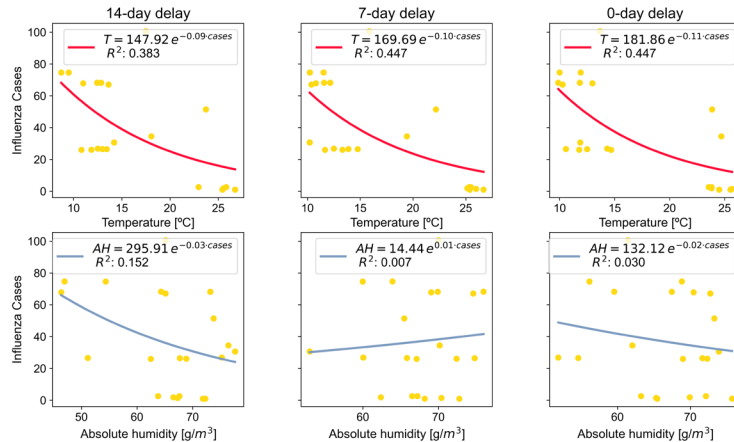


Figure 4.30. Exponential fits of daily influenza cases as a function of temperature or absolute humidity with 3 different lags (14, 7 and 0 days) at the moment where the thresholds of infections (1, 26 and 57 cases for all seasons but 2023-2024 where they are of 1, 50, 100 cases) are overcome.

There is no observable relationship between AH and influenza cases, while temperature shows a slightly better association, especially for the 7- and 0-days delay but showing considerable results for the 14-days lag too. For modelling purposes, the 0-day delay has been neglected, as it makes no physical sense that the daily temperature affects daily cases of influenza, since there is an interval between exposure and infection ([Section 1.2](#)).

Therefore, we computed the transmissivity as a function of temperature with a 1- and a 2-weeks delay, as seen in [Figure 4.31](#) and [Figure 4.32](#), respectively. This association showed to be higher but stayed below 0.65.

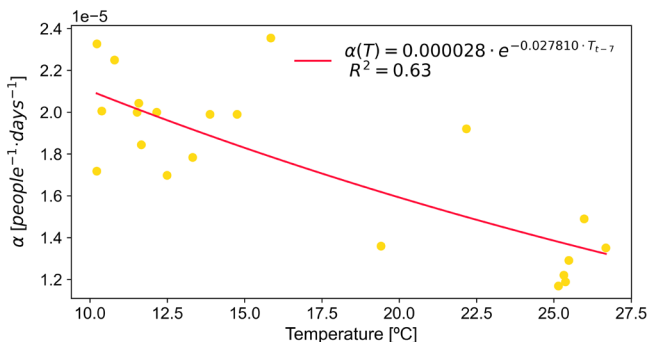


Figure 4.31. Transmissivity as a function of the daily temperature a week before the estimated cases.

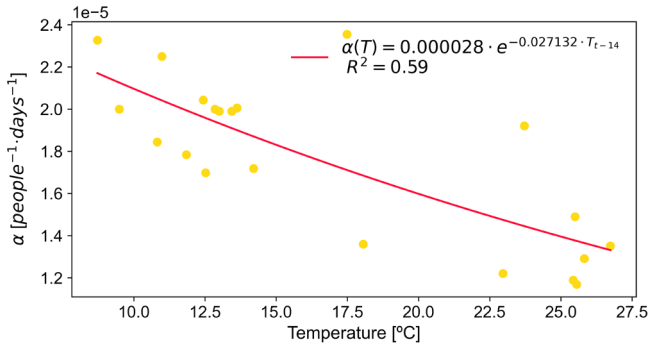


Figure 4.32. Transmissivity as a function of the daily temperature two weeks before the estimated cases.

With these functions, we modified our SEIR base model to introduce the transmissivities depending on temperature instead of the fixed value for α_2 . Therefore, we constructed a model depending on the temperature a week ([Figure 4.33](#)) and two weeks ([Figure 4.34](#)) prior to the estimated infections. Its parameter values (f , α_1 , α_3) and metrics can be observed in [Table 4.6](#) and [Table 4.7](#) respectively.

Chapter 4 – Influenza: Modelling the influenza epidemic

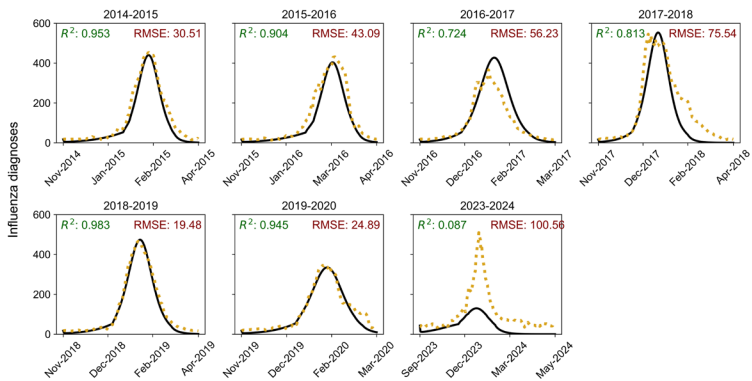


Figure 4.33. SEIR model adjustment to every epidemic season of study, with metrics R^2 and RMSE. For the model with α_2 as a function of temperature a week prior to estimated infections.

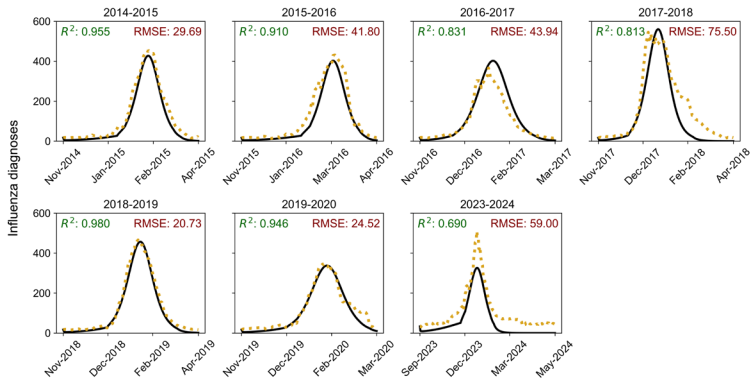


Figure 4.34. SEIR model adjustment to every epidemic season of study, with metrics R^2 and RMSE. For the model with α_2 as a function of temperature two weeks prior to estimated infections.

Interestingly, the model defining transmissivity as a function of temperature with two weeks of delay is the one that obtains the best performance from the three models of study, capturing with the lowest error the magnitude of season 2023-2024 and also its epidemic peak precisely.

Table 4.6. Estimated parameters and performance metrics of the SEIR model for influenza diagnoses in Barcelona using transmissivity as a function of the temperature a week before the estimated cases.

Seasons	f	$\alpha_1 \cdot 10^{-5}$ [people ⁻¹ ·days ⁻¹]	$\alpha_3 \cdot 10^{-5}$ [people ⁻¹ ·days ⁻¹]	R ²	RMSE [cases]	Weeks of delay	wM (%)
2014-2015	0.010 (0.010-0.011)	1.29 (1.29-1.30)	2.47 (2.38-2.61)	0.95	30.51	0	-6.38
2015-2016	0.010 (0.010-0.011)	1.31 (1.23-1.38)	2.47 (2.18-2.76)	0.90	43.09	-1	-5.41
2016-2017	0.011 (0.010-0.012)	1.49 (1.48-1.50)	2.00 (1.76-2.24)	0.72	56.23	1	28.53
2017-2018	0.012 (0.012-0.013)	1.39 (1.33-1.44)	2.00 (1.93-2.07)	0.81	75.54	1	4.43
2018-2019	0.012 (0.012-0.012)	1.23 (1.20-1.25)	2.00 (1.91-2.09)	0.98	19.48	0	2.68
2019-2020	0.010 (0.010-0.010)	1.41 (1.35-1.47)	2.00 (1.95-2.05)	0.94	24.89	0	-0.54
2023-2024	0.008 (0.007-0.010)	1.43 (1.09-1.77)	2.01 (1.07-2.95)	0.09	100.56	-1	-72.29

Table 4.7. Estimated parameters and performance metrics of the SEIR model for influenza diagnoses in Barcelona using transmissivity as a function of the temperature two weeks before the estimated cases.

Seasons	f	$\alpha_1 \cdot 10^{-5}$ [people ⁻¹ ·days ⁻¹]	$\alpha_3 \cdot 10^{-5}$ [people ⁻¹ ·days ⁻¹]	R ²	RMSE [cases]	Weeks of delay	wM (%)
2014-2015	0.010 (0.010-0.011)	1.21 (1.17-1.25)	2.37 (2.19-2.54)	0.96	29.69	0	-8.62
2015-2016	0.010 (0.010-0.011)	1.22 (1.21-1.22)	2.39 (2.15-2.63)	0.91	41.80	-1	-6.15
2016-2017	0.011 (0.010-0.012)	1.49 (1.45-1.53)	2.00 (1.79-2.21)	0.83	43.94	1	19.66
2017-2018	0.012 (0.011-0.013)	1.28 (1.27-1.28)	2.00 (1.71-2.29)	0.81	75.50	1	5.79
2018-2019	0.011 (0.011-0.012)	1.17 (1.17-1.18)	2.01 (1.92-2.10)	0.98	20.73	0	-0.86
2019-2020	0.010 (0.010-0.011)	1.34 (1.34-1.35)	2.01 (1.87-2.14)	0.95	24.52	0	0.12
2023-2024	0.010 (0.009-0.011)	1.18 (1.08-1.29)	2.25 (1.84-2.66)	0.69	59.00	0	-31.68

In fact, in this latest model, the fraction of the population susceptible to infection during the 2023-2024 season was estimated at a similar magnitude to that of previous seasons, implying that approximately 1% of the population was ultimately infected with influenza. In contrast, earlier models tended to estimate this parameter at values lower than 1%. Additionally, the transmissivity coefficient for α_1 in this model is notably lower compared to previous seasons, suggesting that a slower initial growth rate – indeed, one of the slowest observed at the start of the epidemic – may better capture the dynamics of the 2023-2024 season. At the same time, a higher α_3 value appears to align more

closely with the observed progression of the epidemic. These results indicate that, while the epidemic may have exhibited a slower onset than in previous years, once a certain infection threshold was reached, transmission accelerated markedly.

The results presented in this section raise an important question regarding the actual influence of meteorological factors on influenza transmission. Notably, temperature alone as a predictor for influenza transmissivity provided a reliable estimation of epidemic progression across several influenza seasons in Catalonia. This observation highlights the need to deepen our understanding of how meteorological variables interact with the dynamics of influenza epidemics. From what we currently know, meteorological conditions may influence influenza transmission through two primary mechanisms: first, as discussed in **Section 1.2.1**, environmental factors such as temperature and humidity affect mucosal integrity and the survival of the virus, directly influencing susceptibility and transmissibility; second, colder or rainy days tend to alter human behaviour, especially in Catalonia, increasing the likelihood of gatherings in enclosed, poorly ventilated spaces, which facilitates viral spread. Nevertheless, the use of this model for mid-term predictive purposes is limited, as it would entail the use of meteorological models to predict the temperature dynamics which, if feasible, would increase the model uncertainty. Consequently, the principal value of this model lies in enhancing our understanding of the underlying mechanisms that drive transmission processes.

This study is not without limitations. The reliance on influenza diagnosis data without microbiological confirmation introduces potential inaccuracies, as other respiratory pathogens with similar clinical presentations could be misclassified as influenza. Additionally, while daily temperature and absolute humidity data offer high temporal resolution for modelling the influenza epidemic, they are inherently variable. Establishing direct associations between daily case numbers and daily meteorological conditions is more stochastic than using aggregated weekly data. Although daily data allow for more detailed adjustments and forecasting, weekly data might better capture the broader epidemiological patterns influenced by sustained meteorological trends.

However, aggregating meteorological data on a weekly basis presents its own challenges, as there is no universally established method for doing so without potentially losing meaningful fluctuations relevant to transmission dynamics. Furthermore, while this study explored transmissivity thresholds based on infection counts, identifying transmissivity functions driven directly by meteorological variables could pave the way for defining meteorologically based thresholds for epidemic control; an area that remains underexplored and warrants further investigation.

Another unresolved aspect relates to the role of other respiratory pathogens, particularly RSV, in shaping influenza epidemic patterns. Our analyses suggest that factors beyond meteorology may be significant, potentially explaining why children become more prominently involved later in the epidemic but not in the beginning ([Section 4.3.1](#)), possibly due to viral competition or interaction effects early in the season.

To summarise

This study demonstrates that it is possible to model influenza epidemics both with and without the inclusion of meteorological variables, recognizing their influence on transmissivity values and epidemic behaviour. The findings support the relevance of meteorological factors in influenza modelling, while also revealing the complexity of disentangling these effects from other biological and social drivers of transmission. As such, this work should be viewed as a precursor study that opens important avenues for future research, emphasizing the need for refined modelling approaches, more robust data, and an integrated perspective on respiratory epidemic dynamics.

Chapter 5

Respiratory Syncytial Virus

“Canviar de resposta és evolució. Canviar de pregunta és revolució.”

Jorge Wagensberg

If the reader is a parent, they may feel imperilled by the mention of such formidable agent that lends its name to this chapter. Yet I implore you, dear reader, to stand not in fear but in resolve, for ignorance grants no shield, while knowledge arms us against the unseen foe. The scourge of bronchiolitis, mainly wrought by the relentless hand of RSV, has long cast its shadow over infants, its tides as relentless as the seasons, striking with an unforgiving regularity. But take heart, for we have deciphered its patterns, unravelling the hidden threads that weave its rise and fall, wielding models that allow us to foresee its peak before it arrives. Though once we stood defenceless, at the mercy of this affliction, science has now gifted us a mighty protector—nirsevimab, a sentinel forged through knowledge and perseverance. With its arrival, the burden of bronchiolitis has been lessened, the risk diminished, and the youngest among us granted a newfound shield against the tempest. Lord bless science, Lord bless knowledge—our steadfast shield and lasting homage.

In this chapter we will find more about the RSV, empirically model its epidemics and study the effects and effectiveness of nirsevimab, a new immunizing component, on bronchiolitis and RSV dynamics and on RSV-severity related outcomes, based on the following published and peer-reviewed articles:

Scientific work article III: Perramon-Malavez, A., *et al.* Pediatric infectious diseases journal. 2025.

Scientific work article VIII: Perramon-Malavez, A., *et al.* European journal of pediatrics. 2024.

Scientific work article X: Villanueva, M., *et al.* Scientific reports. 2024.

Scientific work article XIII: Coma, E., *et al.* Archives of disease in childhood. 2024.

5.1. Characteristics of the respiratory syncytial virus

The respiratory syncytial virus is one of the most common viral pathogens globally, responsible for a significant burden of acute LRTIs, particularly in infants, but also contributing to serious respiratory illness among older adults and immunocompromised individuals [216]. From the *Pneumoviridae* family, together with the human metapneumovirus (hMPV), it is an enveloped RNA virus (Figure 5.1) with a genome that encodes 11 proteins, including key surface G proteins that play critical roles in viral entry (mucosal attachment) and immune evasion, as explained for influenza in Section 4.1. In addition, the viral envelope also contains the fusion (F) glycoprotein, and the small hydrophobic (SH) protein [217], [218].

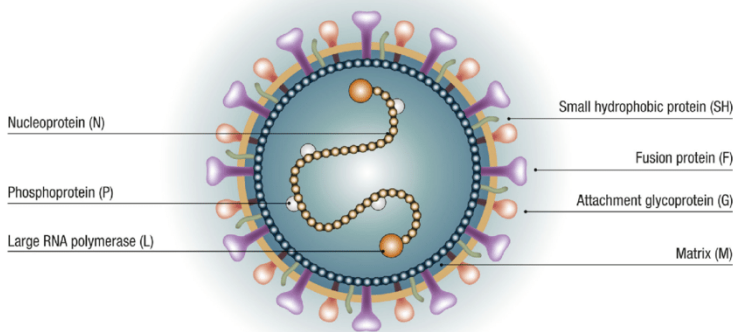


Figure 5.1. The RSV structure. Retrieved from [219].

The G protein and the F protein are the primary antigenic targets and are crucial to RSV pathogenesis and host cell entry, but the SH protein is not required in these processes [217]. The G protein facilitates viral attachment to host epithelial cells and is highly glycosylated and variable, allowing for a rapid generation of mutations, contributing to immune escape and antigenic diversity between subtypes [220], [221]. This is why immunisation strategies have focused on the F protein [218], [220]. This protein is more conserved and plays a central role in the fusion of the viral and host membranes, allowing entry into the host cell. Inactivation of the F protein effectively prevents the virus from infecting host cells. Importantly, RSV exhibits pleomorphism, meaning its

morphology can vary from spherical to filamentous depending on environmental conditions and stage of replication. Correspondingly, the F protein can exist in two distinct structural states: a metastable prefusion form, and a more stable post fusion form (**Figure 5.2**). The prefusion conformation is the target of potent neutralizing antibodies because it shows specific parts of the virus – called epitopes – that trigger strong immune responses. These parts are either hidden or changed in the post fusion form, so targeting the prefusion form is more effective for preventing infection, which has informed the design of prophylactic monoclonal antibodies such as nirsevimab and palivizumab, both of which specifically bind the F protein [222], [223].

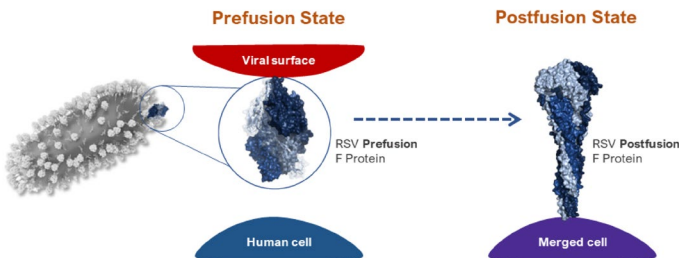


Figure 5.2. States of the RSV F protein. Prefusion State (left): In its prefusion state, the RSV F protein is attached to the viral surface and helps the virus attach to host cells. Post fusion State (right): After the virus recognizes a human cell, the F protein irreversibly transitions from its prefusion to its post fusion state, and the virus merges with the human cell. This allows the virus to infect the host. Retrieved from [224].

The RSV is classified into two major antigenic subgroups, A and B, based primarily on genetic variability in the attachment G protein [221]. Both subtypes co-circulate during seasonal epidemics, although subgroup A has often been associated with more severe clinical outcomes [225]. However, this assertion remains controversial, with studies showing overlapping severity and alternation in dominance between strains across seasons [217].

5.2. Bronchiolitis disease

The RSV infects indiscriminately but it affects differently depending on the age of the infected person. Besides, some studies show a greater severity in males, although females often experiencing more adverse reactions to treatments [226], [227]. To healthy adults in children over 5 years old, its clinical manifestation varies from asymptomatic carriage through signs of URTI. Nasal congestion, rhinorrhoea and even fever are common symptoms 3 to 5 days after infection [228]. However, the virus is more prompt to cause LRTI in infants <6 months and the elderly, causing a more severe clinical presentation, with bronchi and bronchioles inflammation and respiratory distress [103]. In fact, it is the main cause of hospitalization per infectious disease in infants in the Global North, since the RSV is responsible for approximately 70%-80% of bronchiolitis, a very severe inflammation of the bronchioles that can lead to hospitalization and even to the need for PICU admission [102], [167]. In addition, severe disease caused by an RSV infection has been related to asthma developing and recurrent wheezing [229].

In Catalonia, RSV represents a considerable burden on the healthcare system. A study conducted by Vila, J. et al. [4] in one of the region's major tertiary hospitals estimated the direct cost per patient for treating children with LRTIs, primarily caused by the RSV, at approximately €500 per year. This figure greatly exceeds the average annual per capita healthcare expenditure in the region, given that the Catalan Health Institute's – that controls 8 hospitals and 322 primary care centres – per capita budget consists of approximately €1,200-1,500 per year. Hence, a single hospital – although one of the biggest – requires a third of this contribution.

Efforts are driven towards prevention of respiratory syncytial virus severe disease instead of treatment, due to challenging decisions on intervention and high costs.

Clinical guidelines often advocate for supportive (rather than interventional) treatment in bronchiolitis (focusing primarily on hydration and oxygen support) [167] but the complete de-implementation of unnecessary interventions – and

the challenge that is defining what is *unnecessary* when we are dealing with new-borns' lives – remains a major confrontation. This difficulty in managing bronchiolitis, coupled with its high healthcare and economic burden, has driven efforts toward prevention rather than treatment. Palivizumab, commercialized in Spain under the name *Synagis*© [230], [231], was the first preventive strategy implemented. It is a monoclonal antibody that targets a specific epitope of the RSV F protein, neutralizing both RSV subtypes A and B by inhibiting viral fusion [232]. It is administered intramuscularly once a month for five months during the RSV season. While palivizumab reduces RSV-related hospitalizations by up to 60%, it shows little to no effect on mortality or severe adverse events. Furthermore, its use is typically limited to high-risk infants due to its high cost and the need for repeated doses [233].

To address these limitations, the European Medicines Agency (EMA) approved a new monoclonal antibody, nirsevimab, in 2022 [234]. Introduced in Catalonia in October 2023 under the brand name *Beyfortus*© [235], [236], nirsevimab provides longer lasting and broader protection than palivizumab. Unlike palivizumab, which targets both prefusion and post fusion forms, nirsevimab specifically induces potent neutralizing antibodies against the prefusion F protein, resulting in roughly ten times higher and more sustained neutralizing antibody levels [237]. It was expected to prevent up to 80% of severe RSV-related cases in infants, which has been ascertained in real-world analyses and will be discussed in [Section 5.5](#). Following the commercialization of nirsevimab, maternal vaccines [238] and vaccines for the adult population [239] have been or are under development, even introduced in some countries. Under the commercial name of *ABRYSVOC*© [240] the first maternal vaccine against RSV is now available in the United Kingdom (UK) [241], Australia [242] and the US [243] among others. These strategies will change eventually what we know about bronchiolitis severity and the epidemiological dynamics of RSV.

5.3. Epidemiology of the respiratory syncytial virus

Before these immunisation strategies were introduced, RSV dynamics were highly stable and predictable, especially when looking at all-causes bronchiolitis cases, which were the only available indicator for RSV surveillance prior to the COVID-19 pandemic. In **Figure 5.3**, this can be ascertained, as we used SIVIC data of bronchiolitis from 2014 to 2019 to compute the mean pre-pandemic bronchiolitis epidemic and compared it to post COVID-19 pandemic seasons. Given that 70-80% of bronchiolitis cases are attributed to RSV [167], trends in this disease are commonly used as a proxy for RSV surveillance. As you can see, the bronchiolitis onset comes hand-to-hand with school opening, an event that was not observed for influenza, for example, suggesting a clearer relationship of influenza to meteorological events or behavioural changes while RSV transmission is closely aligned to scholar interaction, which is also a hypothesis on why season 2020-2021 could occur in high-temperature conditions (spring-summer epidemic) [244], [245].

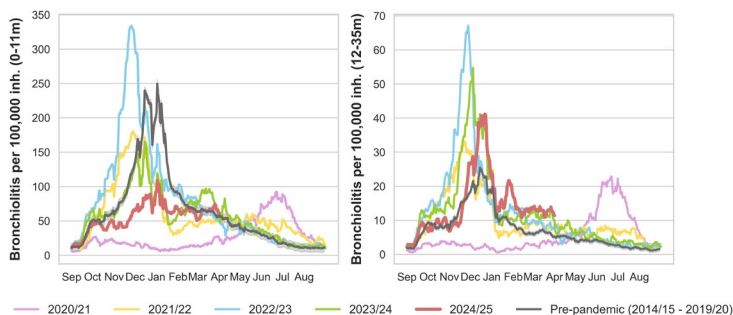


Figure 5.3. Bronchiolitis diagnoses per 100,000 inhabitants for children 0-11 months old (left) and 12-35 months old (right). Pre-pandemic mean season is plotted in dark grey and 2020-2021 to 2024-2025 seasons are depicted individually in pink, yellow, blue, green and red, respectively. Season 2024-2025 is available until 31st March 2025 at the moment of writing.

Although microbiological confirmation of RSV has been publicly available since 2020, data on RSV subtypes is still not accessible. However, a study by Piñana, M. et al. [218] from the Vall d'Hebron Research Institute (VHIR, in Catalan) analysed the co-circulation patterns of RSV-A and RSV-B between the 2013-2014 and 2022-2023 seasons. They observed cyclical shifts in subtype

predominance, with RSV-A being more prevalent approximately every three seasons (**Figure 5.4**), specifically in 2015-2016 and 2019-2020. The authors, aligned with previously published literature, associated this pattern with a short-lived acquired immune response, which allows reinfection by previously circulating subtypes and with the higher genetic variability of RSV-B.



Figure 5.4. Circulation of RSV-A (namely, HRSV-A) and -B throughout 2013–2023 seasons. Seasons 2020–2021 and 2021–2022 are comprised in the represented season 2020–2022, as both peaks were considered to belong to the same epidemic. Retrieved from Piñana, M. *et al.* [218].

However, and as one may notice from **Figure 5.3** too, the dynamics of bronchiolitis have shifted since the introduction of nirsevimab in Catalonia (see **Section 5.5**). In a recently published article [105], we discussed how the historical seasonal patterns changed following the launch of the immunisation campaign in October 2023. This will be explored in **Section 5.5.1**.

5.4. Modelling the respiratory syncytial virus epidemic

Given the substantial clinical and economic burden posed by seasonal RSV epidemics – particularly among infants and the elderly – there has been growing interest in developing models to predict their progression. While traditionally less modelled than influenza, recent efforts have begun to focus on RSV dynamics, especially following the disruptions caused by the COVID-19 pandemic. Moreover, the introduction of preventive measures such as nirsevimab has posed a major challenge to existing modelling approaches, opening up a new and evolving epidemiological landscape. Some studies have explored mechanistic models, including compartmental frameworks like SIR or SEIR variants [246], [247], [248]. Of particular interest for this thesis are those developed by Acedo, L. et al. [249], [250] in Valencia, Spain. AI-based models have started to emerge in this area as well [251], [252], though they are still limited due to the relatively short and incomplete historical datasets available for RSV compared to influenza, for instance. Furthermore, most predictive work to date has concentrated on hospital admissions, with few models addressing RSV trends in primary care or capturing early community transmission, although this is a hard task due to testing limitation in primary care, since the RSV clinical presentation can be very unspecific (see [Section 5.2](#)). In Catalonia, predictive modelling for RSV had not been incorporated into the public health system until recently. In this section, we present the initial modelling approaches developed and shared with the Catalan Public Health Secretariat to enhance RSV epidemic preparedness and anticipate peaks in RSV-related bronchiolitis. The modelling approach is the same presented for influenza (see [Section 4.4.1](#)), but we introduce a novel methodology to obtain RSV-bronchiolitis from all-causes bronchiolitis diagnoses in primary care. This research is under review at the time of writing.

5.4.1. Empirical modelling of the respiratory syncytial virus epidemics

In this section, we will explore the application of the methodology explained in [Section 4.4.1](#) for influenza but to model RSV-bronchiolitis epidemics. For that, we have to extract RSV-caused bronchiolitis from all-causes bronchiolitis

diagnoses in PCP. While it may seem unnecessary, given that most bronchiolitis cases are caused by RSV, it is important to note that early in the season, bronchiolitis can be triggered by a variety of viruses, such as rhinovirus, human metapneumovirus, or even influenza [253], [254]. This viral diversity introduces high stochasticity at the beginning of the epidemic, which is problematic for modelling, as most models are highly sensitive to initial conditions. Therefore, we aim to work with a more stable signal by focusing specifically on bronchiolitis cases attributed to RSV, as it is the pathogen responsible for driving the main epidemic wave once it becomes dominant in the viral landscape.

Methods

Data gathering

We used publicly available data on daily clinical diagnoses for all-causes bronchiolitis in children under 2 years of age, covering the period from September 1st, 2018 to August 31st, 2024. We also gathered the referral population for these data, yearly. All these data were obtained from SIVIC ([Section 1.3.1](#)) [61].

To estimate RSV-confirmed bronchiolitis from all-causes bronchiolitis cases, we gathered data on all-causes and RSV-confirmed bronchiolitis hospital admissions from the CMBD (see [Section 1.3.1](#)) healthcare dataset, spanning September 1st, 2018, to August 9th, 2023. Additionally, we also collected data on daily RSV-confirmed RAT conducted in paediatric PCPs from the SIVIC system, covering the period from September 1st, 2021, to August 31st, 2024. The CMBD data covers the whole Catalan population hospitalizations, but it is only available under demand. The RAT data is only available for the paediatric population with respiratory symptoms in PCPs, but it is available in a daily manner.

Data pre-processing

The data pre-processing for bronchiolitis diagnoses was already described in [Section 2.2.1](#). However, to model bronchiolitis diagnoses, we needed to extract

RSV-bronchiolitis from all-causes bronchiolitis in PCPs (**Figure 5.5**). This distinction is critical, as previously introduced, because the early stages of the bronchiolitis epidemic are driven by multiple viruses. Over time, however, RSV emerges as the dominant contributor, typically becoming the primary driver of cases later in the season [167], [255].

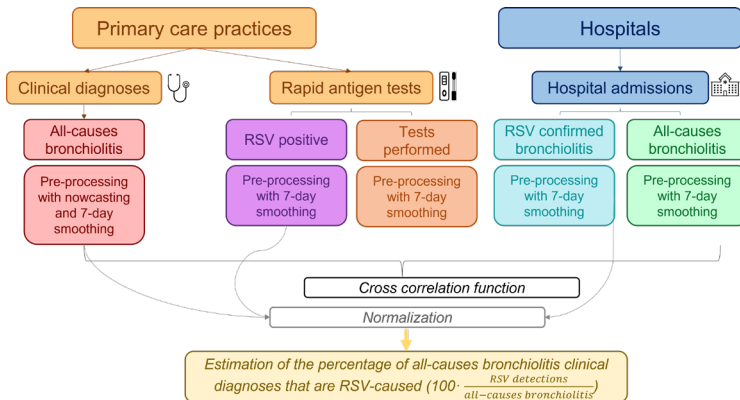


Figure 5.5. Flowchart of the process for the estimation of RSV-caused bronchiolitis.

To address this, we utilized CMBD data and RAT results to estimate the proportion of all-causes bronchiolitis attributable to RSV. For each season (defined as September 1st to August 31st of the following year), we calculated the cross-correlation function (CCF) between all-causes bronchiolitis diagnoses, and all-causes and RSV-bronchiolitis hospital admissions. The series were normalized, combining RSV-caused hospitalizations and RSV-confirmed RAT to ensure the continuity of the data. The percentage of RSV-bronchiolitis hospitalizations or RSV-positive RATs representative of each season was applied to the normalize all-causes bronchiolitis data. This allowed us to estimate the number of RSV-bronchiolitis diagnoses in PCPs for each season. To take into account the fact that RSV is responsible for 70-80% of bronchiolitis [102], we finally took the 75% of the obtained estimated RSV-bronchiolitis diagnoses. This decision only affects conceptually, but the outcome of the model would remain the same whether taking the whole data or the 75%, it is just a scaling factor [102].

Modelling epidemics

This section replicates the methodology previously described in [Section 4.4.1](#) for influenza, now applied to RSV-related bronchiolitis. To avoid repetition, we will only highlight the aspects that are specific to bronchiolitis.

The empirical reproductive number estimation now was defined as the number of newly infected divided by the number of newly infected τ days ago, where τ is the infectious period. For influenza this value was of 2 days, but it is $\tau = 5$ for bronchiolitis [102], [119]. To determine the predictive ability of the model, we iteratively added data for adjustment until the day of the epidemic peak was reached and from the medium epidemic threshold as defined in [Section 2.2.1](#). However, since epidemic thresholds had not yet been established for RSV-bronchiolitis, it was necessary to calculate them specifically for this disease using the same methodology. We measured incidence as the number of cases per 100,000 inhabitants and identified the beginning of the epidemic as the first day the incidence reached 10 cases per 100,000 inh., a value determined to be the epidemic threshold for RSV-bronchiolitis. The end of the epidemic was defined as the last day this threshold was reached.

We used the same metrics (see [Section 4.4.1](#)) to evaluate our model: the R^2 metric for adjustments, the wop prediction, daily peak magnitude, the MAPE and wM. The model adjustments were performed on a daily basis, while predictions were expressed on a weekly scale to align with the weekly framework of publicly available data.

For the prediction phase, we established parameter boundaries based on the minimum and maximum values derived from prior adjustments for the same disease. However, two exceptions were made. The first exception, for the 2022-2023 season, because there are disruptions on the regularity of the epidemic caused by the COVID-19 pandemic. The second, in the 2023-2024 season, because of the introduction of nirsevimab in Catalonia, which altered the epidemic's dynamics [105]. Under normal circumstances, parameter boundaries are adjusted iteratively to reflect new data, making seasonal adjustments a standard part of the methodology. For this study, we assessed

the accuracy of predictions at 32, 30, 28, 21, 14, 7 and 0 days prior to the peak. Broader time delays could not be evaluated due to the limited duration of the growth phase leading up to the peak. Some of the time delays could not be assessed for certain seasons for the same reason.

Results

Data pre-processing

The pre-processed data series on bronchiolitis diagnoses in primary care, hospitalizations (all-causes and RSV-caused) and RAT (tests performed and RSV-positive) in Catalonia can be seen in **Figure 5.6**. Note that, for simplicity, the y-label refers to bronchiolitis diagnoses, but RAT are performed to patients with suspect of any respiratory viral infection.

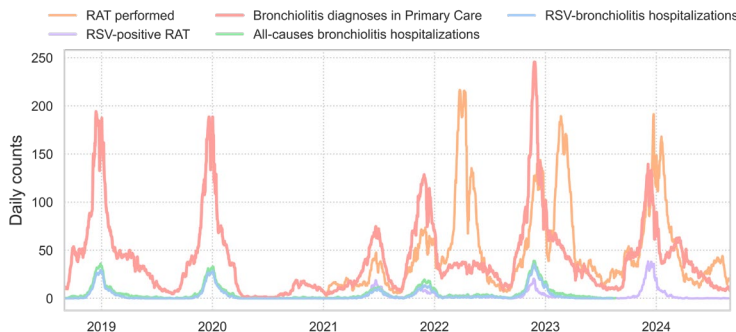


Figure 5.6. All-causes bronchiolitis diagnoses in primary care (red), RAT (orange) and RSV-positive RAT (purple) and all-causes (green) and RSV-caused (blue) hospitalizations for bronchiolitis in Catalonia.

To obtain the final series of RSV-caused bronchiolitis in PCPs, we performed an extensive pre-processing and computed lagged correlations between the bronchiolitis time series in hospitalizations and PCPs. There is no need to do so with RAT since they are undertaken in PCPs. From the CCF analysis (**Figure 5.7**), the highest correlation for hospitalizations and PCPs was observed with no delay or a lag of 1-2 days, indicating that RSV-bronchiolitis cases in PCPs and hospitals exhibit almost simultaneous epidemic trends. This finding suggests that hospitalization data can be reliably used to estimate RSV prevalence in primary care settings with minimal adjustment.

Chapter 5 – Respiratory Syncytial Virus: Modelling the RSV epidemic

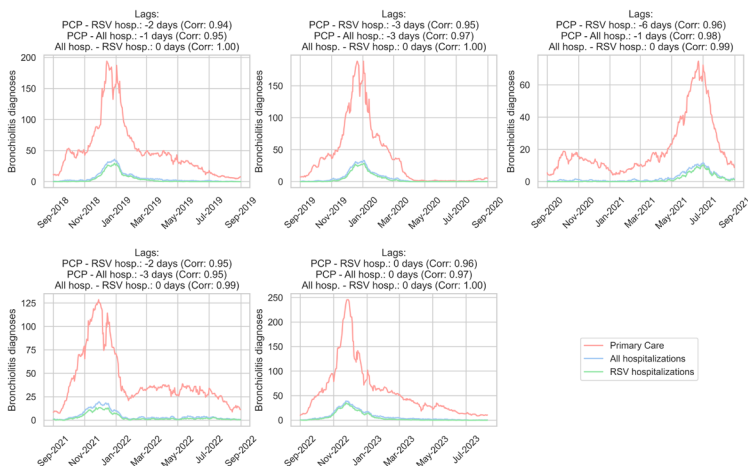


Figure 5.7. Seasonal delayed correlation for all-causes primary care (red), all-causes hospitalization (blue) and RSV hospitalizations (green) bronchiolitis data.

After the normalization of the data (**Figure 5.7**) and proportion extraction, we finally obtained estimated RSV-caused bronchiolitis (**Figure 5.8**). There was no need for alignment of the data previous to the proportion calculation, since maximum correlation between time series was obtained with no delay or 1-2 days of delay.

As it can be seen in **Figure 5.8**, extracting the 75% of the estimated RSV-caused bronchiolitis is a conceptual choice but makes no difference to the epidemic dynamics, therefore it does not affect their model adjustment neither. We also computed the epidemic thresholds for the RSV-bronchiolitis obtained calculating weekly incidence of disease.

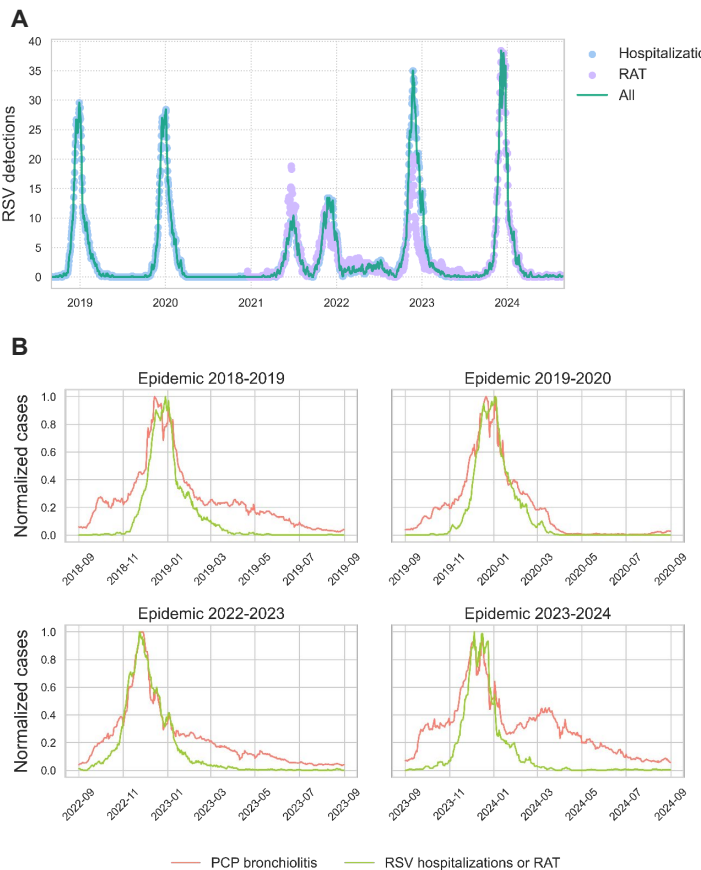


Figure 5.7. (A) RSV daily detections in hospital admissions due to RSV bronchiolitis (blue), RAT in PCPs (purple) and the final series of RSV detections considering hospitalizations until the last day we have the data and RAT from then on (dark green). (B) Normalized cases of all-causes bronchiolitis reported in PCP (light green) and RSV detections (red, related to dark green line in A) per epidemic season of bronchiolitis. The percentage of normalized RSV detections over normalized all causes bronchiolitis (0-100%) is then used to compute estimated RSV-caused bronchiolitis in PCP.

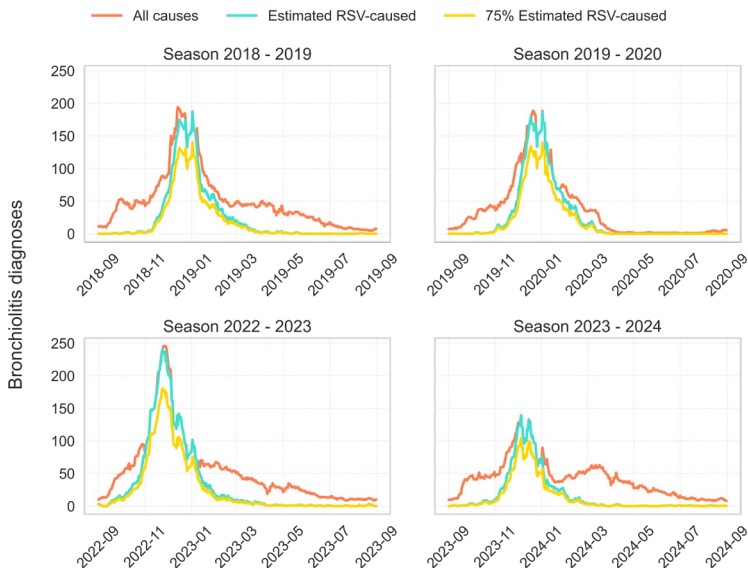


Figure 5.8. Primary care all-causes bronchiolitis diagnoses in red, estimated RSV-caused bronchiolitis diagnoses in turquoise and the final data series for modelling 75% of estimated RSV-caused bronchiolitis in yellow.

The obtained thresholds can be seen in [Figure 5.9](#) and [Table 5.1](#). Notice that we only used four seasons to compute epidemic thresholds, two pre-COVID-19 pandemic and two post-pandemic seasons, as these are the data available.

Table 5.1. Epidemic thresholds for estimated RSV-caused bronchiolitis. Computed from weekly cases per 100,000 inhabitants.

Epidemic level	Weekly cases per 100,000 inh.
Threshold	3
Low	25
Medium	90
High	340
Very high	460

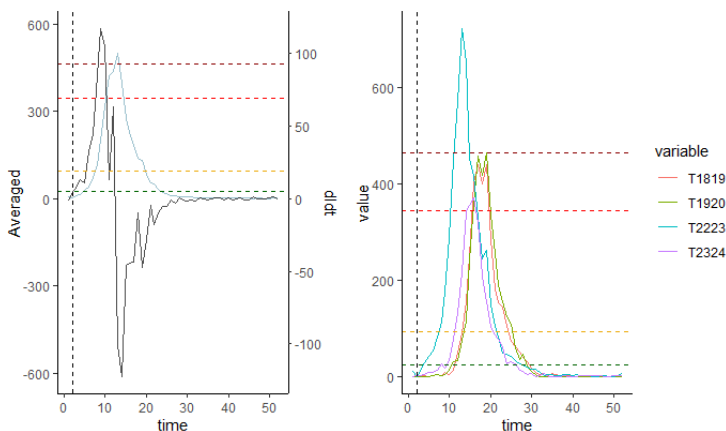


Figure 5.9. Epidemic thresholds for estimated RSV-caused bronchiolitis. Computed from weekly cases per 100,000 inhabitants.

This is going to be used for modelling purposes, but should not be applied for surveillance, as several factors might affect these results, such as interseason variability and the introduction of nirsevimab from October 2023. They should neither be applied to pre-pandemic seasons, since post-pandemic data has been used to compute them and these epidemics have been slightly larger than pre-pandemic epidemics due to immunity debt.

Full-season Gompertz fittings

The Gompertz model was adjusted for all non-pandemic seasons of study. Results for all seasons can be seen in [Figure 5.10](#) to [Figure 5.13](#). The parameters values for all epidemics are reported in [Table 5.2](#).

The RSV-bronchiolitis epidemic of 2022-2023, the second post COVID-19 pandemic season, was a third larger than pre-pandemic seasons. However, the 2023-2024 season had even fewer cases than 2018-2019, a change likely driven by the introduction of nirsevimab, which is estimated to reduce severe RSV-related disease by 80%, as will be discussed in [Section 5.5](#). While we cannot directly quantify this effect, our data indicate a decline in RSV-bronchiolitis cases in 2023-2024 compared to previous seasons.

Table 5.2. Parameter values for the Gompertz model adjustment of estimated RSV-bronchiolitis. The last two columns show the values of empirical reproductive number and specific growth rate at the onset of the fitted epidemic curve.

Season	K (cumulative cases)	a (day ⁻¹)	ρ_0	μ_0 (cases· day ⁻¹)
2018-2019	6,252 (6,220-6,285)	0.057 (0.057-0.058)	2.946	0.324
2019-2020	6,496 (6,470-6,523)	0.055 (0.054-0.055)	2.920	0.316
2022-2023	9,144 (9,091-9,196)	0.043 (0.043-0.044)	2.651	0.271
2023-2024	4,251 (4,232-4,269)	0.059 (0.059-0.060)	2.847	0.320

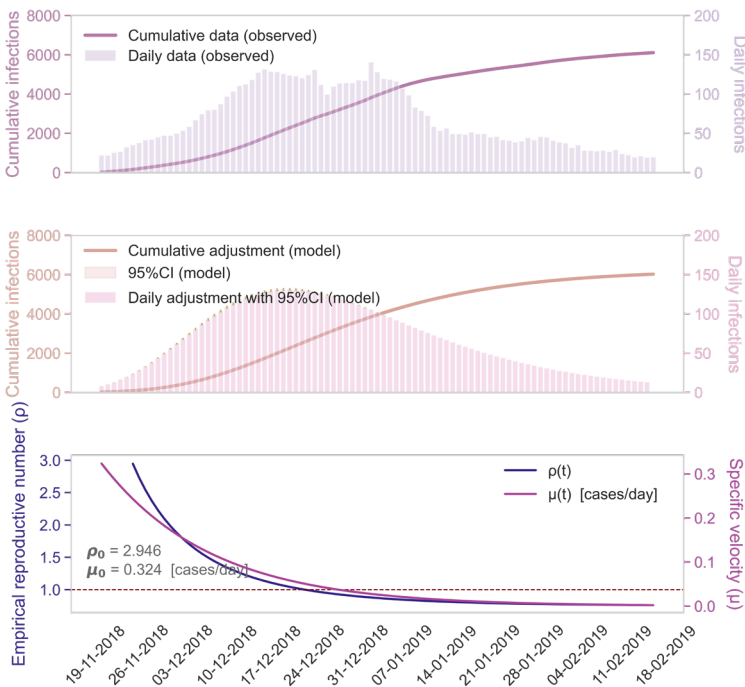


Figure 5.10. Gompertz model adjustments for estimated RSV-bronchiolitis season 2018-2019. Top panel: estimated RSV-caused bronchiolitis from diagnoses counts, assuming a 75% factor. Middle panel: fitted model outcome in terms of cumulative and daily counts. Bottom panel: model-derived specific growth rate and empiric reproductive number, with their initial values; the dotted line represents the $\rho = 1$ threshold, that stands for the inflection point of decrease in caseload.

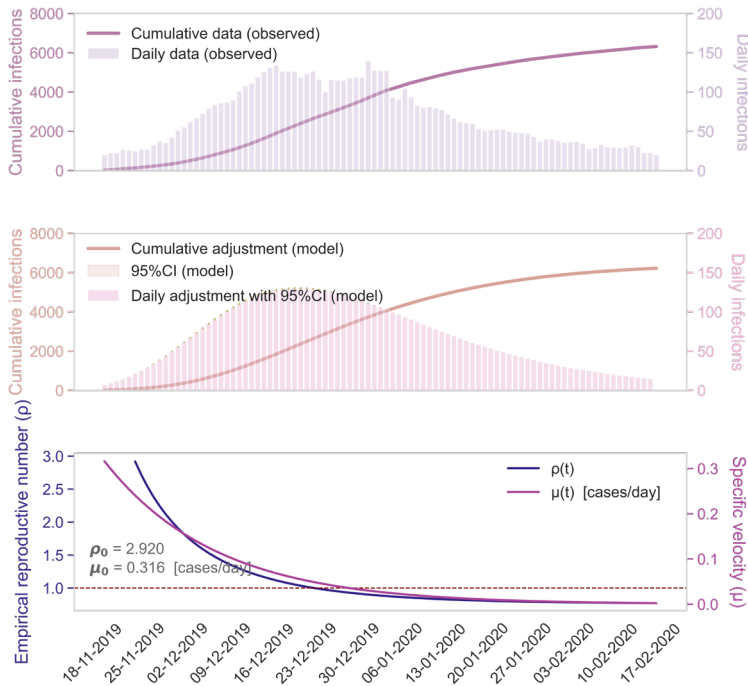


Figure 5.11. Gompertz model adjustments for estimated RSV-bronchiolitis season 2019-2020. Top panel: estimated RSV-caused bronchiolitis from diagnoses counts, assuming a 75% factor. Middle panel: fitted model outcome in terms of cumulative and daily counts. Bottom panel: model-derived specific growth rate and empiric reproductive number, with their initial values; the dotted line represents the $\rho = 1$ threshold, that stands for the inflection point of decrease in caseload.

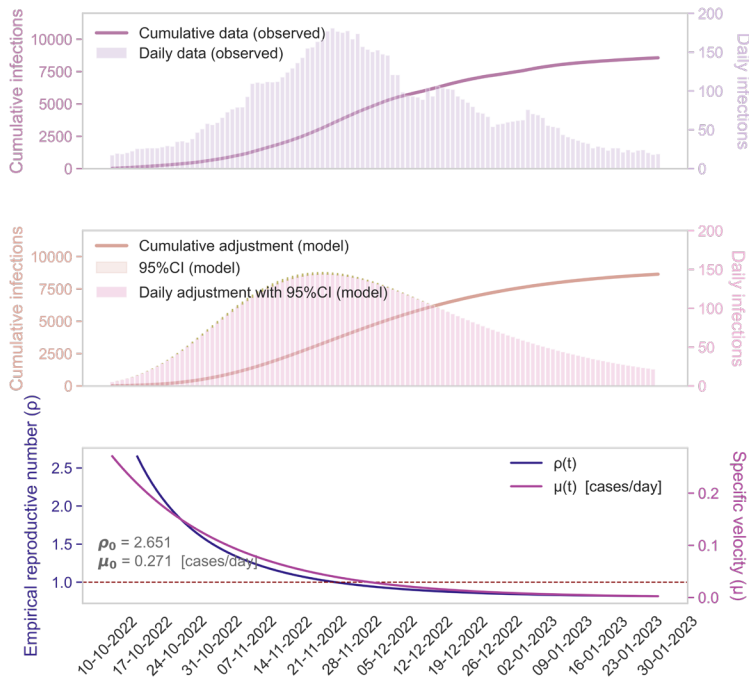


Figure 5.12. Gompertz model adjustments for estimated RSV-bronchiolitis season 2022-2023. Top panel: estimated RSV-caused bronchiolitis from diagnoses counts, assuming a 75% factor. Middle panel: fitted model outcome in terms of cumulative and daily counts. Bottom panel: model-derived specific growth rate and empiric reproductive number, with their initial values; the dotted line represents the $\rho = 1$ threshold, that stands for the inflection point of decrease in caseload.

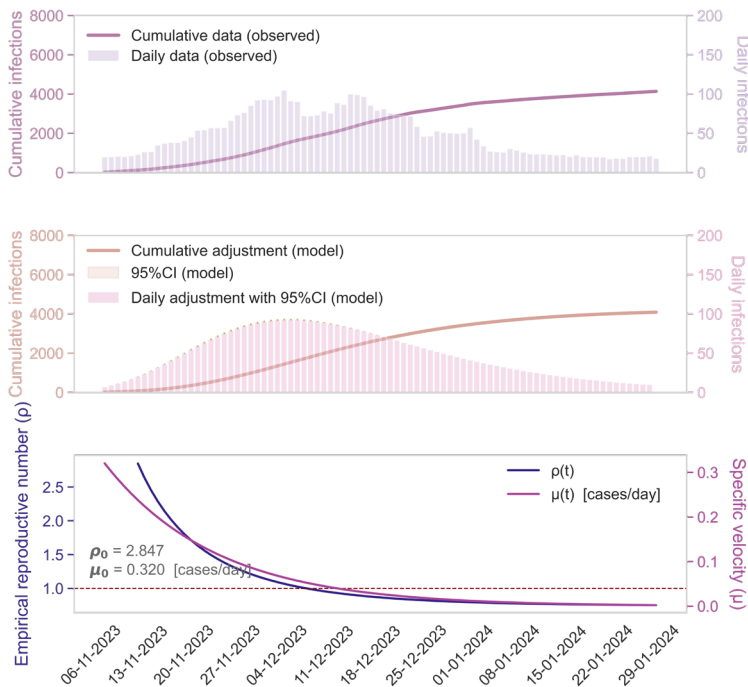


Figure 5.13. Estimated RSV-bronchiolitis Gompertz model adjustments for season 2023-2024. Top panel: estimated RSV-caused bronchiolitis from diagnoses counts, assuming a 75% factor. Middle panel: fitted model outcome in terms of cumulative and daily counts. Bottom panel: model-derived specific growth rate and empiric reproductive number, with their initial values; the dotted line represents the $\rho = 1$ threshold, that stands for the inflection point of decrease in caseload.

Another notable impact of the COVID-19 pandemic is the altered epidemic growth and decline rates. RSV-bronchiolitis now exhibits a slower μ_0 and prolonged decline phases, leading to broader epidemics despite their overall magnitude remaining similar to or exceeding pre-pandemic levels. This slower progression may explain why clinicians perceived post-pandemic epidemics as more severe, even when case numbers were comparable to past seasons.

A visual comparison of historical epidemic trends for RSV-bronchiolitis and influenza (see [Section 4.4.1](#)) as well as parameter analysis reveals distinct patterns. While both diseases exhibit rapid initial growth, influenza cases decline much faster, resulting in a more symmetrical epidemic that spans a shorter time frame. In contrast, RSV-bronchiolitis epidemics are broader, characterized by a sharp increase in cases followed by a prolonged decline, a pattern well captured by the Gompertz model. Additionally, estimates of the empirical reproduction number indicate that each RSV case leads to approximately three new infections, whereas each influenza case resulted in only two secondary infections, comparable to SARS-CoV-2, which shows the rapid transmissibility of RSV.

The RSV transmissibility is larger than influenza's. Besides, influenza epidemics are shorter and more symmetric.

These conclusions have been extracted from the adjustments' parameters, that are as rigorous as to observe $R^2 > 0.99$ in all cases. The model also accurately adjusts to the wop for all epidemics, although with a week in advance for season 2023-2024. Also, the peak magnitude is slightly underestimated, as it was for influenza epidemics. Specifically, the model underestimates the peak magnitude by 11% in season 2023-2024. Although the results vary by season, they demonstrate consistency in capturing the correct week of the peak, as detailed in [Table 5.3](#), with errors in magnitude typically less than 7% across all other seasons that were not affected by the consequences of the COVID-19 pandemic, with greater accuracy for influenza (see [Table 4.3](#)). The magnitude underestimation is computed based on the day the peak in reported cases is reached, which is highly stochastic due to irregularities in case reporting. However, visually, the model captures the peak quite well in general terms.

The discrepancies obtained could be influenced by differences in diagnostic behavior at the epidemic peak, as well as healthcare system capacity constraints, as explained previously. In some cases, peak days coincide with high healthcare demand, potentially leading to underreporting due to saturation or reporting delays, similar to what we discussed for influenza in [Section 4.4.1](#).

Moreover, notably, the pre-pandemic seasons are adjusted with greater accuracy, an effect that we also saw for influenza, which suggests that after the pandemic the Gompertz model may not be able to fully capture disease dynamics. Besides, the RSV epidemics have also been altered due to the introduction of nirsevimab.

Table 5.3. Adjusted and observed week and magnitude (in daily cases) of the peak per season, depending on the data used for forecasting defined as days before the epidemic peak. R^2 of the adjustments.

Season	Adjusted wop	Observed wop	Weeks of delay	Adjusted magnitude	Observed magnitude	Difference in magnitude (%)	R^2
2018-2019	2018-W52	2018-W52	0	131.50	140.46	-6.4	0.999
2019-2020	2019-W52	2019-W52	0	130.47	140.01	-6.8	1.000
2022-2023	2022-W48	2022-W48	0	145.20	180.86	-19.7	0.999
2023-2024	2023-W50	2023-W51	1	92.93	104.57	-11.1	1.000

The model is more accurate in pre-pandemic seasons, suggesting a change in dynamic patterns after the COVID-19 pandemic and the introduction of nirsevimab.

Predictive performance of Gompertz model

In **Table 5.4**, we summarized the predictive accuracy of the model, reporting the predicted week of peak at each iteration as well as its magnitude and comparing these values to the observed data. In addition, we show the accuracy obtained in the simulation of real-time successive predictions, from one month before the peak onwards. We also provide the MAPE of each adjustment. A plot of the model prediction per each iteration and the parameters values evolution are also reported in [Figure 5.14](#) to [Figure 5.17](#) and [Figure 5.18](#) to [Figure 5.21](#), respectively.

For most seasons, our model successfully predicts the epidemic peak week, with an error margin of only one week – being this delay, interestingly, only present for post-pandemic epidemics –, always predicting the peak earlier than the actual occurrence. This early prediction provides public health authorities

with a crucial window to act and allocate resources effectively to mitigate the epidemic's impact. Furthermore, the error in the predicted magnitude of the peak is typically below 20% when predictions are made 28 days in advance and below 10% 21 days in advance. Exceptions to this latter trend include an around 20% magnitude error for the 2022-2023 and 2023-2024 seasons, which are post-pandemic. Notably, the true magnitude of the peak lies within the confidence intervals of the prediction for all seasons.

Table 5.4. Predicted and observed week and maximum magnitude (in terms of weekly diagnoses, wM) of the peak per season, depending on the data used for forecasting defined as days before the epidemic peak. MAPE of the adjustments.

Season	Days before peak	Predicted wop	Observed wop	Weeks of delay	Predicted wM	Observed wM	Difference in magnitude (%)	MAPE (%)
2018-2019	32	2018-W52	2018-W52	0	1,406	876	60.51	43.38
	30	2018-W52		0	1,406		60.51	43.38
	28	2018-W52		0	1,220		39.27	28.91
	21	2018-W52		0	912		4.11	7
	14	2018-W52		0	875		-0.11	8.14
	7	2018-W52		0	869		-0.80	8.39
2019-2020	32	2019-W52	2019-W52	0	1,357	885	53.30	40.49
	30	2019-W52		0	1,109		25.31	20.27
	28	2019-W52		0	983		11.07	10.14
	21	2019-W52		0	826		-6.67	10.70
	14	2019-W52		0	817		-7.68	11.38
	7	2019-W52		0	847		-4.29	9.35
2022-2023	32	2022-W47	2022-W48	-1	1,175	1,220	-3.69	21.62
	30	2022-W47		-1	1,175		-3.69	21.62
	28	2022-W47		-1	1,138		-6.72	18.44
	21	2022-W47		-1	1,015		-16.80	8.26
	14	2022-W48		-1	978		-19.84	8.73
	7	2022-W48		-1	969		-20.57	9.34
2023-2024	21	2023-W50	2023-W51	-1	782	631	23.93	20.01
	14	2023-W50		-1	782		23.93	20.01
	7	2023-W50		-1	651		3.17	6.28

Chapter 5 – Respiratory Syncytial Virus: Modelling the RSV epidemic

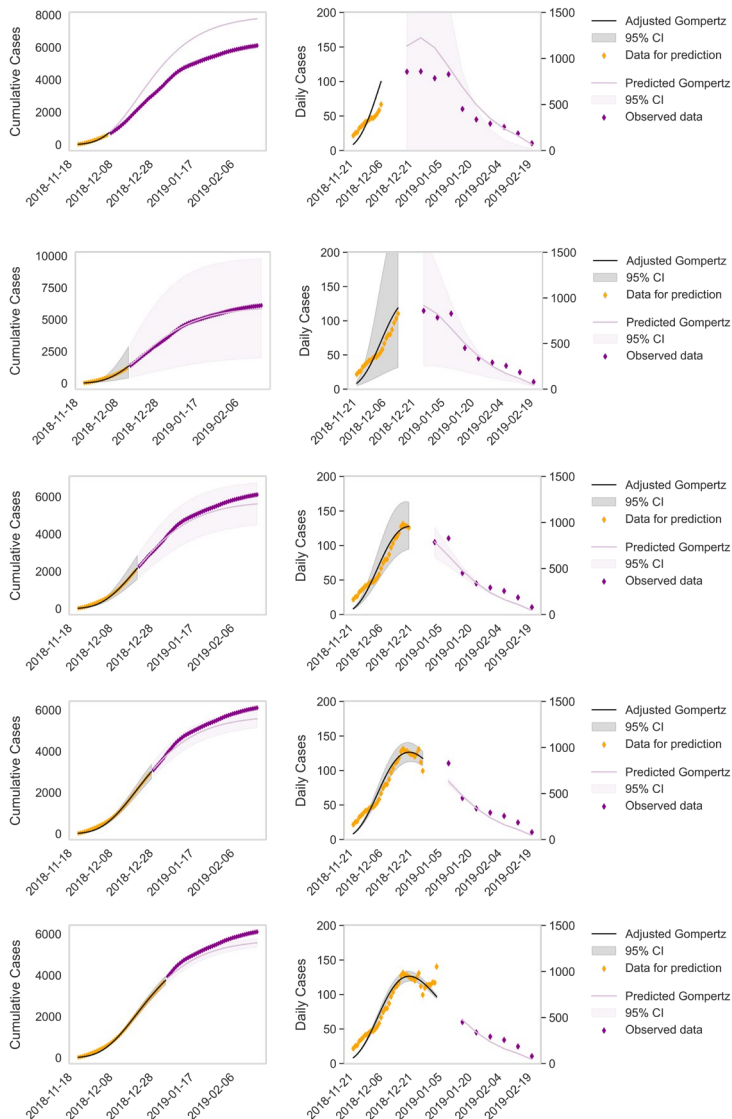


Figure 5.14. Iterative adjustment and predictions for 2018-2019 season of RSV-bronchiolitis. From top to bottom, iteration with data for prediction of 28, 21, 14, 7 and 0 days until the peak.

Chapter 5 – Respiratory Syncytial Virus: Modelling the RSV epidemic

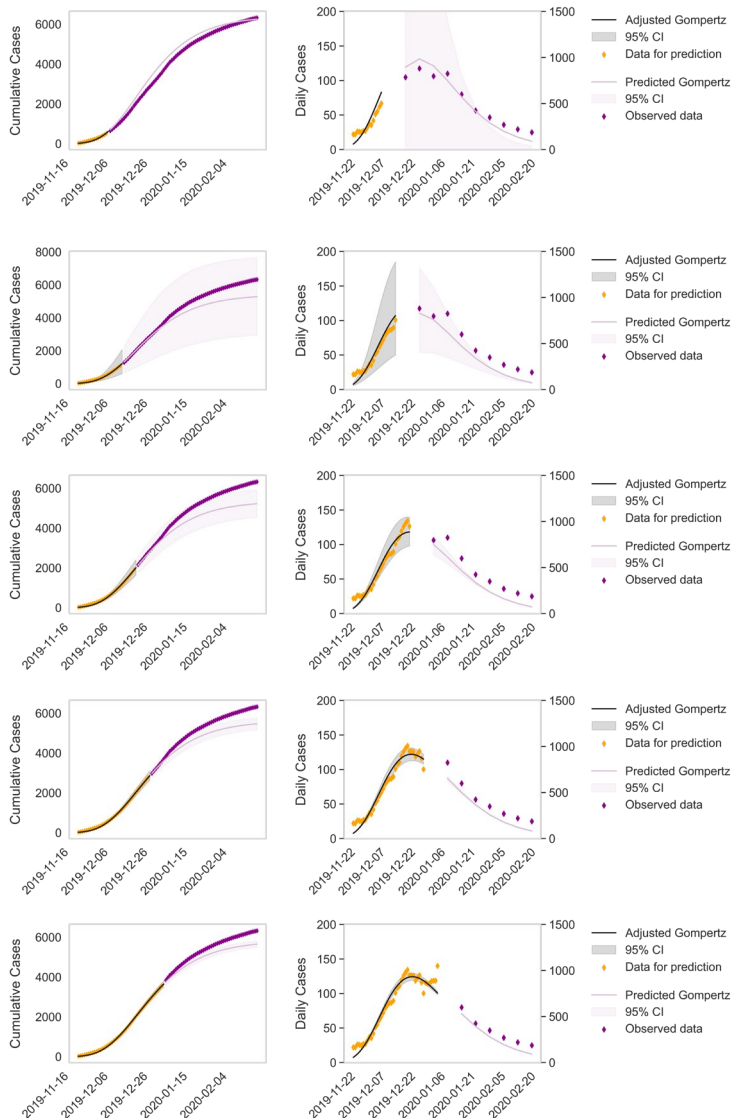


Figure 5.15. Iterative adjustment and predictions for 2019-2020 season of RSV-bronchiolitis. From top to bottom, iteration with data for prediction of 28, 21, 14, 7 and 0 days until the peak.

Chapter 5 – Respiratory Syncytial Virus: Modelling the RSV epidemic

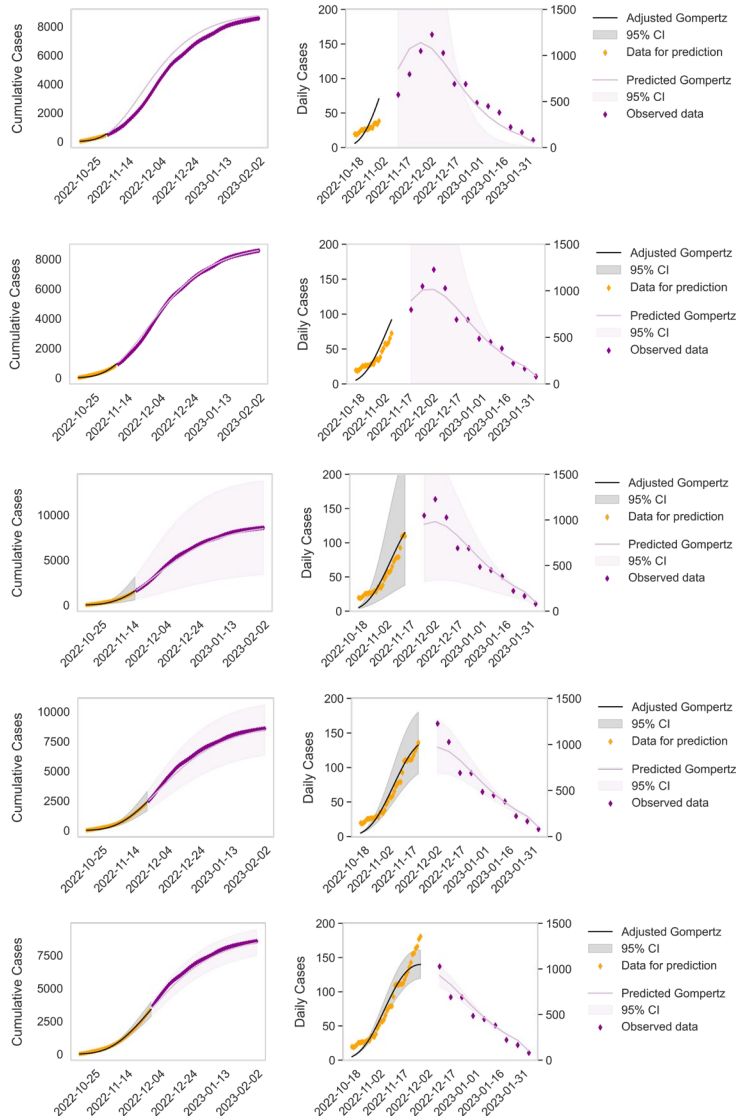


Figure 5.16. Iterative adjustment and predictions for 2022-2023 season of RSV-bronchiolitis. From top to bottom, iteration with data for prediction of 28, 21, 14, 7 and 0 days until the peak.

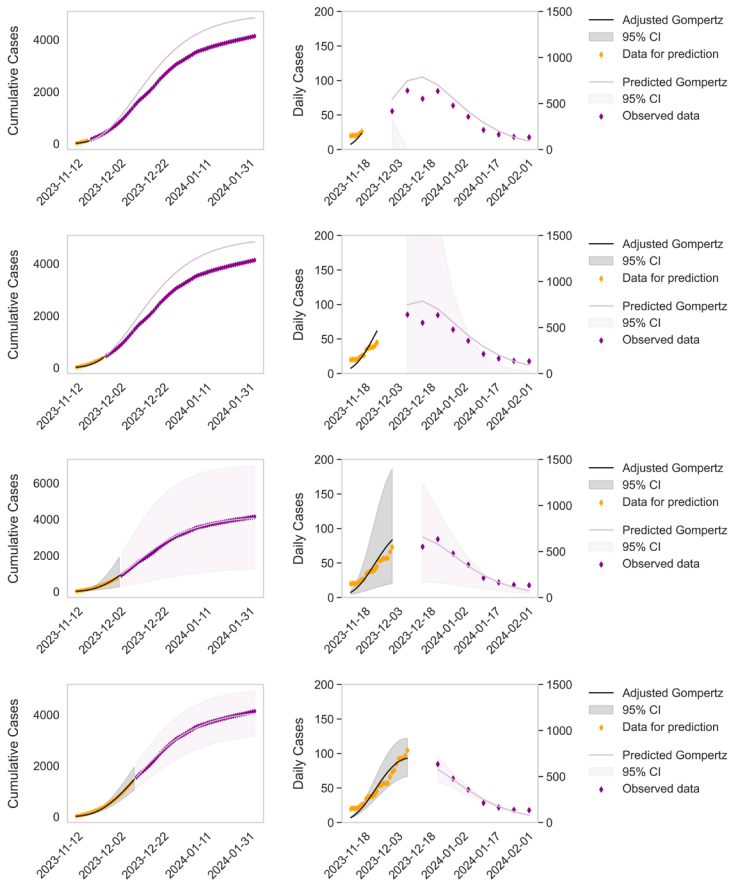


Figure 5.17. Iterative adjustment and predictions for 2023-2024 season of RSV-bronchiolitis. From top to bottom, iteration with data for prediction of 21, 14, 7 and 0 days until the peak.

As we argued for influenza (see [Section 4.4.1](#)) it is important to highlight that the presence of outliers can create discrepancies in identifying the true epidemic peak. This phenomenon is evident in [Figure 5.14](#) or [Figure 5.15](#), where the algorithm identified an outlier as the peak. However, the model's prediction remains accurate, as the outlier occurred during the week with the highest total reported cases, which is the basis for evaluating predictions. In

fact, in all seasons except 2022-2023, the observed cases consistently fall within the confidence intervals of the model's predictions. Nevertheless, it is to note that this might be the reason why the RSV model has a better predictive accuracy than the influenza one, since due to these outliers, the RSV season is being predicted with more data than influenza.

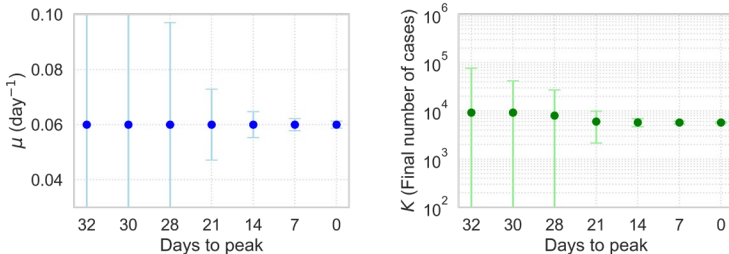


Figure 5.18. Parameter values evolution for the iterative adjustment and predictions for 2018-2019 season of RSV-bronchiolitis. Parameter K values are shown in a logarithmic axis.

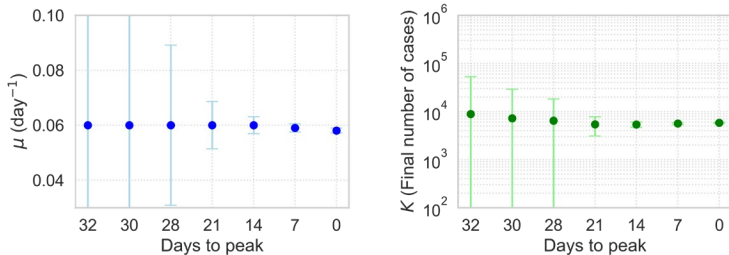


Figure 5.19. Parameter values evolution for the iterative adjustment and predictions for 2019-2020 season of RSV-bronchiolitis. Parameter K values are shown in a logarithmic axis.

As previously discussed, in real-life scenarios, the parameter boundaries are typically adjusted manually to better fit new data. Consequently, while the maximum magnitude prediction error in this study is around 40% of overestimation 28 days in advance, it would likely be significantly lower with human supervision, and it is mostly below 10% 21 days in advance, which is sufficient anticipation for public health practitioners.

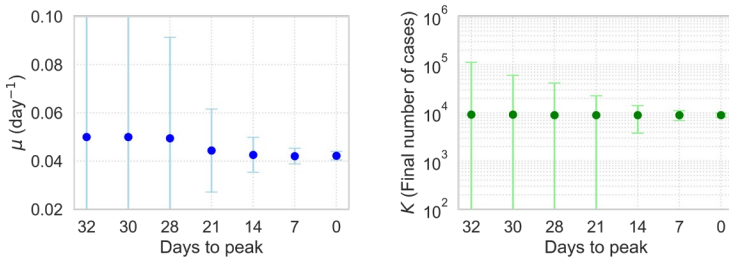


Figure 5.20. Parameter values evolution for the iterative adjustment and predictions for 2022-2023 season of RSV-bronchiolitis. Parameter K values are shown in a logarithmic axis.

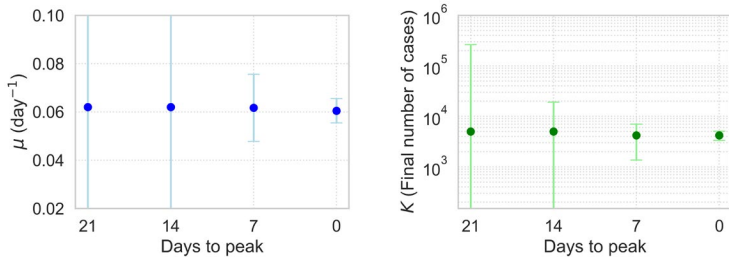


Figure 5.21. Parameter values evolution for the iterative adjustment and predictions for 2023-2024 season of RSV-bronchiolitis. Parameter K values are shown in a logarithmic axis.

Despite this, we successfully adjusted a Gompertz model to influenza and bronchiolitis daily diagnoses data in primary care in Catalonia. We estimated RSV-bronchiolitis from all-causes bronchiolitis in PCPs, which allowed us to accurately predict the week of the peak up to 32 days in advance for most seasons, with a one-week in advance error margin. All magnitudes are estimated with less than 25% of error 28 days before the peak except for 2018-2019 that has less than 5% peak magnitude difference from 21 days before the peak, and the observed magnitude falls upon 95% confidence intervals of the prediction for all seasons. For influenza, these affirmations remain true with slightly better minimum accuracy (see [Section 4.4.1](#)), while the maximum anticipation that we reach is 28 days before the epidemic peak, since the time of growth of the epidemic is shorter between the low epidemic level and the epidemic peak than for RSV-bronchiolitis. Hence, we achieved to predict

epidemic peaks of influenza and RSV-bronchiolitis one month in advance with an anticipated one-week margin and magnitude within 95% confidence intervals. Notably, the predictive capability of the models has been assessed automatically, but it could, and it has demonstrated to be, more accurate in a real-world scenario where human supervision is a vital part of the incorporation of mathematical models in a responsive and effective public health system. These findings are critically important for providing public health managers with timely information, enabling them to take proactive measures to mitigate epidemics and reduce associated health risks and costs.

Some limitations of this study are reported in [Section 4.4.1](#). Specific limitations dealing with RSV-bronchiolitis data are that the introduction of nirsevimab represents a significant change in their epidemiology, potentially altering transmission patterns, seasonal intensity and timing of the epidemic peak. This transformation poses new challenges for real-time prediction, as past epidemic trends may not be directly applicable to future seasons. One of the main uncertainties is the long-term effect of mass immunisation on RSV circulation—whether it will lead to a steady reduction in cases or whether it will introduce new epidemic dynamics, such as longer inter-temporal intervals or delays in epidemic peaks, which will be explored in the next section of this chapter. This is not a limitation of the work by itself, but it does constrain the accuracy in automatically evaluating the model for those years, since in real-time, we supervise and refine the parameter boundaries every iteration to fit the data. Another constraint is the accurate estimation of RSV-bronchiolitis, which is restricted to the available data with which to infer RSV cases from total diagnoses in primary care. Moreover, healthcare databases such as SIVIC and CMBD often suffer from underreporting biases, which tend to be compensated over time. It is also important to note that RSV testing in hospital settings (RSV bronchiolitis from CMBD) and primary care (RSV positive RAT) have different protocols, but both are a representative outline of the RSV epidemic, and we aim to ultimately use the latter while they are still available, as we have daily access to the data. On another note, since the hospitalizations data start in 2018 and RAT in 2021, we computed the RSV-bronchiolitis epidemic thresholds with pre and post pandemic data, while influenza thresholds are computed in pre-

pandemic data (**Section 2.2.1**). These thresholds should be yearly updated, but we assume them constant due to the restricted period in which to compute them. The starting point for modelling defined, as well as the parameter bounds for forecasting, will probably change from pre to post pandemic data once the epidemics stabilize, which has not happened yet.

To summarise

We successfully extracted potential RSV-bronchiolitis cases from primary care data in Catalonia and accurately predicted their evolution, along with that of influenza. Our predictive model demonstrated a capability of forecasting almost a month in advance the epidemic peak, with an error margin of just one week (in advance), and less than 25% error generally in magnitude without supervision, mostly falling within the model's confidence intervals. The performing metrics improve with subsequent real-time iterations, providing more accurate predictions as the peak gets closer. Additionally, incorporating human supervision can further enhance forecasting accuracy by iteratively refining the model adjusting parameter boundaries according to evolving data trends. These results are highly relevant for providing public health professionals with actionable insights, granting them more than two weeks to implement guidance and allocate resources to mitigate the impact of these recurrent epidemics. Besides, our results may offer relief to healthcare practitioners, as they can better anticipate demand in their consultancies.

5.5. Immunisation with nirsevimab

Up to this point, our discussion has largely focused on the challenges posed by RSV, particularly its significant burden on healthcare services – including hospitalizations, PICU admissions, and primary care – to its potential severity in infants, especially those <6 months of age. In some cases, severe RSV-related illness can even result in death. While modelling RSV epidemics is possible, the post-COVID-19 context has disrupted previous assumptions, and the recent introduction of nirsevimab has further altered RSV dynamics.

As previously introduced in [Section 5.2](#), the EMA authorised the administration of nirsevimab in October 2022, although it was not introduced in Catalonia nor any other region until autumn 2023. Nirsevimab is a recombinant human IgG1 kappa monoclonal antibody, in other words, is a lab-engineered antibody that mimics the ones our body naturally produces to fight viruses. It is precisely designed to block RSV by targeting its fusion protein, helping protect infants from serious illness. It is administered as a single intramuscular dose. This is the first strategy that has demonstrated its efficacy and safety in preventing RSV-LRTI in infants during their first epidemic season by, on average, 80% [234], [235]. As said in [Section 5.2](#), this product has been commercialised under the name *Beyfortus®* by Sanofi [236].

Nirsevimab's principle is that it inhibits the F protein from undergoing conversion to the post fusion conformation that is essential for the fusion of the virus with the membranes of the host cells ([Section 5.1](#)). This blockade stops viral entry into host cells thereby inhibiting the infection [237]. The current recommendation is the immunisation with nirsevimab instead of palivizumab since it confers the same protection against RSV as palivizumab with a single dose while palivizumab requires monthly dosing throughout the RSV circulation season. In addition, nirsevimab has 50 times the potency and activity of palivizumab and the duration of the immunity is of at least 5 months [256].

In March 2023, nirsevimab was approved in Spain. In Catalonia, the implementation of the preventive campaign with nirsevimab was launched in October 2023 as part of the infant immunisation program [257]. All infants born

between April and September 2023 were offered to receive a dose of nirsevimab in PCPs during October 2023. Additionally, all newborns born between October 2023 and March 2024 were offered to receive a single dose of nirsevimab in public and private hospitals, or at the PCPs during their first days of life (**Figure 5.22**). Similar strategies were carried out in other regions of Spain [258], [259], [260], France [261], Luxembourg [262], and the US [263]. However, France and the US experienced delays in the launch of their immunisation campaigns [264], [265].

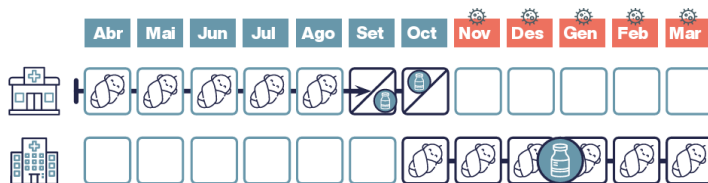


Figure 5.22. Scheme of the immunisation strategy with nirsevimab for infants in Catalonia. Retrieved from Canal Salut [257].

The first results on nirsevimab effectiveness showed a reduction of hospitalizations and PICU admissions of around 80% and 90% respectively. These are the cases of Galicia [258], [266], Murcia [267], the US [263], [268], Luxembourg [262], and France [269]. However, some studies in Valencia [267] and Navarra [260] show a slightly less performance, although studying younger children. Therefore, on one hand we aimed to assess how nirsevimab changed the epidemiological dynamics of RSV in Catalonia and if the age target of the viral infection changed with the immunisation implementation. On the other hand, we wanted to determine nirsevimab's effectiveness in Catalan infants born between April and September 2023 during their first epidemic season (catch-up cohort) [181] and in those born during the RSV season between October 2023 and January 2024 (seasonal cohort) [182]. This differentiation enables us to compare effectiveness among cohorts. A differentiation by sex in the effectiveness of nirsevimab on the seasonal cohort was studied, since RSV can affect males more severely than females and these can have worse responses to treatment (see **Section 5.2**), but this was done under the framework of a master thesis that is not publicly available at the moment of writing.

5.5.1. Dynamic changes after the introduction of nirsevimap

As we anticipated in [Section 5.3](#) and [Section 5.4](#), the historical seasonal patterns of the RSV changed following the launch of the immunisation campaign in October 2023. In this section, we explain how they differed from previous dynamics, and we discuss if these changes can be attributed to nirsevimap. This has been recently published [105].

Methods

Data acquisition

The SIVIC database (see [Section 1.3.1](#)) [61] was used to extract daily all-causes bronchiolitis clinical diagnoses (September 2014 - January 2024) and daily RSV-confirmed cases with RAT (January 2021 - January 2024) in Paediatric PCP. These electronic medical records were classified by age group (0-11 months old, 12-35 months old, >35 months old). The collected data on bronchiolitis diagnoses, include the International Classification of Diseases 10th version (ICD-10) codes J21, J21.0, J21.1, J21.8 and J21.9. This disease should be exclusively reported for infants ≤24 months, but the data source does not have this resolution. Hence, for this analysis, bronchiolitis for infants up to 35 months were considered, knowing that the most burden of the disease affects infants ≤24 months. Moreover, RATs are mostly recommended for children ≤24 months with viral respiratory infection suspicion but are not restricted to infants.

Reference populations per year and by age group were also obtained from the SIVIC database. Access to the PCP system is universal and free in Catalonia.

Statistical analyses

We computed daily incidences of all-causes bronchiolitis disease or RSV infection as reported cases per 100,000 inhabitants. The average pre-pandemic season for description of all-causes bronchiolitis was created as the mean of the epidemics from 2014-2015 to 2019-2020, considering the whole period from September to August. Previous alignment was unnecessary due to the regularity of the bronchiolitis epidemic seasonality in Catalonia (see [Figure 5.3](#)). The average 95% CI was also provided.

For further analysis, we defined a bronchiolitis or RSV season as the period of three months containing the months before, during, and after the epidemic peak, i.e., November to January for all years except 2020-2021, which was delayed to May 2021 - July 2021. For 2021-2022 and 2022-2023, it was anticipated from October to December.

Besides, we comprehensively depicted weekly RSV-infections incidence, RAT incidence named diagnostic effort, and positivity rates, i.e., the percentage of RSV-positive tests regarding the number of tests performed across the different age groups and study periods. A Mann-Whitney U test was employed to compare the most recent season, 2023-2024, and prior seasons, 2020-2021, 2021-2022, and 2022-2023. To account for multiplicity, the Bonferroni correction was implemented. We also analysed the percentage of RSV-confirmed infections for each paediatric age group (0-11m-old, 12-35m-old, >35m-old), computing the percentage of weekly (7-days accumulated) infections corresponding to each age group based on the total number of weekly RSV cases.

In addition, we calculated the incidence rate ratios (RR) and associated 95% CIs for the incidence of all-causes bronchiolitis in 0-11m-old from seasons 2014-2015 to 2023-2024. We selected the 12-35m-old group as a baseline reference. Similarly, the RRs (95%CI) for the incidence of RSV infection in 0-11m-old and 12-35m-old from 2021-2022 to 2023-2024 were obtained, with the >35m-old group as the baseline reference.

To compare last season, 2023-2024, to pre-nirsevimab epidemics, we calculated the mean pre-nirsevimab RR with its 95% CIs. For bronchiolitis, seasons 2020-2021 and 2021-2022 were excluded, and 2022-2023 was compared separately because of the alterations suffered due to the pandemic. The percentage of change in risk for RSV infection or all-causes bronchiolitis was assessed by computing the relative difference of the 2023-2024 RR concerning pre-nirsevimab RRs. To rigorously evaluate the variation in RSV or bronchiolitis incidences between the different seasons, a Mann-Whitney U test was performed in Python v3.11.9.

Results and discussion

RSV infections description

Comparison of 2021/22 and 2022/23 RSV epidemics with 2023/24 by age group

We analysed the percentage of confirmed RSV infections for each age group (**Figure 5.23**). A significant increase in RSV cases in the last season 2023-2024 may be due to a higher diagnostic effort for age groups $\geq 12\text{m-old}$.

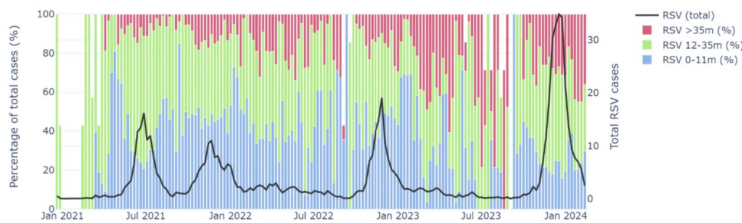


Figure 5.23. Percentage of weekly RSV infections (left axis) corresponding to 0-11m-old (blue), 12-35m-old (green), $>35\text{m-old}$ (magenta) concerning total number of RSV infections (black, right axis). Retrieved from Perramon-Malavez, A. et al. [105]. A higher resolution image can be found in the publisher's website.

However, positivity rates for all age groups were similar to 2020-2021 (summer 2021) (**Figure 5.24**). During the peak of season 2023-2024, 30% of the RSV infections were in children $> 35\text{ m-old}$, compared to 20% in 0-11 m-olds or 50% in 12-35 m-olds. Hence, regardless of the diagnostic effort, findings suggest a significantly increased community transmission of RSV in children $\geq 12\text{ m-old}$ ($p\text{-value} < 0.001$) when compared to the last two seasons.

Conversely, during the peak of season 2023-2024, 30% of the RSV infections were in children $> 35\text{m-old}$, compared to 20% in 0-11m-old or 50% in 12-35m-old. Hence, regardless of the diagnostic effort, findings suggest a significantly increased community transmission of RSV in children $\geq 12\text{m-old}$ ($p\text{-value} < 0.001$).

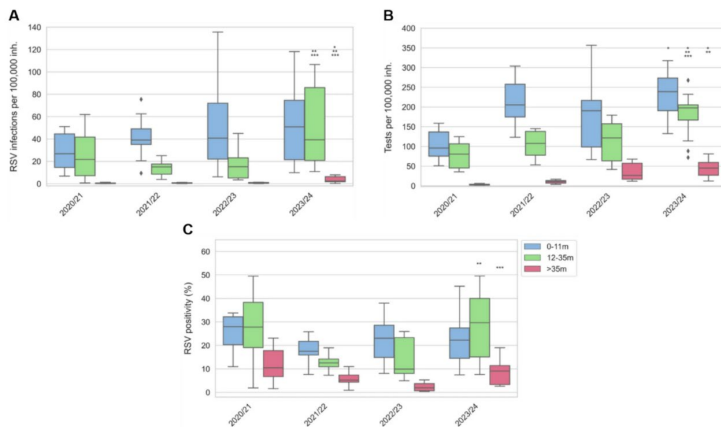


Figure 5.24. (A) Weekly RSV incidence, (B) diagnostic effort and (C) positivity for 0-11m-old (blue), 12-35m-old (green) and >35m-old (magenta) children and the RSV epidemics from 2020/21 to 2023-2024. A Mann-Whitney U test was performed to compare medians between seasons 2023/24 and 2020-2021 (* if $p < 0.05$), 2021/22 (** if $p < 0.05$) and 2022-2023 (** if $p < 0.05$). P -values were corrected using the Bonferroni correction. Retrieved from Perramon-Malavez, A. et al. [105]. A higher resolution image can be found in the publisher's website.

Associated risk of RSV infection to age, per season

For the 0-11 m-old group, the RRs (95% CI) before 2023-2024 were 7.4 (5.6-9.9), 8.8 (6.9-11.3), and 7.1 (5.7-8.9) in 2020-2021, 2021-2022, and 2022-2023, significantly higher than the RR (95% CI) of 1.7 (1.5-2.0) in 2023/2024 ([Figure 5.25](#)). Significant results from the Mann-Whitney U test comparing incidences of the periods mentioned above also showed p -value < 0.001 .

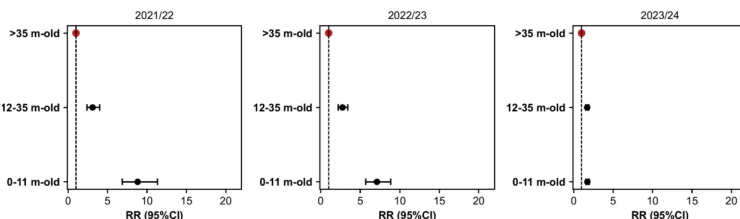


Figure 5.25. Rate Ratio (RR) of RSV infection for age groups 0-11m-old and 12-35m-old, regarding >35m-old, for seasons 2021-2022, 2022-2023 and 2023-2024. Retrieved from Perramon-Malavez, A. et al. [105].

Hence, in 2023-2024, the risk for RSV infection in infants 0-11 m-old compared to > 35 m-old was reduced by 76.7% (73.0-79.9), 80.3% (78.0-82.5), and 75.6% (73.4-77.5) from 2020-2021, 2021-2022, and 2022-2023 epidemics, respectively.

All-causes bronchiolitis description

Comparison of pre-pandemic and post-pandemic all-causes bronchiolitis epidemics with 2023/24

We depicted the incidence of all-causes bronchiolitis across infants 0-11 m-old, 12-35 m-old, and the combined group (all of them, ≤ 35 months), comparing the average incidence from pre-pandemic seasons (95% CI) with the last three epidemics ([Figure 5.26](#), partially updated in [Figure 5.3](#)). In the 2023-2024 season, bronchiolitis incidence notably decreased compared to pre-pandemic years among 0-11 m-olds. Conversely, incidence increased among 12-35 m-old children, in line with the ongoing post-pandemic trend. Analysis of the epidemic's overall impact on the combined ≤ 35 m-old age group revealed a pattern consistent with that observed in the 0-11 m-olds, as expected due to the higher disease burden in this cohort. This analysis indicated an overall reduction in bronchiolitis incidence during the 2023-2024 season, with seasonality closely resembling the pre-pandemic average.

Associated risk of all-causes bronchiolitis by age and per season

For the 0-11 m-old group compared to the 12-35 m-old, the pre-pandemic and 2022-2023 RRs (95%CI) were 9.4 (9.2-9.6) and 6.0 (5.7-6.2), respectively, significantly higher than the RR of 3.6 (3.4-3.8) for 2023-2024. Significance results from the Mann-Whitney U test comparing incidences of the aforementioned periods also showed p -value < 0.001, as one can see in the original article [105]. Hence, in 2023-2024, the risk for all-causes bronchiolitis in infants 0-11 m-old compared to 12-35 m-old was reduced by 61.9% (60.9-62.9) from the pre-pandemic period and by 39.8% (39.3-40.2) from the 2022-2023 epidemic.

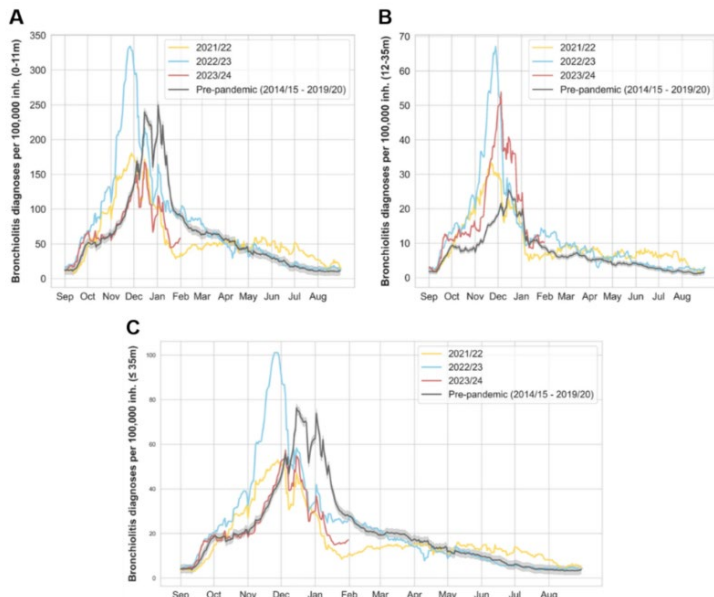


Figure 5.26. Daily bronchiolitis clinical diagnosis data per 100,000 inhabitants for (A) 0-11 m-old, (B) 12-35 m-old, (C) \leq 35 m-old. The grey line represents the average pre-pandemic season (2014-2015 to 2019-2020) with 95% CI. The yellow, blue, and red lines correspond to seasons 2021-2022, 2022-2023, and 2023-2024, respectively. Retrieved from Perramon-Malavez, A. et al. [105]. A higher resolution image can be found in the publisher's website.

All things considered, season 2023-2024 had a significantly lower comparative risk of RSV infection incidence (by 75.6% (73.4-77.5)) and all-cause bronchiolitis incidence (by 39.8% (39.3-40.2)) from 2022-2023 season, in infants 0-11m-old, even in a high RSV season community burden in Catalonia. Besides, children 12-35m-old carried the main burden of community RSV infection in season 2023-2024. During the latter, there have been significantly higher all-causes bronchiolitis and RSV infection incidences in children \geq 12m-old. These differences from previous seasons might be attributed to the introduction of the immunisation campaign with nirsevimab.

As for limitations, we must consider that compliance with the protocol for testing children with a RAT is not necessarily homogeneous among PCP paediatricians despite its availability and that are publicly financed; therefore, data about

community incidence cannot be deduced from RSV-confirmed cases. Nevertheless, we assume there have not been significant changes over time in each particular PCP, so season-to-season compatibility is still feasible. Also, aggregated epidemiological data do not include relevant confounders like those related to socioeconomic factors, which could bias the results.

To summarise

Using data from PCPs in Catalonia, we found out that in season 2023-2024 there was a significantly lower comparative risk of RSV infection incidence (by 75.6% (73.4-77.5)) and all-cause bronchiolitis incidence (by 39.8% (39.3-40.2)) from 2022-2023 season, in infants 0-11m-old, even in a high RSV season community burden in Catalonia. These differences might be attributed to the introduction of the immunisation campaign with nirsevimab to all children in their first RSV epidemic in October 2023. Previous bronchiolitis – and therefore inferred RSV – seasonality followed a very consistent pattern, with epidemics starting after school openings.

Nonetheless, the magnitude of the measured impact is consistent with other results, thus pointing to a minor effect of these confounders. Moreover, when calculating the RR, a historically consistent baseline group should be used to provide robustness when comparing periods. For this reason, the > 35 m-old was used as the control group to assess the divergence in the incidence of RSV infections among epidemics since, in each epidemic, the number of infected > 35 m-olds was similar. However, for all-causes bronchiolitis, we were limited by the diagnosis criteria and the age resolution of the reported data. Thus, we used 12-35 m-olds as the control group, which may have introduced bias into our results. Additionally, recommended immunisation was implemented for infants under 6 months old, so the reduction might be underestimated since the main outcome age range includes children up to 11 months old. Not being able to disaggregate the data by age is a limitation that cannot be compensated for, but that does not significantly impact our conclusions since children born from April 2023 were immunized and the data was extracted in January 2024. Nonetheless, this limitation would only result in

an underestimation of the effect of nirsevimab. In fact, the reductions in RR that we have assessed cannot be quantitatively compared with the outcomes of clinical studies, such as effectiveness, due to differences in objective and study design (e.g., use of RAT instead of PCR, or a population-level focus rather than a patient-level one). In this sense, our study is centred on a real-world evaluation and, as such, relies on the standard practices of paediatricians in primary care settings in Catalonia.

5.5.2. Nirsevimab effectiveness in Catalonia

Therefore, nirsevimab appears to have reduced the relative risk of bronchiolitis in primary care by approximately 70%. However, the key question remains: can this reduction truly be attributed to the introduction of nirsevimab? And more importantly, does its effectiveness in real-world settings align with the efficacy reported in clinical trials and outlined in its technical documentation? [235], [256]

To answer these questions, we assessed the effectiveness of nirsevimab in Catalonia. We did so for the seasonal and the catch-up cohorts separately. The first analysis to be published was the catch-up cohort one, by Coma, E. *et al.* [181]. Later on, we published the study on the seasonal cohort, by Perramon-Malavez, A. *et al.* [182], done during the research stay with the SISAP group at the ICS. Both studies share methodology, and we obtained similar results. However, since I conducted the second study but only collaborated in the first, I will explain both studies focusing more on the seasonal cohort one.

Methods

Study design and settings

We used a retrospective cohort design for the studies. Nirsevimab exposure was obtained from the Catalan Shared Clinical Records, a comprehensive clinical database of electronic medical records at patient level that integrates data from the entire Catalan health system. Data on hospital and PICU admissions were obtained from the CMBD and hospital emergency department visits from the CMBD-UR. Covariables and the eligible population were sourced from the central population register of the Catalan health service. The CMBD downloads data from hospital discharges of all hospitals in Catalonia,

encompassing both public and private hospitals. These datasets were accessed and managed using SQL and the data are not publicly available and were only accessible from the SISAP data centre at ICS (see [Section 1.3](#)).

For the catch-up cohort only, data was linked to the primary care EHRs to analyse primary care-related outcomes. This cannot be done for the seasonal cohort as parents are more likely to bring ill infants to the hospital emergency departments than to primary care paediatricians, hence there is an intrinsic bias in exploring PCP diagnoses for the youngest children.

Ethics committee was required for the studies and approval was given by Clinical Research Ethics Committee of the IDIAP Jordi Gol with reference number 24/015-EOM as it can be seen on Coma, E. *et al.* [181] and Perramon-Malavez, A. *et al.* [182].

[Participants and follow-up](#)

For the catch-up cohort, all infants born between April and September 2023 in Catalonia and deemed eligible for immunisation with nirsevimab were included. For the seasonal cohort, we included all infants born in Catalonia between October 1st, 2023 and January 21st, 2024.

The study period for the outcomes comprised between October 1st, 2023 to January 31st, 2024 for both cohorts. This period corresponds to the RSV epidemic 2023-2024 in Catalonia [181]. For the seasonal cohort, including infants born after January 21 would limit our ability to ensure sufficient follow-up and capture any RSV-related outcomes they may have experienced within the study timeframe.

We excluded patients without a valid health identifier number and those who died or moved outside Catalonia before the start of the immunisation campaign. Besides, we excluded patients who died within 4 days of birth or with missing sociodemographic information. For the seasonal cohort only, we excluded infants not assigned to PCPs in Catalonia, as these infants may have been born in private hospitals where the immunisation data was not reported timely to the Catalan public healthcare system. Private hospitals generally submit health records with delays and sometimes omit essential data points, which could

compromise the accuracy of their immunisation records. By limiting our cohort to infants under the care of public PCPs, we aimed to ensure a more consistent and reliable dataset, minimizing potential gaps in immunity data that could impact our analysis.

Two cohorts were established based on the nirsevimab administration date:

- **Exposed cohort (immunised with nirsevimab):** infants who received a dose of nirsevimab during the study period and this dose was recorded and is accessible.
- **Control cohort (non-immunised):** infants who did not have any record of a dose of nirsevimab during the study period.

For the seasonal cohort, we considered whether the exposed group could serve as controls during the short period before they received immunisation. However, since most newborns were immunised within 2 to 3 days after birth, this approach resulted in very limited follow-up time for those extended controls and was therefore not applied. In contrast, in the catch-up cohort study, exposure status was defined dynamically, i.e., infants who eventually received a dose of nirsevimab contributed person-time to the control group up until the date of immunisation, after which they were considered part of the exposed cohort.

Accordingly, non-immunised participants were followed from the start of the immunisation campaign in Catalonia (1st October 2023) until the earliest of the following events: receipt of a nirsevimab dose (at which point they transitioned to the exposed cohort), occurrence of the outcome, death, or end of follow-up. Immunised infants were followed from the date of nirsevimab administration until the earliest of an outcome, death, or end of the study. In the seasonal cohort study, non-immunised participants were followed from the day of birth until the earliest of the outcome, death, or end of follow-up.

Sensitivity analyses were made for both studies and they can be found in the proper published works [181], [182]. For simplicity, they will not be explored in this thesis.

Study outcomes

To better compare our results with other studies and between the analyses performed in Catalonia, in this thesis we will explore:

- **Hospital ED visits due to bronchiolitis:** any hospital emergency visit for all-cause bronchiolitis or RSV-related bronchiolitis.
- **Hospital admission due to bronchiolitis:** hospital admission with a discharge diagnosis of bronchiolitis due to RSV or all-causes bronchiolitis. In Catalonia, all paediatric patients with suspected acute LRTI who are admitted to the hospital are tested for RSV as well as influenza A and B viruses and SARS-CoV-2.
- **Admission to PICU for bronchiolitis:** any admission to the ICU during the hospital stay due to bronchiolitis caused by RSV or all-causes bronchiolitis.

Additional covariates

The sociodemographic covariates that we included for confounding assessment were week and month of birth, sex, nationality (Spanish or immigrant), rurality and socioeconomic status. We assessed socioeconomic status using the validated socioeconomic index from the Catalan Agency for Healthcare Quality and Assessment, calculated at the health basic area level [270]. For the seasonal cohort, we expressed this index using quartiles of its value, from most deprived (Q4) to least deprived (Q1), while for the catch-up cohort this was explored as a continuous variable. There is not a specific reason for that differentiation, and it does not affect the results. The rurality of residence was measured, with rural areas defined by a population <10,000 inhabitants and a density <150 inhabitants per km², as per regional guidance.

Statistical analyses

We computed monthly coverage for nirsevimab dividing the number of immunised children in a month by the total of born children that month. For descriptive analyses, we expressed continuous variables as median [min, max] – median (interquartile range (IQR)) for the catch-up cohort – and summarised categorical variables as a number (percentages). To provide more information

when analysing days admitted at the hospital or PICU, we included the mean (standard deviation (SD)). We determined the difference between the immunised and non-immunised groups for the descriptive variables through the computation of the p-value at a 95% confidence using the chi-squared test of independence for categorical variables and the standard two-samples t-test for continuous features. We assessed confounding using the standardised mean difference (SMD) of all covariables to compare both cohorts. We considered SMD>0.1 to be imbalanced and adjusted it in multivariable analysis [271]. We computed the cumulative incidence (risk) curves of each outcome using the Kaplan-Meier estimator. Cox proportional hazards (Cox PH) regression models using a calendar time scale [272] were then fitted to calculate hazard ratios (HRs) and 95% CIs for each of the study outcomes according to immunisation status. All Cox models were also adjusted for any confounders with an SMD>0.1. Two models were conducted separately for each of the outcomes, one for the time calendar adjustment and the other for the sensitivity analysis with matching. Visual inspection of Schoenfeld residuals against the transformed time and the diagnosis test of proportional hazards were used to evaluate the fulfilment of the assumptions to use Cox PH models [273], [274]. We estimated effectiveness as the per cent reduction in risk:

$$\text{Effectiveness} = 100 * (1 - \text{HR})$$

Eq. 5.1. ✓

All analyses were conducted using R V.4.4.1 (libraries *survival* and *survminer*).

Results

Before exclusions, 27,121 infants born between April and September 2023 and 17,880 infants born between October 2023 and January 21st, 2024 were eligible for nirsevimab immunisation. Exclusion charts can be found in the published works [181], [182]. In the end, data from 26,525 infants (97.8%) and from 15,341 infants (85.8%) were analysed for the catch-up and seasonal cohorts, respectively. Coverage rates of immunised infants were similar between cohorts, being around 90%. The sociodemographic characteristics of our control and exposed groups for the seasonal cohort are presented in **Table 5.5**. The corresponding table for the catch-up cohort is presented in Coma, E. et al. [172]. Although this cohort is older, the other sociodemographic characteristics

remain comparable between cohorts, perhaps the most different is nationality, as the seasonal cohort shows a greater tax of immigrant participants, but with only a 4-5% of divergence from the catch-up cohort. In both cases, the proportion of males and females was balanced across both immunised and non-immunised groups. In the seasonal cohort, while the groups were similar in terms of sex distribution, they showed differences in other sociodemographic characteristics (p -value < 0.05).

Table 5.5. Sociodemographic characteristics of the patients in our seasonal cohort.

Variable	Non-immunised (N=1,286)	Immunised (N=14,055)	p-value
Sex			
Female	595 (46.3%)	6,833 (48.6%)	
Male	691 (53.7%)	7,222 (51.4%)	0.113
Month of birth			
10/2023	310 (24.1%)	4,075 (29.0%)	
11/2023	321 (25.0%)	3,862 (27.5%)	
12/2023	355 (27.6%)	3,641 (25.9%)	< 0.001
01/2024	300 (23.3%)	2,477 (17.6%)	
Age at the end of the study (days)			
Median [min, max]	60.5 [10.0, 122.0]	69.0 [10.0, 122.0]	< 0.001
Nationality			
Spanish	1,020 (79.3%)	11,915 (84.8%)	
Immigrant	266 (20.7%)	2,140 (15.2%)	< 0.001
Rurality			
Rural	338 (26.3%)	3,181 (22.6%)	
Urban	948 (73.7%)	10,874 (77.4%)	0.003
Socioeconomic index (in quartiles)			
Q1 (least deprived)	281 (21.9%)	2,933 (20.9%)	
Q2	321 (25.0%)	3,687 (26.2%)	
Q3	313 (24.3%)	3,358 (23.9%)	
Q4 (most deprived)	371 (28.8%)	4,077 (29.0%)	0.71

Socioeconomic index was consistent across both groups, with the majority falling into the most deprived quartile. In the immunised cohort, there was a higher proportion of Spanish infants (79.3% vs 84.8% of Spanish nationality), and these infants tended to be slightly older by the end of the study, as most were born in October 2023. This also resulted in an SMD > 0.1, both for the

seasonal (**Figure 5.27**) and the catch-up cohort. Although the majority of participants were from urban areas, a greater proportion of rural infants was observed in the non-immunised cohort (26.3% and 22.6% of rurality), but this variable did not surpass the SMD threshold.

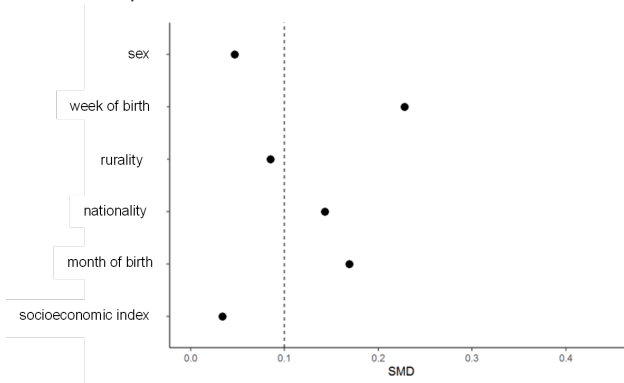


Figure 5.27. Representation of the computation of SMD for the potential confounding variables for the seasonal cohort. Retrieved from Perramon-Malavez, A. et al. [182].

Table 5.6. presents the results of the analysis of hospital and PICU length of stay. While immunised infants tended to have shorter average durations for both hospital stays and PICU admissions compared to non-immunised infants, these differences were not statistically significant (p -value > 0.05). This was not analysed for the catch-up cohort.

Table 5.6. Statistics for the days admitted to hospitals and paediatric intensive care units for patients in our seasonal cohort.

	Non-immunised (N=1,286)	Immunised (N=14,055)	p -value
Days hospitalized due to RSV bronchiolitis Mean (SD) Median [min,max]	5.53 (4.43) 4.5 [0, 24]	5.14 (3.95) 4 [1, 27]	0.645
Days at PICU due to RSV bronchiolitis Mean (SD) Median [min,max]	6.21 (3.68) 4 [2, 12]	5.04 (3.12) 5 [0, 15]	0.323

Kaplan-Meier survival curves were computed for the outcomes of study, and the cumulative incidence of events per outcome are presented in the published works [181], [182], but here we show the curves for the seasonal cohort in **Figure 5.28**.

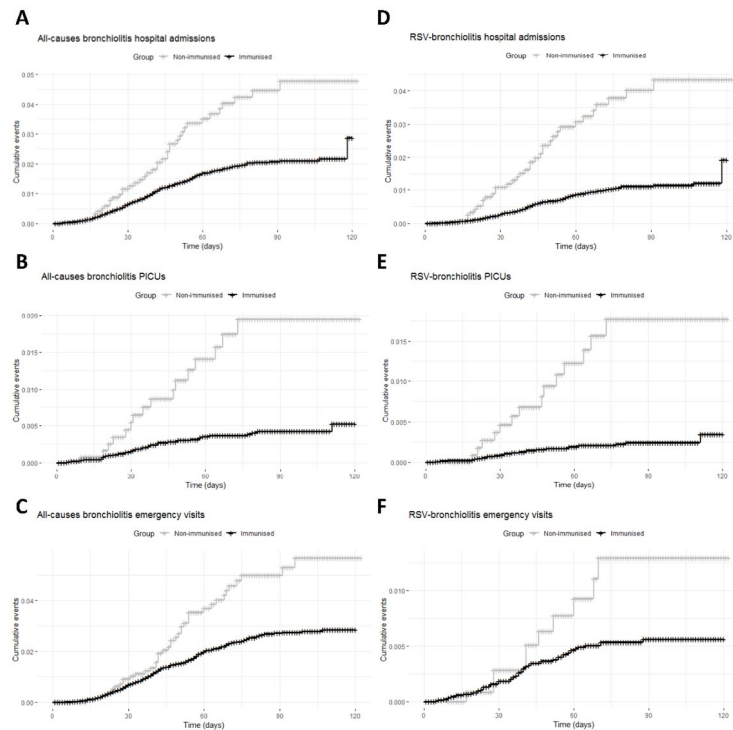


Figure 5.28. Cumulative events plots of the Kaplan-Meier survival curves of hospital admissions, PICUs and emergency department visits for all-causes bronchiolitis (**A-C**, respectively) and RSV bronchiolitis (**D-E**, respectively). For the seasonal cohort, retrieved from Perramon-Malavez, A. et al. [182]. A higher resolution figure can be found in the publisher's website.

Among participants of the study, there were 6.23 vs. 12.65 hospital emergency visits for RSV-associated bronchiolitis per 100,000 person-days, 12.16 vs. 43.57 hospital admissions and 2.78 vs. 17.76 PICU admissions per 100,000 person-days for the immunised vs. control group (**Table 5.7**). In the catch-up cohort, the incidence rates of hospital admission due to RSV bronchiolitis were

2.16 per 100,000 person-days for immunised infants compared to 9.55 for non-immunised participants; for ICU admissions these were of 0.33 and 2.13, and RSV bronchiolitis attended at the ED had incidence rates of 69.7 and 93.9, respectively [172]. In both cases, it is easily observed that children who received nirsevimab have had lower incidences of severe RSV-associated outcomes.

Table 5.7. Number of events, person-days follow-up and incidence (rate of number of events per 100,000 person-days) of the non-immunised and immunised infants in our seasonal cohort, with adjusted HR (aHR) 95%CI and effectiveness 95%CI for the different outcomes explored. Partially retrieved from Perramon-Malavez, A. et al. [182].

Outcomes	Non-immunised		Immunised		aHR	Effectiveness (%)
	Events	Incidence	Events	Incidence		
Hospital admission due to bronchiolitis RSV	34	43.57	109	12.16	0.26 (0.17-0.38)	74 (62-83)
PICU admission due to bronchiolitis RSV	14	17.76	25	2.78	0.15 (0.07-0.28)	85 (72-93)
ED visits due to bronchiolitis RSV	10	12.65	56	6.23	0.46 (0.23-0.90)	54 (10-77)
Hospital admission due to all-causes bronchiolitis	38	48.78	207	23.20	0.45 (0.31-0.63)	55 (37-69)
PICU admission due to all-causes bronchiolitis	16	20.31	44	4.89	0.23 (0.13-0.41)	77 (59-87)
ED visits due to all-causes bronchiolitis	41	52.82	255	28.67	0.49 (0.35-0.68)	51 (32-65)

After adjusting the Cox proportional hazards model for variables with SMD > 0.1, such as nationality and week of birth (a more precise measure than the month of birth), we observed clinically significant results. The adequacy of the

Cox proportional models was verified visualising the Schoenfeld residuals, that have to show a straightish line around 0 (proportional hazards condition fulfilled). To avoid redundancy, we do not provide these plots in this text, but proportionality of hazards can be ascertained if addressing to the published works [181], [182].

A single dose of nirsevimab was associated with a substantial reduction in the risk of hospitalization, with an adjusted hazard ratio (aHR) of 0.26 (95% CI: 0.18-0.39), compared to the 0.12 (95% CI: 0.09 to 0.18) of the catch-up cohort. This corresponds to an approximate 74% (95% CI: 61% to 82%) effectiveness of nirsevimab for the youngest infants vs. an 88% (95% CI: 82% to 91%) for the catch-up group. While these results mean that this same percentage stands for the reduction in the risk of hospitalization compared to untreated individuals, it is noticeable that the catch-up cohort shows a better protection against hospitalization than the seasonal cohort after the administration of nirsevimab, although not statistically significant since the CI overlap. In addition, the impact of nirsevimab immunisation was even more pronounced for PICU admissions, with an aHR of 0.15 (95% CI: 0.08-0.28) for the seasonal cohort, reflecting an 85% (95% CI: 72% to 92%) of reduction in the risk of critical care admission. This outcome is closer to the observed effectiveness for the catch-up cohort, showing aHR of 0.10 (95% CI: 0.04 to 0.24), of comparable magnitude. This finding is particularly significant as PICU admissions indicate severe clinical outcomes and involve substantial healthcare resource utilization. Finally, for emergency department visits, the aHR was 0.46 (95% CI: 0.23-0.90), implying a 54% (95% CI: 10% to 77%) reduction of ED visits due to bronchiolitis caused by RSV. Again, the catch-up cohort showed results of the same order, with an aHR of 0.45 (95% CI: 0.39-0.52). While the effect for ED visits is less marked than for hospitalizations or PICU admissions, it still underscores the effectiveness of nirsevimab in mitigating complications related to RSV, particularly those that require urgent care (**Table 5.7**). Besides, we can see that nirsevimab protects equally the seasonal and catch-up cohorts, with the greatest divergence for RSV-caused bronchiolitis hospital admissions, being the immunisation slightly more effective in the catch-up group. Other autonomous communities in Spain also reported greater effectiveness, such as

Galicia [258] (RSV-related LRTI hospitalizations reduced by 89.8% (IQR 87.5-90.3)), Navarra [260] (preventing hospitalization due to RSV-associated lower respiratory tract disease by 88.7% (95%CI: 69.6% to 95.8%), Murcia [267] (reduction of RSV-associated LRTI hospitalizations of 86.9% (95%CI: 77.1% to 92.9%)), but also to the US [268] first results (effectiveness of 90% (95% CI: 75% to 96%) against RSV-associated hospitalization). Even so, our observations are in line with those of Valencia [267] (reduction of RSV-associated LRTI hospitalizations of 69.3% (95%CI: 36.4% to 86.2%)), France [261], [269] (effectiveness in preventing severe RSV bronchiolitis in infants requiring PICU admission from 75.9% (95%CI: 48.5% to 88.7%) to 80.6% (95%CI: 61.6% to 90.3%) depending on the assumptions) and nirsevimab's clinical trials with a 62.1% (95% CI: -8.6% to 86.8%) in the study published by Hammit, L. L. *et al.* [275]. We present a summary of worldwide results on nirsevimab's effectiveness against RSV-associated hospitalization in **Figure 5.29**.

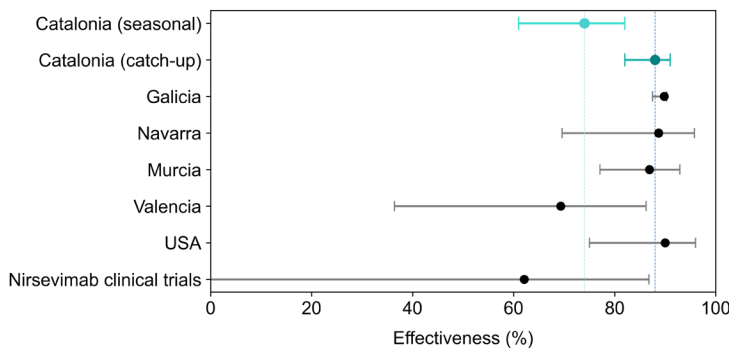


Figure 5.29. Summary of nirsevimab effectiveness against RSV-associated hospitalization outcomes in different regions worldwide.

This marginal decline observed in nirsevimab's effect for the seasonal cohort could be due to confounding effects that are not captured by our model, such as a higher risk of RSV-related severe LRTI in newborn children or maternal protection to infection, but further research would be needed to state a hypothesis. However, in 1994 there was already evidence of passive maternal protection through a maternal IgG antibody [276] more recently corroborated

[277] and under this premise, a maternal vaccine was developed and is already an immunisation strategy (see [Section 5.2](#)) [278], [279]. If this is the case, newborns would have relatively less risk of RSV infection because there would already be a basal defence against infection [42]. Nevertheless, pregnant women have generally had limited exposure to RSV, leading to infrequent natural transfer of antibodies. Concerning the higher risk of severe disease in younger infants, although their chances of infection might be lower than those of older infants, the strength of the symptoms is greater due to a naïve immune system and an immature anatomy. Due to this, nirsevimab would protect infants from RSV infection and derived severe disease but with an increased risk its effectiveness might be comparatively reduced. Nevertheless, even if we consider these factors, there is a clear need for an additional immunisation for RSV infection such as nirsevimab, as it has reduced hospitalizations by 74%.

To summarise

Nirsevimab has shown effectiveness in preventing 85% (95%CI: 72% to 93%) of RSV-associated bronchiolitis-caused admissions to PICU, 74% (95%CI: 61% to 83%) of admissions to hospitals and 54% (95%CI: 10% to 77%) of emergency visits to infants born during the RSV season (October 2023 – January 2024). For the slightly older infants forming the catch-up cohort, the observed effectiveness was of 90.1% (95%CI: 76.3% to 95.9%), 87.6% (95%CI: 82.1% to 91.4%) and 55% (95%CI: 48% to 61%), respectively. The marginal decrease in effectiveness for the seasonal cohort regarding hospitalizations prevention can be explained by a higher risk of RSV severe disease. Additionally, nirsevimab proved effective in mitigating all-cause bronchiolitis-related outcomes. These results were validated through sensitivity analyses employing patient matching.

These studies have some limitations that should be acknowledged, especially the seasonal cohort one. First, the exceptionally high coverage of nirsevimab in Catalonia, exceeding 90%, resulted in a limited number of control cases, which reduced the ability to explore nirsevimab effectiveness across all subgroups and

led to wider confidence intervals for some estimates. Additionally, while we adjusted for key confounders to ensure the robustness of our findings, residual confounding cannot be entirely ruled out. It is possible that unmeasured factors, such as specific environmental exposures or variations in access to healthcare, may have influenced the observed outcomes.

Furthermore, approximately 27% of births in Catalonia (latest published data corresponding to 2022 [11]) occur in private hospitals and the availability in the Catalan shared databases of the recording of doses administered in this type of hospitals may be late and/or less than in public hospitals. Therefore, for the seasonal cohort study patients without follow-up in primary care were excluded, as their immunisation status could not be reliably confirmed. Since for the catch-up cohort the immunisation was made at the PCP instead of at the hospital of birth, this information was more reliable. This exclusion likely underestimated the true effectiveness of nirsevimab for the seasonal cohort, as the inclusion of private hospital data could have provided a more comprehensive view of the population. Besides, this issue was particularly evident in subgroup analyses, such as those evaluating effectiveness by sex and for PICU admissions, where the low number of cases resulted in less precise estimates and lack of statistical power.

Despite these limitations, the comprehensive population coverage of these studies is remarkable, achieved by leveraging data from nearly all children in Catalonia, made possible by our universal and free healthcare system. This extensive coverage ensured a representative sample, offering robust and generalizable estimates of nirsevimab's effectiveness within the studied population. Besides, the use of a sensitivity analysis employing matching is another strength, as it reinforced the robustness of the primary findings by producing similar results. Additionally, the research considered a wide range of outcomes, including hospital admissions, PICU admissions, emergency visits, and length of hospital stay for the seasonal cohort; but also considering primary care outcomes for the catch-up cohort, which had not been previously done at the time of publishing. This comprehensive approach provided a holistic assessment of nirsevimab's impact on RSV-related disease.

Chapter 6

Conclusions

*Nature is what we know—
Yet have no art to say—
So impotent Our Wisdom is
To her Simplicity.*

Emily Dickinson

A s this thesis draws to an end, I invite the reader to see it not just as research, but as a journey through the ever-shifting realms of infectious diseases. From the bustling lands of Catalonia, we began by exploring the guardians of public health and the silent workings of the immune system. We faced the storm of SARS-CoV-2 and its aftermath in children, and learned how surveillance and epidemic thresholds guide our defences. Then came influenza, the shapeshifter, whose seasonal return we tracked through models and meteorological whispers. Finally, we met RSV—subtle, elusive—and the promise of new weapons like nirsevimab. At the heart of it all stood the young, our boldest knights, often first to charge into battle. May this work serve as both map and memory for those who continue the watch.

6.1. Summary of results and discussion

In this thesis, we have explored the epidemic dynamics of SARS-CoV-2, RSV and influenza in Catalonia, with particular focus on the role of children in the spread of these seasonal infections.

Extending surveillance panels to incorporate predictive indicators

Firstly, we established epidemic indicators to construct a semi-empirical risk panel for real-time epidemic surveillance. In doing so, we redefined the EPG indicator, demonstrating its ability to anticipate changes in epidemic incidence by approximately 4-5 days for bronchiolitis and 6-7 days for influenza. This index, combined with a semi-empirical reproduction number, weekly incidence changes and growth rates, formed the basis of our surveillance panel, an evolution of earlier work applied to COVID-19 monitoring [113].

In fact, the COVID-19 pandemic highlighted the critical need for robust, accessible infectious disease surveillance systems, especially for airborne-transmitted pathogens. While several countries have implemented public epidemic monitoring systems (such as the USA [110], UK [280], Canada [281], and Australia [282]), at the time of writing none offered short-term predictive indicators easily interpretable by the general public or decision-makers without a strong background in mathematical modelling. Given that infectious disease modelling relies heavily on data quality and technical expertise, EPG offers a practical alternative for very short-term forecasting. By anticipating epidemic thresholds and potential peaks nearly a week in advance and presenting this information in incidence terms – a widely used metric in clinical and public health settings – it becomes a valuable tool for operational decision-making. Additionally, our proposal to visualise EPG through a risk diagram provides a simple, intuitive representation of epidemic progression. Moreover, this indicator could also be integrated into more complex mathematical models to improve their forecasting accuracy.

Besides, to compliment the previous indicators we presented consistent epidemic thresholds for influenza and bronchiolitis through appropriate data pre-processing and adjustment for weekly reporting biases. These thresholds

have proven robust, even when accounting for data inconsistencies, particularly in bronchiolitis surveillance. Crucially, when weekly cases surpass a certain threshold combined with a defined growth rate, a substantial epidemic wave reliably follows in the subsequent weeks. Although we have not focused our research on predicting when this threshold will be surpassed, finding an incidence level from which the epidemic only grows has clear implications for future surveillance and preparedness, offering the potential to alert healthcare services ahead of anticipated increases in patient demand.

While the inclusion of hospitalization data would enhance the sensitivity and specificity of our monitoring panel, relying on clinical diagnoses offers practical advantages. The pandemic has accelerated the development and availability of centralised databases containing primary care clinical records, making this approach feasible and scalable in other settings ([110], [280], [281], [282]). The semi-empirical indicators we propose can be easily incorporated into such databases, providing a straightforward, actionable tool for epidemic management and public health surveillance.

Mathematical models to support influenza and bronchiolitis management

In parallel to these empirical indicators, we developed mathematical models to improve our understanding of transmission dynamics and support predictive efforts. While risk indicators are essential for operational and public communication, modelling provides deeper insight into underlying mechanisms and supports forecasting in a more scientific framework. In this context, we applied both empirical models, using the Gompertz equation for influenza and RSV-bronchiolitis epidemics, and mechanistic models, developing a SEIR-like framework incorporating a two-step transmissivity function, which we successfully modelled as a function of temperature with an associated delay.

Our empirical models enabled us to predict the week of the epidemic peak for both influenza and bronchiolitis with a maximum margin of error of one week, and frequently in advance. While the models typically underestimated the peak magnitude for both influenza and bronchiolitis, predictions consistently fell within the 95%CIs. These results align with previous studies where the

Gompertz model was used to predict COVID-19 cases [67], revealing this model as a robust empirical approach to provide mid-term predictive capacity. Notably, since 2021, these models have been actively used to inform public health authorities and paediatricians within the COPEDICAT network about the expected timing of influenza and bronchiolitis peaks in Catalonia. The primary distinction between these operational forecasts and the work presented in this thesis lies in the degree of human supervision applied during model validation. In real-world settings, parameter boundaries are continually refined as new data become available, allowing models to better adapt to emerging trends and to be even more accurate than the results presented hereby.

A significant contribution of this thesis has been the modelling of RSV-bronchiolitis epidemics using both hospitalization data and RAT results. While modelling RSV epidemics is conceptually similar to influenza, publicly accessible microbiological confirmation data for RSV in Catalonia only became available in 2021. Furthermore, the current RAT testing protocol primarily targets children under 15 years with clinical suspicion of respiratory infection, but testing is up to the paediatrician. This limits the dataset's size and scope for broader modelling purposes. As such, clinical diagnoses of bronchiolitis provide a more reliable proxy for anticipating RSV epidemics. Nevertheless, modelling bronchiolitis epidemics poses challenges, as other respiratory viruses can also cause similar presentations, leading to plateaus before and after epidemic peaks and introducing stochasticity into the data. To address this, we sought access to RSV hospitalization records and combined them with RAT results to estimate the proportion of bronchiolitis attributable to RSV, an approach that can be continually updated as new RAT data become available alongside all-cause bronchiolitis diagnoses. This methodology can also be applied to surveillance purposes whenever the main cause for bronchiolitis incidence is relevant, as for instance when designing immunisation campaigns.

Although hospitalizations data possess the advantage of having microbiological confirmation of infectious pathogens, one clear benefit of using primary care data for epidemic prediction is its ability to provide early signals of disease activity before cases escalate to hospital settings. As most influenza and RSV-

bronchiolitis cases are managed in outpatient care, primary care records capture the early spread of infections, offering valuable opportunities for timely public health interventions. In contrast, hospital-based forecasts are inherently delayed, as patients typically seek hospital care at later stages of illness. By enabling earlier trend detection, primary care-based models, such as our Gompertz-based approach, offer a practical tool for improving epidemic preparedness and response.

Besides, it also allowed us to compare the epidemic dynamics of influenza and RSV-bronchiolitis, revealing notable differences. Both diseases exhibited rapid initial growth, yet influenza epidemics declined more quickly, resulting in a shorter and more symmetrical epidemic curve. Conversely, RSV-bronchiolitis epidemics displayed a sharp rise followed by a more prolonged decline – patterns that were well captured by the Gompertz model. Moreover, empirical estimates of the reproduction number suggested a higher initial transmission potential for RSV-bronchiolitis, with each case generating approximately three secondary infections, compared to two for influenza. It is important to acknowledge, however, that our RSV analysis was limited to children under two years, as bronchiolitis diagnoses are restricted to this age group. Given that RSV also affects older children and adults – groups not captured in these data – comparisons between influenza and RSV transmission dynamics should be made cautiously.

It is important to note that modelling infectious diseases does not necessarily aim solely for predictive purposes. In this thesis, while both our empirical Gompertz-based models and mechanistic SEIR approach achieved comparable accuracy in reproducing the epidemic peak and magnitude for influenza, the SEIR framework provided valuable insights into the underlying mechanisms of disease transmissibility. Notably, it allowed us to characterise transmissivity as a two-step function, ultimately identifying a relationship between transmissivity and ambient temperature, which follows a decreasing exponential pattern with a two-week delay. While this work remains preliminary and open to refinement, it lays the groundwork for further exploration of the

relationship between influenza transmission and meteorological factors or, at the very least, the secondary effects one may have on the other.

Furthermore, this modelling strategy opens up the possibility of defining transmissivity as a function of other variables. For example, one previous study successfully quantified the relationship between transmissivity and human mobility patterns [283], but there remains a notable gap in applying similarly straightforward, effective approaches to meteorological variables. Some existing models addressing these questions tend to be overly complex and lack accessibility for public health practitioners [284]. The simple, adaptable modelling strategy proposed in this thesis thus offers a promising avenue for advancing this line of research.

On the new paediatric viral scenario during and after the pandemic: lessons learned and challenges

In addition to our modelling work, we addressed specific epidemiological questions for each virus under study. For SARS-CoV-2, a central concern was whether the virus would eventually follow a seasonal pattern, similar to influenza and RSV, or whether it would persist in a more sporadic, endemic form, like rhinovirus or adenovirus. To date, the evidence suggests the latter. Although it remains premature to definitively exclude the possibility of future waves of COVID-19, five years of pandemic evolution indicate that successive mutations, culminating in the global dominance of Omicron subvariants, have resulted in a virus with reduced severity compared to earlier strains. From a paediatric perspective, severe complications, including MIS-C, have significantly decreased since the Delta wave, and recent surveillance data in Catalonia suggest very few infections among children. At the time of writing, no new MIS-C studies reporting new cases have been published since 2022. This trend is reassuring, given growing evidence of possible long-term consequences of MIS-C, particularly in mental health and cardiovascular outcomes [285], [286].

Our findings also underscore the value of children as a sentinel population for infectious disease surveillance. During the COVID-19 pandemic, widespread use of RATs in primary care and schools made children a particularly well-

monitored group. However, this also raises an ethical concern on how much responsibility we place on children for community health. Historically, children have frequently suffered the burden of restrictive NPIs and have often been labelled as key transmitters of epidemics, frequently without robust evidence. In Spain, for example, children were subjected to prolonged mask mandates in schools, measures that have since been questioned in light of their limited epidemiological justification and potential negative effects on child development [287].

Similarly, it has long been assumed that children drive influenza epidemics, yet our analysis suggests otherwise. While children, particularly the 3-5 years old, inevitably accumulate a high disease burden during epidemics due to their more unrestricted social interactions, this does not necessarily imply that they initiate these outbreaks. Rather, it is possible that adults – often asymptomatic or mildly symptomatic – act as vectors, transmitting viruses such as RSV to more vulnerable paediatric populations, who then experience more severe disease. Despite this, public health interventions have traditionally targeted children first, including, more recently, the influenza vaccination campaign in Catalonia, which now is also directed to all children under five years of age [288]. This is not a drawback by itself but raises an important ethical question about our collective approach to epidemic prevention and surveillance. It remains questionable why adults, as the group most capable of understanding and managing preventive health behaviours, have not consistently shared in the burden of surveillance measures, vaccination campaigns, and NPIs to the same extent as children. A shift towards a more balanced distribution of preventive strategies, including adult vaccination and increased testing and surveillance in adults, would help to protect vulnerable children without disproportionately affecting their daily lives and development.

One example of this is nirsevimab. It has been proven highly effective in preventing severe RSV disease in infants, but there are other prevention strategies being developed such as maternal vaccination. However, this approach has not been verified to have the same effectiveness as nirsevimab, and it is a relatively new research line [279]. Until such strategies reach their full

potential, achieving high immunisation coverage in young children remains crucial to prevent RSV-associated hospitalizations and admissions to intensive care, with the potential to reduce these by more than 80%, as we have seen in this thesis. Nevertheless, important considerations remain regarding the high costs associated with nirsevimab (approx. €200 per dose [289]) and the implications of targeting the entire infant population. Balancing clinical benefits, economic sustainability, and equity in access will be a key challenge for health authorities moving forward.

Limitations of this thesis

Our results do not come without limitations. One of the major challenges we encountered was the restricted access to hospitalization data. Obtaining such data requires a laborious, time-consuming administrative process, and by the time access is granted, the data may already be outdated. This issue highlights a broader problem that extends beyond Catalonia: the global need for timely, high-quality, publicly available health data, particularly from electronic medical records, to support evidence-based public health research and response. While Catalonia benefits from a relatively coherent and integrated publicly available healthcare data system, expanding our analyses and methodologies to other regions would require substantial efforts from governments worldwide to improve both the availability and quality of public health data, since conducting meaningful analyses becomes complex when data originate from diverse sources with differing diagnostic systems and data structures.

An operational limitation also exists in the day-to-day reporting of diagnoses. Case numbers reported on Mondays typically double those of the weekend, reflecting both healthcare-seeking behaviours and reporting delays. Although we attempted to mitigate this by pre-processing and weighting the data, our methodology is not yet flawless. Greater collaboration with healthcare providers, particularly through access to data on primary care attendances, could enable the identification of these patterns more accurately and improve the reliability of epidemic forecasting.

Chapter 6 – Conclusions

Furthermore, the absence of microbiological confirmation for many infectious diagnoses remains a constraint. The overlap of different pathogens causing similar clinical syndromes complicates the modelling of epidemic waves, rendering them more stochastic and sensitive to initial conditions. Incorporating microbiological confirmation – either universal or by means of a paediatric representative sampling that allows for a specific monitoring of infections among children – would enhance the precision of future epidemic analyses and models. Moreover, our modelling approach depends on the epidemic levels defined for the diseases studied. As previously discussed, these thresholds will require periodic revision, particularly in light of post-pandemic trends and the introduction of immunisation strategies such as nirsevimab. Similarly, increased promotion of influenza vaccination among children in Catalonia [288] is expected to influence epidemic patterns over time, underscoring the importance of updating models and thresholds as additional seasons of data become available.

Nevertheless, there is reason for optimism regarding paediatric infectious disease outcomes. Public health systems are increasingly prioritising immunisation and disease prevention, as evidenced by expanded influenza and COVID-19 vaccination campaigns and the rollout of RSV immunisation programmes. Furthermore, there is growing interest in integrating surveillance and predictive modelling into routine public health decision-making. During the pandemic, such analyses proved profitable, and in the years since, the Catalan public health system has shown continued interest in epidemic forecasting to support healthcare planning.

However, it must be acknowledged that information alone does not lead to meaningful change: action and policy implementation do. While predictive models and surveillance systems provide essential tools for anticipating and managing health crises, their true value lies in how effectively public health authorities and policymakers translate these insights into timely, equitable, and evidence-based interventions.

6.2. Conclusions

The aim of this PhD thesis was to characterise and better understand the dynamics of SARS-CoV-2, influenza, and RSV in childhood in Catalonia over the past decade. While fully disentangling the nature of viral behaviour and disease transmission is an ambitious goal, this work has achieved substantial progress in describing how SARS-CoV-2 has settled into the viral landscape of Catalonia, how it currently affects children, and how influenza and RSV-bronchiolitis epidemics compare and interact. We have characterised the age-dependent profile of influenza epidemics, particularly in relation to their initial growth, and proposed new research lines investigating the relationship between influenza transmissivity and external environmental or social factors such as meteorology. Furthermore, we successfully differentiated RSV-bronchiolitis from all-cause bronchiolitis and developed predictive models for these and for influenza, creating a public health surveillance toolkit with newly defined epidemic indicators, such as the EPG and risk diagrams. In addition, this work evaluated the effectiveness and public health potential of RSV-preventive interventions, particularly nirsevimab, demonstrating its capacity to significantly reduce bronchiolitis-related morbidity and healthcare burden. Below, the specific conclusions for each objective are summarised:

- 1. To define epidemiological indicators and thresholds for the surveillance and early detection of respiratory diseases in Catalonia, with special focus on the paediatric population.*

We successfully defined and validated epidemic indicators including the EPG (effective potential growth), the semi-empirical reproduction number and risk diagrams adapted to paediatric respiratory diseases. These tools improved real-time surveillance and decision-making capacity within the public healthcare system, particularly when predicting epidemic peaks and monitoring severity levels, which we also defined using pre-pandemic data but that need readjustment once the epidemics reach post-pandemic stationarity.

Chapter 6 – Conclusions

2. *To describe and analyse changes in the epidemiological patterns of respiratory viral infections in children before, during, and after the COVID-19 pandemic, through prospective monitoring and dynamic modelling.*

The pandemic substantially altered the seasonality and transmission patterns of influenza and RSV in children. While influenza and RSV had a very stable synchronic seasonality, SARS-CoV-2 arose disturbing this stable system. During the pandemic period, RSV and influenza demonstrated disrupted epidemic curves, likely influenced by public health interventions. At the moment of writing, they are recovering pre-pandemic dynamics although new interventions such as nirsevimab have altered the recovery of their stationary state. Meanwhile, SARS-CoV-2 remains non-seasonal and with low incidence levels after vaccination campaigns and the predominance of the Omicron variant.

3. *To analyse pre-pandemic data on RSV and influenza epidemics in children in Catalonia using empirical epidemiological models (based on the Gompertz equation) to describe their epidemic dynamics.*

Empirical modelling with the Gompertz equation accurately captured the epidemics of RSV-bronchiolitis and influenza. Additionally, this modelling approach allowed us to characterise differences in the speed of epidemic growth and decline for RSV and influenza, finding that RSV exhibited a more transmissible pattern and more asymmetrical epidemics, while influenza had shorter but more steep outbreaks.

4. *To develop compartmental epidemiological models for influenza, incorporating meteorological factors as potential modulators of transmissivity.*

Our SEIR model for influenza allowed us to infer a two-step transmissivity function influenced by temperature with a two-week lag effect and discard significant effect of absolute humidity. This demonstrated the feasibility of integrating environmental variables into transmissivity estimation and opens a promising research line for modelling seasonal respiratory epidemics with environmental and social predictors.

Chapter 6 – Conclusions

5. *To assess the predictive performance of the models at short- and mid-term and their potential application in public health monitoring and response systems.*

The Gompertz model showed a high predictive performance anticipating the epidemic peak almost a month in advance with an error of just one week (usually in advance). Magnitude differences remain greater, of up to the 25% in the two weeks prior to the epidemic peak, but predictions get better with human intervention when iteratively new data is added. These models have proven operationally valuable for paediatric and public health authorities in Catalonia. Moreover, the interest shown by paediatricians from the COPEDICAT group, who reach out annually for epidemic forecasts, illustrates the applicability and trust of our models in supporting real-time clinical preparedness.

6. *To analyse the epidemiological characteristics and impact of multisystem inflammatory syndrome in children associated with SARS-CoV-2 in Catalonia.*

MIS-C incidence sharply declined following the dominance of the Omicron variant and vaccination campaigns. Since 2022, no new cases of MIS-C have been reported in Catalonia, a finding consistent with both its inherently low prevalence and the markedly reduced circulation of SARS-CoV-2 within the paediatric population.

7. *To evaluate the role of the paediatric population as a sentinel group for detecting and anticipating respiratory virus epidemics in the general population, particularly during the COVID-19 pandemic.*

During the COVID-19 pandemic, children were consistently tested in schools and PCPs with RAT. In addition, whole classes and bubble groups were also tested once a case was detected. This provided earlier signals of respiratory virus circulation than hospital data, making children a great surveillance group for infectious respiratory diseases. However, while effectively reflecting epidemic prevalence, our analysis challenges the assumption that they were predominantly infected in the early stages of the pandemic, showing similar or lower incidence taxes than the adult population.

8. To assess the role of children in the transmission dynamics of seasonal influenza epidemics in Catalonia.

Our findings suggest that children, especially the youngest, are not necessarily the initiators of influenza epidemics but disproportionately suffer from them due to higher exposure through unrestricted social interaction combined with limited previous contact with this virus, revealing a pattern of progressive transmission from broader community circulation. This insight questions historical assumptions about paediatric superspreading and highlights the importance of adult-driven transmission chains that are currently not monitored.

9. To analyse the epidemiological impact of new immunisation strategies for RSV in children in Catalonia, through statistical analysis and dynamic modelling approaches.

Nirsevimab demonstrated a high effectiveness in preventing severe RSV disease, with potential reductions in bronchiolitis-related hospitalizations and PICU admissions exceeding 80% both for the catch-up and seasonal cohorts. At the population level, a reduction in all-causes bronchiolitis diagnoses in PCPs was also observed. Furthermore, RSV circulation exhibited a notable shift in its primary affected group, moving from infants aged 0-11 months to older paediatric age groups.

6.3. Future work

These four years of research have, inevitably, raised more questions than they have answered. But this is the nature of science: a sometimes frustrating yet deeply rewarding pursuit that constantly returns us to the childlike impulse to ask *why* and *how*. While there are countless options for further research, this section will attempt to summarise the most pertinent and realistic lines of future work.

Firstly, the inclusion of hospitalisation and primary care attendance data would enable the development of additional epidemiological indicators, further enhancing the current risk panel. These data sources would be particularly valuable for refining RSV-bronchiolitis estimations and for improving early warning systems.

From a modelling perspective, the asymmetric structure of the Gompertz model proved highly effective for capturing the dynamics of bronchiolitis and influenza epidemics. However, the near-symmetrical epidemic pattern of influenza suggests that alternative models, such as the logistic model, may offer an improved fit. The Richards model, which was not tested in this work due to its increased complexity, could also be explored in future studies. While this thesis aimed for simpler models with fewer parameters to ensure accessibility and interpretability for public health professionals, the use of other empirical models may improve predictive accuracy without compromising usability.

An important next step would be to replicate a real-world forecasting context by iteratively updating parameter boundaries with newly acquired data to assess model accuracy over time. Although this would challenge the automated nature of the current framework, it would more closely simulate operational epidemic forecasting. Integrating an algorithm capable of adjusting parameter boundaries automatically in response to incoming data is another exploratory path. Some AI algorithms could prove particularly valuable for that aim. In fact, AI can also be used for modelling purposes and could help us identify hidden patterns, but some more years of data gathering are needed to be able to incorporate them into post pandemic surveillance and prediction of epidemics.

At a broader level, integrating these empirical models into international disease surveillance systems could substantially strengthen epidemic forecasting capacities and inform pandemic preparedness strategies. While real-time predictive modelling gained prominence during the COVID-19 pandemic [67], [79], this thesis underscores the importance of maintaining and expanding such practices. Ensemble modelling was very relevant during the pandemic and implemented in a European Hub in which we participated [290]. In an increasingly interconnected world, the health of one region cannot be considered in isolation from the global landscape. It is imperative that public health continues to adopt a global perspective, even when working with local data, through collaborative modelling hubs and shared forecasting platforms. Europe has demonstrated a pioneering attitude in this regard with the development of *Respicast* (<https://respicast.ecdc.europa.eu/>) [291].

In terms of data infrastructure, sustained access to rapid antigen tests for epidemic surveillance remains essential, and public health authorities must continue to invest in them. Furthermore, a robust healthcare information system that facilitates secure and timely access to high-quality, standardised data is crucial. This would allow for greater applicability of Catalan data in global research initiatives and improve comparability between studies.

This thesis also highlights two particularly promising lines of future research. The first involves further investigation into meteorological drivers of influenza epidemics. Preliminary results suggest that incorporating environmental factors, such as temperature and absolute humidity, can improve predictive accuracy and assist in identifying the necessary conditions for epidemic onset and peak. Developing transmissivity functions that integrate environmental, social, and behavioural factors could provide us with invaluable information to greatly enhance epidemic mitigation strategies.

The second research line calls for a critical re-examination of the assumed role of children in the initiation and propagation of respiratory epidemics. The availability of microbiologically confirmed infection data for all ages would enable a more accurate understanding of the contribution of different age groups to a certain disease epidemic. Developing age-structured SEIR-like models or agent-based models in combination with clinical studies about household viral transmission could be particularly informative for both influenza and RSV dynamics, with the potential to inform targeted immunisation strategies. For instance, while RSV immunisation currently focuses on infants, it may be valuable to explore the effectiveness of adult-targeted immunisation campaigns.

In this regard, although nirsevimab has demonstrated high effectiveness in preventing severe RSV disease, the economic burden of achieving sufficient immunisation coverage at the population level remains a challenge. Not all governments have the resources to adopt universal prevention strategies, often opting for treatment-centred approaches that, while cheaper in the short term, overlook the long-term economic and health consequences associated with post-infection comorbidities in children. It is essential to advocate for the long-

Chapter 6 – Conclusions

term value of preventive measures and to generate robust, actionable evidence that can guide public health authorities in negotiating fair and sustainable access to these interventions, an effort in which pharmaceutical companies must also assume their share of responsibility.

Finally, the pandemic reminded us that public health threats do not recognise borders. As demonstrated by COVID-19, a disease affecting one region inevitably affects others. Global cooperation in health systems, surveillance, immunisation coverage, and resource sharing remain indispensable if we are to effectively safeguard population health. This principle extends to vaccination coverage, as no disease can be eradicated without achieving critical population immunity thresholds. The ongoing challenge lies in ensuring that evidence-based preventive strategies reach all populations equitably, and that governments and public health authorities continue to advocate for their adoption.

Science, as well as healthcare, must be available for everyone, everywhere.

Note on language support

Throughout the writing of this thesis, artificial intelligence tools such as ChatGPT by OpenAI [292] were occasionally used to assist with grammar correction, vocabulary refinement, and stylistic enhancement, particularly in chapter introductions where a more narrative or creative tone was intended. These tools were employed solely to improve clarity and linguistic quality and were not used to generate, interpret, or analyse any scientific content. All scientific ideas, results, and interpretations presented in this work are entirely my own.

References

- [1] R. E. Neale *et al.*, "Balancing the risks and benefits of sun exposure: A revised position statement for Australian adults," *Aust N Z J Public Health*, vol. 48, no. 1, p. 100117, Feb. 2024, doi: 10.1016/j.anzjph.2023.100117.
- [2] R. Zampieri *et al.*, "Prevention and treatment of autoimmune diseases with plant virus nanoparticles," *Sci Adv*, vol. 6, no. 19, May 2020, doi: 10.1126/sciadv.aaz0295.
- [3] N. H. L. Leung, "Transmissibility and transmission of respiratory viruses," *Nature Reviews Microbiology*, vol. 19, no. 8, pp. 528-545, Mar. 2021, doi: 10.1038/s41579-021-00535-6.
- [4] J. Vila *et al.*, "The burden of non-SARS-CoV2 viral lower respiratory tract infections in hospitalized children in Barcelona (Spain): A long-term, clinical, epidemiologic and economic study," *Influenza Other Respir Viruses*, vol. 17, no. 1, p. e13085, Jan. 2023, doi: 10.1111/irv.13085.
- [5] P. V. Dasaraju and C. Liu, "Infections of the Respiratory System," *Concise Handbook of Infectious Diseases*, pp. 65–65, 1996, doi: 10.5005/jp/books/14120_12.
- [6] C. Troeger *et al.*, "Estimates of the global, regional, and national morbidity, mortality, and aetiologies of lower respiratory infections in 195 countries, 1990-2016: a systematic analysis for the Global Burden of Disease Study 2016," *Lancet Infect Dis*, vol. 18, no. 11, pp. 119-1210, 2018, doi: 10.1016/S1473-3099(18)30310-4.
- [7] "Respiratory Viruses and Young Children | Respiratory Illnesses | CDC." Accessed: Jul. 23, 2024. [Online]. Available: <https://www.cdc.gov/respiratory-viruses/risk-factors/young-children.html>
- [8] "VizHub - GBD Compare." Accessed: May 02, 2023. [Online]. Available: <https://vizhub.healthdata.org/gbd-compare/>

- [9] "Idescat. Indicadors bàsics de Catalunya. Població. Per grups d'edat." Accessed: Jul. 29, 2024. [Online]. Available: <https://www.idescat.cat/indicadors/?id=basics&n=10329>
- [10] "Estructura per edats de la població a Catalunya - Observatori de la mobilitat a Catalunya (OMC) - ATM." Accessed: Jul. 29, 2024. [Online]. Available: <https://omc.cat/ca/w/estructura-per-edats-de-la-poblacio-a-catalunya#>
- [11] "Idescat. Estadística de naixements. Nascuts vius segons sexe. Catalunya." Accessed: Jul. 29, 2024. [Online]. Available: <https://www.idescat.cat/pub/?id=naix&n=364>
- [12] M.J. Macías Reyes *et al.*, "Prevalence of Respiratory Infections during the 2018–2020 Period in the Paediatric Population of Primary Care Centres in Central Catalonia," *Healthcare (Switzerland)*, vol. 11, no. 9, p. 1252, May 2023, doi: 10.3390/healthcare11091252.
- [13] J. P. Allinson *et al.*, "Early childhood lower respiratory tract infection and premature adult death from respiratory disease in Great Britain: a national birth cohort study," *The Lancet*, vol. 401, no. 10383, pp. 1183-1193, Apr. 2023, doi: 10.1016/S0140-6736(23)00131-9.
- [14] L. Bont *et al.*, "Long-term consequences of respiratory syncytial virus (RSV) bronchiolitis," *Paediatr Respir Rev*, vol. 1, no. 3, pp. 221-227, Sep. 2000, doi: 10.1053/prrv.2000.0052.
- [15] R. W. Wilmott, "Long-term effects of severe lower respiratory tract infections in early childhood," *Journal of Pediatrics*, vol. 165, no. 1, pp. 1–3, Jul. 2014, doi: 10.1016/j.jpeds.2014.05.006.
- [16] C. C. Wang *et al.*, "Airborne transmission of respiratory viruses," *Science* (1979), vol. 373, no. 6558, 2021, doi: 10.1126/science.abd9149.
- [17] J. W. Tang *et al.*, "Hypothesis: All respiratory viruses (including SARS-CoV-2) are aerosol-transmitted," *Indoor Air*, vol. 32, no. 1, p. e12937, Jan. 2022, doi: 10.1111/ina.12937.

- [18] M. Drexler, "How Infection Works," 2010, Accessed: Aug. 05, 2024. [Online]. Available: <https://www.ncbi.nlm.nih.gov/books/NBK209710/>
- [19] D. A. J. Tyrrell and R. F. Sellers. "How Do Viruses Invade Mucous Surfaces? [And Discussion]." *Philosophical Transactions of the Royal Society of London*, vol. 303, no. 1114, pp. 75–83, 1983. [Online]. Available: <http://www.jstor.org/stable/3030120>.
- [20] G. McFadden *et al.*, "Cytokine determinants of viral tropism," *Nature Reviews Immunology*, vol. 9, no. 9, pp. 645-655, Aug. 2009, doi: 10.1038/nri2623.
- [21] J. L. Geoghegan *et al.*, "Virological factors that increase the transmissibility of emerging human viruses," *Proc Natl Acad Sci USA*, vol. 113, no. 15, pp. 4170-4175, Apr. 2016, doi: 10.1073/pnas.1521582113
- [22] J. E. Jones, V. Le Sage, and S. S. Lakdawala, "Viral and host heterogeneity and their effects on the viral life cycle," *Nature Reviews Microbiology* 2020 19:4, vol. 19, no. 4, pp. 272–282, Oct. 2020, doi: 10.1038/s41579-020-00449-9.
- [23] R. Sanjuán and P. Domingo-Calap, "Mechanisms of viral mutation," *Cellular and Molecular Life Sciences*, vol. 73, no. 23, pp. 4433-4448, Jul. 2016, doi: 10.1007/s00018-016-2299-6.
- [24] R. Sanjuán and P. Domingo-Calap, "Genetic Diversity and Evolution of Viral Populations," *Encyclopedia of Virology*, vol. 1-5, p. 53, Jan. 2021, doi: 10.1016/b978-0-12-809633-8.20958-8.
- [25] G. A. Somsen *et al.*, "Small droplet aerosols in poorly ventilated spaces and SARS-CoV-2 transmission," *Lancet Respir Med*, vol. 8, no. 7, pp. 658-659, Jul. 2020, doi: 10.1016/s2213-2600(20)30245-9.
- [26] L. Owen, M. Shivkumar, and K. Laird, "The Stability of Model Human Coronaviruses on Textiles in the Environment and during Health Care Laundering," *mSphere*, vol. 6, no. 2, Apr. 2021, doi: 10.1128/mSphere.00316-21.

- [27] P. Vasickova *et al.*, "Issues Concerning Survival of Viruses on Surfaces," *Food Environ Virol*, vol. 2, no. 1, p. 24, Mar. 2010, doi: 10.1007/s12560-010-9025-6.
- [28] S. Ashokkumar *et al.*, "Persistence of Coronavirus on Surface Materials and Its Control Measures Using Nonthermal Plasma and Other Agents," *Int J Mol Sci*, vol. 24, no. 18, p. 14106, Sep. 2023, doi: 10.3390/ijms241814106.
- [29] M. Biasin *et al.*, "UV-C irradiation is highly effective in inactivating SARS-CoV-2 replication," *Scientific Reports*, vol. 11, no. 1, pp. 1-7, Mar. 2021, doi: 10.1038/s41598-021-85425-w.
- [30] C. D. Lytle and J. L. Sagripanti, "Predicted Inactivation of Viruses of Relevance to Biodefense by Solar Radiation," *J Virol*, vol. 79, no. 22, p. 14244, Nov. 2005, doi: 10.1128/jvi.79.22.14244-14252.2005.
- [31] M. Moriyama, W. J. Hugentobler, A. Iwasaki, "Seasonality of Respiratory Viral Infections," *Annu Rev Virol*, vol. 7, no. 1, pp. 83-101, Sep. 2020, doi: 10.1146/annurev-virology-012420-022445.
- [32] J. S. Walker *et al.*, "Accurate Representations of the Microphysical Processes Occurring during the Transport of Exhaled Aerosols and Droplets," *ACS Cent Sci*, vol. 7, no. 1, pp. 200-209, Jan. 2021, doi: 10.1021/acscentsci.0c01522.
- [33] A. C. Lowen, J. Steel, S. Mubareka, and P. Palese, "High Temperature (30°C) Blocks Aerosol but Not Contact Transmission of Influenza Virus," *J Virol*, vol. 82, no. 11, pp. 5650-5652, Jun. 2008, doi: 10.1128/jvi.00325-08.
- [34] P. Wolkoff, "Indoor air humidity revisited: Impact on acute symptoms, work productivity, and risk of influenza and COVID-19 infection," *Int J Hyg Environ Health*, vol. 256, p. 114313, Mar. 2024, doi: 10.1016/j.ijeh.2023.114313.
- [35] K. Lin and L. C. Marr, "Humidity-Dependent Decay of Viruses, but Not Bacteria, in Aerosols and Droplets Follows Disinfection Kinetics," *Environ Sci Technol*, vol. 54, no. 2, pp. 1024-1032, Jan. 2020, doi: 10.1021/acs.est.9b04959.

- [36] C. Xu, X. Zheng, and S. Shen, "A numerical study of the effects of ambient temperature and humidity on the particle growth and deposition in the human airway," *Environ Res*, vol. 200, p. 111751, Sep. 2021, doi: 10.1016/j.envres.2021.111751.
- [37] C. E. A. Winslow, L. P. Herrington, and J. H. Nelbach, "The influence of atmospheric temperature and humidity upon the dryness of the oral mucosa," *Am J Epidemiol*, vol. 35, no. 1, pp. 27-39, Jan. 1942, doi: <https://doi.org/10.1093/oxfordjournals.aje.a118784>.
- [38] M. Glenet *et al.*, "Asymptomatic COVID-19 Adult Outpatients identified as Significant Viable SARS-CoV-2 Shedders," *Scientific Reports*, vol. 11, no. 1, pp. 1-6, Oct. 2021, doi: 10.1038/s41598-021-00142-8.
- [39] H. Chu *et al.*, "Host and viral determinants for efficient SARS-CoV-2 infection of the human lung," *Nature Communications*, vol. 12, no. 1, pp. 1-15, Jan. 2021, doi: 10.1038/s41467-020-20457-w.
- [40] J. Hou *et al.*, "Integrated multi-omics analyses identify anti-viral host factors and pathways controlling SARS-CoV-2 infection," *Nature Communications*, vol. 15, no. 1, pp. 1-14, Jan. 2024, doi: 10.1038/s41467-023-44175-1.
- [41] J. E. Kohlmeier and D. L. Woodland, "Immunity to respiratory viruses," *Annu Rev Immunol.*, vol. 27, pp. 61-82, 2009, doi: 10.1146/annurev.immunol.021908.132625.
- [42] A. Gambadauro *et al.*, "Immune Response to Respiratory Viral Infections," *International Journal of Molecular Sciences*, vol. 25, no. 11, p. 6178, Jun. 2024, doi: 10.3390/ijms25116178.
- [43] A. H. Newton, A. Cardani, and T. J. Braciale, "The host immune response in respiratory virus infection: balancing virus clearance and immunopathology," *Semin Immunopathol*, vol. 38, no. 4, pp. 471-482, Jul. 2016, doi: 10.1007/s00281-016-0558-0.
- [44] T. J. Braciale, J. Sun, and T. S. Kim, "Regulating the adaptive immune response to respiratory virus infection," *Nature Reviews Immunology*, vol. 12, no. 4, pp. 295-305, Mar. 2012, doi: 10.1038/nri3166.

- [45] S. P. Commins, L. Borish, and J. W. Steinke, “Immunologic messenger molecules: Cytokines, interferons, and chemokines,” *Journal of Allergy and Clinical Immunology*, vol. 125, no. 2, Feb. 2010, doi: 10.1016/j.jaci.2009.07.008.
- [46] V. Sencio, M. G. Machado, and F. Trottein, “The lung–gut axis during viral respiratory infections: the impact of gut dysbiosis on secondary disease outcomes,” *Mucosal Immunology*, vol. 14, no. 2, pp. 296-304, Jan. 2021, doi: 10.1038/s41385-020-00361-8.
- [47] D. Zheng, T. Liwinski, and E. Elinav, “Interaction between microbiota and immunity in health and disease,” *Cell Research*, vol. 30, no. 6, pp. 492-506, May 2020, doi: 10.1038/s41422-020-0332-7.
- [48] I. Boncheva, J. Poudrier, and E. L. Falcone, “Role of the intestinal microbiota in host defense against respiratory viral infections,” *Curr Opin Virol*, vol. 66, p. 101410, Jun. 2024, doi: 10.1016/j.coviro.2024.101410.
- [49] V. Marrella, F. Nicchiotti, and B. Cassani, “Microbiota and Immunity during Respiratory Infections: Lung and Gut Affair,” *International Journal of Molecular Sciences*, vol. 25, no. 7, p. 4051, Apr. 2024, doi: 10.3390/ijms25074051.
- [50] “Serveis sanitaris. CatSalut. Servei Català de la Salut.” Accessed: Dec. 31, 2024. [Online]. Available: <https://catsalut.gencat.cat/ca/serveis-sanitaris/>
- [51] M. Castells Oliván *et al.*, “Capítol 2. El sistema de salut a Catalunya: estructura i dinàmica,” in Modernització tecnològica, canvi organitzatiu i serveis als usuaris en el sistema de salut de Catalunya. Informe de recerca (volum II), Universitat Oberta de Catalunya. Internet Interdisciplinary Institute (IN3), 2007, ch. 2. [Online]. Available: <http://www.uoc.edu/in3/pic>
- [52] “Regions sanitàries. CatSalut. Servei Català de la Salut.” Accessed: Dec. 31, 2024. [Online]. Available: <https://catsalut.gencat.cat/ca/coneix-catsalut/catsalut-territori/>
- [53] “Quin CAP correspon a una adreça?. CatSalut. Servei Català de la Salut.” Accessed: Dec. 31, 2024. [Online]. Available: <https://catsalut.gencat.cat/ca/centres-sanitaris/quin-cap-correspon-a-una-adreca/>

- [54] “El sistema sanitari públic. CatSalut. Servei Català de la Salut.” Accessed: Dec. 30, 2024. [Online]. Available: <https://catsalut.gencat.cat/ca/coneix-catsalut/presentacio/informes-memories-activitat/infografies/sistema-sanitari-public/index.html>
- [55] “El SISCAT: sistema sanitari integral d'utilització pública de Catalunya. CatSalut. Servei Català de la Salut.” Accessed: Dec. 30, 2024. [Online]. Available: <https://catsalut.gencat.cat/ca/coneix-catsalut/presentacio/model-sanitari-catala/siscat/>
- [56] “Sistema sanitari català: assistència de qual... - Govern.cat.” Accessed: Dec. 30, 2024. [Online]. Available: <https://govern.cat/salaprensa/notes-premsa/228333/sistema-sanitari-catala-assistencia-de-qualitat-per-a-tots-els-ciutadans>
- [57] “Catalunya gasta 1.250 euros per persona i any en salut.” Accessed: Dec. 30, 2024. [Online]. Available: <https://www.3cat.cat/324/catalunya-gasta-1-250-euros-per-persona-i-any-en-salut/noticia/299261/>
- [58] “Pressupost 2023. CatSalut. Servei Català de la Salut.” Accessed: Dec. 30, 2024. [Online]. Available: <https://catsalut.gencat.cat/ca/coneix-catsalut/transparencia/economia-patrimoni/pressupostos/pressupost-2023/>
- [59] “Catàleg | Dades obertes de Catalunya.” Accessed: Dec. 31, 2024. [Online]. Available: <https://analisi.transparenciacatalunya.cat/?sortBy=relevance&page=1&pageSize=20>
- [60] “Dades Obertes Catalunya - Salut.” Accessed: Dec. 30, 2024. [Online]. Available: <https://analisi.transparenciacatalunya.cat/browse?category=Salut&sortBy=relevance&page=1&pageSize=20>
- [61] “SIVIC - Inici.” Accessed: Feb. 16, 2023. [Online]. Available: <https://sivic.salut.gencat.cat/>
- [62] “Dades meteorològiques de la XEMA | Dades obertes de Catalunya.” Accessed: Dec. 09, 2024. [Online]. Available:

https://analisi.transparenciacatalunya.cat/Medi-Ambient/Dades-meteoroligiques-de-la-XEMA/nzvn-apee/about_data

- [63] "Conjunt mínim bàsic de dades (CMBD). CatSalut. Servei Català de la Salut." Accessed: Dec. 31, 2024. [Online]. Available: <https://catsalut.gencat.cat/ca/proveidors-professionals/registres-catalegs/registres/cmbd/index.html>
- [64] "Idescat. Institut d'Estadística de Catalunya." Accessed: Dec. 31, 2024. [Online]. Available: <https://www.idescat.cat/>
- [65] R. Rosenfeld and R. J. Tibshirani, "Epidemic tracking and forecasting: Lessons learned from a tumultuous year," *Proc Natl Acad Sci USA*, vol. 118, no. 51, pp. 1-6, 2021, doi: 10.1073/pnas.2111456118.
- [66] A. Perramon-Malavez *et al.*, "A semi-empirical risk panel to monitor epidemics: multi-faceted tool to assist healthcare and public health professionals," *Front Public Health*, vol. 11, no. January, pp. 1-13, 2023, doi: 10.3389/fpubh.2023.1307425.
- [67] M. Català *et al.*, "Empirical model for short-time prediction of COVID-19 spreading," *PLoS Comput Biol*, vol. 16, no. 12, p. e1008431, Dec. 2020, doi: 10.1371/journal.pcbi.1008431.
- [68] F. Brauer, C. Castillo-Chavez, and Z. Feng, "Mathematical Models in Epidemiology," *Springer New York*, New York, 2019, doi: 10.1007/978-1-4939-9828-9.
- [69] K. Sherratt *et al.*, "Predictive performance of multi-model ensemble forecasts of COVID-19 across European nations," *Elife*, vol. 12, Apr. 2023, doi: 10.7554/elife.81916.
- [70] N. Ouerfelli *et al.*, "Empirical Modeling of COVID-19 Evolution with High/Direct Impact on Public Health and Risk Assessment," *Int J Environ Res Public Health*, vol. 19, no. 6, p. 3707, Mar. 2022, doi: 10.3390/ijerph19063707.

- [71] D. Kucharavy and R. De Guio, "Application of Logistic Growth Curve," *Procedia Eng*, vol. 131, pp. 280–290, Jan. 2015, doi: 10.1016/j.proeng.2015.12.390.
- [72] E. Pelinovsky *et al.*, "Logistic equation and COVID-19," *Chaos Solitons Fractals*, vol. 140, p. 110241, Nov. 2020, doi: 10.1016/j.chaos.2020.110241.
- [73] N. Bacaër, "Verhulst and the logistic equation (1838)," in *A Short History of Mathematical Population Dynamics*, Springer, London, 2011, pp. 35-39. doi: 10.1007/978-0-85729-115-8_6.
- [74] R. D. Berger, "Comparison of the Gompertz and Logistic Equations to Describe Plant Disease Progress," *Phytopathology*, vol. 71, pp. 716-719, Aug. 1980.
- [75] H. Fujikawa, A. Kai, and S. Morozumi, "A new logistic model for Escherichia coli growth at constant and dynamic temperatures," *Food Microbiol*, vol. 21, no. 5, pp. 501-509, 2004, doi: 10.1016/j.fm.2004.01.007.
- [76] K. M. C. Tjørve and E. Tjørve, "The use of Gompertz models in growth analyses, and new Gompertz-model approach: An addition to the Unified-Richards family," *PLoS One*, vol. 12, no. 6, p. e0178691, Jun. 2017, doi: 10.1371/journal.pone.0178691.
- [77] C. P. Winsor, "The Gompertz curve as a growth curve," in *Proceedings Of The National Academy Of Sciences*, vol. 18, no. 1, pp. 1-8, Jan. 1932, doi: 10.1073/pnas.18.1.1.
- [78] C. Vaghi *et al.*, "Population modeling of tumor growth curves and the reduced Gompertz model improve prediction of the age of experimental tumors," *PLoS Comput Biol*, vol. 16, no. 2, p. e1007178, 2020, doi: 10.1371/journal.pcbi.1007178.
- [79] I. Villanueva *et al.*, "Country-report pattern corrections of new cases allow accurate 2-week predictions of COVID-19 evolution with the Gompertz model," *Sci Rep*, vol. 14, no. 1, pp. 1-11, 2024, doi: 10.1038/s41598-024-61233-w.

- [80] V. K. R. Chimmula and L. Zhang, "Time series forecasting of COVID-19 transmission in Canada using LSTM networks," *Chaos Solitons Fractals*, vol. 135, 2020, doi: 10.1016/j.chaos.2020.109864.
- [81] İ. Kirbaş *et al.*, "Comparative analysis and forecasting of COVID-19 cases in various European countries with ARIMA, NARNN and LSTM approaches," *Chaos Solitons Fractals*, vol. 138, 2020, doi: 10.1016/j.chaos.2020.110015.
- [82] "A simple overview of RNN, LSTM and Attention Mechanism | by Manu Chauhan | The Startup | Medium." Accessed: Jan. 27, 2025. [Online]. Available: <https://medium.com/swlh/a-simple-overview-of-rnn-lstm-and-attention-mechanism-9e844763d07b>
- [83] "Deep Learning para la predicción de series temporales: Redes Neuronales Recurrentes (RNN) y Long Short-Term Memory (LSTM)." Accessed: Jan. 27, 2025. [Online]. Available: <https://cienciadedatos.net/documentos/py54-forecasting-con-deep-learning>
- [84] J. Brownlee, *Long Short-Term Memory Networks With Python*, vol. 1, no. 1. 2017.
- [85] R. R. Guerra *et al.*, "Forecasting LoRaWAN RSSI using weather parameters: A comparative study of ARIMA, artificial intelligence and hybrid approaches," *Computer Networks*, vol. 243, p. 110258, Apr. 2024, doi: 10.1016/j.comnet.2024.110258.
- [86] E. Kolemen *et al.*, "A new deep recurrent hybrid artificial neural network of gated recurrent units and simple seasonal exponential smoothing," *Granular Computing*, vol. 9, no. 1, pp. 1-10, Mar. 2024, doi: 10.1007/s41066-023-00444-4.
- [87] A. Wiratsudakul, P. Suparit, and C. Modchang, "Dynamics of Zika virus outbreaks: An overview of mathematical modeling approaches," *PeerJ*, vol. 2018, no. 3, 2018, doi: 10.7717/peerj.4526.
- [88] K. K. Steinhöfel, D. Heslop, and C. R. MacIntyre, "Agent-Based Models of Virus Infection," *Current Clinical Microbiology Reports*, vol. 12, no. 1, pp. 1-7, Jan. 2025, doi: 10.1007/s40588-024-00238-5.

- [89] P. J. Thomas and A. Marvell, "Scaling of agent-based models to evaluate transmission risks of infectious diseases," *Scientific Reports*, vol. 13, no. 1, pp. 1-15, Jan. 2023, doi: 10.1038/s41598-022-26552-w.
- [90] C. Nitzsche and S. Simm, "Agent-based modeling to estimate the impact of lockdown scenarios and events on a pandemic exemplified on SARS-CoV-2," *Scientific Reports*, vol. 14, no. 1, pp. 1-17, Jun. 2024, doi: 10.1038/s41598-024-63795-1.
- [91] M. Català *et al.*, "The impact of prioritisation and dosing intervals on the effects of COVID-19 vaccination in Europe: an agent-based cohort model," *Sci Rep*, vol. 11, no. 1, Dec. 2021, doi: 10.1038/s41598-021-98216-0.
- [92] M. Kretzschmar and J. Wallinga, "Mathematical Models in Infectious Disease Epidemiology," *Modern Infectious Disease Epidemiology*, vol. 28, pp. 209-221, Jul. 2009, doi: 10.1007/978-0-387-93835-6_12.
- [93] S. Alonso *et al.*, "Age-dependency of the Propagation Rate of Coronavirus Disease 2019 Inside School Bubble Groups in Catalonia, Spain," *Pediatric Infectious Disease Journal*, vol. 40, no. 11, pp. 955-961, 2021, doi: 10.1097/inf.0000000000003279.
- [94] D. C. P. Jorge *et al.*, "Estimating the effective reproduction number for heterogeneous models using incidence data," *R Soc Open Sci*, vol. 9, no. 9, Sep. 2022, doi: 10.1098/rsos.220005.
- [95] A. Cori *et al.*, "A new framework and software to estimate time-varying reproduction numbers during epidemics," *Am J Epidemiol*, vol. 178, no. 9, pp. 1505-1512, 2013, doi: 10.1093/aje/kwt133.
- [96] A. Annunziato and T. Asikainen, "Effective reproduction number estimation from data series," *Publications Office of the European Union*, 2020.
- [97] "BOE-A-2020-3692 Real Decreto 463/2020, de 14 de marzo, por el que se declara el estado de alarma para la gestión de la situación de crisis sanitaria ocasionada por el COVID-19." Accessed: Feb. 24, 2025. [Online]. Available: <https://www.boe.es/buscar/doc.php?id=BOE-A-2020-3692>

- [98] "Crisis sanitaria COVID-19 - Atención e información - Punto de Acceso General." Accessed: Feb. 24, 2025. [Online]. Available: https://administracion.gob.es/pag_Home/atencionCiudadana/Crisis-sanitaria-COVID-19.html
- [99] G. Armero *et al.*, "Non-Pharmacological Interventions During SARS-CoV-2 Pandemic: Effects on Pediatric Viral Respiratory Infections," *Arch Bronconeumol*, vol. 60, no. 10, pp. 612-618, Oct. 2024, doi: 10.1016/j.arbres.2024.05.019.
- [100] D. García-García *et al.*, "Assessing the effect of non-pharmaceutical interventions on COVID-19 transmission in Spain, 30 August 2020 to 31 January 2021," *Eurosurveillance*, vol. 27, no. 19, p. 2100869, May 2022, doi: 10.2807/1560-7917.es.2022.27.19.2100869.
- [101] V. Guadalupe-Fernández *et al.*, "Investigating epidemiological distribution (temporality and intensity) of respiratory pathogens following COVID-19 de-escalation process in Catalonia, September 2016-June 2021: Analysis of regional surveillance data," *PLoS One*, vol. 19, no. 2, p. e0285892, Feb. 2024, doi: 10.1371/journal.pone.0285892.
- [102] S. R. Dalziel *et al.*, "Bronchiolitis," *Lancet*, vol. 400, no. 10349, pp. 392-406, Jul. 2022, doi: 10.1016/S0140-6736(22)01016-9.
- [103] G. Piedimonte and M. K. Perez, "Respiratory syncytial virus infection and bronchiolitis," *Pediatr Rev*, vol. 35, no. 12, pp. 519-530, Dec. 2014, doi: 10.1542/pir.35-12-519.
- [104] "La Moncloa. 04/07/2023. El Consejo de Ministros declara el fin de la crisis sanitaria del COVID-19 y elimina la obligatoriedad de las mascarillas [Consejo de Ministros/Resúmenes]." Accessed: Feb. 24, 2025. [Online]. Available: <https://www.lamoncloa.gob.es/consejodeminstros/resumenes/paginas/2023/040723-rp-cministros.aspx>
- [105] A. Perramon-Malavez *et al.*, "Introduction of nirsevimab in Catalonia, Spain: description of the incidence of bronchiolitis and respiratory syncytial virus

in the 2023/2024 season,” *Eur J Pediatr*, vol. 183, no. 12, pp. 5181-5189, Sep. 2024, doi: 10.1007/s00431-024-05779-x.

- [106] “Immunització contra les infeccions pel virus respiratori sincicial (VRS). Canal Salut.” Accessed: Oct. 26, 2024. [Online]. Available: <https://canalsalut.gencat.cat/ca/salut-a-z/v/vacunacions/infantil/vrs/>
- [107] CatSalut, “Tests ràpids d’infeccions respiratòries pediàtriques,” Dec. 2020. Accessed: Feb. 24, 2025. [Online]. Available: <https://scientiasalut.gencat.cat/handle/11351/5523?show=full>
- [108] “Weekly U.S. Influenza Surveillance Report | CDC.” Accessed: May 02, 2023. [Online]. Available: <https://www.cdc.gov/flu/weekly/index.htm#ILINet>
- [109] “COVID-19 Pandemic Planning Scenarios | CDC.” Accessed: May 02, 2023. [Online]. Available: <https://www.cdc.gov/coronavirus/2019-ncov/hcp/planning-scenarios.html>
- [110] “National Respiratory and Enteric Virus Surveillance System | CDC.” Accessed: May 08, 2023. [Online]. Available: <https://www.cdc.gov/surveillance/nrevss/index.html>
- [111] “Flu News Europe: Weekly influenza updates.” Accessed: May 02, 2023. [Online]. Available: <https://www.ecdc.europa.eu/en/seasonal-influenza/surveillance-and-disease-data/flu-news-europe>
- [112] “Surveillance and outbreak tools.” Accessed: Mar. 01, 2025. [Online]. Available: <https://www.ecdc.europa.eu/en/tools/outbreak-surveillance-tools>
- [113] M. Català *et al.*, “Risk Diagrams Based on Primary Care Electronic Medical Records and Linked Real-Time PCR Data to Monitor Local COVID-19 Outbreaks During the Summer 2020: A Prospective Study Including 7,671,862 People in Catalonia,” *Front Public Health*, vol. 9, p. 890, Jul. 2021, doi: 10.3389/fpubh.2021.693956.
- [114] C. Aguilar Martín *et al.*, “Concordance between the Clinical Diagnosis of Influenza in Primary Care and Epidemiological Surveillance Systems

(PREVIGrip Study)," *Int J Environ Res Public Health*, vol. 19, no. 3, Jan. 2022, doi: 10.3390/ijerph19031263.

[115] A. Altmejd, J. Rocklöv, and J. Wallin, "Nowcasting COVID-19 Statistics Reported with Delay: A Case-Study of Sweden and the UK," *Int J Environ Res Public Health*, vol. 20, no. 4, p. 3040, 2023, doi: 10.3390/ijerph20043040.

[116] T. Vega *et al.*, "Influenza surveillance in Europe: Establishing epidemic thresholds by the Moving Epidemic Method," *Influenza Other Respir Viruses*, vol. 7, no. 4, pp. 546-558, 2013, doi: 10.1111/j.1750-2659.2012.00422.x.

[117] T. Vega *et al.*, "Influenza surveillance in Europe: comparing intensity levels calculated using the moving epidemic method," *Influenza Other Respir Viruses*, vol. 9, no. 5, pp. 234-246, Sep. 2015, doi: 10.1111/irv.12330.

[118] "Influenza (seasonal)." Accessed: Mar. 03, 2025. [Online]. Available: https://www.who.int/health-topics/influenza-seasonal#tab=tab_1

[119] "Recommendations | Bronchiolitis in children: diagnosis and management | Guidance | NICE".

[120] J. Wallinga and P. Teunis, "Different Epidemic Curves for Severe Acute Respiratory Syndrome Reveal Similar Impacts of Control Measures," *Am J Epidemiol*, vol. 160, no. 6, pp. 509-516, Sep. 2004, doi: 10.1093/aje/kwh255.

[121] K. M. Gostic *et al.*, "Practical considerations for measuring the effective reproductive number, Rt," *PLoS Comput Biol*, vol. 16, no. 12, p. e1008409, Dec. 2020, doi: 10.1371/journal.pcbi.1008409.

[122] Red Nacional de Vigilancia Epidemiológica and Instituto de Salud Carlos III, "Vigilancia centinela de Infección Respiratoria Aguda en Atención Primaria (IRAs) y en Hospitales (IRAG) Gripe, COVID-19 y otros virus respiratorios," 2023.

[123] "Pediatric viral respiratory infections in Catalonia – EPIDEMIOLOGIA MATEMÀTICA – CATALUNYA." Accessed: Mar. 02, 2025. [Online]. Available: <https://epidemiologia.upc.edu/pediatric/>

- [124] "Bioart." Accessed: Jan. 29, 2025. [Online]. Available: <https://bioart.nih.gov/>
- [125] H. Yang and Z. Rao, "Structural biology of SARS-CoV-2 and implications for therapeutic development," *Nature Reviews Microbiology*, vol. 19, no. 11, pp. 685-700, Sep. 2021, doi: 10.1038/s41579-021-00630-8.
- [126] P. V. Markov *et al.*, "The evolution of SARS-CoV-2," *Nature Reviews Microbiology*, vol. 21, no. 6, pp. 361-379, Apr. 2023, doi: 10.1038/s41579-023-00878-2.
- [127] V. L. de Rioja *et al.*, "Mathematical modeling of SARS-CoV-2 variant substitutions in European countries: transmission dynamics and epidemiological insights," *Front Public Health*, vol. 12, May. 2024, doi: 10.3389/fpubh.2024.1339267.
- [128] S. Steiner *et al.*, "SARS-CoV-2 biology and host interactions," *Nature Reviews Microbiology*, vol. 22, no. 4, pp. 206-225, Jan. 2024, doi: 10.1038/s41579-023-01003-z.
- [129] L. S. Canas *et al.*, "Early detection of COVID-19 in the UK using self-reported symptoms: a large-scale, prospective, epidemiological surveillance study," *Lancet Digit Health*, vol. 3, no. 9, pp. e587-e598, Sep. 2021, doi: 10.1016/s2589-7500(21)00131-x.
- [130] N. Chams *et al.*, "COVID-19: A Multidisciplinary Review," *Front Public Health*, vol. 8, p. 557296, Jul. 2020, doi: 10.3389/fpubh.2020.00383.
- [131] S. Chatterjee *et al.*, "A Detailed Overview of SARS-CoV-2 Omicron: Its Sub-Variants, Mutations and Pathophysiology, Clinical Characteristics, Immunological Landscape, Immune Escape, and Therapies," *Viruses*, vol. 15, no. 1, p. 167, Jan. 2023, doi: 10.3390/v15010167.
- [132] C. Bonanad *et al.*, "The Effect of Age on Mortality in Patients With COVID-19: A Meta-Analysis With 611,583 Subjects," *J Am Med Dir Assoc*, vol. 21, no. 7, pp. 915-918, Jul. 2020, doi: 10.1016/j.jamda.2020.05.045.

- [133] J. M. Antoñanzas *et al.*, "Symptom-based predictive model of covid-19 disease in children," *Viruses*, vol. 14, no. 1, 2022, doi: 10.3390/v14010063.
- [134] F. P. Esper *et al.*, "Alpha to Omicron: Disease Severity and Clinical Outcomes of Major SARS-CoV-2 Variants," *J Infect Dis*, vol. 227, no. 3, pp. 344-352, Feb. 2023, doi: 10.1093/infdis/jiac411.
- [135] D. Hattab *et al.*, "SARS-CoV-2 journey: from alpha variant to omicron and its sub-variants," *Infection*, vol. 52, no. 3, pp. 767-786, Jun. 2024, doi: 10.1007/s15010-024-02223-y.
- [136] E. Manirambona *et al.*, "Evolution and implications of SARS-CoV-2 variants in the post-pandemic era," *Discover Public Health*, vol. 21, no. 1, pp. 1-12, Jun. 2024, doi: 10.1186/s12982-024-00140-x.
- [137] E. Molteni *et al.*, "Illness Characteristics of COVID-19 in Children Infected with the SARS-CoV-2 Delta Variant," *Children*, vol. 9, no. 5, p. 652, May 2022, doi: 10.3390/children9050652.
- [138] P. Relan *et al.*, "Severity and outcomes of Omicron variant of SARS-CoV-2 compared to Delta variant and severity of Omicron sublineages: a systematic review and metanalysis," *BMJ Glob Health*, vol. 8, no. 7, p. 12328, Jul. 2023, doi: 10.1136/bmjgh-2023-012328.
- [139] N. Radhakrishnan *et al.*, "Comparison of the clinical characteristics of SARS-CoV-2 Delta (B.1.617.2) and Omicron (B.1.1.529) infected patients from a single hospitalist service," *BMC Infect Dis*, vol. 23, no. 1, pp. 1-11, Dec. 2023, doi: 10.1186/s12879-023-08714-x.
- [140] L. A. Vella *et al.*, "Deep immune profiling of MIS-C demonstrates marked but transient immune activation compared to adult and pediatric COVID-19," *Sci Immunol*, vol. 6, no. 57, pp. 1-18, 2021, doi: 10.1126/sciimmunol.abf7570.
- [141] R. Pino *et al.*, "Multisystem inflammatory syndrome in children and SARS-CoV-2 variants: a two-year ambispective multicentric cohort study in Catalonia, Spain," *Eur J Pediatr*, vol. 182, no. 4, pp. 1897-1909, 2023, doi: 10.1007/s00431-023-04862-z.

[142] V. L. de Rioja *et al.*, "Severity of Omicron Subvariants and Vaccine Impact in Catalonia, Spain," *Vaccines (Basel)*, vol. 12, no. 5, p. 466, May 2024, doi: 10.3390/vaccines12050466/s1.

[143] S. Walsh *et al.*, "Do school closures and school reopenings affect community transmission of COVID-19? A systematic review of observational studies," *BMJ Open*, vol. 11, no. 8, p. e053371, Aug. 2021, doi: 10.1136/bmjopen-2021-053371.

[144] A. Soriano-Arandes *et al.*, "Policies on children and schools during the SARS-CoV-2 pandemic in Western Europe," *Front Public Health*, vol. 11, pp. 1-20, Jul. 2023, doi: 10.3389/fpubh.2023.1175444.

[145] A. Gatell-Carbó *et al.*, "State of child and adolescent mental health during the first wave of the COVID-19 pandemic and at the beginning of the 2020-2021 school year," *Anales de Pediatría (English Edition)*, vol. 95, no. 5, pp. 354-363, Nov. 2021, doi: 10.1016/j.anpede.2021.08.004.

[146] Y. Zhu *et al.*, "The role of children in transmission of SARS-CoV-2 variants of concern within households: an updated systematic review and meta-analysis, as at 30 June 2022," *Eurosurveillance*, vol. 28, no. 18, p. 2200624, May 2023, doi: 10.2807/1560-7917.es.2023.28.18.2200624.

[147] A. Perramon-Malavez *et al.*, "Schools as a Framework for COVID-19 Epidemiological Surveillance of Children in Catalonia, Spain: A Population-Based Study," *Front Pediatr*, vol. 9, pp. 1-10, Sep. 2021, doi: 10.3389/fped.2021.754744.

[148] "Dades actualitzades COVID-19. Agència de Salut Pública de Catalunya (ASPCAT)." Accessed: Apr. 26, 2025. [Online]. Available: <https://salutpublica.gencat.cat/ca/details/Article/Dades aktualitzades-COVID-19>

[149] "Salut inicia la vacunació amb segones dosis ... - Govern.cat." Accessed: Apr. 13, 2025. [Online]. Available: <https://govern.cat/salapremsa/notes-premsa/410411/salut-inicia-vacunacio-segones-dosis-dels-collectius-essencials>

- [150] S. Rhedin *et al.*, “Risk factors for multisystem inflammatory syndrome in children – A population-based cohort study of over 2 million children,” *The Lancet Regional Health - Europe*, p. 100443, Jun. 2022, doi: 10.1016/j.lanepe.2022.100443.
- [151] D. Buonsenso *et al.*, “Multisystem Inflammatory Syndrome in Children in Western Countries? Decreasing Incidence as the Pandemic Progresses?: An Observational Multicenter International Cross-sectional Study,” *Pediatric Infectious Disease Journal*, vol. 41, no. 12, pp. 989-993, 2022, doi: 10.1097/inf.0000000000003713.
- [152] F. P. Lyngse *et al.*, “Effect of vaccination on household transmission of SARS-CoV-2 Delta variant of concern,” *Nature Communications*, vol. 13, no. 1, pp. 1-8, Jun. 2022, doi: 10.1038/s41467-022-31494-y.
- [153] I. Eleftheriou *et al.*, “Decreasing Incidence of the Multisystem Inflammatory Syndrome in Children Over 3 Pandemic Waves,” *Pediatr Infect Dis J*, vol. 42, no. 2, p. 122, Feb. 2022, doi: 10.1097/inf.0000000000003766.
- [154] F. La Torre *et al.*, “Incidence and Prevalence of Multisystem Inflammatory Syndrome in Children (MIS-C) in Southern Italy,” *Children*, vol. 10, no. 5, p. 766, May 2023, doi: 10.3390/children10050766.
- [155] CUSABIO TECHNOLOGY, “Influenza Virus.” Accessed: Mar. 26, 2025. [Online]. Available: <https://www.cusabio.com/infectious-diseases/influenza-virus.html>
- [156] “Types of Influenza Viruses | Influenza (Flu) | CDC.” Accessed: Mar. 19, 2025. [Online]. Available: <https://www.cdc.gov/flu/about/viruses-types.html>
- [157] “Influenza (seasonal).” Accessed: Mar. 26, 2025. [Online]. Available: [https://www.who.int/news-room/fact-sheets/detail/influenza-\(seasonal\)](https://www.who.int/news-room/fact-sheets/detail/influenza-(seasonal))
- [158] R. F. Nuwarda, A. A. Alharbi, and V. Kayser, “An overview of influenza viruses and vaccines,” *Vaccines (Basel)*, vol. 9, no. 9, 2021, doi: 10.3390/vaccines9091032.

- [159] C. Andrés *et al.*, “Molecular influenza surveillance at a tertiary university hospital during four consecutive seasons (2012-2016) in Catalonia, Spain,” *Vaccine*, vol. 37, no. 18, pp. 2470-2476, Apr. 2019, doi: 10.1016/j.vaccine.2019.03.046.
- [160] “Browsing - Pla d’informació de les infeccions respiratòries agudes a Catalunya (PIDIRAC): balanç temporada gripal by Issue Date.” Accessed: Apr. 03, 2025. [Online]. Available: https://scientiasalut.gencat.cat/handle/11351/4319/browse?rpp=20&sort_by=2&type=dateissued&offset=0&etal=-1&order=ASC
- [161] S. Caini *et al.*, “Probable extinction of influenza B/Yamagata and its public health implications: a systematic literature review and assessment of global surveillance databases,” *Lancet Microbe*, vol. 5, no. 8, p. 100851, Aug. 2024, doi: 10.1016/s2666-5247(24)00066-1.
- [162] A. S. Monto, M. Zambon, and J. P. Weir, “The End of B/Yamagata Influenza Transmission — Transitioning from Quadrivalent Vaccines,” *New England Journal of Medicine*, vol. 390, no. 14, pp. 1256-1258, Apr. 2024, doi: 10.1056/nejmp2314801.
- [163] “Global Influenza Programme.” Accessed: Mar. 26, 2025. [Online]. Available: <https://www.who.int/teams/global-influenza-programme/vaccines/who-recommendations>
- [164] C. Andrés *et al.*, “Detection of reassortant influenza B strains from 2004 to 2015 seasons in Barcelona (Catalonia, Spain) by whole genome sequencing,” *Virus Res*, vol. 330, p. 199089, Jun. 2023, doi: 10.1016/j.virusres.2023.199089.
- [165] M. B. Bull *et al.*, “Universally immune: How infection permissive next generation influenza vaccines may affect population immunity and viral spread,” *Viruses*, vol. 13, no. 9, 2021, doi: 10.3390/v13091779.
- [166] X. Wang *et al.*, “Global burden of respiratory infections associated with seasonal influenza in children under 5 years in 2018: a systematic review and

modelling study," *Lancet Glob Health*, vol. 8, no. 4, pp. e497-e510, Apr. 2020, doi: 10.1016/s2214-109x(19)30545-5.

[167] T. A. Florin, A. C. Plint, and J. J. Zorc, "Viral bronchiolitis," *The Lancet*, vol. 389, no. 10065, pp. 211-224, Jan. 2017, doi: 10.1016/s0140-6736(16)30951-5.

[168] M. Eccleston-Turner, A. Phelan, and R. Katz, "Preparing for the Next Pandemic — The WHO's Global Influenza Strategy," *New England Journal of Medicine*, vol. 381, no. 23, pp. 2192-2194, Dec. 2019, doi: 10.1056/nejmp1905224.

[169] "Influenza fact sheet." Accessed: Mar. 26, 2025. [Online]. Available: https://www.health.nsw.gov.au/Infectious/factsheets/Pages/influenza_factsheet.aspx

[170] N. Harding, R. Spinney, and M. Prokopenko, "Phase Transitions in Spatial Connectivity during Influenza Pandemics," *Entropy*, vol. 22, no. 2, p. 133, Jan. 2020, doi: 10.3390/e22020133.

[171] M. Soler-Font *et al.*, "Costs and Factors Associated with Hospitalizations Due to Severe Influenza in Catalonia (2017–2020)," *Int J Environ Res Public Health*, vol. 19, no. 22, p. 14793, Nov. 2022, doi: 10.3390/ijerph192214793.

[172] C. J. Worby *et al.*, "On the relative role of different age groups in influenza epidemics," *Epidemics*, vol. 13, pp. 10-16, Dec. 2015, doi: 10.1016/j.epidem.2015.04.003.

[173] J. Nayak, G. Hoy, and A. Gordon, "Influenza in Children," *Cold Spring Harb Perspect Med*, vol. 11, no. 1, p. a038430, Jan. 2021, doi: 10.1101/cshperspect.a038430.

[174] N. R. Waterlow *et al.*, "Competition between RSV and influenza: Limits of modelling inference from surveillance data," *Epidemics*, vol. 35, p. 100460, Jun. 2021, doi: 10.1016/j.epidem.2021.100460.

[175] S. C. Kramer *et al.*, "Characterizing the interactions between influenza and respiratory syncytial viruses and their implications for epidemic control," *Nature*

Communications, vol. 15, no. 1, pp. 1-14, Nov. 2024, doi: 10.1038/s41467-024-53872-4.

[176] A. Perramon-Malavez *et al.*, "Transition from the old to the new viral normality: Where are we?", *Enfermedades Emergentes*, vol. 22, no. 2, pp. 71-75, 2023.

[177] J. Tamerius *et al.*, "Global influenza seasonality: Reconciling patterns across temperate and tropical regions," *Environ Health Perspect*, vol. 119, no. 4, pp. 439-445, 2011, doi: 10.1289/ehp.1002383.

[178] S. Caini *et al.*, "Characteristics of seasonal influenza A and B in Latin America: Influenza surveillance data from ten countries," *PLoS One*, vol. 12, no. 3, p. e0174592, Mar. 2017, doi: 10.1371/journal.pone.0174592.

[179] J. M. Pascale *et al.*, "Burden of Seasonal Influenza A and B in Panama from 2011 to 2017: An Observational Retrospective Database Study," *Infect Dis Ther*, vol. 10, no. 4, pp. 2465-2478, Dec. 2021, doi: 10.1007/s40121-021-00501-y.

[180] L. Chen *et al.*, "Immunity Debt for Seasonal Influenza After the COVID-19 Pandemic and as a Result of Nonpharmaceutical Interventions: An Ecological Analysis and Cohort Study," *Advanced Science*, p. 2410513, Apr. 2025, doi: 10.1002/advs.202410513.

[181] E. Coma *et al.*, "Effectiveness of nirsevimab immunoprophylaxis against respiratory syncytial virus-related outcomes in hospital and primary care settings: a retrospective cohort study in infants in Catalonia (Spain)," *Arch Dis Child*, vol. 109, pp. 736-741, 2024, doi: 10.1136/archdischild-2024-327153.

[182] A. Perramon-Malavez *et al.*, "Effectiveness of Nirsevimab Immunoprophylaxis Against Respiratory Syncytial Virus-related Outcomes in Hospital Care Settings: A Seasonal Cohort Study of Infants in Catalonia (Spain)," *Pediatr Infect Dis J*, vol. 44, no. 5, pp. 394-398, May 2025, doi: 10.1097/inf.0000000000004672.

[183] C. Andrés *et al.*, "Respiratory viral coinfections in pediatric patients in the primary care setting: a multicenter prospective study within the COPEDICAT

network," *J Infect Dis*, vol. 230, no. 6, pp. 1337-1341, Dec. 2024, doi: 10.1093/infdis/jiae279.

[184] A. Míguez, A. Iftimi, and F. Montes, "Temporal association between the influenza virus and respiratory syncytial virus (RSV): RSV as a predictor of seasonal influenza," *Epidemiol Infect*, vol. 144, no. 12, pp. 262-2632, Sep. 2016, doi: 10.1017/s095026881600090x.

[185] "SIVIC - Infeccions respiratòries - Grip - Vacunació." Accessed: Apr. 08, 2025. [Online]. Available: https://sivic.salut.gencat.cat/grip_vacunacio

[186] E. Castro Blanco *et al.*, "A Predictive Model of the Start of Annual Influenza Epidemics," *Microorganisms*, vol. 12, no. 7, p. 1257, Jun. 2024, doi: 10.3390/microorganisms12071257.

[187] L. C. Brooks *et al.*, "Nonmechanistic forecasts of seasonal influenza with iterative one-week-ahead distributions," *PLoS Comput Biol*, vol. 14, no. 6, pp. 1-29, 2018, doi: 10.1371/journal.pcbi.1006134.

[188] J. Shaman and A. Karspeck, "Forecasting seasonal outbreaks of influenza," *Proc Natl Acad Sci USA*, vol. 109, no. 50, pp. 20425-20430, Dec. 2012, doi: 10.1073/pnas.1208772109.

[189] G. González-Parra *et al.*, "Modeling the epidemic waves of AH1N1/09 influenza around the world," *Spat Spatiotemporal Epidemiol*, vol. 2, no. 4, pp. 219-226, 2011, doi: 10.1016/j.sste.2011.05.002.

[190] F. Brauer, C. Castillo-Chavez, and Z. Feng, "Models for Influenza," in Mathematical Models in Epidemiology, *Springer*, New York, ch. 9. Models, pp. 311-350. doi: 10.1007/978-1-4939-9828-9_9.

[191] B. Wang, Y. Hu, Z. Cen, J. Huang, T. He, and A. Xu, "A SIR Model with Incomplete Data for the Analysis of Influenza A Spread in Ningbo," *Discrete Dyn Nat Soc*, vol. 2024, no. 1, p. 7694770, Jan. 2024, doi: 10.1155/2024/7694770.

[192] K.-H. Yang and J.-Y. Hsu, "A New SIR-based Model for Influenza Epidemic," *International Journal of Health and Medical Engineering*, vol. 6, no. 7, pp. 701-706, 2012.

- [193] M. M. Saito *et al.*, “Extension and verification of the SEIR model on the 2009 influenza A (H1N1) pandemic in Japan,” *Math Biosci*, vol. 246, no. 1, pp. 47-54, Nov. 2013, doi: 10.1016/j.mbs.2013.08.009.
- [194] P. Guo *et al.*, “Monitoring seasonal influenza epidemics by using internet search data with an ensemble penalized regression model,” *Scientific Reports*, vol. 7, no. 1, pp. 1-11, Apr. 2017, doi: 10.1038/srep46469.
- [195] H. Zhu *et al.*, “Study on the impact of meteorological factors on influenza in different periods and prediction based on artificial intelligence RF-Bi-LSTM algorithm: to compare the COVID-19 period with the non-COVID-19 period,” *BMC Infect Dis*, vol. 24, no. 1, pp. 1-22, Dec. 2024, doi: 10.1186/s12879-024-09750-x.
- [196] H. Y. Cheng *et al.*, “Applying machine learning models with an ensemble approach for accurate real-time influenza forecasting in Taiwan: Development and validation study,” *J Med Internet Res*, vol. 22, no. 8, p. e15394, Aug. 2020, doi: 10.2196/15394.
- [197] L. Santamaría and J. Hortal, “COVID-19 effective reproduction number dropped during Spain’s nationwide dropdown, then spiked at lower-incidence regions,” *Sci Total Environ*, vol. 751, p. 142257, Jan. 2020, doi: 10.1016/j.scitotenv.2020.142257.
- [198] J. E. Park *et al.*, “Effects of temperature, humidity, and diurnal temperature range on influenza incidence in a temperate region,” *Influenza Other Respir Viruses*, vol. 14, no. 1, pp. 11-18, Jan. 2020, doi: 10.1111/irv.12682.
- [199] D. Wang *et al.*, “Association between Temperature and Influenza Activity across Different Regions of China during 2010-2017,” *Viruses*, vol. 15, no. 3, p. 594, Mar. 2023, doi: 10.3390/v15030594.
- [200] C. Chen *et al.*, “Associations between temperature and influenza activity: A national time series study in china,” *Int J Environ Res Public Health*, vol. 18, no. 20, Oct. 2021, doi: 10.3390/ijerph182010846.

- [201] J. Shaman and M. Kohn, "Absolute humidity modulates influenza survival, transmission, and seasonality," *Proc Natl Acad Sci USA*, vol. 106, no. 9, pp. 3243-3248, 2009, doi: 10.1073/pnas.0806852106.
- [202] Z. L. Yan *et al.*, "Effects of meteorological factors on influenza transmissibility by virus type/subtype," *BMC Public Health*, vol. 24, no. 1, pp. 1-11, Dec. 2024, doi: 10.1186/s12889-024-17961-9.
- [203] Y. Li *et al.*, "Global patterns in monthly activity of influenza virus, respiratory syncytial virus, parainfluenza virus, and metapneumovirus: a systematic analysis," *Lancet Glob Health*, vol. 7, no. 8, pp. e1031-e1045, 2019, doi: 10.1016/s2214-109x(19)30264-5.
- [204] B. S. Finkelman *et al.*, "Global patterns in seasonal activity of influenza A/H3N2, A/H1N1, and B from 1997 to 2005: Viral coexistence and latitudinal gradients," *PLoS One*, vol. 2, no. 12, 2007, doi: 10.1371/journal.pone.0001296.
- [205] E. K. S. Lam *et al.*, "The impact of climate and antigenic evolution on seasonal influenza virus epidemics in Australia," *Nature Communications*, vol. 11, no. 1, 2020, doi: 10.1038/s41467-020-16545-6.
- [206] "Llistat d'estacions meteorològiques automàtiques de Catalunya | Meteocat." Accessed: Dec. 09, 2024. [Online]. Available: <https://www.meteo.cat/observacions/llistat-xema>
- [207] D. Koutsoyiannis, "Clausius–Clapeyron equation and saturation vapour pressure: simple theory reconciled with practice," *Eur J Phys*, vol. 33, no. 2, p. 295, Jan. 2012, doi: 10.1088/0143-0807/33/2/295.
- [208] Y. Sun, Z. Zhang, and Y. Sun, "Calculation Method and Application of Time-Varying Transmission Rate via Data-Driven Approach," *Mathematics*, vol. 11, no. 13, p. 2955, Jul. 2023, doi: 10.3390/math11132955.
- [209] Y. Yang, Y. Asai, and H. Nishiura, "A method for estimating the transmissibility of influenza using serial cross-sectional seroepidemiological data," *J Theor Biol*, vol. 511, p. 110566, Feb. 2021, doi: 10.1016/j.jtbi.2020.110566.

- [210] X. Liu and P. Stechlinski, “Infectious disease models with time-varying parameters and general nonlinear incidence rate,” *Appl Math Model*, vol. 36, no. 5, pp. 1974-1994, May 2012, doi: 10.1016/j.apm.2011.08.019.
- [211] “Idescat. El municipi en xifres. Barcelona (Barcelonès).” Accessed: Apr. 22, 2025. [Online]. Available: <https://www.idescat.cat/emex/?id=080193>
- [212] “GitHub - scmassey/model-sensitivity-analysis: Latin hypercube sampling and partial rank correlation coefficients.” Accessed: Apr. 22, 2025. [Online]. Available: <https://github.com/scmassey/model-sensitivity-analysis/tree/master>
- [213] C. Song and R. Kawai, “Monte Carlo and variance reduction methods for structural reliability analysis: A comprehensive review,” *Probabilistic Engineering Mechanics*, vol. 73, p. 103479, Jul. 2023, doi: 10.1016/j.probengmech.2023.103479.
- [214] M. D. McKay, R. J. Beckman, and W. J. Conover, “Comparison of three methods for selecting values of input variables in the analysis of output from a computer code,” *Technometrics*, vol. 21, no. 2, pp. 239-245, 1979, doi: 10.1080/00401706.1979.10489755.
- [215] A. Sorokin and I. Goryanin, “FBA-PRCC. Partial Rank Correlation Coefficient (PRCC) Global Sensitivity Analysis (GSA) in Application to Constraint-Based Models,” *Biomolecules*, vol. 13, no. 3, Mar. 2023, doi: 10.3390/biom13030500.
- [216] “Respiratory syncytial virus (RSV).” Accessed: Apr. 06, 2025. [Online]. Available: [https://www.who.int/news-room/fact-sheets/detail/respiratory-syncytial-virus-\(rsv\)](https://www.who.int/news-room/fact-sheets/detail/respiratory-syncytial-virus-(rsv))
- [217] A. T. Borchers *et al.*, “Respiratory syncytial virus - A comprehensive review,” *Clin Rev Allergy Immunol*, vol. 45, no. 3, pp. 331-379, Dec. 2013, doi: 10.1007/s12016-013-8368-9.
- [218] M. Piñana *et al.*, “Genomic evolution of human respiratory syncytial virus during a decade (2013-2023): bridging the path to monoclonal antibody surveillance,” *J Infect*, vol. 88, no. 5, May 2024, doi: 10.1016/j.jinf.2024.106153.

- [219] C. Azzari *et al.*, "Epidemiology and prevention of respiratory syncytial virus infections in children in Italy," *Ital J Pediatr*, vol. 47, no. 1, pp. 1-12, Dec. 2021, doi: 10.1186/s13052-021-01148-8.
- [220] L. J. Anderson *et al.*, "Functional Features of the Respiratory Syncytial Virus G Protein," *Viruses*, vol. 13, no. 7, p. 1214, Jul. 2021, doi: 10.3390/v13071214.
- [221] I. Raffaldi and E. Castagno, "The Epidemiology of Respiratory Syncytial Virus: New Trends and Future Perspectives," *Viruses*, vol. 16, no. 7, p. 1100, Jul. 2024, doi: 10.3390/v16071100.
- [222] E. Andreano *et al.*, "The respiratory syncytial virus (RSV) prefusion F-protein functional antibody repertoire in adult healthy donors," *EMBO Mol Med*, vol. 13, no. 6, p. e14035, Jun. 2021, doi: 10.15252/emmm.202114035.
- [223] A. Agac *et al.*, "Host Responses to Respiratory Syncytial Virus Infection," *Viruses*, vol. 15, no. 10, p. 1999, Sep. 2023, doi: 10.3390/v15101999.
- [224] "Safe and Effective RSV Protein Vaccines | NIAID: National Institute of Allergy and Infectious Diseases." Accessed: Apr. 06, 2025. [Online]. Available: <https://www.niaid.nih.gov/diseases-conditions/safe-and-effective-rsv-protein-vaccines>
- [225] N. G. Papadopoulos *et al.*, "Does respiratory syncytial virus subtype influences the severity of acute bronchiolitis in hospitalized infants?," *Respir Med*, vol. 98, no. 9, pp. 879-882, Sep. 2004, doi: 10.1016/j.rmed.2004.01.009.
- [226] R. L. Ursin and S. L. Klein, "Sex Differences in Respiratory Viral Pathogenesis and Treatments," *Annu Rev Virol*, vol. 8, pp. 393-414, Sep. 2021, doi: 10.1146/annurev-virology-091919-092720.
- [227] Y. Nagayama *et al.*, "Gender analysis in acute bronchiolitis due to respiratory syncytial virus," *Pediatric Allergy and Immunology*, vol. 17, no. 1, pp. 29-36, Feb. 2006, doi: 10.1111/j.1399-3038.2005.00339.x.
- [228] H. H. Nam and M. G. Ison, "Respiratory syncytial virus infection in adults," *BMJ Publishing Group*, vol. 366, Sep. 2019, doi: 10.1136/bmj.l5021.

- [229] E. Binns *et al.*, “Respiratory syncytial virus, recurrent wheeze and asthma: A narrative review of pathophysiology, prevention and future directions,” *J Paediatr Child Health*, vol. 58, no. 10, pp. 1741-1746, Oct. 2022, doi: 10.1111/jpc.16197.
- [230] “CIMA. FICHA TECNICA SYNAGIS 50 mg/0,5 ml SOLUCION INYECTABLE.” Accessed: Dec. 08, 2024. [Online]. Available: https://cima.aemps.es/cima/dochtml/ft/199117003/FT_199117003.html
- [231] “CIMA. FICHA TECNICA SYNAGIS 100 mg/1 ml SOLUCION INYECTABLE.” Accessed: Apr. 10, 2025. [Online]. Available: https://cima.aemps.es/cima/dochtml/ft/199117004/FT_199117004.html
- [232] L. Garegnani *et al.*, “Palivizumab for preventing severe respiratory syncytial virus (RSV) infection in children,” *Cochrane Database Syst Rev*, vol. 11, no. 11, Nov. 2021, doi: 10.1002/14651858.cd013757.pub2.
- [233] P. K. Tang, “Palivizumab prophylaxis in preterm infants,” *Lancet Respir Med*, vol. 5, no. 3, p. 171, Mar. 2017, doi: 10.1016/s2213-2600(17)30050-4.
- [234] “Beyfortus | European Medicines Agency.” Accessed: Jun. 18, 2024. [Online]. Available: <https://www.ema.europa.eu/en/medicines/human/EPAR/beyfortus>
- [235] E. M. Agency, “BEYFORTUS: Summary of Product Characteristics,” 2013. [Online]. Available: https://www.ema.europa.eu/en/documents/product-information/beyfortus-epar-product-information_en.pdf
- [236] “CIMA. PROSPECTO BEYFORTUS 50 MG SOLUCION INYECTABLE EN JERINGA PRECARGADA.” Accessed: Apr. 10, 2025. [Online]. Available: https://cima.aemps.es/cima/dochtml/p/1221689001/P_1221689001.html
- [237] D. Wilkins *et al.*, “RSV Neutralizing Antibodies Following Nirsevimab and Palivizumab Dosing,” *Pediatrics*, vol. 154, no. 5, Nov. 2024, doi: 10.1542/peds.2024-067174.

[238] "During Pregnancy | ABRYSVO® (Respiratory Syncytial Virus Vaccine) | Risk Info." Accessed: Jul. 16, 2024. [Online]. Available: <https://www.abrysvo.com/pregnant-women>

[239] A. Papi *et al.*, "Respiratory Syncytial Virus Prefusion F Protein Vaccine in Older Adults," *New England Journal of Medicine*, vol. 388, no. 7, pp. 595-608, Feb. 2023, doi: 10.1056/nejmoa2209604.

[240] "CIMA. FICHA TECNICA ABRYSVO POLVO Y DISOLVENTE PARA SOLUCION INYECTABLE." Accessed: Apr. 10, 2025. [Online]. Available: https://cima.aemps.es/cima/dochtml/ft/1231752001/FT_1231752001.html

[241] "A guide to RSV vaccination for pregnant women - GOV.UK." Accessed: Apr. 10, 2025. [Online]. Available: <https://www.gov.uk/government/publications/respiratory-syncytial-virus-rsv-maternal-vaccination/a-guide-to-rsv-vaccination-for-pregnant-women>

[242] "National Immunisation Program update – maternal respiratory syncytial virus (RSV) vaccine | Australian Government Department of Health and Aged Care." Accessed: Apr. 10, 2025. [Online]. Available: <https://www.health.gov.au/news/national-immunisation-program-update-maternal-respiratory-syncytial-virus-rsv-vaccine>

[243] "Immunizations to Protect Infants | RSV | CDC." Accessed: Apr. 10, 2025. [Online]. Available: <https://www.cdc.gov/rsv/vaccines/protect-infants.html>

[244] M. N. Billard *et al.*, "International changes in respiratory syncytial virus (RSV) epidemiology during the COVID-19 pandemic: Association with school closures," *Influenza Other Respir Viruses*, vol. 16, no. 5, pp. 926-936, Sep. 2022, doi: 10.1111/irv.12998.

[245] Y. Li *et al.*, "Understanding the Potential Drivers for Respiratory Syncytial Virus Rebound During the Coronavirus Disease 2019 Pandemic," *J Infect Dis*, vol. 225, no. 6, p. 957, Mar. 2022, doi: 10.1093/infdis/jiab606.

[246] M. Leecaster *et al.*, "Modeling the variations in pediatric respiratory syncytial virus seasonal epidemics," *BMC Infect Dis*, vol. 11, 2011, doi: 10.1186/1471-2334-11-105.

- [247] H. C. Moore *et al.*, “Modelling the Seasonal Epidemics of Respiratory Syncytial Virus in Young Children,” *PLoS One*, vol. 9, no. 6, p. e100422, Jun. 2014, doi: 10.1371/journal.pone.0100422.
- [248] A. T. Gebremedhin *et al.*, “Developing a prediction model to estimate the true burden of respiratory syncytial virus (RSV) in hospitalised children in Western Australia,” *Sci Rep*, vol. 12, no. 1, pp. 1-12, 2022, doi: 10.1038/s41598-021-04080-3.
- [249] L. Acedo *et al.*, “Using random networks to study the dynamics of respiratory syncytial virus (RSV) in the Spanish region of Valencia,” *Math Comput Model*, vol. 54, no. 7-8, pp. 1650-1654, 2011, doi: 10.1016/j.mcm.2010.11.068.
- [250] L. Acedo *et al.*, “Mathematical modelling of respiratory syncytial virus (RSV): Vaccination strategies and budget applications,” *Epidemiol Infect*, vol. 138, no. 6, pp. 853-860, 2010, doi: 10.1017/s0950268809991373.
- [251] C. F. Tso *et al.*, “Machine learning early prediction of respiratory syncytial virus in pediatric hospitalized patients,” *Front Pediatr*, vol. 10, Aug. 2022, doi: 10.3389/fped.2022.886212.
- [252] M. R. Cogollo, G. González-Parra, and A. J. Arenas, “Modeling and Forecasting Cases of RSV Using Artificial Neural Networks,” *Mathematics*, vol. 9, no. 22, p. 2958, Nov. 2021, doi: 10.3390/math9222958.
- [253] P. Xepapadaki *et al.*, “Human metapneumovirus as a causative agent of acute bronchiolitis in infants,” *Journal of Clinical Virology*, vol. 30, no. 3, p. 267, Jul. 2004, doi: 10.1016/j.jcv.2003.12.012.
- [254] C. J. Stewart *et al.*, “Respiratory Syncytial Virus and Rhinovirus Bronchiolitis Are Associated With Distinct Metabolic Pathways,” *J Infect Dis*, vol. 217, no. 7, pp. 1160-1169, Mar. 2018, doi: 10.1093/infdis/jix680.
- [255] R. J. Pickles and J. P. DeVincenzo, “Respiratory syncytial virus (RSV) and its propensity for causing bronchiolitis,” *J Pathol*, vol. 235, no. 2, p. 266, Jan. 2014, doi: 10.1002/path.4462.

- [256] J. Reina and C. Iglesias, “Nirsevimab: Towards universal child immunization against respiratory syncytial virus,” *Vacunas*, vol. 24, no. 1, pp. 68-73, Jan. 2023, doi: 10.1016/j.vacun.2022.10.002.
- [257] D. de S. G. de Catalunya, “Programa d’immunització contra el virus respiratori sincicial (VRS) en infants a Catalunya,” 2023.
- [258] S. Ares-Gómez *et al.*, “Effectiveness and impact of universal prophylaxis with nirsevimab in infants against hospitalisation for respiratory syncytial virus in Galicia, Spain: initial results of a population-based longitudinal study,” *Lancet Infect Dis*, vol. 24, no. 8, pp. 817-828, Apr. 2024, doi: 10.1016/s1473-3099(24)00215-9.
- [259] M. López-Lacort *et al.*, “Nirsevimab Effectiveness Against Severe RSV Infection in the Primary Care Setting,” *Pediatrics*, vol. 155, no. 1, p. e2024066393, Oct. 2024, doi: 10.1542/peds.2024-066393/199595.
- [260] G. Ezpeleta *et al.*, “Effectiveness of Nirsevimab Immunoprophylaxis Administered at Birth to Prevent Infant Hospitalisation for Respiratory Syncytial Virus Infection: A Population-Based Cohort Study,” *Vaccines*, vol. 12, no. 4, p. 383, Apr. 2024, doi: 10.3390/vaccines12040383.
- [261] J. Paireau *et al.*, “Nirsevimab Effectiveness Against Cases of Respiratory Syncytial Virus Bronchiolitis Hospitalised in Paediatric Intensive Care Units in France, September 2023–January 2024,” *Influenza Other Respir Viruses*, vol. 18, no. 6, p. e13311, Jun. 2024, doi: 10.1111/irv.13311.
- [262] C. Ernst *et al.*, “Impact of nirsevimab prophylaxis on paediatric respiratory syncytial virus (RSV)-related hospitalisations during the initial 2023/24 season in Luxembourg,” *Eurosurveillance*, vol. 29, no. 4, p. 2400033, Jan. 2024, doi: 10.2807/1560-7917.es.2024.29.4.2400033.
- [263] H. Xu *et al.*, “Estimated Effectiveness of Nirsevimab Against Respiratory Syncytial Virus,” *JAMA Netw Open*, vol. 8, no. 3, pp. e250380-e250380, Mar. 2025, doi: 10.1001/jamanetworkopen.2025.0380.
- [264] G. Emery, “Beyfortus®(Nirsevimab): Priorisation temporaire des patients à immuniser,” 2023.

[265] "Health Alert Network (HAN) - 00499 | Limited Availability of Nirsevimab in the United States—Interim CDC Recommendations to Protect Infants from Respiratory Syncytial Virus (RSV) during the 2023–2024 Respiratory Virus Season." Accessed: Jan. 31, 2024. [Online]. Available: <https://emergency.cdc.gov/han/2023/han00499.asp>

[266] Dirección Xeral De Saúde Pública, "Follow-up report on immunization with nirsevimab in Galicia," Santiago de Compostela, 2024.

[267] M. López-Lacort *et al.*, "Early estimates of nirsevimab immunoprophylaxis effectiveness against hospital admission for respiratory syncytial virus lower respiratory tract infections in infants, Spain, October 2023 to January 2024," *Eurosurveillance*, vol. 29, no. 6, p. 2400046, Feb. 2024, doi: 10.2807/1560-7917.es.2024.29.6.2400046.

[268] H. L. Moline *et al.*, "Early Estimate of Nirsevimab Effectiveness for Prevention of Respiratory Syncytial Virus–Associated Hospitalization Among Infants Entering Their First Respiratory Syncytial Virus Season — New Vaccine Surveillance Network, October 2023–February 2024," *MMWR Morb Mortal Wkly Rep*, vol. 73, no. 9, pp. 209-214, Mar. 2024, doi: 10.15585/mmwr.mm7309a4.

[269] R. Carbajal *et al.*, "Real-world effectiveness of nirsevimab immunisation against bronchiolitis in infants: a case–control study in Paris, France," *Lancet Child Adolesc Health*, vol. 8, no. 10, pp. 730-739, Oct. 2024, doi: 10.1016/s2352-4642(24)00171-8.

[270] C. Colls, M. Mias, and A. García-Altés, "[A deprivation index to reform the financing model of primary care in Catalonia (Spain)]," *Gac Sanit*, vol. 34, no. 1, pp. 44-50, Jan. 2020, doi: 10.1016/j.gaceta.2018.07.015.

[271] T. L. Nguyen *et al.*, "Double-adjustment in propensity score matching analysis: choosing a threshold for considering residual imbalance," *BMC Med Res Methodol*, vol. 17, no. 1, pp. 1-8, Apr. 2017, doi: 10.1186/s12874-017-0338-0.

- [272] L. C. Lund *et al.*, "Cox regression using a calendar time scale was unbiased in simulations of COVID-19 vaccine effectiveness & safety," *J Clin Epidemiol*, vol. 156, pp. 127-136, Apr. 2023, doi: 10.1016/j.jclinepi.2023.02.012.
- [273] P. M. Grambsch and T. M. Therneau, "Proportional hazards tests and diagnostics based on weighted residuals," *Biometrika*, vol. 81, no. 3, pp. 515-526, Sep. 1994, doi: 10.1093/biomet/81.3.515.
- [274] M. J. Stensrud and M. A. Hernán, "Why Test for Proportional Hazards?," *JAMA*, vol. 323, no. 14, pp. 1401-1402, Apr. 2020, doi: 10.1001/jama.2020.1267.
- [275] L. L. Hammitt *et al.*, "Nirsevimab for Prevention of RSV in Healthy Late-Preterm and Term Infants," *New England Journal of Medicine*, vol. 386, no. 9, pp. 837-846, Mar. 2022, doi: 10.1056/nejmoa2110275.
- [276] J. A. Englund, "Passive protection against respiratory syncytial virus disease in infants: the role of maternal antibody," *Pediatric Infectious Disease Journal*, vol. 13, no. 5, pp. 449-453, 1994.
- [277] A. B. Kachikis *et al.*, "Transfer of Respiratory Syncytial Virus Prefusion F Protein Antibody in Low Birthweight Infants," *Open Forum Infect Dis*, vol. 11, no. 7, Jul. 2024, doi: 10.1093/ofid/ofae314.
- [278] B. Kampmann, D. Radley, and I. Munjal, "Bivalent Prefusion F Vaccine in Pregnancy to Prevent RSV Illness in Infants. Reply.,," *N Engl J Med*, vol. 389, no. 11, pp. 1053-1055, Sep. 2023, doi: 10.1056/nejmc2307729.
- [279] D. Hodgson *et al.*, "Protecting infants against RSV disease: an impact and cost-effectiveness comparison of long-acting monoclonal antibodies and maternal vaccination," *The Lancet Regional Health - Europe*, vol. 38, p. 100829, Mar. 2024, doi: 10.1016/j.lanepe.2023.100829.
- [280] "Weekly national flu reports - GOV.UK." Accessed: May 08, 2023. [Online]. Available: <https://www.gov.uk/government/collections/weekly-national-flu-reports>

- [281] "Flu (influenza): FluWatch surveillance - Canada.ca." Accessed: May 08, 2023. [Online]. Available: <https://www.canada.ca/en/public-health/services/diseases/flu-influenza/influenza-surveillance.html>
- [282] "National Notifiable Diseases Surveillance System (NNDSS) | Australian Government Department of Health and Aged Care." Accessed: May 08, 2023. [Online]. Available: <https://www.health.gov.au/our-work/nndss>
- [283] R. Cai, Z. Spencer, and N. Ruktanonchai, "Exploring infectious disease spread as a function of seasonal and pandemic-induced changes in human mobility," *Front Public Health*, vol. 12, p. 1410824, Aug. 2024, doi: 10.3389/fpubh.2024.1410824.
- [284] J. P. Gutiérrez-Jara *et al.*, "Effects of human mobility and behavior on disease transmission in a COVID-19 mathematical model," *Sci Rep*, vol. 12, no. 1, pp. 1-18, Dec. 2022, doi: 10.1038/s41598-022-14155-4.
- [285] C. K. Rollins *et al.*, "Neurological and Psychological Sequelae Associated With Multisystem Inflammatory Syndrome in Children," *JAMA Netw Open*, vol. 6, no. 7, pp. e2324369-e2324369, Jul. 2023, doi: 10.1001/jamanetworkopen.2023.24369.
- [286] I. Jaxybayeva, R. Boranbayeva, M. Bulegenova, N. Urazalieva, V. Gerein, and L. Manzhuova, "Long-term outcomes and immune profiling in children with multisystem inflammatory syndrome (MIS-C)," *Acta Biomed*, vol. 94, no. 6, pp. e2023233-e2023233, Dec. 2023, doi: 10.23750/abm.v94i6.14788.
- [287] E. Coma *et al.*, "Unravelling the role of the mandatory use of face covering masks for the control of SARS-CoV-2 in schools: A quasi-experimental study nested in a population-based cohort in Catalonia (Spain)," *Arch Dis Child*, vol. 108, no. 2, pp. 131-136, Aug. 2022, doi: 10.1136/archdischild-2022-324172.
- [288] "Campanya de vacunació contra la grip i la covid. gencat.cat." Accessed: Apr. 25, 2025. [Online]. Available: <https://web.gencat.cat/ca/actualitat/detail/Comenca-la-campanya-de-vacunacio-contra-la-grip-i-la-covid>

[289] “Informació de la publicació - Plataforma de Serveis de Contractació Pública.” Accessed: Apr. 25, 2025. [Online]. Available: <https://contractaciopublica.cat/ca/detall-publicacio/0c7345ca-be79-468e-a4c6-6a6333095511/200144108>

[290] “European Covid-19 Forecast Hub.” Accessed: Apr. 25, 2025. [Online]. Available: <https://covid19forecasthub.eu/>

[291] “RespiCast | ECDC Respiratory Diseases Forecasting Hub.” Accessed: May 13, 2025. [Online]. Available: <https://respicast.ecdc.europa.eu/>

[292] “Introducing ChatGPT | OpenAI.” Accessed: Apr. 06, 2025. [Online]. Available: <https://openai.com/index/chatgpt/>

